Polymer Carriers of Toll-Like Receptor-7/8 Agonists as Vaccine Adjuvants

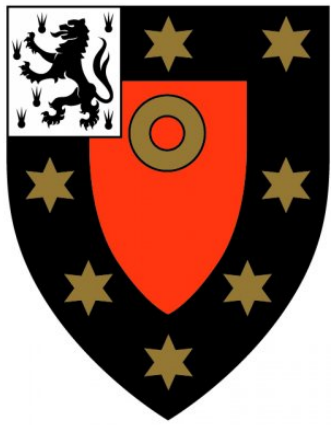

Geoffrey Martin Lynn
Saint John's College
University of Oxford

A thesis submitted for the degree of
Doctor of Philosophy
To the faculty of Nuffield Department of Medicine
Trinity Term 2014

Acknowledgements

This work was conducted under the supervision of Professor Leonard Seymour at the University of Oxford (Department of Oncology) and Dr Robert Seder at the National Institutes of Health (NIH, Vaccine Research Center) in Washington, DC. I am grateful for their generous support and thoughtful leadership, as well as their unwavering enthusiasm in the face of any experimental outcome. They have an infectious passion for science and they are truly dedicated to their students. It was a great privilege to work with these two inspiring supervisors and I hope that this body of work reflects positively on their contributions to my growth as a scientist.

While I am grateful for the support of many colleagues and friends who cannot all be recognized here, several should be noted for their direct experimental contributions. Dr Richard Laga (Oxford / Institute of Macromolecular Chemistry, Prague) has been both a mentor and friend who I worked closely with on the synthesis and characterisation of many of the polymers described herein. Dr Patricia "Tricia" Darrah (NIH) is a mentor and friend who guided my transition from a chemist to an immunologist and was instrumental in not only the experimental planning and execution of the biological experiments described herein but also assisted with many of the *in vivo* immunological studies. Tricia specifically carried out the *Leishmania major* challenges in mice. Andrew Ishizuka (NIH) provided invaluable insights as well as direct assistance with the development of staining panels for the flow cytometry studies. Alexandra Balaci, Ayako Yamomoto and Barbara Flynn (NIH) were invaluable in supporting many of the biological studies.

This work was supported by two training grants administered by the NIH, a Medical Scientist Training Program grant and an Intramural AIDS Research Fellowship.

Finally, I wish to acknowledge my friends and family whose loving support and encouragement has been the bedrock from which I have been able to pursue my ambitions in science and medicine.

Declaration of Authentication

The work presented herein was performed by me and in no way forms part of another thesis from this or any other university. Contributions made by others have been acknowledged. This work was performed under the supervision of Professor Leonard Seymour within the Department of Oncology under the Division of Medical Sciences at the University of Oxford.

Geoffrey M Lynn

Oxford University

Trinity Term 2014

Abstract

There is currently a need for vaccine adjuvants that are effective for eliciting Th1-type CD4 and CD8 T cell responses when formulated with protein and peptide-based subunit vaccines. Some of the most promising adjuvants in this regard are combined small molecule Toll-like receptor-7/8 agonists (TLR-7/8a). However, poor pharmacokinetic properties have precluded TLR-7/8a for use in vaccines.

In this thesis, polymer carriers were used to control pharmacokinetics and to modulate activity of TLR-7/8a for use as vaccine adjuvants. Combinatorial synthesis and *in vivo* structure-activity studies were used to evaluate how properties of Polymer-TLR-7/8a conjugates (Poly-7/8a) influence innate immune activation in lymph nodes that drain the site of vaccine administration. The most striking finding was that particle formation by Poly-7/8a strongly enhances the magnitude and duration (>14 days) of innate immune activation in lymph nodes by restricting agonist biodistribution and promoting uptake by dendritic cells. Particle-forming Poly-7/8a optimized for activity were found to induce only local innate immune activation (not systemic) and were effective for eliciting Th1-type CD4 and CD8 T cells that mediated protection against infectious challenge. Based on the importance of particle formation for activity of Poly-7/8a, thermo-responsive Poly-7/8a were developed that exist as single water-soluble macromolecules in solution but undergo temperature-driven particle formation *in vivo*. In conclusion, polymer carriers of TLR-7/8a represent a versatile and effective platform for modulating innate immune activity and warrant further investigation as a class of adjuvants for vaccines.

Table of Contents

1 Introduction 11

1.1 Vaccines and public health 11

1.2 Vaccination platforms 12

1.3 Vaccine adjuvants 14

1.4 Toll-Like Receptors (TLRs) 16

1.5 TLR signalling 18

1.6 Agonists of TLRs promote T cell responses 19

1.7 TLRa induce Type I IFNs and IL-12 that promote CD8 T cell responses to protein antigen 25

1.8 Agonists of TLR-7 and TLR-8 induce IL-12 and Type-I IFNs 27

1.9 Discovery of agonists of TLR-7 and TLR-8 30

1.10 Clinical uses of TLR-7/8a 31

1.11 Mechanism and pharmacokinetics of TLR-7/8a 33

1.12 Formulation of TLR-7/8a for use as vaccine adjuvants 34

1.13 Protein-TLR-7/8a conjugate vaccines 35

1.14 Synthetic carriers of TLR-7/8a for protein vaccines 37

1.15 Mechanisms accounting for activity of TLR-7/8a formulations 41

1.16 Hypothesis and specific aims 45

2 Materials and Methods 47

2.1 Chemicals 47

2.2 Synthesis of nucleophilic small molecule TLR-7/8a and negative control ligands 48

2.3 Synthesis of SM TLR-7/8a dye conjugates 58

2.4 Synthesis of amine-reactive copolymers 59

2.5 Synthesis of polymer-TLR-7/8a (Poly-7/8a) conjugates 60

2.6 Instrumentation for synthesis, purification and chemical characterisation 61

2.7 Determination of polymer molecular weights 62

2.8 Determination of the amount and density of TLR-7/8a attached to polymer carriers 62

2.9 Particle size and morphology characterisation 65

2.10 Transition temperature determination for thermo-responsive polymers 65

2.11 Evaluation of TLR-7/8a activity in vitro 66

2.12 Animals 67

2.13 Animal use ethics statement 67

2.14 *Ex vivo* lymph node cultures for cytokine determination 68

2.15 Cytokine measurements by ELISA 68

2.16 Cytokine measurements by bead array / multiplex 69

2.17 Whole animal imaging (biodistribution and kinetics) 70

2.18 Flow cytometry analysis of innate immune cells from lymph nodes and spleen 70

2.19 Tetramer staining of CD8 T cells from whole blood 72

2.20 Analysis of polyfunctional CD4 T cell responses 73

2.21 Flow cytometry 74

2.22 Listeria monocytogenes 74

2.23 *Listeria monocytogenes* infectious challenge 74

2.24 *Leishmania major* challenge 75

2.25 Serum antibody measurements 75

2.26 Hapten antibody determination 76

2.27 Statistics and graphs 76

3 Combinatorial synthesis of polymer carriers of TLR-7/8a and *in vivo* structure-activity relationship studies 77

3.1 Introduction 77

3.2 Synthesis of conjugatable TLR-7/8a agonists 80

3.3 Synthesis of amine-reactive HPMA-based polymers 81

3.4 Synthesis of polymer-TLR-7/8a (Poly-7/8a) conjugates 83

3.5 Combinatorial synthesis of Poly-7/8a and physicochemical characterisation 85

3.6 *In vivo* screening of a combinatorial library of polymer-TLR-7/8a conjugates 90

3.7 Increasing TLR-7/8a density on polymers induces particle formation 93

3.8 Increasing TLR-7/8a density and particle formation are associated with increased lymph node cytokine production 94

3.9 Lymph node cytokine production is dependent on TLR-7 but independent of the inflammasome 97

3.10 Polymer-TLR-7/8a conjugates are inactive *in vitro* 100

3.11 Discussion 101

4 Influence of Poly-7/8a pharmacokinetics and DC uptake on the location, magnitude and duration of innate immune activation 104

4.1 Introduction 104

4.2 Dye-labelled constructs for whole animal imaging and flow cytometry 106

4.3 Biodistribution and kinetics of SM 7/8a and Poly-7/8a 107

4.4 Adjuvant uptake by lymph node DC populations 111

4.5 Magnitude and spatiotemporal characteristics of innate immune activation 115

4.6 Magnitude and spatiotemporal characteristics of cytokine production 118

4.7 CD8 T cell and antibody responses to a model immunogen 119

4.8 Poly-7/8a co-administered with protein antigen ensures efficient co-delivery to lymph node DCs 123

4.9 Increasing agonist potency and dose are associated with persistent lymph node cytokine production and higher magnitude CD8 T cell responses 125

4.10 Discussion 129

5 Polymer-TLR-7/8a conjugates elicit protective CD8 T cell and Th1-type CD4 T cell responses 132

5.1 Introduction 132

5.2 Magnitude and spatiotemporal characteristics of innate immune activation 134

5.3 Magnitude and protective efficacy of CD8 T cell responses elicited by immunization with ovalbumin 141

5.4 Magnitude and isotype (Th1 vs. Th2) of antibodies elicited 145

5.5 SIV Gag immunization: magnitude of CD8 T cell responses and protective efficacy 146

5.6 Magnitude and quality of Th1-type CD4 T cell responses elicited by immunization with the MML protein derived from *Leishmania major* 148

5.7 Th1-type CD4 T cells induced by Poly-7/8a mediate protection following infectious challenge with *Leishmania major* 153

5.8 Discussion 155

6 Second-generation polymer-TLR-7/8a conjugates 159

6.1 Introduction 159

6.2 Controlling the timing of onset of innate immune activation 162

6.3 Micelle-forming Poly-7/8a 166

6.4 *In vivo* particle formation using thermoresponsive polymers 171

6.5 Discussion 177

7 Conclusions and future directions 180

7.1 Conclusions 180

7.2 Future directions 186

8 Literature cited 188

/	per
Ab	antibody
AEMA-BOC	n-(t-BOC-2-*aminoethyl*)*methacrylamide*
Ahx	aminohexanoic acid
AIBN	2,2′-azobis(2-methylpropionitrile)
APC	antigen-presenting cell
BCR	b cell receptor
CTA	4-cyano-4-(phenylcarbonothioylthio)pentanoic acid
CD	cluster of differentiation
CpG	cytosine-phosphate-guanosine rich DNA
Da	dalton
DC	dendritic cell
DLS	dynamic light scattering
DMAP	4-(dimethylamino)pyridine
DIPEA	n,n′-diisopropylethylamine
dsRNA	double stranded RNA
EDC	n-(3-dimethylaminopropyl)-N′-ethylcarbodiimide
EDTA	Ethylenediaminetetraacetic acid
ELISA	enzyme linked immunosorbent assay
ENV	envelope protein
EtMI	n-ethylmaleimide
g	gram
GPC	gel permeation chromatography
HLA	human leukocyte antigen
HPLC	high performance liquid chromatography
HPMA	n-(2-hydroxypropyl)methacrylamide
IFN	interferon
Ig	immunoglobulin
IL	interleukin
IP-10	inducible protein-10 (CXCL-10)
IR	infrared
L	litre
LC-MS	liquid chromatography mass spectrometry
LPS	lipopolysaccharide
m	metre
MA	methacrylamide
mM	millimoles
m<u>M</u>	millimolar
Mn	number average molecular weight
mg	milligram
mL	millilitre
MHC	major histocompatibility complex
MML	polyprotein from *leishmania major*
Mw	weight average molecular weight

MW	molecular weight
MPL	monophosphoryl lipid a
n	mole
nM	nanomolar
nm	nanometre
NMR	nuclear magnetic resonance spectroscopy
ODN	oligodeoxynucleotide
OVA	ovalbumin
PAMP	pathogen associated molecular pattern
PC	polymer coil
pDC	plasmacytoid dendritic cell
PgMA	n-propargyl methacrylamide
PM	polymer micelle
PP	polymer particle
PPG	poly(propylene glycol)
Poly	polymer
PRR	pattern recognition receptor
SAR	structure-activity relationship
SEAP	secreted embryonic alkaline phosphatase
SM	small molecule
ssRNA	single stranded RNA
TB	tuberculosis
TCR	t cell receptor
Th	t helper cell
TIR	toll / interleukin-1 receptor domain
TLR	toll-like receptor
TT	thiazoline-2-thione
TT	transition temperature
μ	micro
μL	microlitre
μm	micromoles
μM	micromolar
UV-Vis	ultraviolet-visible spectroscopy
VLP	virus-like particle
WT	wild type

1 Introduction

1.1 Vaccines and public health

Vaccines remain humanity's most cost-effective and efficacious means of reducing global infectious disease burden worldwide. Life expectancy in most developed nations has nearly doubled over the last two centuries, with most of these gains directly attributable to the impact of vaccines on reducing the impact of communicable diseases[1]. During the period from 1993-2014, in the US alone, the Centres for Disease Control and Prevention estimates that widespread childhood vaccination programs averted nearly 300 million infections and saved nearly $1.5 trillion in costs that would have otherwise been attributable to treatment and rehabilitation[2].

Despite the many triumphs of vaccines, over 5 million people worldwide will continue to die each year from infectious diseases for which there are no licensed vaccines or for which current vaccines are inadequate[3]. Impediments to the development of successful vaccination strategies for many infectious diseases are related to the limitations of contemporary vaccine technology. Accordingly, whereas existing vaccines primarily mediate protection through elicitation of broad-based antibody responses, vaccines against HIV, malaria and tuberculosis will likely require the elicitation of high magnitude and durable T cell responses[4-6] and / or the elicitation of broadly neutralizing antibodies that target defined, invariant epitopes of pathogens (e.g., v1/v2 loop of HIV Envelope protein)[3, 7-9].

While either or both T cells and antibodies will likely be important for protective immunity against many infectious diseases, this thesis focuses on the development of novel technologies for eliciting T cell responses using protein antigens.

1.2 Vaccination platforms

Vaccination platforms can be generally divided into two broad categories depending on whether the vaccine is derived from a (1) whole pathogen or is a (2) subunit (component) of the pathogen (see Table 1.1).

Vaccine platform		Advantages	Limitations	Examples
Whole organism	Live-attenuated	- Endogenous antigen production - Antigenic breadth - Highly immunogenic and induces durable immunity	- Reactogenicity and potential for reversion - Antigenic breadth can dilute immune response - Immunodominant responses not always best for protection	- Smallpox (cowpox) - Tuberculosis (BCG vaccine)
	Inactivated / killed	- Antigenic breadth - Highly immunogenic and induces durable immunity - Increased safety profile as compared with live vaccines	- Reactogenicity - Antigenic breadth can dilute immune response - Immunodominant responses not always best for protection	- Typhoid fever - Influenza
Subunit	Protein	- Highly defined and permit responses against subdominant epitopes - Safe and scalable - Permit repeated administration	- Protein alone is poorly immunogenic and requires adjuvants - Exogenously delivered antigen often less efficient at inducing T cell responses	- Tetanus (purified toxoid) - Hepatitis B (recombinant protein)
	Gene delivery-based (DNA)	- Highly defined and permit responses against subdominant epitopes - Easiest vaccine technology to manufacture and rapidly deploy - Effective in heterologous prime-boost immunization	- Poorly immunogenic - Requires electroporation or formulation with non-viral vector to enhance gene expression	- None currently licensed - Undergoing development for use as prime in heterologous prime-boost with viral vectors
	Gene delivery-based (viral vectors)	- Best platforms for inducing T cell responses - Highly defined and permit responses against subdominant epitopes	- Anti-vector immunity prevents repeated administration - Reactogenicity - Immunodominant responses against vector proteins	- None currently licensed - Human and chimpanzee adenoviruses and pox vectors most clinically advanced

Table 1.1: Vaccination platforms widely used for licensed and experimental vaccines.

Whole organism vaccines

Whole organism vaccines account for the largest share of currently licensed vaccines and represent some of the oldest and most effective vaccination platforms[10]. The principal advantage of whole organisms is that they provide a high breadth of antigens and naturally have immunostimulatory components. Whereas live-attenuated whole organism vaccines can produce endogenous antigen that is effective for the elicitation of cytotoxic lymphocytes (CTLs), inactivated / killed organisms are not able to produce endogenous antigen and are often restricted to elicitation of antibodies and only modest CD4 T cell responses[11]. The utility of whole organism vaccines is limited principally by the potential for reversion (for live-attenuated), as well as reactogenicity and high antigenic breadth. While high antigenic breadth may be an advantage in certain disease settings (e.g., Malaria)[6], elicitation of broadly-neutralizing antibodies against HIV and Influenza will likely require focused immune responses against highly conserved and defined epitopes present on pathogen surface proteins[12, 13].

Subunit vaccines

Subunit vaccines comprised of a single protein antigen derived from an infectious pathogen offer a more defined vaccine platform than whole organism-based vaccines[7, 10, 14]. Safety and high chemical definition of the antigen are the principal advantages of this platform. By focusing the immune response on a single protein antigen, it is possible to direct antibodies and T cells against what may otherwise be a subdominant epitope. There are three different strategies for delivering the subunit antigen, which include whole protein, DNA plasmids and vectored (e.g., viral, bacterial, etc.) vaccines. DNA vaccines are the lowest cost and, in principle, the most simple to

develop but have so far shown only limited efficacy in humans[15]. In contrast, viral vectors are the most potent platform for eliciting cellular immunity but are often limited by reactogenicity and / or anti-vector immunity that restricts their use to a single administration[16-20]. As compared with gene delivery-based vaccines, protein antigens are often less effective for eliciting cellular immunity but are safe and can be given repeatedly either alone or in combination with viral vectors. However, highly purified protein antigens are weakly immunogenic when used alone and require formulation with vaccine adjuvants to elicit T cell responses[14, 21]. A potential advantage is that specific formulations and adjuvant systems can be used to tune qualitative characteristics of T and B cell responses with little influence from the protein antigen alone.

The remainder of this thesis will focus on how adjuvants can be used to improve T cell responses to protein-based subunit vaccines.

1.3 Vaccine adjuvants

Adjuvants, from the Latin root Adjuvar, to help, can be defined as any component added to a vaccine that enhances or modifies the immune response to an antigen[21-24]. Whereas many pharmaceutical compounds are classified according to their chemical class, adjuvants are often classified broadly according to their presumed, often poorly understood, mechanism of action. A simple scheme is to classify adjuvants as either (1) delivery systems or (2) immune potentiators.

Delivery systems

Delivery systems are believed to primarily mediate their effects by altering the pharmacokinetics and cellular uptake of protein antigens[22, 25]. Though, recently it has emerged that many delivery systems also activate cells of the innate immune system[26], suggesting that contemporary classification schemes for adjuvants are inadequate. Through improved delivery and direct activation of innate immune cells, delivery systems have been shown to be effective for improving antibody titres but are often limited in their capacity to elicit T cell responses when used alone.

Delivery systems as adjuvants were discovered somewhat serendipitously in 1924 following the observation that Diphtheria toxin bound to Aluminum hydroxide microparticles induced higher antibody titres as compared with the toxin administered alone[22]. This seminal finding introduced adjuvants as a concept and established Aluminum salts, or Alum, as safe and effective tool for boosting immunity for a variety of vaccines. Remarkably, Alum remained the only adjuvant approved for clinical use until 1997. Today, certain compositions of emulsions and liposomes are also approved as delivery systems, in addition to Alum used alone and Alum in combination with an immune potentiator, Monophosphoryl lipid A (MPL)[1, 22].

Immune potentiators

Immune potentiators can be classified as molecularly defined adjuvants that enhance humoral and cellular immune responses to vaccines by directly activating cells of the innate immune system through defined receptors and signalling pathways[22, 27]. Whereas Alum delivery systems have been used in vaccines since the 1920s, it was not until 2005 that the first immune potentiator, MPL, was licensed for clinical use.

While the definition of an immune potentiator permits broader inclusion, most compounds that are being developed as immune potentiators are agonists of Toll-like receptors (TLRs), a specific class of Pattern Recognition Receptor (PRR) that functions in the innate recognition of pathogens[28].

The next sections describe how agonists of TLRs can be used as adjuvants for vaccines.

1.4 Toll-Like Receptors (TLRs)

PRRs represent a broad and diverse class of receptors that specialize in the recognition of conserved structures of pathogens, referred to as pathogen associated molecular patterns (PAMPs)[21, 23, 28]. The role of Toll-like receptors (TLRs) as PRRs was first recognized in 1997 after the discovery of a human homologue of the Toll protein associated with anti-fungal responses in fruit flies[29, 30]. Since the discovery, a total of 13 TLRs have been identified in humans and have been found on many different cell types, ranging from hepatocytes[31] and endothelial cells[32] to immune cells[28, 33, 34]. All TLRs are transmembrane proteins with an N-terminal outer-domain that functions in pathogen recognition and a C-terminal inner (Toll-IL-1 receptor, TIR) domain that binds adaptor proteins to mediate intracellular signalling (Figure 1.1A).

Cellular localization and functional specialization of TLRs

TLR cellular localization largely reflects their functional specialization. Whereas surface TLRs (TLR 1, 2, 4, 5, 6, 11, 12) recognize extracellular components of pathogens, endosomally localized TLRs (TLR 3, 7, 8, 9 and 13) are specialized for

the recognition of nucleic acids (Figure 1.1B)[28, 35]. The functional significance of the localization of TLRs not only relates to the accessibility of PAMPs (e.g., surface TLRs are specialized to recognize extracellular pathogens) but also has consequences for downstream signalling and the type of immune responses that are induced through TLR binding[35]. The functional specialization of TLRs through distinct signalling pathways is described below.

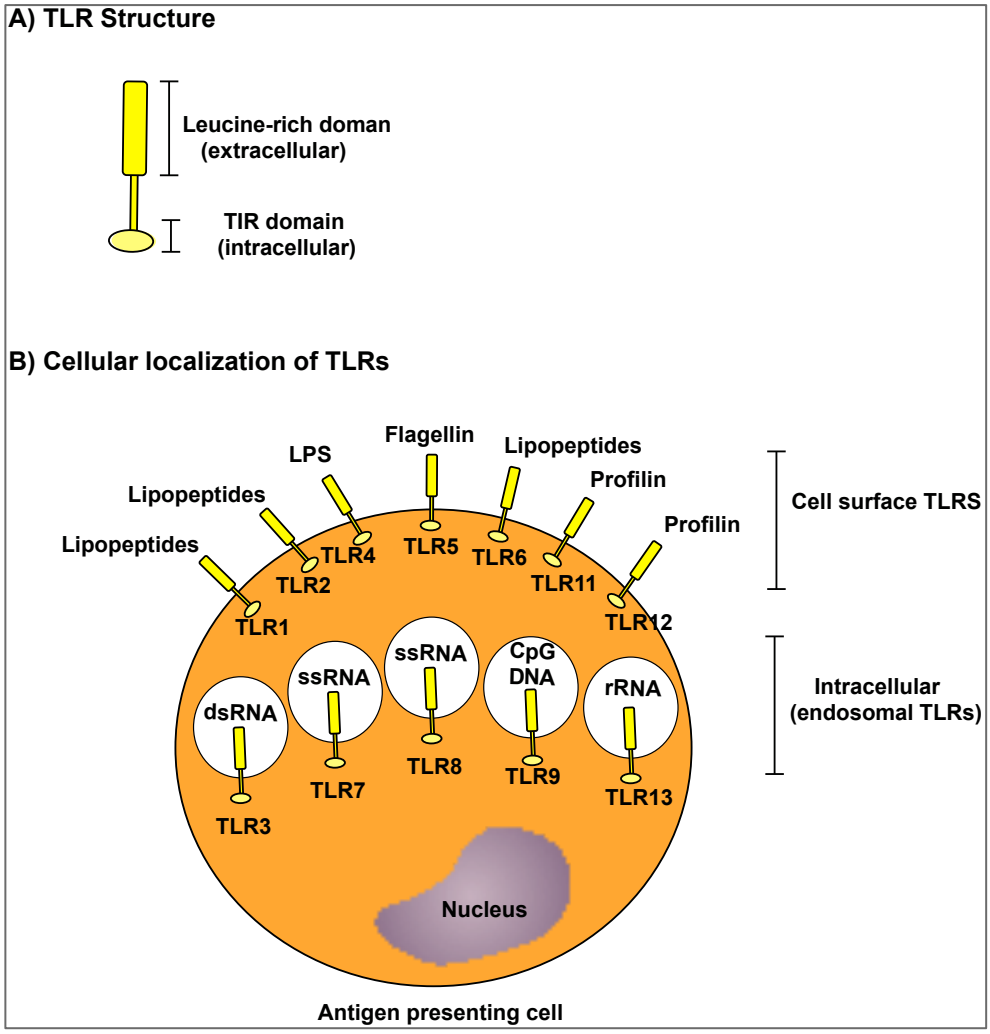

Figure 1.1: Structure and cellular localization of TLRs. (A) TLRs are comprised of an extracellular Leucine-rich domain that functions in PAMP recognition, a transmembrane domain and an intracellular Toll/-IL-1 receptor (TIR) domain. (B) Thirteen TLRs have been identified in humans. The cellular localization of the receptors reflects their functional specialization. Whereas surface TLRs are specialized for recognition of structural proteins of extracellular pathogens, endosomally localized TLRs are specialized for recognition of nucleic acid sequences.

1.5 TLR signalling

TLRs are expressed on cell surfaces or within endosomal compartments. Agonist binding to TLRs results in dimerization and recruitment of adaptor proteins through the TIR domain[36]. While other adaptor molecules play a role, myeloid differentiation primary-responses gene 88 (MyD88) is used by many TLRs and is the most studied. MyD88 contains a death domain that allows binding of IL-1 receptor associated kinase 4 (IRAK4), which serves as nucleation point for IRAK1 and IRAK2 that collectively form what is referred to as the "Myddosome[36]." The Phosphorylated Myddosome complex can then bind tumor necrosis factor receptor-associated factor 6 (TRAF6), which leads downstream to the recruitment and activation of the inhibitor of kappa kinase α/β (IKKα/β)[36, 37]. Activated IKKα/β, as the name implies, phosphorylates the inhibitor of kappa-B (IkB), which marks IkB for degradation and thereby permits the release of NF-kB. Free NF-kB translocates to the nucleus and mediates gene transcription that results in cellular activation and cytokine production[35, 38, 39].

Endosomal TLRs use distinct signalling pathways that lead to IFNs

With the exception of TLR-3, which only uses the adaptor molecule TRIF, TLRs use the different adaptor molecules, such as MyD88, to mediate downstream signalling that culminates in the nuclear translocation of NF-kB[35]. Within innate immune cells, particularly antigen presenting cells (APCs), nuclear translocation of NF-kB results in cellular activation and production of pro-inflammatory cytokines, including IL-1, IL-6 and TNFα. In contrast to surface TLRs that primarily mediate gene transcription through NF-kB, signalling through endosomally localized TLRs leads to nuclear translocation of NF-kB as well as Interferon regulatory factor (IRF) family

transcription factors[37]. The important distinction is that gene products downstream of NF-kB are primarily general markers of inflammation, whereas IRF leads to production of interferons (IFNs) and other gene products that are important for mediating anti-viral immune responses. Differences in signalling pathways and downstream gene products between surface and endosomally localized TLRs highlight the important functional specialization of these receptors and suggests that specific immune responses can be tailored by selectively targeting TLRs[40].

1.6 Agonists of TLRs promote T cell responses

TLR agonists (TLRa) primarily mediate their effects by activating cells of the innate immune system that are specialized for antigen uptake and presentation[21, 27]. The two main cells types involved are macrophages and professional antigen presenting cells (APCs), known as dendritic cells (DCs)[41]. These and other APCs act as sentinels of the innate immune system and are able to sense pathogens (or vaccines) through TLRs and other PRRs (Figure 1.2). Binding of agonists to cognate TLRs on or within APCs leads to a downstream signalling cascade (described above) and APC maturation. “Mature” (or activated) APCs (1) migrate to draining lymph nodes, (2) upregulate antigen presentation and co-stimulatory molecule expression on the cell surface and (3) produce selective cytokines[14, 21, 23].

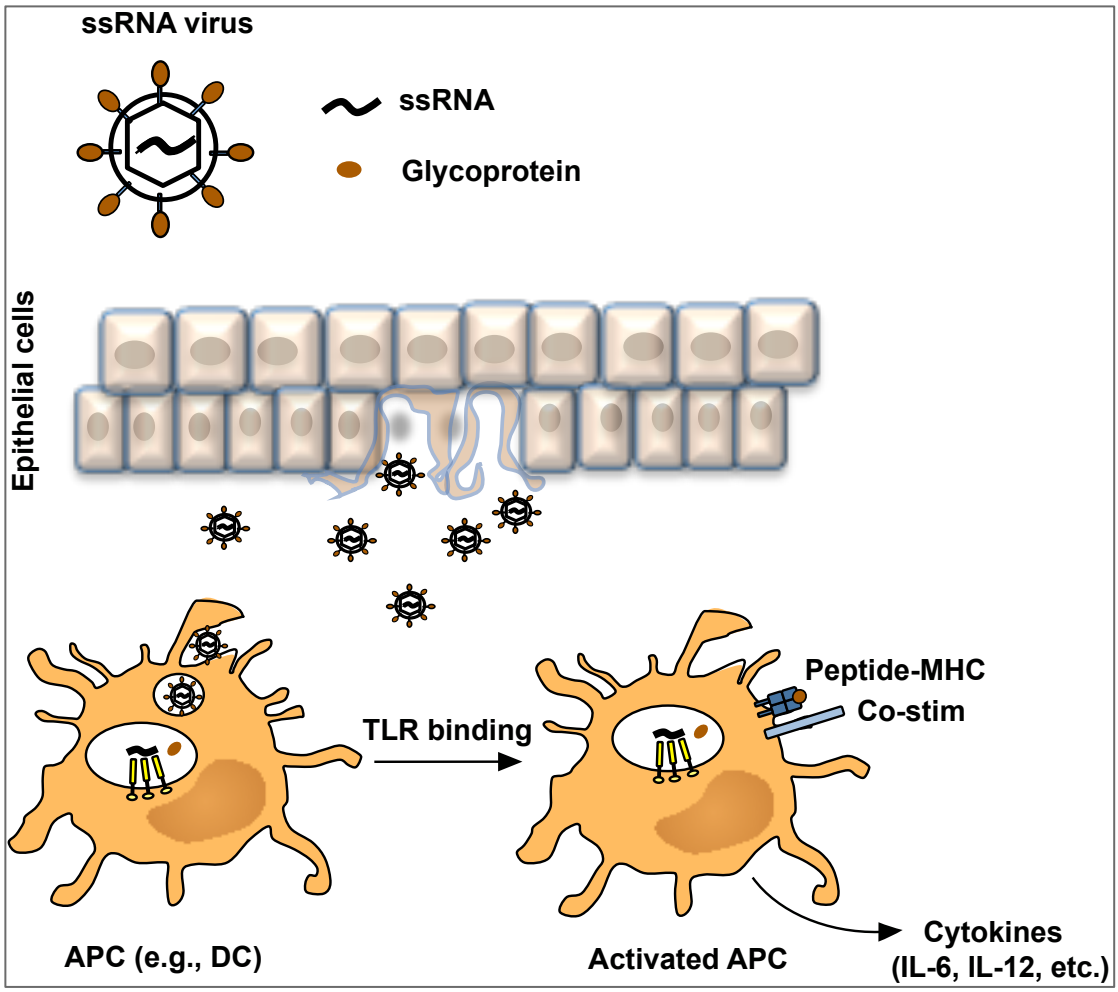

Figure 1.2: Dendritic cells (DCs) are professional antigen-presenting cells (APCs) that act as sentinels in peripheral tissues. As shown in this cartoon schematic, a DC is responding to a viral infection. Uptake and degradation of the virus within the endo-lysozomal compartment of the DC releases RNA and results in hydrolysis of structural proteins into peptide fragments that can be presented within the context of MHC molecules. TLRs in the endosome (e.g., TLR-7 or TLR-8) may bind the viral RNA and promote DC activation. The activated DC will migrate to lymph nodes (via CCR7 expression) where it produces cytokines and presents antigen and co-stimulatory molecules to T cells.

TLRs provide the 3 signals required for T cell priming and differentiation

The capacity of TLRa to induce DC maturation and cytokine production satisfies the three "signals" required for priming and differentiating T cells[23, 24]. As shown in Figure 1.3, DCs activated by TLRa (signal 0) present protein antigen on the cell surface in the form of peptide-MHC complexes, upregulate expression of costimulatory molecules (e.g., CD80, CD86) and produce selective cytokines. CD4 or CD8 T cells that recognize antigen (signal 1) in the context of MHC class II or MHC class I molecules, respectively, and receive adequate co-stimulatory molecule input (signal 2) are licensed to respond to antigen and initiate antigen-specific responses. Importantly, cytokines that are present during T cell priming are described as a critical 3rd factor (signal 3) that influences the differentiation of CD4 T helper cells (Th) towards distinct phenotypes that are defined by their expression of certain cytokines and transcription factors that dictate their effector functions.

CD4 Th cells can differentiate towards several distinct phenotypes that are specialized for protecting against certain infections but have also been implicated in autoimmune diseases and allergies. Classically, CD4 Th cells were thought to differentiate towards either Th1 or Th2 lineages[42, 43]. In this model, recently activated CD4 T cells in the presence of IL-12 and IFNγ become Th1-type CD4 cells that are characterized by their production of IFNγ and TNFα and the expression of the transcription factor T-bet. Th1 cell characteristic cytokines, which include IFNγ and TNFα, promote APCs to eliminate intracellular pathogens. This effect of Th1 cytokines has been cited as a mechanism to account for how Th1-type CD4 cells mediate protection against intracellular pathogens, such as Tuberculosis and Leishmania[44, 45]. Despite their important role in protecting against intracellular pathogens, Th1 responses have also

been implicated in certain autoimmune diseases, such as systemic lupus erythematosus and multiple sclerosis[46]. As an alternative to Th1 differentiation, IL-4 present during CD4 T cell activation has been shown to promote the differentiation of cells towards a Th2 phenotype that are characterized by production of the cytokines IL-4, IL-5 and IL-13 and the expression of the transcription factor GATA3. While the role of Th2 cells in providing protection against infection or promoting tolerance to prevent immune mediated diseases in normal physiology are areas of activate investigation, Th2 responses have been strongly implicated in the pathogenesis of asthma[47]. The role of Th2 cells in asthma can be partially explained by their effector functions, since IL-4 is known to promote B cell antibody class switching towards IgE, which mediates allergic immune responses and mast cell degranulation, while the production of IL-5 is known to promote eosinophil infiltration and activation that can lead to lung tissue fibrosis. Mast cells activated by IgE antibodies promoted by Th2 responses produce IL-4 that further reinforces the Th2 response and leads to histamine release, which results in smooth muscle contraction and vasodilation leading to airway obstruction[48]. While Th2 responses have historically been considered “humoral-mediated” immune responses, the capacity of Th2 cells to recruit and activate many innate cells in the pathology of asthma highlights the limitations of this classical Th1 (cell mediated immunity) / Th2 (humoral mediated immunity) paradigm.

In the last two decades, additional Th subsets have been identified, including Th17, T follicular helper (Tfh) and regulatory T (Treg) cells[42, 46, 49-51]. Treg cells are characterized by their production of the anti-inflammatory cytokine IL-10 and the expression of the transcription factor FOXP3. Treg cells provide an important

function in preventing over activation of immune responses and can be either thymic derived or induced in the periphery. Th17 cells, in contrast, are characterized by their expression of the transcription factor RORγt and the production their characteristic cytokine, IL-17, which promotes the recruitment and activation of a variety of innate immune cells, particularly neutrophils, that produce pro-inflammatory cytokines such as TNFα and IL-1β. While Th17 cells are believed to be important for mediating protection against extracellular bacteria, these cells have also been implicated in pathogenesis of asthma and other autoimmune diseases. In contrast to the other Th phenotypes that have direct roles in peripheral responses to pathogens, Tfh cells are characterized by their localization within the B cell follicle of lymph nodes and the expression of the transcription factor bcl6. This close proximity to B cells allows Tfh cells to enhance antibody responses by promoting antibody class switching and affinity maturation. Additional Th cells, including Th9 and Th22 have been recently identified and are currently being investigated for their roles in health and disease.

While Th subsets were long believed to be terminally differentiated, recent data suggests that Th cells have a great deal of plasticity and can change transcription factor expression depending on external stimuli[49]. For instance, Treg cells have recently been shown to lose their expression of FoxP3 and begin producing pro-inflammatory cytokines in responses to type I IFNs. Additionally, Th17 cells can gain the capacity to produce IFNγ, a Th1 characteristic cytokine, while Th1, Th2 and Th17 cells have all been shown to have the capacity to differentiate towards Tfh cell phenotypes.

While these data highlight the tremendous phenotypic heterogeneity and plasticity of Th CD4 cell subsets, vaccines against certain infectious diseases (e.g., malaria, TB and HIV) and cancers will likely require Th1 responses that provide the appropriate effector functions for clearance of intracellular pathogens and the promotion of high affinity, broadly neutralizing antibodies. Based on the need for more effective vaccines against HIV, malaria and TB, as well as therapeutic vaccines against cancers, the remainder of this thesis will focus on how TLRs can be used in vaccines to promote the appropriate cytokine milieu required for priming Th1-type CD4 T cell responses to protein antigens.

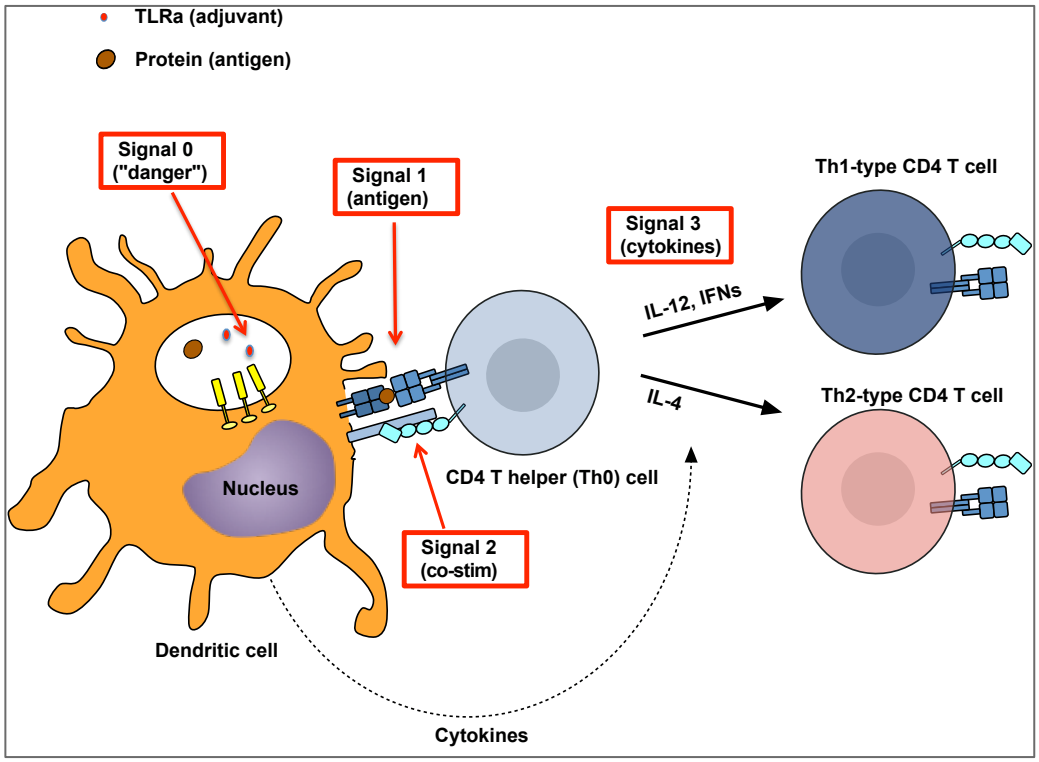

Figure 1.3: TLRa provide the three "signals" required for T cell priming and differentiation. Recognition of a PAMP activates APCs (e.g., DCs) and is referred to as Signal 0, or the "danger signal." T cell receptor (TCR) binding to the peptide-MHC complex is Signal 1, "recognition." Signal 2 is provided by co-stimulatory molecules on the DC that provide "verification" to T cells that Signal 1 is "non-self" in origin. Cytokines present during T cell priming provide Signal 3, which drives differentiation of T helper (Th) cells towards distinct subsets. Th1-type CD4 cells are characterized by their capacity to produce IFNγ, IL-2 and TNFα, whereas Th2-type CD4 cells are characterized by their capacity to produce IL-4, IL-5, IL-10 and IL-13.

1.7 TLRa induce cytokines that promote CD8 T cell responses

The prior section described the role of specific cytokines in promoting the differentiation of CD4 helper T (Th) cells towards distinct functional phenotypes. In addition to their role in driving CD4 Th cell differentiation, certain cytokines, particularly type I IFNs and IL-12, also play diverse and important roles in promoting CD8 T cell responses to exogenously delivered protein antigen. The role of Type I IFNs and IL-12 in promoting CD8 T cell immunity is discussed below.

Type-I IFNS

Type I IFNs represent a broad family of related cytokines (IFNβ and multiple isoforms of IFNα) that can be induced by viral infection or by synthetic or naturally occurring molecules, such as TLRa (e.g., CpG, Imidazoquinolines, etc.). These molecules have potent antiviral properties owing to their capacity to directly suppress viral replication within host cells as well as their ability to promote robust immunological responses against viral infection. The capacity of Type I IFNs to promote antiviral responses can be exploited to promote CD8 T cell immunity to exogenously delivered protein antigen during vaccination.

An important role of Type I IFNs for promoting CD8 T cell responses is their capacity to promote upregulation of MHC-I and co-stimulatory molecule expression by professional APCs. More recently, Type I IFNs have also been shown to essentially "rewire" antigen presentation pathways to allow for presentation of exogenously delivered protein antigen within the context of MHC-I[52]. This mechanism for allowing exogenously delivered protein antigen to be presented on MHC-I, a process referred to as cross-presentation, is critical for ensuring that protein

delivered by vaccination can promote CD8 T cell priming. Otherwise, in the absence of this mechanism, protein antigen delivered during vaccination is limited to presentation within the context of MHC-II and can only promote the generation of CD4 T cell responses. Another potentially important mechanism is that Type I IFNs induce macrophages and other APC populations to produce IFN-inducible protein 10 (IP-10, also known as CXCL10), which promotes recruitment of CD8 T cells to the sites where both antigen and the stimulus (i.e., Type I IFNs) are present and thus provides another means to promote CD8 T cell priming[53]. While additional mechanisms are likely present, these examples highlight some of the diverse mechanisms through which type I IFNs can enhance CD8 T cell responses by promoting cross-presentation, increasing antigen and co-stimulatory molecule expression and recruiting CD8 T cells to the sites of priming.

IL-12

In addition to the important role of IL-12 for driving differentiation of Th0 to Th1-type cells, IL-12 has also recently been recognized to play an important role in driving the expansion of CD8 T cells[54, 55]. Recent data shows that IL-12 induces the upregulation of the high affinity IL-2 receptor on CD8 T cells that promotes their proliferation and expansion through autocrine or paracrine production of IL-2. Studies using IL-12 and Type I IFN knockout mice have also suggested that IL-12 and type I IFNs work concertedly to promote CD4 and CD8 T cell responses[56, 57]. Altogether, these data suggest that vaccines for optimizing T cell responses to protein antigens should use TLRa or other immune potentiators that able to induce the production of both IL-12 and Type-I IFNs.

1.8 Agonists of TLR-7 and TLR-8 induce IL-12 and Type-I IFNs

Unique DC subsets show remarkable functional specialisation for producing cytokines and presenting antigen, allowing for immune responses to be tailored depending on which DC subsets are activated[41, 58-61]. For instance, as shown in Figure 1.4, the major DC subsets found in humans are BDCA3$^+$ DCs, conventional DCs (cDC) and plasmacytoid DCs (pDCs)[41, 59]. BDCA3$^+$ DCs are the main DC population responsible for cross-priming CD8 T cells (considered the human equivalent of murine CD8$^+$ DCs) and also produce IL-12 and IFN-β[59]. In contrast, cDCs are specialised for priming CD4 T cells and for producing IL-12[61]. pDCs are not believed to play an important role in presenting antigen to T cells during natural infection or immunization, but these cells are the principal source of Type I IFNs and seem to be specialised in their capacity to recognise viruses[60]. The functional specialization of DC subsets suggests that select TLR agonists can be used to activate unique combinations of DCs for inducing the desired immune outcome. Thus, understanding TLR expression patterns across distinct subsets provides a means of understanding how different TLRa can be used to induce unique innate immune response profiles. TLR expression patterns in humans and mice are described below.

TLR expression across DC subsets

The functional specialisation of DC subsets suggests that optimising T cell responses to protein antigen requires activation of all the major human DC subsets to promote both Th1 priming and cross presentation. However, different DC subsets show unique patterns of TLR expression and are differentially activated by TLR agonists. This suggests that optimizing T cell responses to protein antigen requires the appropriate TLRa, or combination of TLRa, to induce broad-based DC activation and the

production of specific cytokines that promote T cell immunity. Of the most pre-clinically advanced TLRa (see Figure 1.4), which includes agonists of TLR 3, 4, 7/8 and 9, only the imidazoquinoline-based molecules with combined TLR-7 and TLR-8 activity are able to directly activate all major human APC subsets, which includes all DC subsets, as well as macrophages and B cells[21, 33, 58, 62, 63]. The capacity of combined TLR-7/8a to induce such broad-based APC activation has been hypothesized to provide the optimal innate immune stimulus for eliciting T cell immunity[21].

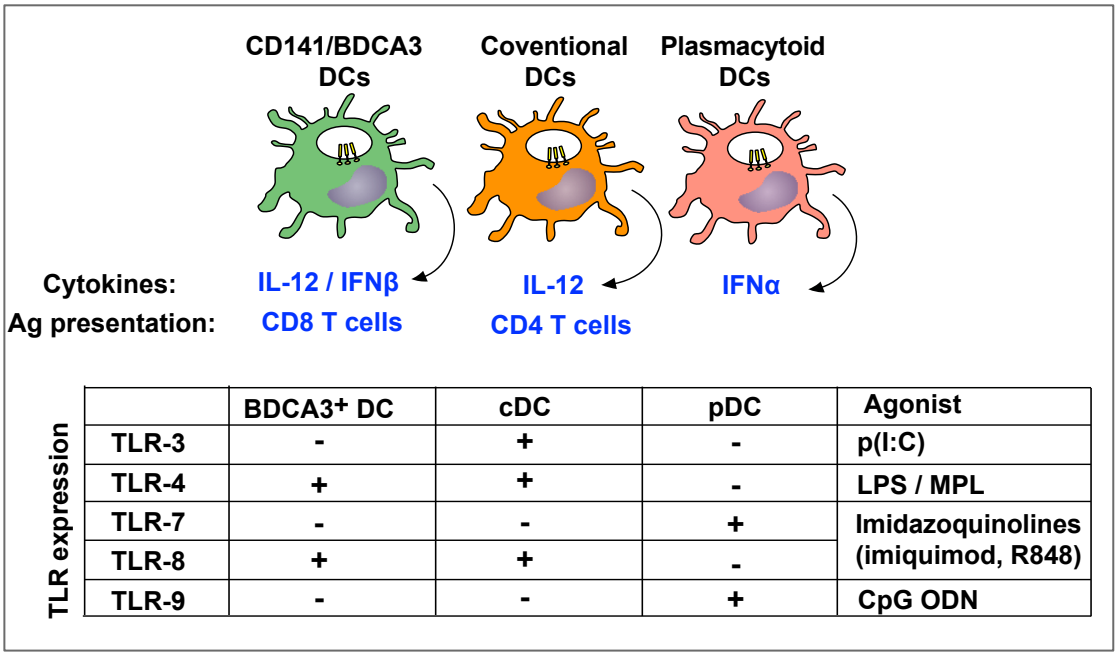

TLR expression

	BDCA3+ DC	cDC	pDC	Agonist
TLR-3	-	+	-	p(I:C)
TLR-4	+	+	-	LPS / MPL
TLR-7	-	-	+	Imidazoquinolines (imiquimod, R848)
TLR-8	+	+	-	
TLR-9	-	-	+	CpG ODN

Figure 1.4: Functional specialisation of major human DC subsets and patterns of TLR expression. The three major human DC subsets are shown. BDCA3+ DCs are specialised for IL-12 and IFN-β production, as well as antigen presentation to CD8 T cells. cDCs are specialised for IL-12 production and antigen presentation to CD4 T cells. pDCs are specialised for production of type I IFNs. The table shows the TLR expression patterns for each of the 3 major DC subsets. Note that no single TLR is found in all subsets but that combined TLR-7/8a (imidazoquinolines) can activate all major DC subsets through TLR-7 and TLR-8.

While combined TLR-7/8a are recognized by all major APC subsets in humans, TLR-7/8a are more limited for directly activating APC subsets in mice (Figure 1.5). For instance, until recently, TLR-8 was believed to be inactive in mice. While more recent

data has implicated TLR-8 in viral recognition and even protection against autoimmunity[64, 65], it is presently unknown whether TLR-8 activity accounts for immune responses in mice induced by combined TLR-7/8a. While the role of TLR-8 in mice is unknown, TLR-7 is expressed by pDCs, macrophages, monocyte-derived DCs, CD8- DCs, and B cells, but TLR-7 is not expressed by the CD8+ DCs in mice, which are the murine ortholog of human BDCA3+ DCs that are specialized for antigen cross-presentation.[28, 34, 63] Despite their lack of TLR-7 expression, use of TLR-7/8a in mice still leads to activation of CD8+ DCs, suggesting indirect activation of these DCs due to the inflammatory milieu[63].

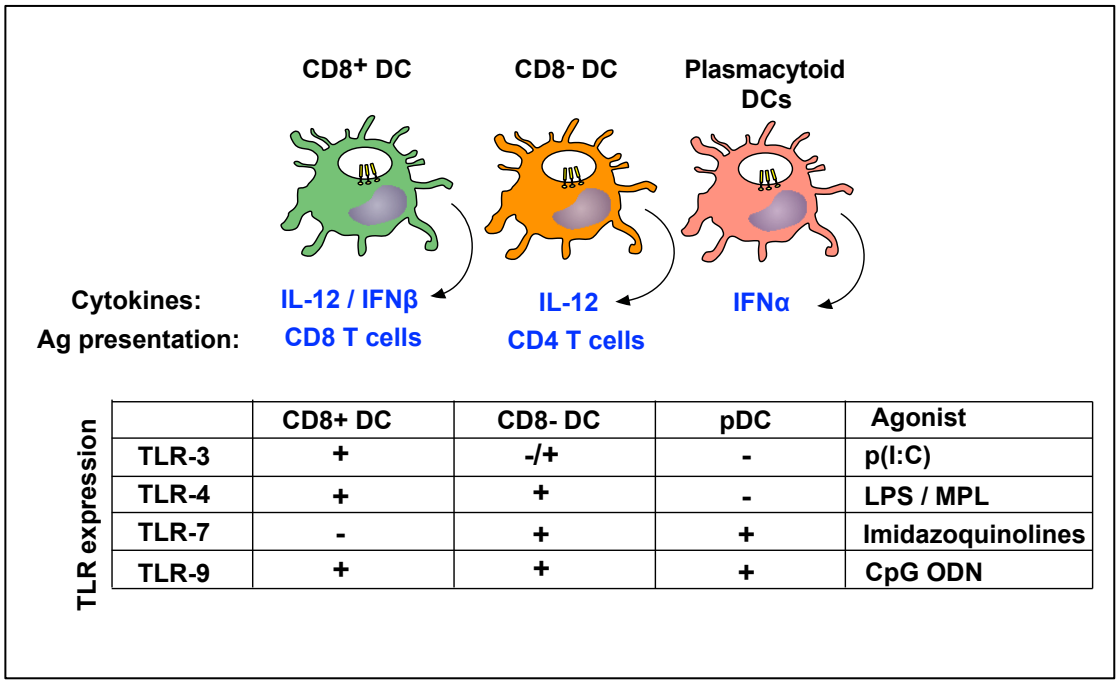

TLR expression	CD8+ DC	CD8- DC	pDC	Agonist
TLR-3	+	-/+	-	p(I:C)
TLR-4	+	+	-	LPS / MPL
TLR-7	-	+	+	Imidazoquinolines
TLR-9	+	+	+	CpG ODN

Figure 1.5: Functional specialisation of major murine DC subsets and patterns of TLR expression. The above table provides a simplified classification that relates murine DC phenotypes with their human orthologs shown in Figure 1.4. Note that CD8- DCs are a heterogeneous population of lymph node resident and skin derived DCs, but that these DCs share similar qualities with conventional DCs in humans.

The capacity imidazoquinoline-based TLR-7/8a to broadly activate APC subsets and promote a favourable cytokine milieu for inducing T cells responses served as the fundamental basis for choosing these molecules for this thesis. The remainder of the

discussion will focus on properties of these molecules and will emphasise the contemporary limitations surrounding the use of TLR-7/8a as vaccine adjuvants to highlight how polymer carriers can be used as delivery platforms to improve their activity for use in vaccines.

1.9 Synthetic agonists of TLR-7 and TLR-8

The discovery of synthetic agonists that induce Type I IFN production predates the discovery of TLRs and occurred somewhat serendipitously by researchers at 3M pharmaceuticals in the 1980s[66]. In their search for herpes simplex virus (HSV) treatments, researchers discovered that imidazoquinoline-based compounds (see Figure 1.6) could inhibit HSV infection *in vivo* but not during *in vitro* studies. Researchers later identified that inhibition of viral replication *in vivo* was indirectly due to the production of Type I IFN by immune cells, rather than by direct inhibition of the viral replication machinery[67].

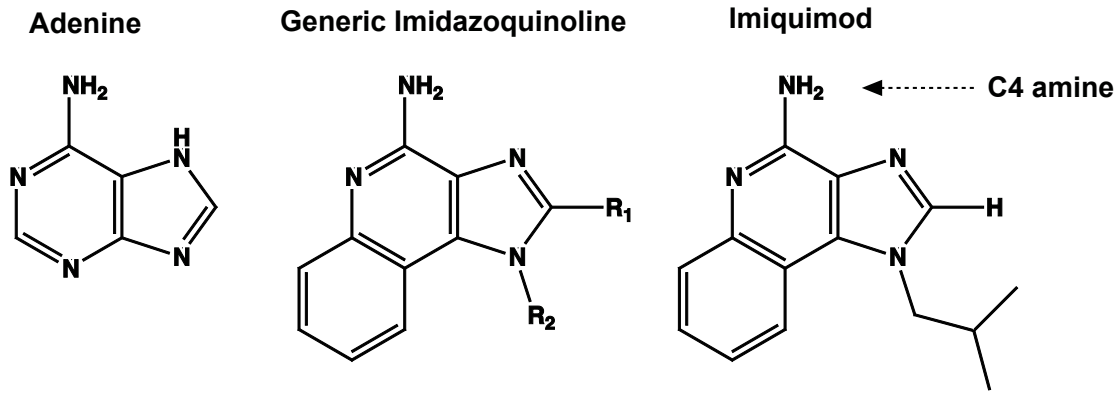

Figure 1.6: Structures of the nucleotide base adenine and imidazoquinolines. Note that R1 and R2 can be any substituent. Imiquimod is a representative imidazoquinoline compound where R1 = hydrogen and R2 = isobutyl. Note that the C4 amine (indicated by the arrow) is critical for TLR-7 and TLR-8 binding.

Following the seminal discovery that TLRs are the class of receptors that mediate recognition of LPS in the late 1990s[29, 30], it was later shown that TLR-7 and TLR-8 are the receptors that mediate Type I IFN production by the imidazoquinoline-based compounds[67]. Discovery of the receptors led to the rapid identification of several additional classes of compounds with a range of potencies for either or both TLR-7 and TLR-8[66, 68-72]. All of the synthetic small molecule agonists for these receptors resemble purine nucleotide bases and share a common structural motif that includes an aromatic amine (C4 position; see Figure 1.6) that is critical for receptor dimerization and downstream biological activity[66, 73]. While many synthetic compounds with TLR-7 and TLR-8 activity had already been identified, it was not until 2004 that ssRNA was identified as the natural ligand for both TLR-7 and -8, suggesting that these receptors have evolved to recognize viruses (e.g., influenza, yellow fever, HIV, etc.)[74, 75].

1.10 Clinical uses of TLR-7/8a

Following 3M's discovery that imidazoquinolines can inhibit viral replication by inducing Type I IFNs, there have been many efforts to use TLR-7/8a for a variety of disease indications ranging from cutaneous pathologies to chronic Hepatitis C infection and metastatic cancers[76-80]. While use of TLR-7/8a for treatment of cutaneous viral infections and skin cancers has proven effective[79-82], use of TLR-7/8a for treatment of systemic diseases (e.g., Hepatitis and metastatic cancers) has been limited by poor activity and often dose-limiting toxicity[76, 77, 83, 84]. The next sections summarize the clinical uses of TLR-7/8a as well as the immunological mechanisms that account for efficacy and toxicity.

Cutaneous uses of TLR-7/8a

An imidazoquinoline-based TLR-7/8a was the first TLRa to be approved by the FDA for clinical use. In 1997, the FDA granted approval for 3M to begin marketing and selling a topical cream containing the imidazoquinoline-based compound, Imiquimod (Aldara®), for treatment of human papilloma virus (warts)[82]. Indications were later expanded to include treatment of basal cell carcinoma[78, 80] and actinic keratosis[79]. Since this time, Imiquimod and a more potent and water-soluble imidazoquinoline-based compound, Resiquimod, have both been explored for treatment of other cutaneous pathologies, including herpes simplex virus (HSV)[85] and melanoma[86]. Adverse events associated with TLR-7/8a cutaneous therapy include localised erythema, pain and swelling[79, 80, 85, 87, 88].

Systemic uses of TLR-7/8a

Recombinant Type I IFN has been used in the treatment of hepatitis B virus infection since the late 1980s[89] and it has been speculated that systemic use of type I IFN may also be useful for treatment of metastatic cancers and viral infections[90, 91]. However, development of anti-IFN antibodies[92] and intolerable "flu-like" symptoms[93] by recombinant IFN therapy has prompted a search for safer and less immunogenic alternatives. This need for systemic inducers of Type I IFNs has led many researchers to evaluate the potential clinical utility of imidazoquinoline-based TLR-7/8a for use as systemic treatments for diseases ranging from chronic viral infections[77, 94, 95] to metastatic cancers[76, 83, 84, 96]. However, none of these studies have reported efficacy for the treatment of systemic disease. Instead, all clinical trials evaluating systemic administration of imidazoquinoline-based TLR-7/8a report dose-limiting toxicities, including lymphopenia and "flu-like" symptoms[77, 83, 84, 97]. Mechanisms that account

for differences in clinical efficacy between local and systemic uses of imidazoquinoline-based TLR-7/8a are discussed in the next section and provide a foundation for understanding the limitations of TLR-7/8a for use as vaccine adjuvants.

1.11 Mechanism and pharmacokinetics of TLR-7/8a

The capacity of TLR-7/8a to clear cutaneous viral infections and cancers but not systemic diseases relates to the mechanism of action and pharmacokinetics of imidazoquinoline-based TLR-7/8a.

Mechanism of action

Imidazoquinoline-based TLR-7/8a have shown remarkable efficacy for clearing cutaneous pathologies and are thought to mediate their effects through indirect and direct immunological mechanisms[81]. Through their capacity to activate APCs and induce cytokines (e.g., IL-12 and type I IFNs), TLR-7/8a have been shown to prime adaptive immune responses (Th1-type CD4 and CD8 T cells) against cutaneous antigens[87, 98]. These responses are presumably primed in lymph nodes downstream of the sites of imidazoquinoline administration. Recent data suggests that TLR-7/8a may even play a direct role in clearing cutaneous pathologies by endowing DCs with "tumouricidal" activity[99-102]. There is also evidence that TLR-7/8a can augment pro-inflammatory cytokine production by inhibiting adenosine receptors and / or may even directly induce apoptosis of cancerous or virally infected cells, though the relative significance of these mechanisms is unknown[81].

Pharmacokinetic limitations

Administration of small molecule TLR-7/8a by oral or parenteral routes results in dose-limiting toxicity and poor efficacy[77, 83, 96]. These observations are likely explained by the pharmacokinetic properties of the agonist. Whereas topical application of TLR-7/8a creams provide a sustained source of agonist for activating APCs at local tissue sites and in draining lymph nodes, subcutaneously (sc) or orally delivered TLR-7/8a enter systemic circulation and are cleared from the blood with half-lives ranging from 2.5 to 8 hours[97, 103]. Broad biodistribution and rapid clearance of the agonist leads to transient systemic innate immune activation that is associated with toxicity and immune dysfunction. For instance, a high concentration of TLR-7/8a in the blood induces high levels of Type-I IFNs and pro-inflammatory cytokines that are temporally associated with "flu-like" symptoms in patients[97]. Another negative consequence of systemic cytokines is that blood vessels throughout the body upregulate selectins that bind and sequester circulating leukocytes[32]. This effectively decreases white blood cell counts (lymphopenia) and has been associated with the impaired capacity of animals to elicit either primary immune responses to vaccination or hypersensitivity responses to secondary antigen exposure (at draining lymph nodes and skin, respectively)[104].

1.12 Formulation of TLR-7/8a for use as vaccine adjuvants

Eliciting optimal T cell and antibody responses to protein antigens requires persistent innate immune activation and antigen presentation in lymph nodes that drain the sites of vaccine administration. However, the transient systemic innate immune activation induced by small molecule TLR-7/8a provides only limited innate immune activation at the sites of immune priming (i.e., lymph nodes). To improve activity of TLR-7/8a

for use as vaccines adjuvants, it is necessary to use formulation and delivery approaches that spatially restrict agonist distribution to the sites of administration and draining lymph nodes. Several strategies have recently been described that use either macromolecular or particle-based carriers as a means of improving TLR-7/8a pharmacokinetics, and all of these strategies have been shown to markedly improve antibody and T cell responses as compared with use of the free TLR-7/8a. The next sections describe the relative advantages and limitations of the different TLR-7/8a formulation and delivery strategies (see sections 1.13 and 1.14), as well as the mechanisms that account for the improvements in activity that are observed (see section 1.15).

1.13 Protein-TLR-7/8a conjugate vaccines

One method for improving the activity of TLR-7/8a is to physically link (conjugate) the agonist directly to protein antigens. In the first example of this approach, Wille-Reece and colleagues used a UV light-catalysed cross-linker to attach multiple imidazoquinoline-based TLR-7/8a to nucleophilic residues (e.g., lysine) on HIV Gag protein to generate a Gag-TLR-7/8a conjugate vaccine[105-107]. Immunisation with the Gag-TLR-7/8a conjugate compared with Gag + free (unlinked) TLR-7/8a resulted in a significantly higher magnitude of Gag-specific Th1-type CD4 T cells and CD8 T cells, as well as a higher magnitude of Gag-specific antibody endpoint titres. Later studies found that improved immunogenicity of the conjugate was dependent on aggregation (particle formation) that resulted from the chemical conjugation process[108]. Overall, these studies provided an important proof-of-principle that the activity of TLR-7/8a for use as vaccine adjuvants can be improved through the use of

formulation and delivery approaches that restrict agonist biodistribution and improve co-delivery of the agonist with protein antigens.

Second-generation protein-TLR-7/8a conjugates

Later studies built on Wille-Reece's findings by introducing more reproducible and controlled chemical methodologies for linking TLR-7/8a to protein antigens. Shukla et al report on several chemical methodologies for controlling the site and number of TLR-7/8a linked to proteins[109]. By using TLR-7/8a modified with a primary amine, isothiocyanate, or maleimide linkers, the authors show that they can control the site and number of TLR-7/8a attached to the protein antigens either through reducing sugars, or cysteine or lysine residues, respectively. Additional site-selective bioconjugation strategies have recently been described and should allow for the controlled attachment of TLR-7/8a to a range of different protein and peptide antigens using reactive chemistries available to native proteins or proteins using non-natural amino acids[110-115].

In a later study, Vecchi et al describe a process that allows for the attachment of high densities of TLR-7/8a to protein antigens without inducing aggregation of the resulting conjugate[116]. The authors observed that the soluble protein-TLR-7/8a conjugate is not immunogenic *in vivo* unless the conjugate is adsorbed to Alum microparticles and is effectively made particulate. These observations corroborate Wille-Reece's earlier findings that particle formation is critical for activity of the protein-TLR-7/8a conjugate and suggest that future studies should focus on the use of particulate carriers of TLR-7/8a. Altogether, these studies show that chemically

defined and controlled formulation strategies can be implemented for producing protein-TLR-7/8a conjugates vaccines.

Limitations and prospects

There are several issues that may preclude the use of protein-TLR-7/8a conjugates as vaccines. A major limitation of this technology is that the attachment of TLR-7/8a to protein antigens can alter and / or mask important epitopes and inhibit binding by neutralizing antibodies[117]. While it may be possible to circumvent this limitation by attaching TLR-7/8a to sites that do not interfere with recognition by neutralizing antibodies, the requirements to reproducibly and site-selectively attach TLR-7/8a to the protein will likely add to labour and financial costs that will reduce the relative appeal of this technology compared with alternatives. Given the technical limitations and access to potentially superior alternative technologies (see section 1.14), it remains unclear whether this technology will be adopted for routine clinical use[118].

1.14 Synthetic carriers of TLR-7/8a for protein vaccines

Several synthetic macromolecular- and particle-based carriers of TLR-7/8a have recently been described and are reported to enhance both antibody and T cell responses to protein antigen. In contrast to direct protein-TLR-7/8a conjugation strategies, use of synthetic carriers to control delivery of TLR-7/8a circumvents the need to chemically modify the protein antigen and permits control over pharmacokinetics independent of properties of the protein antigen. While other classification schemes are possible, carrier approaches can be defined as either (1) ***non-covalent formulations*** (e.g., emulsions and liposomes) that incorporate TLR-7/8a through hydrophobic interactions, or (2) ***covalent formulations*** that require

chemical modification to incorporate TLR-7/8a to macromolecular and particulate scaffolds. Examples of these strategies, as well as the relative advantages and limitations of each of these approaches are discussed in the sections below.

Non-covalent formulations

All of these strategies take advantage of the lipophilic properties of TLR-7/8a, which allows for incorporation of the agonists into hydrophobic compartments of particulate carriers. The principal advantage of these approaches is that they do not require covalent modification of the platform or the agonists. However, major limitations of these approaches are that they provide only limited control over the amount of TLR-7/8a (or other materials) that are incorporated into the carriers and many properties of these systems (e.g., rate of TLR-7/8a release from the particles) are empirically determined and are difficult to control. Several of the most promising and advanced approaches are described here.

1. ***Poly(lactic-co-glycolic acid) (PLGA)-based nanoparticles.*** PLGA has been developed as a material for use in vaccines because it is biodegradable and has been used safely in humans for other applications (e.g, sutures, implants). Several studies have described strategies for incorporating imidazoquinoline-based TLR-7/8a agonists (R837 and R848) into the hydrophobic compartments of PLGA nanoparticles that are ~ 300 nm in diameter[119, 120]. Kasturi et al observed that R837 (Imiquimod) co-encapsulated in PLGA nanoparticles with the TLR-4 agonist, MPL, markedly enhanced both antibody and T cell responses to protein antigen but that optimal antibody responses required the antigen to be delivered in separate nanoparticles[119]. Based on the observed persistence of germinal centre

formation in tissue draining lymph nodes, the authors speculate that the improved immunogenicity is due to the capacity of the PLGA nanoparticles to increase persistence of antigen and adjuvant.

2. ***Liposomes and polymersomes-*** Whereas PLGA particles have entirely hydrophobic interiors that are used to encapsulate the TLR-7/8a, both liposomes and polymersomes are bilayer vesicles surrounded by an aqueous phase. In these approaches, lipophilic TLR-7/8a are incorporated or intercalated within the bilayer of the particles. To facilitate incorporation of TLR-7/8a into liposomal bilayers, Smirnov and colleagues produced a TLR-7/8a with a fatty acid (C18) tail, referred to as 3M-052[121]. The authors observed that liposomal formulations of 3M-052, as compared with free R848, co-administered with protein antigen leads to significantly higher titres of total IgG antibodies and Th1-skewing of the antibody responses (i.e., higher IgG2a compared with IgG1 titres). Importantly, whereas R848 led to high levels of serum cytokines, 3M-052 incorporated into liposomes did not induce any serum cytokines. An alternative, but similar, approach is to use synthetic polymers that, like liposomes, form particles with lamellar membranes referred to as polymersomes. This approach was recently described by Scott et al who used poly(propylene sulphide) (PPS) and PEG block copolymers to form polymersome nanoparticles between 100-200 in diameter to incorporate R848[122]. Whether this approach improves *in vivo* activity of the agonist remains to be determined.

3. ***Stabilized emulsions-*** Use of emulsions to encapsulate R837 was recently described by Vicente et al[123]. In this this approach, R837 was added to a mixture

of medium chain triglycerides and an emulsifying agent was used to stabilize the nanoparticle-sized (~ 200 nm) oil droplets that were formed in aqueous conditions. Immunization with the "nanocapsule" and protein antigen significantly enhanced Th1-polarized antibody responses, a finding that is consistent with earlier findings by Smirnov et al who delivered TLR-7/8a in liposomes[121]

Covalent formulations

There are a variety of macromolecular and particle-based delivery platforms that can be used for covalent attachment of TLR-7/8a. The principle advantage of this approach is that conjugation of TLR-7/8a to delivery platforms allows for more precise control over physicochemical properties that include the number, location and orientation of agonists attached to the delivery platform, as well as the rate of release of the agonists from the platform. A limitation of this approach is that it requires chemical modification of the agonist and the delivery platform, which requires additional purification and characterisation steps that increase the labour and material costs in manufacturing these adjuvant systems. Several examples of these strategies are discussed below.

1. ***Covalently modified PLGA-*** While prior studies have used PLGA to encapsulate R848 and R837 through non-covalent interactions, Ilyinski et al recently described the evaluation of a PLGA-based nanoparticle carrier that was used to covalently attach the agonist[124]. While there were no detailed descriptions of the material composition, it is possible that R848 was linked to terminal carboxylic acids of the copolymer chains and is incorporated within the interior of the particles. Incorporation of R848 into the PLGA particles was shown to significantly

decrease serum cytokines while markedly enhancing the magnitude of lymph node cytokine production. Vaccination with PLGA-R848 particles that also incorporate a model protein antigen led to significant increases in CD8 T cell responses, suggesting that the capacity of the PLGA-R848 particles to spatially restrict agonist activity is important for enhancing adaptive CD8 T cell responses.

2. ***Linear polymers-*** Heuking et al recently reported the use of linear polymer chains as scaffolds for the delivery of TLR-7a[125]. In this study, hydroxy-adenine based TLR-7a were attached to a cationic polymer that was complexed with a DNA plasmid. While only limited immunological evaluation was shown, such a strategy may be useful for improving immune responses to gene delivery systems.

3. ***Alum / TLR-7a-*** A recent strategy developed by Novartis is to modify TLR-7a with phosphate groups that allows for their binding to Alum microparticles[126]. The phosphate linker on the TLR-7/8a can link to Alum particles either through ion exchange or through electrostatic interactions. Data in mice shows that TLR-7a linkage to Alum is an effective means for spatially restricting agonist activity to the sites of vaccine administration and draining lymph nodes and that this improved local innate immune activity results in significantly improved antibody and T cell responses to protein antigen.

1.15 Mechanisms accounting for activity of TLR-7/8a formulations

While a number of seemingly disparate formulation and delivery strategies have been developed to improve the activity of TLR-7/8a for use as vaccine adjuvants, several common mechanisms may account for the improved activity that has been observed.

Local retention / persistence of innate immune activation

It is generally presumed that attaching small molecule TLR-7/8a to macromolecular or particulate carriers is an effective means of restricting agonist biodistribution and increasing local retention. Covalent and non-covalent formulations of TLR-7/8a with macromolecular or particulate scaffolds have been shown to significantly increase local cytokine production while reducing serum cytokines, suggesting that the agonist is restricted locally by the carrier[120, 121, 124, 127]. Furthermore, recent studies have shown that PLGA nanoparticles carrying TLR-7/8a leads to increased magnitude and persistence (> 4 days) of lymph node cytokine production that is associated with improved CD8 T cell responses to co-administered protein antigen[124]. It is possible that improved T cell responses to particulate carriers may be due to increased persistence of innate immune activation in draining lymph nodes, which separate studies have shown is important for priming T cell responses[128-131].

Particles promote enhanced uptake by APCs

The capacity of particulate carriers to improve APC uptake has been previously established[22, 132-135] and is likely another mechanism that accounts for the improved activity of macromolecular- and particle-based carriers of TLR-7/8a. Indeed, the potential importance of this mechanism is supported by Kastenmuller's observations that aggregates of protein-TLR-7/8a conjugates, as compared with monomeric conjugates, lead to uptake by a markedly higher proportion of APCs in draining lymph nodes, as well as higher uptake on a per cell basis[108]. Furthermore, Kastenmuller[108] and Vecchi[116] independently showed that particulate, but not monomeric, protein-TLR-7/8a conjugates are immunogenic *in vivo*. Altogether, this

suggests that improved uptake by particles may be critical for the capacity of TLR-7/8a to access endosomally-localized TLR-7 and TLR-8.

Co-delivery / Toll-dependent selection of antigens

By restricting agonist biodistribution and improving uptake by APCs, macromolecular and particle-based carriers may increase the probability that APCs at the injection site or draining lymph nodes internalize both TLR-7/8a and protein antigen. Improved co-delivery has two important functional consequences. First, co-delivery of TLR-7/8a with protein antigen ensures that APCs induce T cell activation rather than tolerance[136, 137]. Secondly, co-delivery of TLRa with protein antigen may lead to improved antigen presentation through what Blander and colleagues refer to as "Toll-dependent selection of microbial antigens."[138-141]. For instance, Blander et al observe that the efficiency of antigen presentation is enhanced when APCs internalize both antigen and TLRa within the same endosomal compartment rather than distinct compartments within the same APC, which suggests that optimal antigen presentation and T cell responses require co-delivery of TLRa with protein antigen.

Improved binding and receptor clustering through multimeric agonist presentation

Multivalent display of ligands on the surfaces of macromolecular or particle-based scaffolds is known to increase avidity of binding to cognate receptors and / or improve receptor clustering[142-144]. Therefore it is possible that delivery of multiple TLR-7/8a on macromolecules or particles may have a similar influence on receptor multimermization that is important for mediating downstream signalling[36, 73]. This hypothesis is supported by the observations that multimeric CpG, CpG-A, but not monomeric CpG, CpG-B, leads to robust signalling through IRF-7 and downstream

production of type-I IFN [145]. Furthermore, while monomeric CpG-B does not induce Type-I IFN, multimermization of CpG-B by attaching a poly-G tail, or by complexing with the cationic particle, DOTAP, leads to IRF-7 dependent type-I IFN production[146, 147], suggesting that multimeric presentation of TLRa may be important for improved TLR binding and / or downstream signalling.

Lymphatic trafficking and uptake by DC populations

A final consideration is how particle size (hydrodynamic radii) of the macromolecular and particulate carriers of TLR-7/8a influences lymphatic drainage and uptake by different APC populations. Earlier work has shown that small particles (< 100 nm) passively traffic to lymph nodes and target subcapsular macrophages and lymph node resident DCs, whereas larger particles (100-1000 nm) require uptake and trafficking to lymph nodes primarily by migratory and monocyte-derived DCs[148-150]. All particulate TLR-7/8a delivery platforms that have been evaluated in vaccine models in animals have used particles that are ~ 200-400 nm in diameter[119, 121, 124], suggesting that migratory and monocyte-derived DCs may be important for the activity of these platforms. However, it is still not clear which sizes of particles may be optimal for eliciting T cell responses[22, 135]. Additional studies will be required to evaluate how the size of the TLR-7/8a carrier influences adaptive immune responses.

1.16 Hypothesis and specific aims

Collectively, prior studies have established that macromolecular and particle-based carriers can be used to improve activity of TLR-7/8a as vaccine adjuvants for protein-based vaccines. However, it is currently unknown how physicochemical parameters of TLR-7/8a delivery platforms directly influence innate immune activation *in vivo,* and how these parameters lead to improved antibody and T cell responses in the context of vaccination with protein antigens.

Approach and principal aims

Using linear biocompatible polymers as scaffolds for the delivery of TLR-7/8a, the principal aims of this thesis are to define the physiochemical parameters of TLR-7/8a delivery that are critical for inducing persistent innate immune activation in tissue draining lymph nodes, and to evaluate whether persistent local (lymph node) innate immune responses are necessary and sufficient for eliciting protective Th1-type CD4 and CD8 T cell responses to protein antigen.

Principal hypotheses

1. Multivalent display of TLR-7/8a on linear biocompatible polymers will lead to increased magnitude and more persistent innate immune responses through higher avidity binding and / or enhanced receptor clustering.
2. Conjugation of TLR-7/8a to linear biocompatible polymers will lead to increased magnitude and persistence of innate immune activation in lymph nodes by restricting agonist biodistribution to the site of injection and draining lymphatics.

3. Persistent local (lymph node) innate immune activation induced by polymer-TLR-7/8a conjugates is necessary and sufficient for eliciting protective T cell responses to co-administered protein antigens.

Specific aims

1. Synthesize Polymer-TLR-7/8a conjugates
2. Use *in vivo* structure-activity relationship studies to define physicochemical parameters of TLR-7/8a delivery that are critical for activity
3. Evaluate the influence of physicochemical properties of TLR-7/8a delivery on pharmacokinetics (whole animal) and APC uptake (lymph nodes)
4. Optimize the magnitude and persistence of lymph node innate immune activation induced by polymer-TLR-7/8a conjugates
5. Evaluate the capacity of lead polymer-TLR-7/8a conjugates to elicit Th1-type CD4 and CD8 T cells that mediate protection following infectious challenge
6. Synthesize and characterize second-generation polymer-TLR-7/8a conjugates that address limitations of first-generation technologies

2 Materials and Methods

2.1 Chemicals

All chemicals were purchased from Sigma-Aldrich (St. Louis, MO) as reagent grade or higher purity, unless stated otherwise. Ethoxyacetic acid was obtained from Alfa Aesar (Ward Hill, MA). Boc-15-amino-4,7,10,13-tetraoxapentadecanoic acid (PEG4) was purchased from EMD Millipore (Darmstadt, Germany). N-Boc-1,4-diaminobutane[151] and 2-Chloro-4,6-dimethoxy-1,3,5-triazine (CDMT)[152] were prepared as previously described. Green fluorescent reactive dyes Alexa Fluor® 488 carboxylic acid tetrafluorophenyl ester and Alexa Fluor® 488 cadaverine were purchased from Life Technologies (Carlsbad, CA). Amine reactive infrared fluorescent reactive dye IRDye® 800CW NHS Ester was purchased from LI-COR (Lincoln, Nebraska). Nucleophilic infrared fluorescent reactive dye, CruzFluor sm™ 8 amine, was purchased from Santa Cruz Biotechnology (Dallas, Texas). Dibenzocyclooctyne (DBCO) modified PEG spacer (DBCO-PEG4-Amine) was purchased from Click Chemistry Tools (Scottsdale, Arizona).

2.2 Synthesis of nucleophilic small molecule TLR-7/8a and negative control ligands

Synthesis of nucleophilic imidazoquinoline-based TLR-7/8a was based on previous reports[66, 69, 153-155] and is described in more detail below.

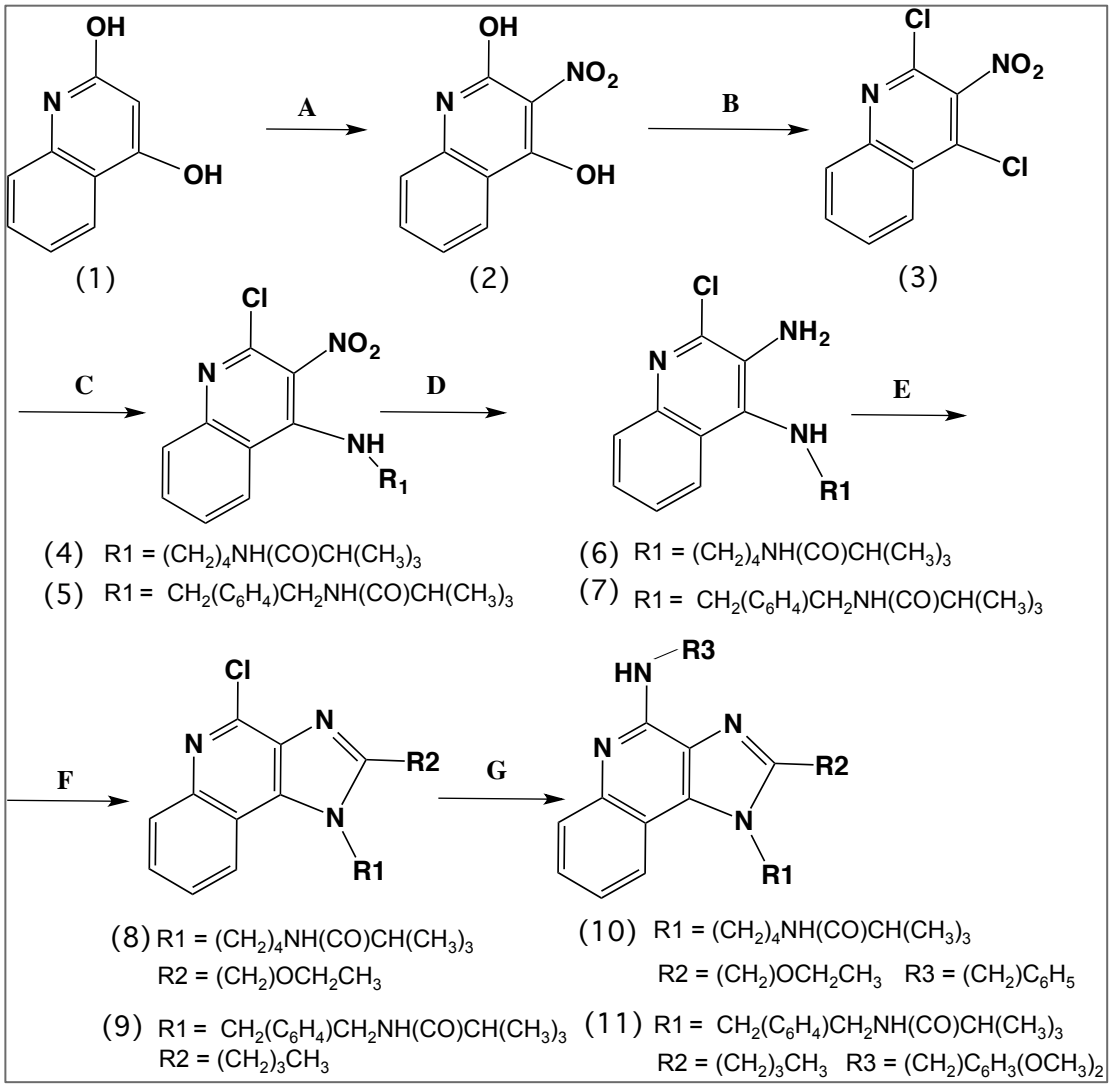

Figure 2.1: Synthesis of nucleophilic imidazoquinoline-based TLR-7/8a: (A) HNO_3, heat; (B) $PhPOCl_2$, heat; (C) NH_2R1, Et_3N, heat; (D) 10% Pt/c, H_2 (g) 55 PSI, Ethyl acetate; (E) R_2COOH, CDMT, NMM, EtOAc; (F) CaOH, heat, MeOH; (G) NH_2R3, Et_3N, MeOH, heat, 150 PSI; (H) H_2SO_4, heat

(1-4) The synthesis of *tert*-butyl (4-((2-chloro-3-nitroquinolin-4-yl)amino)butyl)carbamate was carried out as previously described[153]. ^{1}H NMR (400 MHz, $CDCl_3$) δ 8.11 (d, J = 7.6 Hz, 1H), 7.91 (dd, J = 8.4, 1 Hz, 1H), 7.74 (m, 1H) 7.52 (m, 1H), 6.40 (br s, 1H), 4.66 (br s, 1H), 3.48 (m, 2H), 3.20 (m, 2H), 1.80 (m, 2H), 1.65 (m, 2H), 1.47 (br s, 9H). MS (APCI) calculated for $C_8H_{23}ClN_4O_4$, *m/z,* 394.1, found 394.9 $(M+H)^+$.

(5) The synthesis of *tert*-butyl (4-(((2-chloro-3-nitroquinolin-4-yl)amino)methyl)benzyl) carbamate was carried out as previously described[155]. ^{1}H NMR (400 MHz, DMSO-d6) δ 8.51 (d, J = 8.5 Hz, 1H), 8.46 (t, J = 6.4 Hz, 1H), 7.88 – 7.78 (m, 2H), 7.65 (dd, J = 8.4, 5.5 Hz, 1H), 7.33 (t, J = 6.2 Hz, 1H), 7.17 (q, J = 8.2 Hz, 4H), 4.39 (d, J = 6.2 Hz, 2H), 4.07 (d, J = 6.2 Hz, 2H), 1.36 (s, 9H). MS (APCI) calculated for $C_{22}H_{23}ClN_4O_4$, *m/z,* 442.1, found 464.9 $(M+Na)^+$.

(6) *tert*-butyl (4-((3-amino-2-chloroquinolin-4-yl)amino)butyl)carbamate. A 23 g solution of ***(5)*** and 230 mg of Na_2SO_4 in 200 mL of ethyl acetate was bubbled with Argon for 5 minutes to remove oxygen. To this solution, 230 mg of 10% pt/c was added and the mixture was flushed with argon for an additional 5 minutes and then pressurized with H_2(g) to 55 mm Hg. The reaction mixture was agitated with a mechanical shaker. The reaction was considered complete (~ 3 hours) once the pressure remained constant at a constant volume of H_2(g). The reaction mixture was filtered through celite and evaporated to dryness to obtain yellow oil. Trituration with 1:1 hexanes / ether yielded white crystals that were collected by filtration. Drying overnight under vacuum yielded 20.12 g (94.7 % yield) of spectroscopically pure (>95% at 254 nm) white crystals. ^{1}H NMR (400 MHz, DMSO-d6) δ 8.03 – 7.95 (m,

1H), 7.70 – 7.61 (m, 1H), 7.44 – 7.34 (m, 2H), 6.73 (s, 1H), 5.14 (t, J = 6.7 Hz, 1H), 5.00 (s, 2H), 3.19 (q, J = 7.0 Hz, 2H), 2.87 (q, J = 6.5 Hz, 2H), 1.55 – 1.34 (m, 4H), 1.33 (s, 9H). MS (APCI) calculated for $C_{18}H_{25}ClN_4O_2$, *m/z,* 364.2, found 365.2 $(M+H)^+$.

(7) *tert*-butyl 4-(((3-amino-2-chloroquinolin-4-yl)amino)methyl)benzylcarbamate. The synthetic protocol is the same as for ***(6),*** except 5 g of ***(5)*** was used as the starting material. Product was spectroscopically pure (>95% at 254 nm) following passage through celite. Solvent was removed under vacuum and yielded 4.57 g (93% yield) of white crystals. ^{1}H NMR (400 MHz, DMSO-d6) δ 8.00 – 7.93 (m, 1H), 7.63 (dd, J = 8.0, 1.7 Hz, 1H), 7.35 (tt, J = 6.9, 5.2 Hz, 2H), 7.31 – 7.25 (m, 3H), 7.11 (d, J = 7.9 Hz, 2H), 5.79 (t, J = 7.1 Hz, 1H), 5.04 (s, 2H), 4.40 (d, J = 7.2 Hz, 2H), 4.04 (d, J = 6.2 Hz, 2H), 1.36 (s, 9H). MS (APCI) calculated for $C_{22}H_{25}ClN_4O_2$, *m/z,* 412.2, found 413.2 $(M+H)^+$.

(8) *Tert*-butyl (4-(4-chloro-2-(ethoxymethyl)-1*H*-imidazo[4,5-*c*]quinolin-1-yl)butyl)carbamate. To 2.5 mL of 2-ethoxyacetic acid (0.026 mol, 1.2 eq) in 150 mL of ethyl acetate were added 4.6 g (0.026 mol, 1.2 eq) CDMT, followed by dropwise addition of 6.0 mL (0.055 mol, 2.5 eq) of N-methylmorpholine (NMM). After 5 minutes, 8 g (0.022 mol, 1.0 eq) of ***(6)*** was added and the reaction was refluxed over an oil bath. A white precipitate was obvious after several minutes and corresponds to the NMM.Cl salt. After 16 hours, the reaction mixture was filtered and washed 3x150 mL with 1M HCl. The organic phase was dried with Na_2SO_4, filtered and evaporated to dryness. The resulting crude product was added to 20 mL of methanol with 800 mg (10 % wt/wt) CaO and then microwaved at 100^0 C for 3 h. The CaO was removed by

filtration and the resulting solution was evaporated to dryness to obtain oily product that was purified by flash chromatography using a 0-6% methanol in DCM gradient, yielding 9.44 g of clear oil. Recrystallization from 5:1 Hexane / Ethyl acetate yielded 5.59 g (58.9 % yield) of spectroscopically pure (>95% at 254 nm) white crystals. ^{1}H NMR (400 MHz, DMSO-d6) δ 8.37 – 8.28 (m, 1H), 8.11 – 8.04 (m, 1H), 7.81 – 7.70 (m, 2H), 6.83 – 6.75 (m, 1H), 4.84 (s, 2H), 4.65 (t, J = 7.9 Hz, 2H), 3.62 – 3.52 (m, 2H), 2.96 (q, J = 6.4 Hz, 2H), 1.85 (t, J = 7.9 Hz, 2H), 1.56 (t, J = 7.7 Hz, 2H), 1.30 (s, 9H), 1.20 – 1.12 (m, 3H). MS (APCI) calculated for $C_{22}H_{29}ClN_4O_3$ *m/z* 432.2, found 433.2 $(M+H)^+$.

(9) *Tert*-butyl 4-((2-butyl-4-chloro-1*H*-imidazo[4,5-*c*]quinolin-1-yl)methyl) benzylcarbamate. The synthetic protocol is the same as for ***(8)***, except 2 g of ***(7)*** was used as the starting material and pentanoic acid was used in place of 2-ethoxyacetic acid. Flash purification was not required, but the product was recrystallized from methanol to obtain 1.4 g (58% yield) of spectroscopically pure (>95% at 254 nm) yellow crystals. NMR (400 MHz, DMSO-d6) δ 8.08 (d, J = 8.3 Hz, 1H), 8.02 (d, J = 8.4 Hz, 1H), 7.63 (dd, J = 8.2, 6.8 Hz, 1H), 7.50 (t, J = 7.7 Hz, 1H), 7.30 (t, J = 8 Hz, 1H), 7.15 (d, J = 7.9 Hz, 2H), 7.01 – 6.94 (m, 2H), 5.94 (s, 2H), 4.04 (d, J = 6.2 Hz, 2H), 2.96 (t, J = 7.7 Hz, 2H), 1.73 (q, J = 7.6 Hz, 2H), 1.38 (q, J = 7.4 Hz, 2H), 1.33 (s, 9H), 0.86 (t, J = 7.3 Hz, 3H). MS (APCI) calculated for $C_{27}H_{31}ClN_4O_2$ *m/z* 478.2, found 479.2 $(M+H)^+$.

(10) *Tert*-butyl (4-(4-(benzylamino)-2-(ethoxymethyl)-1*H*-imidazo[4,5-*c*]quinolin-1-yl)butyl)carbamate. 6.5 g of ***(8)*** (0.015 mol, 1 eq) was added to 16 mL of benzylamine (0.15 mol, 10 eq) and reacted for 6 hours at 110 °C in a microwave apparatus. After

completion, the reaction mixture was added to 100 mL of DCM and washed 4x100 mL with 1 M HCl. The resulting yellow oil was recrystallized from 4:1 hexane / ethyl acetate to obtain 7.3g (97.1%) of spectroscopically pure (>95% at 254 nm) white crystals. ^{1}H NMR (400 MHz, DMSO-d6) δ 7.99 (d, J = 8.0 Hz, 1H), 7.66 – 7.55 (m, 2H), 7.41 (d, J = 7.3 Hz, 3H), 7.25 (td, J = 7.5, 5.6 Hz, 3H), 7.20 – 7.12 (m, 1H), 6.80 (t, J = 5.7 Hz, 1H), 4.79 – 4.72 (m, 4H), 4.53 (t, J = 7.8 Hz, 2H), 3.54 (q, J= 7.0 Hz, 2H), 2.95 (q, J = 6.5 Hz, 2H), 1.85 (m, 2H), 1.54 (t, J = 7.7 Hz, 2H), 1.31 (s, 9H), 1.15 (t, J = 7.0 Hz, 3H). MS (APCI) calculated for $C_{29}H_{37}N_5O_3$ *m/z* 503.3, found 504.3 $(M+H)^+$.

(11) *Tert*-butyl 4-((2-butyl-4-((2,4-dimethoxybenzyl)amino)-1*H*-imidazo[4,5-*c*]quinolin-1-yl)methyl)benzylcarbamate. The synthetic protocol was the same as for ***(10)***, except 300 mg of ***(9)*** was used as the starting material and 2,4-dimethoxy benzylamine was used in place of benzylamine. Product was recrystallized rom 3:1 hexane / ethyl acetate to obtain 272 mg (78% yield) of a spectroscopically pure product (>95% at 254 nm). ^{1}H NMR (400 MHz, DMSO-d6) δ 9.64 (s, 1H), 8.16 (s, 1H), 7.91 (s, 1H), 7.60 (t, J = 7.8 Hz, 1H), 7.34 (q, J = 7.1, 6.1 Hz, 2H), 7.18 (d, J = 8.0 Hz, 3H), 7.02 (d, J = 8.0 Hz, 2H), 6.60 (d, J = 2.3 Hz, 1H), 6.49 (dd, J = 8.3, 2.4 Hz, 1H), 5.91 (s, 2H), 4.89 (s, 2H), 4.05 (d, J = 6.2 Hz, 2H), 3.77 (s, 3H), 3.74 (s, 3H), 2.92 (t, J = 7.7 Hz, 2H), 1.75 – 1.66 (m, 2H), 1.37-1.19 (m, 11H), 0.84 (t, J = 7.3Hz, 3H). MS (APCI) calculated for $C_{36}H_{43}N_5O_4$ *m/z* 609.3, found 610.3 $(M+H)^+$.

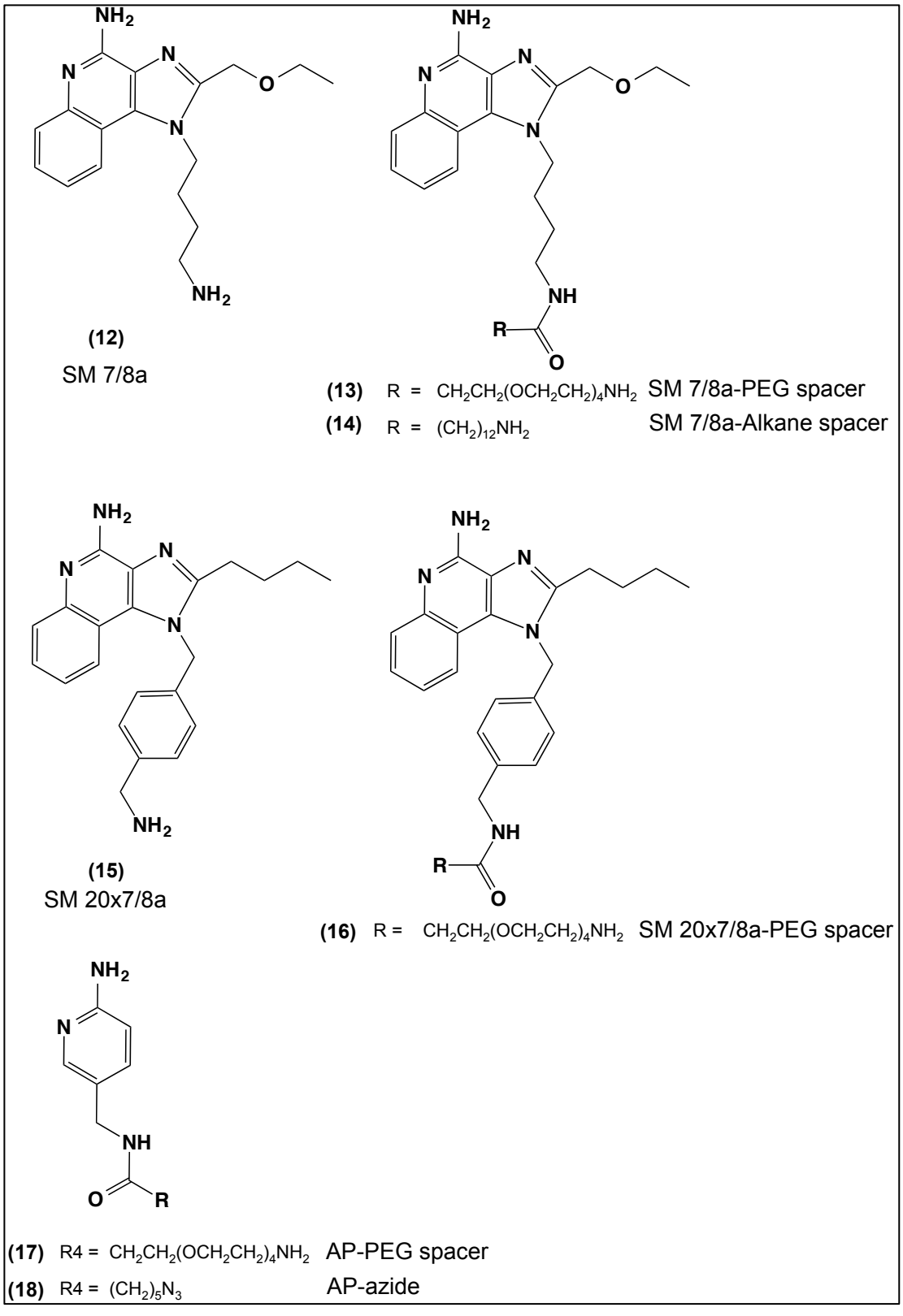

Figure 2.2: Nucleophilic small molecule Toll-like receptor-7/8 agonists (TLR-7/8a) and nucleophilic aromatic heterocyclic base control ligands based on 4-aminopyridine (AP).

(*12*) SM 7/8a, 1-(4-aminobutyl)-2-(ethoxymethyl)-1*H*-imidazo[4,5-*c*]quinolin-4-amine. Simultaneous debenzylation and boc removal was achieved by adding 36 mL of H_2SO_4 to 7.2 g (0.014 mol) of **(*10*)**. The solution turned from slight yellow to cloudy orange over several minutes. Reaction progress was monitored by HPLC. After 3 hours, the reaction mixture was slowly added to 200 mL of DI H_2O and stirred at room temperature for 30 minutes. This mixture was filtered through celite and the resulting clear aqueous solution was adjusted to pH 10 using 10 M NaOH. The aqueous layer was extracted with 6x100 mL DCM. The organic layer was dried with Na_2SO_4 and then evaporated to dryness, yielding 4.03 g (89.6% yield) of a spectroscopically pure (>95% at 254 nm) white powder. ^{1}H NMR (400 MHz, DMSO-d6) δ 8.02 (dd, J = 16.6, 8.2 Hz, 1H), 7.63 – 7.56 (m, 1H), 7.47 – 7.38 (m, 1H), 7.30 – 7.21 (m, 1H), 6.55 (s, 2H), 4.76 (s, 2H), 4.54 (q, J = 6.3, 4.4 Hz, 2H), 3.54 (q, J = 7.0 Hz, 2H), 2.58 (t, J = 6.9Hz, 2H), 1.93-1.81 (m, 2H), 1.52 (m, 2H), 1.15 (t, J = 7.0Hz, 3H). MS (APCI) calculated for $C_{17}H_{23}N_5O$ *m/z* 313.2, found 314.2 $(M+H)^+$.

(*13*) SM 7/8a-PEG, 1-amino-*N*-(4-(4-amino-2-(ethoxymethyl)-1*H*-imidazo[4,5-*c*]quinolin-1-yl)butyl)-3,6,9,12-tetraoxapentadecan-15-amide. To 20 mL of ethyl acetate was added 500 mg (1.6 mmol, 1 eq) of (***12***), 281 mg (1.6 mmol, 1 eq) of CDMT and 643 mg (1.8 mmol, 1.1 eq) of Boc-15-amino-4,7,10,13-tetraoxapentadecanoic acid (PEG4), followed by the dropwise addition of 441 µl (4.0 mmol, 2.5 eq) of NMM, while stirring vigorously. After 16 hours at room temperature, the reaction mixture was filtered and then washed 3x50 mL with 1 M HCl. The organic phase was dried with Na_2SO_4 and then evaporated to dryness. The resulting solid was purified by flash chromatography using a 2-15% methanol / dichloromethane gradient. The resulting clear oil was added to 5 mL of 30%

TFA/DCM and reacted for 1 hour at room temperature. The TFA/DCM was removed by evaporation and the resulting residue was dissolved in 1M HCl and filtered. The filtrate was made alkaline by the addition of 10 M NaOH, followed by extraction with 3x50 mL of DCM. The organic phase was dried with Na_2SO_4 and evaporated to dryness to obtain 455 mg (51% yield) of spectroscopically pure (>95% at 254 nm) clear oil. ^{1}H NMR (400 MHz, DMSO-d6) δ 7.98 (d, J = 8 Hz 1H), (7.83 (t, J = 5.7 Hz, 1H), 7.60 (dd, J = 8.4, 1.3 Hz, 1H), 7.43 (dd, J = 8.4, 6.9 Hz, 1H), 7.25 (t, J = 7.7 Hz, 1H), 6.56 (s, 2H), 4.75 (s, 2H), 4.59 – 4.50 (m, 2H), 4.07 (d, J = 5.8 Hz, 4H), 3.59–3.39 (m, 16 H) 3.09 (q, J = 6.5Hz, 2H), 2.63 (t, J= 5.9Hz, 2H), 2.24 (t, J = 6.5Hz, 2H), 1.83 (m, 2H), 1.56 (t, J = 7.5Hz, 2H), 1.15 (t, J = 7.0Hz, 3H). MS (APCI) calculated for $C_{28}H_{44}N_6O_6$ *m/z* 560.3, found 561.3 $(M+H)^+$.

(*14*) SM 7/8a-Alkane, 12-amino-*N*-(4-(4-amino-2-(ethoxymethyl)-1*H*-imidazo[4,5-*c*]quinolin-1-yl)butyl)dodecanamide. To 20 mL of ethyl acetate was added 200 mg (0.64 mmol, 1 eq) of (***12***), 112 mg (0.64 mmol, 1eq) of CDMT and 222 mg (0.70 mmol, 1.1 eq), of N-boc-aminodecanoic acid followed by the dropwise addition of 176 µl (1.6 mmol, 2.5 eq) of NMM while stirring vigorously. After 16 hours at room temperature, the reaction mixture was filtered and washed 3x50 mL with 1 M HCl. The organic phase was dried with Na_2SO_4 and then evaporated to dryness. The resulting solid was suspended in 5 mL of 30% TFA/DCM and reacted for 1 hour at room temperature. The TFA/DCM was removed by evaporation and the resulting residue was dissolved in 1M HCl and filtered. The filtrate was made alkaline by the addition of 10 M NaOH, followed by extraction with 3x50 mL of DCM. The organic phase was then dried with Na_2SO_4 and evaporated to dryness to obtain 279 mg (85.4% yield) of spectroscopically pure (>95% at 254 nm) white solid. ^{1}H NMR (400

MHz, DMSO-d6) δ 7.98 (d, J = 8.1 Hz, 1H), 7.74 (t, J = 5.7 Hz, 1H), 7.60 (d, 8 Hz, 1H), 7.42 (t, J = 7.6 Hz, 1H), 7.24 (t, J = 7.5 Hz, 1H), 6.56 (s, 2H), 4.75 (s, 2H), 4.53 (t, J = 7.9 Hz, 2H), 3.54 (q, J = 7.0 Hz, 2H), 3.07 (q, J = 6.4Hz, 2H), 2.60 (t, J = 7.1Hz, 2H), 1.97 (t, J = 7.4Hz, 2H), 1.87–1.78 (m, 2H), 1.55 (t, J = 7.6 Hz, 2H), 1.43–1.34 (m, 5H), 1.24–1.10 (m, 18H). MS (APCI) calculated for $C_{29}H_{46}N_6O_2$ *m/z* 510.4, found 511.4 $(M+H)^+$.

(*15*) SM 20x7/8a, 1-(4-(aminomethyl)benzyl)-2-butyl-1*H*-imidazo[4,5-*c*]quinolin-4-amine. Deprotection of (***11***) required milder conditions as compared with (***12***) so as to avoid removal of the xylene diamine linker. Simultaneous removal of the 2,4-dimethoxybenzyl and Boc groups was achieved by adding 300 mg of (***11***) to a 30 mL solution of 40% TFA/DCM that was stirred at room temperature for 30 h. Reaction progress was monitored by HPLC. After completion, the reaction mixture was evaporated to dryness and the resulting yellow solid was suspended in 200 mL of 1 M HCl. Insoluble material was removed by filtration and the resulting clear aqueous solution was adjusted to pH 10 using 10 M NaOH. The Aqueous layer was extracted 6x100 mL using DCM as the organic phase. The organic layer was dried with Na_2SO_4 and evaporated to dryness, yielding 172 mg (89.6% yield) of a spectroscopically pure (>95% at 254 nm) white powder. ^{1}H NMR (400 MHz, DMSO-d6) δ 7.77 (dd, J = 8.4, 1.4 Hz, 1H), 7.55 (dd, J = 8.4, 1.2 Hz, 1H), 7.35 – 7.28 (m, 1H), 7.25 (d, J = 7.9 Hz, 2H), 7.06 – 6.98 (m, 1H), 6.94 (d, J = 7.9 Hz, 2H), 6.50 (s, 2H), 5.81 (s, 2H), 3.64 (s, 2H), 2.92–2.84 (m, 2H), 2.15 (s, 2H), 1.71 (q, J = 7.5Hz, 2H), 1.36 (q, J = 7.4Hz, 2H), 0.85 (t, J = 7.4 Hz, 3H). MS (APCI) calculated for $C_{22}H_{25}N_5$ *m/z* 359.2, found 360.3 $(M+H)^+$.

(*16*) SM 20x7/8a-PEG, 1-(4-(aminomethyl)benzyl)-2-butyl-1*H*-imidazo[4,5-*c*]quinolin-4-amine. The same reaction conditions and purification scheme were used as for the preparation of **(*13*)**, except 100 mg of (***15***) was used in place of (***12***). 126.2 mg (96% yield) of spectroscopically pure (>95% at 254 nm) clear oil was obtained. ^{1}H NMR (400 MHz, DMSO-d6) δ 8.31 (t, J = 6.0 Hz, 1H), 7.93 (d, J = 8.4 Hz, 1H), 7.78 (d, J = 8.3 Hz, 1H), 7.71 (s, 4H), 7.61 (t, J = 7.8 Hz, 1H), 7.35 (t, J = 7.8 Hz, 1H), 7.18 (d, J = 8.0 Hz, 2H), 7.00 (d, J = 8.0 Hz, 2H), 5.92 (s, 2H), 4.20 (d, J = 5.9 Hz, 2H), 3.62–3.44 (m, 16H), 3.00–2.90 (m, 4H), 2.33 (t, J = 6.4 Hz, 2H), 1.75—1.67 (m, 2H), 1.37 (q, J = 7.4 Hz, 2H), 0.85 (t, J = 7.3 Hz, 3H). MS (APCI) calculated for $C_{33}H_{46}N_6O_5$ *m/z* 606.4, found 607.3 $(M+H)^+$.

(*17*) AP-PEG, 1-amino-*N*-((6-aminopyridin-3-yl)methyl)-3,6,9,12-tetraoxapentadecan-15-amide. The same reaction conditions and purification scheme were used as for the preparation of (***13***), except 50 mg of *tert*-Butyl 5-(aminomethyl)-2-pyridinylcarbamate was used in place of (***12***). 73 mg (88% yield) of spectroscopically pure (>95% at 254 nm) clear oil was obtained. ^{1}H NMR (400 MHz, DMSO-d6) δ 8.32 (t, J = 5.9 Hz, 1H), 7.76 (d, J = 2.1 Hz, 1H), 7.66 (dd, J = 9.0, 2.2 Hz, 1H), 7.51 (s, 2H), 6.81 (d, J = 9.0 Hz, 1H), 4.10 (d, J = 5.8 Hz, 2H), 3.67 – 3.37 (m, 16H), 2.96 (s, 2H), 2.53 (p, J = 1.9 Hz, 1H), 2.43 (p, J = 1.9 Hz, 1H), 2.33 (t, J = 6.4 Hz, 2H). MS (APCI) calculated for $C_{17}H_{30}N_4O_5$ *m/z* 370.2, found 371.2 $(M+H)^+$.

(*18*) AP-azide, *N*-((6-aminopyridin-3-yl)methyl)-5-azidopentanamide. The same reaction conditions and purification scheme were used as for the preparation of (***13***), except 50 mg of *tert*-Butyl 5-(aminomethyl)-2-pyridinylcarbamate was used in place of (***12***). 21.4 mg (39% yield) of spectroscopically pure (>95% at 254 nm) clear oil

was obtained. ^{1}H NMR (400 MHz, DMSO-d6) δ 8.25 (t, J = 5.7 Hz, 1H), 7.75 (d, J = 2.2 Hz, 1H), 7.65 – 7.57 (m, 1H), 7.22 (s, 2H), 6.75 (d, J = 8.9 Hz, 1H), 4.07 (d, J = 5.8 Hz, 2H), 3.34 (s, 2H), 3.24 (s, 2H), 2.53 (p, J = 2.0 Hz, 1H), 2.43 (p, J = 1.9 Hz, 1H), 2.11 (t, J = 7.0 Hz, 2H), 1.50 (m, 4H). ^{1}H NMR (400 MHz, DMSO-d6) δ 8.25 (t, J = 5.7 Hz, 1H), 7.75 (d, J = 2.2 Hz, 1H), 7.65 – 7.57 (m, 1H), 7.22 (s, 2H), 6.75 (d, J = 8.9 Hz, 1H), 4.07 (d, J = 5.8 Hz, 2H), 2.43 (m, 2H), 2.11 (t, J = 7.0 Hz, 2H), 1.50 (m, 4H). MS (APCI) calculated for $C_{11}H_{16}N_6O$ *m/z* 248.1, found 249.1 $(M+H)^+$.

2.3 Synthesis of SM TLR-7/8a dye conjugates

(*19*) SM 7/8a-AF488.

The AF488 dye conjugate of the small molecule TLR-7/8a was synthesized by reacting 2 mg (2.3 μmoles, 1 eq) of Alexa Fluor® 488 carboxylic acid tetrafluorophenyl ester with 0.85 mg (2.7 μmoles, 1.2 eq) of (***12***) in 300 uL of anhydrous DMSO. The reaction was monitored by HPLC and the product, (***19***), was purified by semi-prep HPLC using a 25% to 35% ACN/H_2O gradient over 16 minutes. The reaction mixture was injected over 3 runs. Fractions containing (***19***) were consolidated, frozen and lyophilized to yield 1.6 mg (85.5% yield) of spectroscopically pure (>95% at 254 nm) product. MS (ESI) calculated for $C_{38}H_{33}N_7O_{11}S_2$ *m/z* 827.2, found 827.7 $(M+H)^+$.

(*20*) SM 7/8a-IRDye800

For the IR Dye conjugate of the SM 7/8a, a PEG spacer was required to increase solubility. The same reaction conditions and purification scheme were used as for the preparation of (***19***), except 4 mg (3.4 μmoles, 1 eq) of IR Dye 800cw NHS ester was used as the dye and reacted with 2.3 mg (4.1 μmoles, 1 eq) of (***13***). 3.8 mg (71%

yield) of spectroscopically pure (>95% at 254 nm) product was obtained. MS (ESI) calculated for $C_{74}H_{96}N_8O_{20}S_4$ *m/z* 1546, found 1547 $(M+H)^+$.

2.4 Synthesis of amine-reactive copolymers

HPMA-based copolymers

The amine reactive HPMA-based statistical copolymer, **p[(HPMA)-*co*-(Ma-ε-Ahx-TT)**, was synthesized by free radical solution polymerization as previously described[156]. Briefly, a mixture of HPMA (9.8 wt%), Ma-ε-Ahx-TT (5.2 wt%) and AIBN (1.5 wt%) was dissolved in DMSO (83.5 wt%) and polymerized at 60°C for 6 h under argon atmosphere. Polymer was isolated by precipitation into a 1:1 mixture of acetone and diethyl ether and purified by re-precipitation from methanol solution into a 3:1 mixture of acetone and diethyl ether. The content of TT reactive groups determined by UV-Vis spectrophotometry was 14.8 mol% (ε_{305} =10,300 L/mol); the weight- and number-average molecular weights determined by SEC were M_w = 31,850 g/mol and M_n = 20,330 g/mol, respectively.

NIPAM-based (thermo-responsive) copolymers

The amine reactive NIPAM-based (thermoresponsive) statistical copolymer **p[(NIPAM)-*co*-(Ma-Ahx-TT)]** was prepared by free radical solution polymerization as described elsewhere[157]. Briefly, a mixture of NIPAM (10.2 wt%), Ma-ε-Ahx-TT (4.8 wt%) and AIBN (1.5 wt%) was dissolved in DMSO (83.5 wt%) and polymerized at 60°C for 18 h under argon atmosphere. The reaction mixture was diluted with an HCl aqueous solution (pH 2) and the reaction mixture was extracted to dichloromethane (3x). The combined organic phases were dried over anhydrous $MgSO_4$, filtered and evaporated. The residue was dissolved in methanol and

precipitated into a 3:1 mixture of acetone and diethyl ether. The content of TT reactive groups determined by UV-Vis spectrophotometry was 10.2 mol% (ε_{305} =10,300 L/mol); the weight- and number-average molecular weights determined by SEC were M_w = 26,830 g/mol and M_n = 17,650 g/mol, respectively.

2.5 Synthesis of polymer-TLR-7/8a (Poly-7/8a) conjugates

p[(HPMA)-co-(Ma-ε-Ahx-7/8a)] and p[(NIPAM)-co-(Ma-Ahx-7/8a)]

Poly-7/8a were synthesized in a combinatorial approach by reacting varying amounts of nucleophilic TLR-7/8a (compounds 12, 13, 14, 15 or 16) with amine reactive copolymers in anhydrous methanol while stirring vigorously for 16 h at room temperature. For dye-conjugated polymers, nucleophilic dyes (Alexa Fluorophore 488 Cadaverine or Cruz Fluor 8 amine) were added and reacted with the amine reactive copolymers for 2 h prior to the addition of the nucleophilic TLR-7/8a. Unreacted TT groups were removed by adding excess 1-amino-2-propanol. Reaction mixtures were purified by dialysis or gel permeation chromatography to yield solutions of polymer that were evaporated to dryness and characterized as described below.

Example: To generate p[(HPMA)-*co*-(Ma-ε-Ahx-PEG4-7/8a)] with an agonist density of ~ 10 mol% TLR-7/8a, 10 mg (8.4 μmole TT, 1 eq) of amine reactive copolymer p[(HPMA)-*co*-(Ma-ε-Ahx-TT)] with ~ 14 mol% TT was added to 1 mL of anhydrous methanol. To this solution, 4.7 mg (6.0 μmole, 0.7 eq) of ***(13)*** (SM 7/8-PEG4) in a solution of anhydrous DMSO at 10 mg/mL was added slowly to the polymer solution while stirring vigorously. After 16h, 1.25 mg (16.8 μmole, 2 eq) of 1-amino-2-propanol was added to remove unreacted TT groups. After an additional 2 hours, the reaction mixture was dialyzed against methanol using Spectra/Por7

Standard Regenerated Cellulose dialysis tubing with a molecular weight cut-off (MWCO) of 25 kDa purchased from Spectrum Labs (Rancho Dominguez, CA). The dialysis tube was suspended in 1000 mL of methanol and the dialysis buffer was changed twice each day for 3 days to ensure efficient removal of unreacted small molecules. The methanol solution containing Poly-7/8a was evaporated to dryness and yielded 11.4 mg of p[(HPMA)-*co*-(Ma-ε-Ahx-PEG4-7/8a)] that was suspended in 1140 μL of anhydrous DMSO for storage. Determination of the amount of TLR-7/8a attached, molecular weight and particle size in aqueous solution were determined as described below. For this example, a 0.3 mg/mL 1% triethylamine / methanol solution of this Poly-7/8a measured an average absorption at 325 nm of 0.64 (TLR-7/8a content; ε_{325} =5,012 L/mol), corresponding to 0.42 μmole of TLR-7/8a/mg of polymer, or ~ 8.14 mol% Ma-ε-Ahx-PEG4-7/8a.

2.6 Instrumentation for synthesis, purification and chemical characterisation

Microwave irradiation was carried out in a CEM Discover Synthesizer with 150 watts max power. Flash column chromatography was performed on a Biotage SP4 Flash Purification system (Uppsala Sweden) using Biotage® SNAP Cartridges and SNAP Samplet Cartridges with KP-Silica 60 mm. Analytical HPLC analyses were performed on an Agilent 1200 Series instrument equipped with multi-wavelength detectors using a Zorbax Stable Bond C-18 column (4.6 x 50 mm, 3.5 mm) with a flow rate of 0.5 mL/min or 1.0 mL/min. Solvent A was 0.05% trifluoroacetic acid (TFA) in water (H_2O), solvent B was 0.05% TFA in acetonitrile (ACN), and a linear gradient of 5% B to 95% B over 10 minutes was used. ESI or APCI mass spectrometry (MS) were performed on an LC/MSD TrapXCl Agilent Technologies

instrument or on a 6130 Quadrupole LC/MS Agilent Technologies instrument equipped with a diode array detector. ^{1}H NMR spectra were recorded on a Varian spectrometer operating at 400 MHz. Ultraviolet-Visible (UV-Vis) light spectroscopy was performed on a Lambda25 UV/Vis system from PerkinElmer (Waltham, MA) and fluorescence spectroscopy was carried out on a PerkinElmer brand Fluorescence Spectrometer, model LS 55.

2.7 Determination of polymer molecular weights

Molecular weights and polydispersities of polymers and copolymers were measured by gel permeation chromatography using an HPLC system (Shimadzu, Japan) equipped with refractive index (RI), UV and multiangle light scattering (MALS) DAWN 8 EOS detectors (Wyatt Technology, USA). Either a Superose 6 column (GE Healthcare, USA was used with a 0.3 M acetate buffer (pH 6.5) eluent at 0.5 mL min^{-1}, or a MicroSuperose 6 column was used with PBS (pH 7.4) as the eluent at 0.1 mL min^{-1}. Weight-average molecular weights (M_w) were calculated from the light-scattering detector based on the known injected mass while assuming 100% mass recovery. Number-average molecular weights (M_n) were determined by refractive index measurements and were calculated assuming a dn/dc value of 0.167 mL/g. Polydispersity is defined as (M_w/M_n).

2.8 Determination of the amount and density of TLR-7/8a attached to polymer carriers

The amount of ligand attached to the copolymers was determined by UV-Vis spectroscopy using the Beer-Lambert law relationship ($A = \varepsilon * c$; where A = absorption and c = mol/L). Samples were suspended in solutions of 1% triethylamine

/ methanol at known densities (mg/mL) and added to quartz cuvettes with a path length of 1 cm. Absorption was recorded over a spectrum from 250 – 775 nm using a Lambda25 UV-Vis spectrometer from Perkin Elmer. For example, a 0.1 mg/mL solution of Poly-7/8a in 1% triethylamine/methanol (λ_{max} = 325 nm, ε_{325} = 5012 L/mol) has an optical density (OD, arbitrary units) of 0.25 at 325 nm. The concentration of TLR-7/8 can be calculated by solving for c in the Beer-Lambert law relationship and is 5e-5 mol/L, which can be expressed as the amount of TLR-7/8a per mass of copolymer (5e-4 mmol/mg).

The Beer-Lambert relationship was used to determine the amount of ligand and dye molecules attached to the polymers using known extinction coefficients (Table 2.1).

Ligand	Max absorption (λ_{max}, nm)	Extinction coefficient, (L/mol) 1% triethylamine / methanol	A_{325} / A_{max}
Aminopyridine	305	3,511	---
TLR-7/8a (SM 7/8a)	325	5,012	1.00
AF488	495	167,415	0.12
Cruz Fluor 8	775	71,493	0.09

Table 2.1: Absorption maxima and extinction coefficients were determined for different ligand and dye molecules in 1% triethylamine/methanol. Note, for copolymers with both TLR-7/8a and dye (AF488 or Cruz Fluor 8), the contribution of absorption at 325 nm by the dye was determined using the relationships described in the above table.

Agonist density (mol% TLR-7/8a) determination

UV-Vis can be used to estimate the agonist density (mol%) of co-monomers. Mol% of co-monomer y, for a statistical copolymer comprised of monomers x and y is estimated using the following relationship: $mol\%_y = \left(\frac{1}{1+(\frac{\rho \times \varepsilon}{A \times Mw_x} - \frac{Mw_y}{Mwx})}\right) * 100$

mol%$_y$ (TLR-7/8a density) = percentage of copolymer that is y (e.g., TLR-7/8a containing monomer), for copolymer comprised of x and y monomers

ρ = volumetric mass density (mg/mL) of copolymer during UV-Vis measurement

ε = molar extinction coefficient for monomer y (e.g. TLR-7/8a = 5,012)

A = Absorbance

Mw$_x$ = molecular weight (g/mol) of majority monomer

Mw$_y$ = molecular weight (g/mol) of minority monomer

Example calculation:

For poly-7/8a comprised of the majority monomer HPMA (Mw_{HPMA} = 143.2) and minority monomer containing the TLR-7/8a (MA-Ahx-PEG4-7/8a; $Mw_{MA\text{-}PEG47/8a}$ = 741.9) that is suspended in methanol at 0.1 mg/mL and measures an average absorbance of 0.25 at 325 nm, the mol% of the minority unit, MA-PEG4-7/8a is:

$$mol\%_{MA-Ahx-PEG4-7/8a} = \left(\frac{1}{1+(\frac{0.1 \times 5012}{0.25 \times 143.2} - \frac{741.9}{143.2})}\right) * 100 = 10.2\%$$

2.9 Particle size and morphology characterisation

Particle size determination by dynamic light scattering

Z-average diameter (nm) of copolymers in PBS (pH 7.4) was determined by dynamic light scattering using a Zetasizer Nano ZS purchased from Malvern (Malvern Instruments, Malvern, United Kingdom).

Cryo-EM sample preparation and imaging

Vitrified specimens were prepared by first treating CF150 continuous carbon grids (Protochips, Raleigh, NC, USA) for 8 sec in a Gatan Solarus plasma cleaner (Gatan, Pleasanton, CA, USA) and then adding 3 μL of copolymers in PBS pH 7.4 to the grid before blotting and plunge freezing in an Vitrobot Mk VI (FEI Company, Hillsboro, OR, USA). Frozen grids were loaded in a Tecnai G2 Polara transmission electron microscope (FEI Company, Hillsboro, OR, USA) operated at 200 kV and equipped with an energy filter and 2K × 2K postenergy filter CCD (Gatan, Pleasanton, CA, USA). The specimens were maintained at approximately -182 °C in the microscope, and were imaged at 9,300× magnification (14 Â pixel size).

2.10 Transition temperature determination for thermo-responsive polymers

Thermo-responsive polymers were suspended in 0.1 mg/mL PBS (pH 7.4) and 200 μL volumes of each solution of polymer were added in triplicate to Costar polystyrene 96 well flat bottom culture plates obtained from Corning (Corning, NY). Absorption of the solutions as a function of temperature was evaluated on a SpectraMax Plus spectrophotometer (Molecular Devices). Absorption was measured at 490 nm and

temperature was increased at 1°C/5 min steps. Absorption increases with particle formation due to Rayleigh scattering. The data was analysed using PRISM and non-linear regression fit was used to calculate transition temperature (~ temperature at ½ max absorbance).

2.11 Evaluation of TLR-7/8a activity in vitro

Evaluation of TLR-7 activity in vitro using HEK293 reporter cells

HEK293 cells expressing human TLR-7 (HEK-TLR7) were purchased from Invivogen (San Diego, CA) and used according to the manufacturer's guidelines. Briefly, cells were cultured in DMEM supplemented with 4.5 g/l glucose, 10% (v/v) fetal calf serum, 50 U/ml penicillin, 50 µg/ml streptomycin, 100 µg/ml Normocin and 2 mM L-glutamine. Antibiotics were used according to manufacturer's protocol to select for HEK293 that were transfected with a plasmid expressing antibiotic resistance genes, as well as TLR-7 and a reporter enzyme, secreted embryonic alkaline phosphatase (SEAP). To screen compounds for TLR-7 activity, 40,000 HEK-TLR7 cells were added to each well of 96-well flat bottom plates and incubated with adjuvants or controls for 20 hours. After this time, 20 µl of supernatant from each well was removed and added to flat bottom plates containing 180 µl of QUANTI-Blue solution (Invivogen), a proprietary substrate that is converted by Secreted Embryonic Alkalkine Phopshatase. Conversion of the substrate was read on a UV-Vis spectrophotometer at 620 nm and is proportional to TLR-7 signalling.

Cytokine production by human PBMCs

Human whole blood-leukoreduction filters (white blood cell cones) were obtained from the National Health Service Blood and Transplant Division (NHSBT, Oxford, UK), and hPBMCs were isolated as previously described[158, 159]. Briefly, PBMCs were isolated by density gradient separation using ficoll-paque PLUS (GE Healthcare, Pittsburgh, PA) according to manufacturer's guidelines. PBMCs were enumerated and suspended in RPMI supplemented with 10% (v/v) fetal calf serum, 50 U/ml penicillin, 50 μg/ml streptomycin and 2 mM L-glutamine. PBMCs were seeded at a final concentration of $5x10^5$ cells/well in 96 well plates. Cells were then incubated with either adjuvant or controls. After 20 hours, supernatant was removed and evaluated for the presence of cytokines by ELISA or cytokine bead array.

2.12 Animals

BALB/c mice, C57BL/6 (B6) mice, and B6N.129S2-Casp1tm1Flv/J (Caspase 1/11 (Inflammasome) KO) mice were obtained from the Jackson Laboratory and maintained in the Vaccine Research Center's Animal Care Facility under pathogen-free conditions. TLR7 KO mice were generously provided by Ross Kedl at the University of Colorado, Denver, Colorado, USA) and were bred and maintained at the Vaccine Research Center (Bethesda, MD, USA).

2.13 Animal use ethics statement

All animal experiments were conducted at the National Institutes of Health (Bethesda, MD, USA) and were in compliance with the guidelines set by the Association for the Assessment and Accreditation of Laboratory Animal Care International (AAALAC), as well as by the Institutional Animal Care and Use Committee (ACUC). All

experimental animal protocols underwent review and were approved by the Vaccine Research Center ACUC prior to the start of experiments. Efforts were made to refine experiments and to find alternative, *in vitro,* model systems as a means of reducing the number of animals used in this thesis.

2.14 *Ex vivo* lymph node cultures for cytokine determination

Following subcutaneous footpad administration of different adjuvants or controls in 50 μL PBS (pH 7.4), proximal draining lymph nodes (popliteal lymph nodes) were harvested at serial timepoints as described in the figure legends. Lymph nodes were placed in 300 μL of RPMI supplemented with 10% (v/v) fetal calf serum, 50 U/ml penicillin, 50 μg/ml streptomycin and 2 mM L-glutamine in 1.5 mL DNase, RNase, Pyrogen free Kontes Pellet Pestle Grinders (Kimble-Chase, Vineland, NJ) sitting on ice. Lymph nodes were gently mechanically disrupted using sterile pestles. The resulting lymph node cell suspensions were vortexed for 5 seconds and added to a 96 well round bottom culture plate that was incubated at 37°C, 5% CO_2 for 8h. After the incubation was complete, samples were spun down to pellet cells and debris and the supernatant was collected and stored at - 80°C until analysed by ELISA or cytokine bead array.

2.15 Cytokine measurements by ELISA

ELISA kits for either murine or human IL-12p40, IP-10 and IFNγ were purchased from Peprotech (Rocky Hill, NJ) and used for the determination of cytokines in the supernatant of hPBMC or lymph node cell suspension cultures (see above). Preparation and development of ELISA plates was carried out according to the guidelines recommended by the manufacturer. Briefly, supernatants were diluted in

ELISA diluent (0.1% FBS / PBS) and added to Nunc-Immuno 96 Microwell plates (Nunc A/S, Roskilde, Denmark) coated with capture antibodies. ELISA plates were developed according to manufacture recommendations and ABTS (2′-Azino-bis (3-ethylbenzthiozoline-6-sulfonic acid)) was used as a substrate for peroxidase conjugated secondary antibodies. Absorption was evaluated at 405 nm using a SpectraMax Plus plate reader (Molecular Devices). Concentrations of cytokines in the supernatant were determined using a fit from a standard curve. Concentrations of murine IFNα in the supernatant of the lymph node cell suspensions was evaluated in a similar fashion using VeriKine™ Mouse IFN Alpha ELISA Kit purchased from PBL Assay Science (Piscataway, NJ).

2.16 Cytokine measurements by bead array / multiplex

Cytokine bead array was used to determine the concentration of 12 or more cytokines in 25 μL aliquots of lymph node culture supernatant as described in the figure legends. Customized mouse cytokine / chemokine magnetic bead panels were purchased from EMD Millipore (Billerica, MA). Plates were developed according to the guidelines recommended by the manufacturer. Briefly, culture supernatants were incubated overnight with a mixture of different magnetic beads each specific for a unique cytokine. After washing, Biotin-conjugated detection antibodies were added, followed by the addition of PE-conjugated streptavidin for visualization. Samples were washed and then run on a Luminex (Austin, Texas) FLEX MAP3D multiplex system according to the manufacturer's guidelines. Concentrations of individual cytokines in the supernatants were determined from standard curves.

2.17 Whole animal imaging (biodistribution and kinetics)

Biodistribution and kinetics of IR Dye-labelled polymers or small molecule controls were evaluated on a Bruker (Billerica, MA) In Vivo Xtreme combined optical and x-ray small animal imaging system. Briefly, IR Dye-labelled polymers or small molecule controls in 50 μL of PBS were administered subcutaneously in the left rear footpad of BALB/c mice. Mice were imaged at serial timepoints thereafter using an imaging protocol comprised of 2 steps: In the first step, mice were illuminated by epifluorescence (excitation = 760 nm; emission = 830 nm; 0.915 second exposure). In the second step, X-ray (45 kVp) with 1.0-second exposure was applied to visualize anatomical landmarks. For biodistribution studies, doses were normalized for irradiance as well as TLR-7/8a dose to directly compare images. For kinetics experiments, polymers and small molecules were normalized for TLR-7/8a dose. Amount of TLR-7/8a (nmoles) within a region of interest (ROI) was calculated using standard curves (log(photons mm-2 seconds-1) versus TLR-7/8a amount (nmoles)) that were determined for each IR dye-labelled polymer or small molecule. Using this method, the amount of TLR-7/8a (nmoles) within draining lymph nodes was evaluated both in live animals, as well as in *ex vivo* lymph node suspensions.

2.18 Flow cytometry analysis of innate immune cells from lymph nodes and spleen

The magnitude, activation status and adjuvant uptake of innate immune cells in draining lymph nodes and spleen were evaluated following subcutaneous administration of adjuvants or controls delivered in 50 μL PBS (pH 7.4) into both hind footpads of C57BL/6 mice. Popliteal lymph nodes from both hind legs were

harvested and added to pestle tubes, as described above. Following mechanical disruption, lymph node cell suspensions were spun down, supernatant was removed and cell suspensions were re-suspended in 1 mL of an enzyme cocktail comprised of 1 mg/ml collagenase D (Roche, Basel, Switzerland) and 100 U/mL recombinant DNase I (Roche) in RPMI for 30 minutes at 37°C. Lymph nodes cells were then washed and resuspended in PBS and added to 96 well plates for staining. To isolate splenocytes, 5 mL of enzyme cocktail was injected directly into spleens that were then incubated at 37°C for 30 minutes. Spleens were mechanically disrupted over 70 μm nylon strainers (Corning) and collected in 50 mL Falcon tubes (Corning). Splenocytes were washed with HBSS and resuspended in 2 mL of ACK lysing buffer (Life Technologies) and incubated for 4 minutes at room temperature. After red blood cell lysis, the splenocytes were washed with PBS, passed through 70 μm nylon strainers and transferred to 96 well plates for staining. Cells were stained with LIVE/DEAD cell stain (Aqua, Life Technologies) for 10 minutes at room temperature. Without washing, cells were stained for 15 minutes with FcR-Block, anti-CD16/CD32 (clone 2.4G2, BD). Without washing, cells were then stained for 20 minutes with Brilliant Violet (BV)510-anti-CD3e (145-2C11), BV421-anti-CD19 (1D3), BV605-anti-Ly-6G (1A8), BV786-anti-CD8 (53-6.7), BV510-anti-NK-1.1 (PK136), Cy7-PE-anti-B220 (RA3-6B2), PE-anti-CD11c (HL3), Ax700-anti-CD11b (M1/70, BioLegend), Cy7-APC-anti-Ly-6C (AL-21), APC-anti-CD86 (GL1, eBiosciences), Cy5-PE-anti-F4/80 (BM8, eBiosciences), and CF594-PE-anti-CD80 (16-10A1). Except where noted, antibodies were purchased from BD Biosciences. Using this same procedure, APC uptake of Alexa Fluor 647-labeled ovalbumin (Life Technologies) was evaluated where noted in the results section of this thesis. Flow

cytometry data were acquired using a modified BD LSR II and analysed using FlowJo software (Tree Star).

2.19 Tetramer staining of CD8 T cells from whole blood

Tetramer+ CD8 T cells were characterized from whole blood as previously described. Briefly, whole blood was collected from immunized mice in heparinized 1.5 mL polypropylene tubes at various time points described in figure legends. Red blood cells were lysed by adding 1.0 mL of ACK Lysing buffer (Life Technologies, Frederick, MD) to each tube and incubating the resulting suspension for 4 minutes at room temperature. Cell suspensions were spun down at 600 rcf and supernatant was removed by vacuum. Cells were resuspended in 250 μL of PBS and added to 96 well plates for staining. Cells were washed with PBS and then stained with the viability dye LIVE/DEAD Fixable Orange (OrViD, Life Technologies) for 10 minutes at room temperature. After washing, cells were stained for 15 minutes with either PE-H2-Kb OVA (SIINFEKL) tetramer (Beckman Coulter, Brea, California) or PE –H2-Db SIV Gag (AAVKNWMTQTL) tetramer. Fc-Block, anti-CD16/CD32 (clone 2.4G2, BD, Franklin Lakes New Jersey), was added for 10 minutes and then stained with the following surface antibodies, APC-Cy7-anti-CD8 (53-6.7, Biolegend, San Diego, California) PE-Cy7-anti-CD62L (MEL-14, AbCam, Cambridge, England), eFluor-660-anti-CD127 (A7R34, ebioscience, San Diego, California) and FITC-anti-KLRG1 (clone 2F1, Southern Biotech, Birmingham, Alabama) which were incubated with the cells for 15 minutes at room temperature. Cells were then fixed and permeabilized using Fix / Perm solution (BD) and incubated at 4°C for 20 minutes. Cells were washed and then suspended in perm wash buffer containing PerCP-Cy5.5-anti-CD3

(clone 145-2C11, BD) and were incubated at 4C for 30 minutes. Cells were washed with perm wash buffer and then analysed by flow cytometry.

2.20 Analysis of polyfunctional CD4 T cell responses

Evaluation of antigen-specific CD4 T cell responses was determined as previously described[44, 45]. Briefly, splenocytes were isolated from vaccinated mice at several timepoints and 1.5×10^6 splenocytes were cultured in 96-well plates with 2 μg/ml α-CD28 (37.51) alone (background response), or in combination with 20 μg/ml MML protein (Leish-111f, derived from Leishmania spp.) or 2 μg/ml (each) MML peptides (Mimotopes Pty Ltd; 15-mers overlapping by 11) for 2 h before addition of 10 μg/ml brefeldin A (BFA; Sigma-Aldrich) for an additional 4 h. After washing with PBS, cells were stained with Violet Dead Cell Stain (ViViD, Life Technologies), then washed and blocked with Fc-Block, anti-CD16/CD32 (clone 2.4G2, BD, Franklin Lakes New Jersey) for 10 minutes at room temperature. After blocking, the following surface antibodies were added for 30 minutes at room temperature: APC-Cy7-anti-CD8 (clone 53-6.7, Biolegend) and Ax700-anti-CD4 (RM4-5). Cells were then fixed and permeabilized using Fix/Perm solution (BD) and incubated at 4^oC for 30 minutes. Cells were washed and then suspended in perm wash buffer containing PE-Cy5-anti-CD3 (clone 145-2C11, BD), APC-anti-IFNγ (clone XMG1.2, BD), PE-anti-IL-2 (clone JES6-5H4, BD), PE-Cy7-anti-TNFα (clone MP6-XT22, BD) and were then incubated for 30 minutes at room temperature. Following staining, cells were washed and suspended in perm wash buffer and then evaluated by flow cytometry.

2.21 Flow cytometry

Samples were resuspended in 0.5% paraformaldehyde before acquisition using a modified LSR II flow cytometer (BD Biosciences). Results were analyzed using FlowJo version 9.3, Pestle version 1.6.2, and SPICE version 5.22 software (Mario Roederer, Vaccine Research Center, National Institute of Allergy and Infectious Diseases, National Institutes of Health, Bethesda, MD).

2.22 Listeria monocytogenes

Recombinant *Listeria monocytogenes* expressing-OVA (LM-OVA) was a gift from H. Shen (University of Pennsylvania, School of Medicine, Philadelphia, Pennsylvania, USA) and attenuated (ΔactA, ΔintB) *L mono* expressing-Gag (LM-Gag) from SIV strain mac239 was provided by ANZA Therapeutics (Concord, CA). Both strains were maintained at -80°C as a stock in brain-heart infusion/50% glycerol (BHI/50% glycerol).

2.23 *Listeria monocytogenes* infectious challenge

Evaluation of CD8 T cell mediated protection using *Listeria monocytogenes* was carried out as previously described[160, 161]. For infection with recombinant *LM*-OVA, mice were infected with $3x10^4$ to $6x10^4$ CFU in 0.3 ml PBS that was delivered intravenously into the tail vein. For infection with recombinant *LM*-Gag, mice were infected with $2x10^7$ CFU in 0.3 mL PBS that was delivered intravenously into the tail vein. Spleens were harvested 48 or 72 hours later, mechanically homogenized in 1 ml of PBS using a Tissue Ruptor (Qiagen, Valencia, CA) and then plated in duplicate as a 10-fold dilution series on brain heart infusion agar (Difco, Detroit, MI). Plates were

incubated at 37°C for 24 hours and colonies were counted to determine total CFU per spleen (bacterial burden).

2.24 *Leishmania major* challenge

L. major clone V1 (MHOM/IL/80/ Friedlin) promastigotes were grown as described previously[44]. Briefly, infectious-stage metacyclic promastigotes of *L. major* were isolated from stationary cultures (4–5 days old) by negative selection using peanut agglutinin (Vector Laboratories). Mice were infected 4 weeks after boost by injecting 750 metacyclic promastigotes intradermally within both ears. Personnel blinded to the vaccination assignments of the infected mice recorded weekly ear measurements using a metric calliper.

2.25 Serum antibody measurements

Immulon 4HBX plates (Thermo Scientific) were coated overnight at 4°C with either OVA or MML proteins diluted in 0.1 M Carbonate Buffer (pH 9.8). Plates were then blocked with 1% FBS/PBS, and plasma from OVA or MML immunized mice was applied in serial 10-fold dilutions in ELISA diluent (0.1% FBS / PBS) and incubated for 1 h at 37°C. For determining total IgG, biotin conjugated goat-anti-mouse total IgG (Jackson Immuno-Research, Westgrove, Pennsylvania) was added and incubated for 1 h at 37°C. Alternatively, for antibody isotyping, either biotin conjugated goat anti-mouse IgG1 (Jackson Immunoresearch) or biotin conjugated goat anti-mouse IgG2c (Jackson Immunoresearch) were added in diluent incubated for 1 h at 37°C. For detection, Avidin-Horse Radish Peroxidase (BD) was added and incubated for 30 minutes at room temperature, followed by the addition of TMB substrate-chromogen (Dako) and a 2N sulfuric acid stop solution. Washing was performed between steps

with PBS + 0.05% Tween 20. Plates were read on a SpectraMax Plus spectrophotometer (Molecular Devices) at 450 nm. Data was analysed in prism to generate a non-linear regression fit to estimate EC50 (midpoint titre) or EC05 (endpoint titres).

2.26 Hapten antibody determination

For assessment of the anti-hapten (anti-TLR-7/8a or anti-AP) antibody titres either SM 7/8a-PEG or AP-PEG, both of which contain a primary amine, were covalently linked to maleic anhydride activated, amine-reactive ELISA plates (Thermo Scientific) according to manufactures recommended guidelines. Serum was evaluated for total IgG titres as described above. Data was analyzed in prism to generate a non-linear regression fit to estimate EC50 (midpoint titres) or EC05 (endpoint titres).

2.27 Statistics and graphs

All data are represented as mean ± standard error of the mean (SEM). Statistical analyses were done using Prism software (GraphPad) and either one-way or two-way analysis of variance (ANOVA) was used as indicated. Bonferroni correction was applied to correct for multiple comparisons. Differences were found to be significant when P was less than 0.05 or 0.01, as indicated by single (*) or double asterisks (**) within the figures. Most graphs were produced using Prism. Flow cytometry data was processed using FlowJo (Tree Star). To evaluate the multifunctional cytokine response for antigen-specific T cells, Boolean gating was performed in Flow Jo and the resulting data was processed in Pestle (M. Roederer, VRC, NIAID, NIH, USA) and graphed using SPICE (http://exon.niaid.nih.gov/spice/; provided by Mario Roederer).

3 Combinatorial synthesis of polymer carriers of TLR-7/8a and *in vivo* structure-activity relationship studies

3.1 Introduction

Parenteral administration of small molecule TLR-7/8a leads to systemic inflammation and limited and only transient (< 24 h) induction of innate immune activation in draining lymph nodes[77, 97, 103, 124]. Systemic toxicity and poor lymph node activity is presumed to be a consequence of high tissue extravasation of small molecule TLR-7/8a that leads to poor local retention and rapid systemic distribution[97].

To overcome the pharmacokinetic limitations of TLR-7/8a, several formulation strategies have been developed as a means of: (1) restricting TLRa biodistribution to the site of injection and tissue draining lymph nodes; (2) prolonging adjuvant activity in draining lymph nodes, which serve as the sites of T cell priming; and, (3) improving co-delivery of the innate immune stimulus (e.g., TLR-7/8a) with admixed or co-formulated protein antigen.

Formulation strategies can be broadly delineated as either non-covalent or covalent approaches. Non-covalent formulations do not require modification of the TLR-7/8a or the delivery platform but instead use either hydrophobic or electrostatic interactions to associate the agonist with the particulate carrier or involve strategies for entrapping the agonist within particles. Such strategies have included the incorporation of TLR-7/8a agonists within oil-in-water emulsions[123], PLGA

particles[119, 120], liposomes[121] and polymersomes[122]. In contrast, covalent formulation approaches require modification of the TLR-7/8a to physically link the agonist to the delivery platform. The principal advantage of this approach is that the covalent bond provides a strong, stable link between the agonist and the delivery platform and also offers greater programmability as the exact amount and orientation of the agonist on the delivery platform can be chemically controlled. Covalent formulation strategies have included the covalent linkage of TLR-7/8a to polymer scaffolds[125], coordination of phosphate containing TLR-7/8a to the mineral salt Alum[126] and even direct attachment of TLR-7/8a to protein antigens[106, 107, 109, 116, 117, 127, 162]. The principal disadvantage of covalent formulation strategies is that they require physiochemical modification of both the agonist and delivery platform and this adds additional synthesis and purification steps, as well as additional levels of regulatory approval as each TLRa-delivery platform conjugate is considered by regulatory medical authorities as a new chemical entity[163].

Formulation strategies that use either macromolecular or particulate systems to restrict TLR-7/8a biodistribution have all been shown to improve the capacity of TLR-7/8a to elicit cellular and humoral immune responses[106, 118, 121, 123]. While improved responses are presumed to arise from increased local retention and improved APC uptake, many of the different physicochemical properties of TLR-7/8a formulation and delivery that influence innate immune activation *in vivo* are currently poorly understood. Without defining these mechanisms, the relative contributions of different components of adjuvant delivery to downstream immune responses remain unknown.

A major objective of this study was to define how physicochemical parameters of TLR-7/8a delivery directly influence innate immune activation in draining lymph nodes, which are the site of T cell priming following vaccination. To modulate delivery, TLR-7/8a were linked to biocompatible polymer scaffolds in a combinatorial process that resulted in a diverse array of Polymer-TLR-7/8a conjugates (Poly-7/8a). Combinatorial libraries of Poly-7/8a were screened for the capacity to induce lymph node cytokine (e.g., IL-12 and Type I IFN) production in mice following parenteral administration. These studies identified physicochemical properties that are important for activity, including scaffold morphology, TLR-7/8a density (spacing of agonists on the scaffold) and linker group composition. Moreover, lymph node cytokine production was dependent on TLR-7 but independent of caspase 1/11, a key mediator of a major Inflammasome pathway. Altogether, this chapter demonstrates that our approach of combinatorial synthesis and *in vivo* structure-activity relationship studies is an effective means of systematically identifying physicochemical parameters that are important for the activity of adjuvant delivery systems.

Experimental aims:

1. Synthesize and characterize combinatorial libraries of Poly-7/8a
2. Screen Poly-7/8a activity using *in vivo* structure-activity relationship (SAR) studies
3. Identify and validate physicochemical characteristics that are critical for Poly-7/8a activity *in vivo*

3.2 Synthesis of conjugatable TLR-7/8a agonists

There are several different classes of synthetic small molecule compounds that are known to bind to either or both TLR-7 and TLR-8[71]. The studies herein focused on analogues of the imidazoquinoline-based compounds, Imiquimod and Resiquimod (R848), which are both combined TLR-7/8a that have been extensively studied and are both approved by the FDA for use in the treatment of cutaneous pathologies[66, 82].

As commercially available imidazoquinoline-based TLR-7/8a lack a reactive handle that allows for their attachment to delivery scaffolds, it was necessary to synthesize conjugatable imidazoquinoline-based small molecule TLR-7/8a (SM 7/8a) from basic precursors in a 7-step reaction scheme (see materials and methods for synthesis and characterisation). As shown in Figure 3.1, the conjugatable analogue of R848, referred to as SM 7/8a, was prepared by replacing the t-butanol side group with a short butyl amine. The primary amine provides a reactive handle that permits attachment to delivery scaffolds. To evaluate the influence of linker length and composition on activity, SM 7/8a were prepared with hydrophobic alkane (SM 7/8a-alkane) and hydrophilic ethylene oxide (SM 7/8a-PEG) linkers with a terminal primary amine group that facilitates attachment to polymer scaffolds (Figure 3.1). To control for the physicochemical properties of the aromatic heterocyclic structure of SM 7/8a, 4-amino pyridine (AP) was used as a negative control ligand.

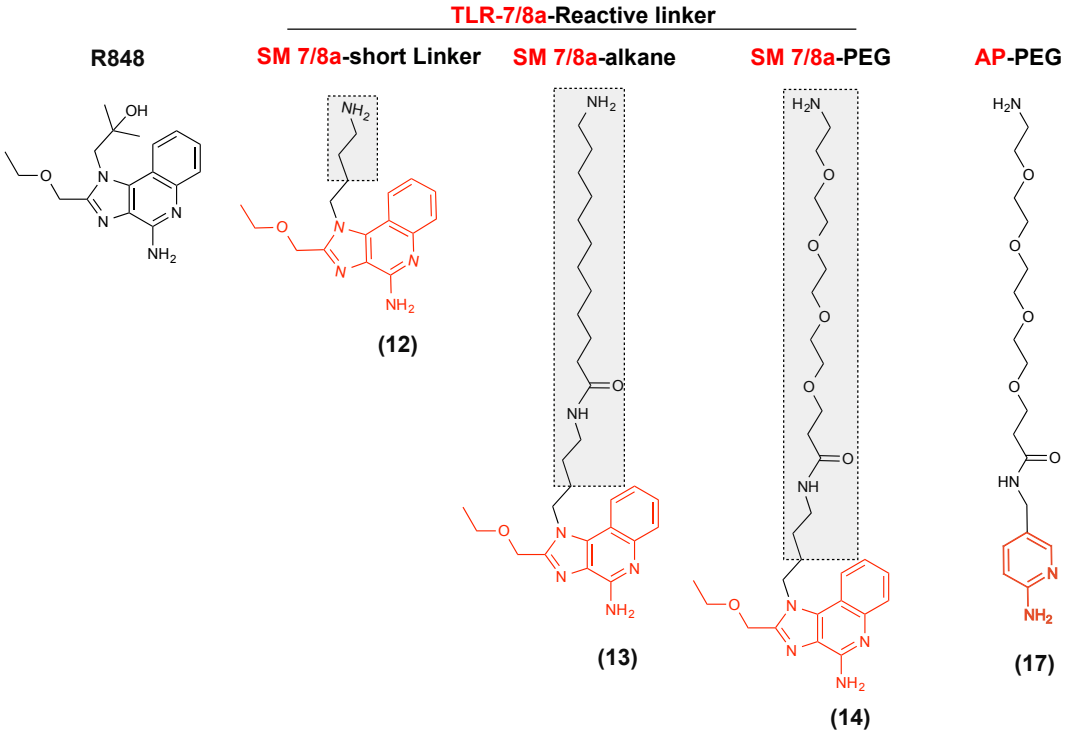

Figure 3.1: Conjugatable TLR-7/8a and controls. R848 is a commercially available TLR-7/8a that is poorly reactive for conjugation to delivery platforms. Several conjugatable analogues of R848 were prepared by replacing the t-butanol group with amine reactive linkers indicated by the shaded boxes: compound (12), SM-7/8a, was prepared as described in the methods section and was used as a precursor for the preparation of compounds (13) and (14) with either alkane (hydrophobic) or ethylene oxide (hydrophilic) linkers, respectively. Compound (17), 4-aminopyridine (AP)-PEG, which shares similar physical and chemical properties with the imidazoquinoline-based TLR-7/8a, was used as a negative control ligand.

3.3 Synthesis of amine-reactive HPMA-based polymers

Linear biocompatible polymers based on HPMA (Figure 3.2) were selected as scaffolds for the delivery of TLR-7/8a based on several key properties[156, 163-166]: (1) HPMA-based polymers are hydrophilic and can improve solubility of hydrophobic ligands (e.g., TLR-7/8a); (2) HPMA-based polymers are highly tunable, allowing for the evaluation of how precise changes in molecular weight, monomer composition, and morphology influences activity of the attached TLR-7/8a; (3) HPMA-based polymers are immunologically inert; and (4) HPMA-based polymers have been used

as carriers of small molecule drugs and have been shown to be safe in both animals and humans[163, 165, 166]. Altogether, HPMA-based polymers are well suited for systematically evaluating properties of TLR-7/8a delivery that influence *in vivo* activity[166].

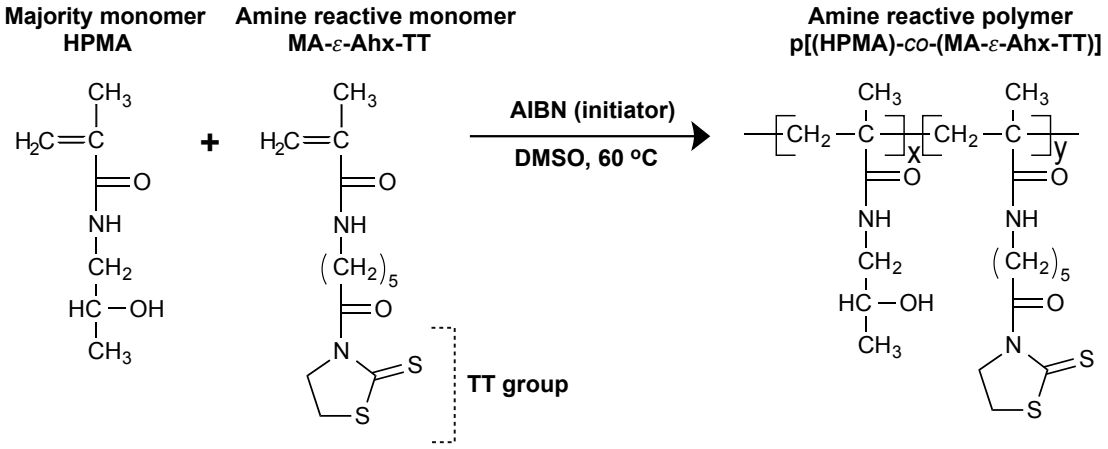

Figure 3.2: Preparation of an amine reactive HPMA-based copolymer. Copolymers N-(2-hydroxypropyl)methacrylamide (HPMA) and N-(6-oxo-6-(2-thioxothiazolidin-3-yl)hexyl)methacrylamide (Ma-ε-Ahx-TT), were added to a reaction vessel at a molar ratio of 9:1 and polymerization was initiated with azobisisobutyronitrile (AIBN).

HPMA homopolymers have limited chemical reactivity and cannot readily incorporate nucleophilic ligands, such as SM 7/8a. Thus, it was necessary to synthesize an HPMA-based copolymer that is comprised of the monomers HPMA and a methacryloylated amine reactive monomer, Ma-ε-Ahx-TT (Figure 3.2). The synthetic procedure to prepare the monomers, HPMA and Ma-ε-Ahx-TT, is described in the materials and methods section. Note that the carbonyl on the Ma-ε-Ahx is activated with a thiazoline-2-thione (TT) leaving group that permits site selective attachment of the nucleophilic TLR-7/8a (SM 7/8a). As shown in Figure 3.2, amine-reactive HPMA-based copolymers were prepared by solution radical polymerization using acrylamide-based monomers and AIBN as the radical initiator. The reaction

was run at elevated temperature (60°C) to catalyze thermolysis of AIBN; each AIBN molecule produces two radical species that can each react with an acrylamide monomer, resulting in two nascent polymer chains. The polymer chains continue reacting with monomers until either all monomers have reacted or until a termination event occurs (e.g., two radicals react to form a stable sigma bond). This process, referred to as chain growth polymerization results in a statistical copolymer with the two monomers randomly distributed along the length of the copolymer chain. The composition of the resulting copolymer is dependent on the ratio of each monomer in the reaction mixture during polymerization. Herein, a 9:1 molar ratio of HPMA to Ma-ε-Ahx-TT was used to generate a copolymer with ~ 10 mol % Ma-ε-Ahx-TT (10 out of 100 monomers in the copolymer). Modulating the amount of initiator allowed for control over molecular weights (degree of polymerization ~ length of polymers) which were generally kept at ~ 45 kDa, which is the previously reported renal excretion limit for HPMA-based copolymers[164].

3.4 Synthesis of polymer-TLR-7/8a (Poly-7/8a) conjugates

Polymer-TLR-7/8a (Poly-7/8a) conjugates were prepared by reacting nucleophilic TLR-7/8a (SM 7/8a) with amine-reactive HPMA-based copolymers in anhydrous conditions. As represented schematically in Figure 3.3, the nucleophilic TLR-7/8a displaces the TT groups and forms a stable amide bond with the polymer, resulting in a protein-sized (~ 30-50 kDa) linear macromolecule with pendantly arrayed TLR-7/8a. This process of polymer analogous reaction was used to prepare different compositions of Poly-7/8a. The process for synthesis, purification and analytical characterisation of the different Poly-7/8a is detailed in the methods section and outlined in Figure 3.4.

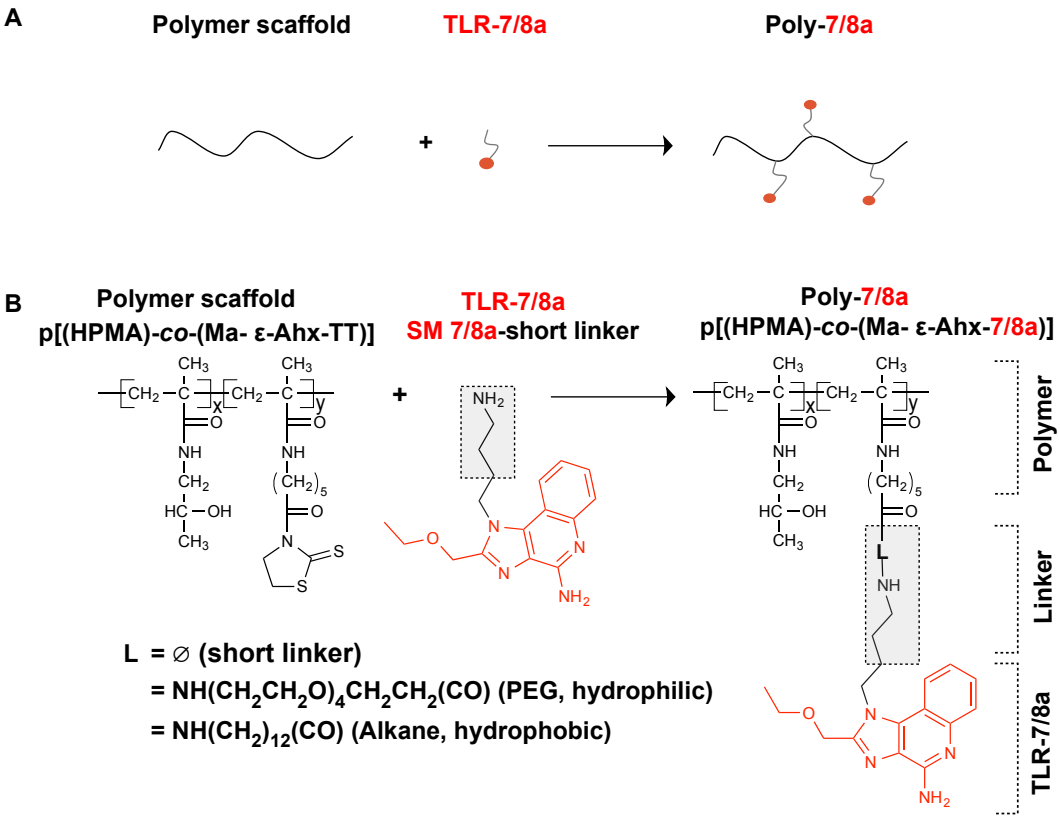

Figure 3.3: Synthesis of Polymer-TLR-7/8a conjugates (Poly-7/8a). Represented in the schematic, Poly-7/8a were prepared by reacting an amine-reactive HPMA-based polymer scaffold with nucleophilic TLR-7/8a to generate Poly-7/8a, a linear copolymer with multiple TLR-7/8a pendantly arrayed along the polymer backbone. (B) Structures of Poly-7/8a and precursors. Each monomer is contained within brackets and the subscripts (x or y) denote the mol% (percentage of total monomers) that each monomer comprises. Note that y is equal to the agonist density, or mol% 7/8a attached to the copolymer. The linker group is represented by the shaded box, where L (linker) = nothing, PEG or Alkane. HPMA = N-(2-hydroxypropylmethacrylamide); MA = Methacrylamide; Ahx = Aminohexanoic acid; TT = Thiazoline-2-thione

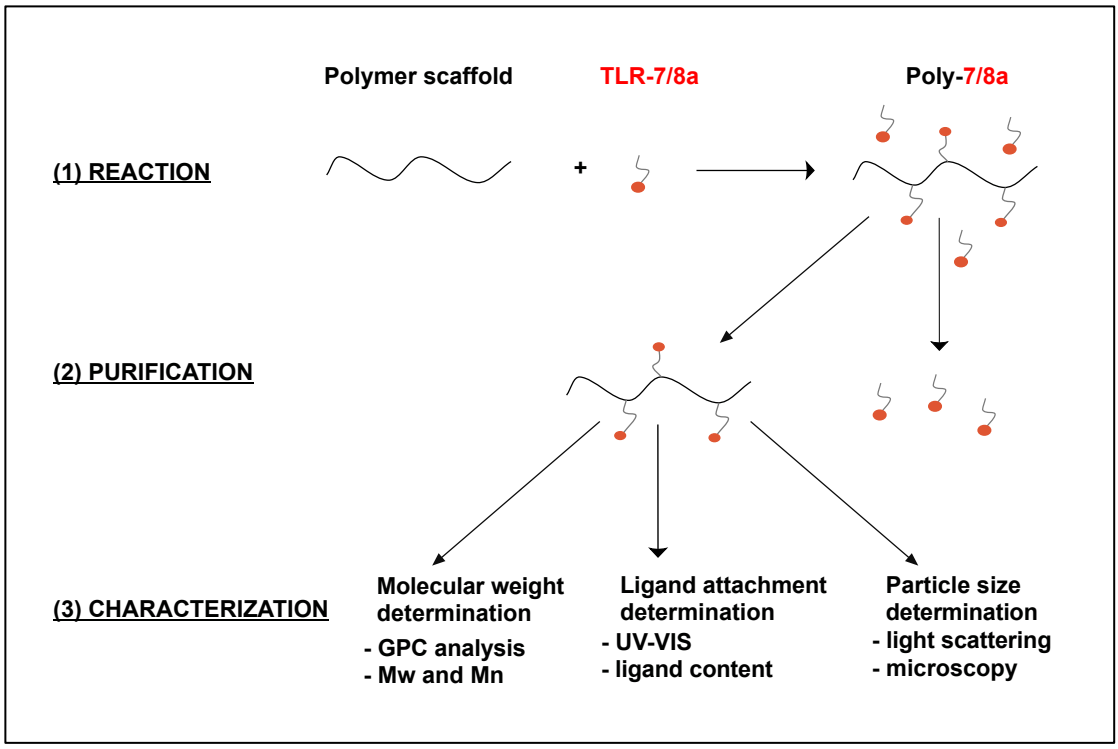

Figure 3.4: Flowchart outlining the process of Poly-7/8a synthesis, purification and characterisation. (1) Polymer-TLR-7/8a conjugates (Poly-7/8a) were synthesized by polymer analogous reaction. (2) Poly-7/8a were purified by size exclusion chromatography or dialysis to remove unreacted small molecules. (3) Purified Poly-7/8a were characterized by gel permeation chromatography (GPC) to determine the average molecular weight of the polymer chains (Mw and Mn); light scattering was used to assess the ligand content on the polymers; and, dynamic light scattering and Cryo-Electron Microscopy were used to assess size and morphology of Poly-7/8s structures in aqueous conditions.

3.5 Combinatorial synthesis of Poly-7/8a and physicochemical characterisation

Combinatorial synthesis was used as a high throughput and systematic process for preparing chemical libraries of Poly-7/8a with diverse physicochemical properties. In this process, the Poly-7/8a is comprised of several tunable components: (1) the TLR-7/8a; (2) the linker group used to attach the TLR-7/8a to the polymer backbone (hydrophilic / hydrophobic, length); (3) the density of TLR-7/8a attached to the

polymer (mol% 7/8a, which relates to the spacing of TLR-7/8a along the polymer backbone); and, (4) the chemical composition of the polymer scaffold (e.g., HPMA). Each of the components represents a variable that can be precisely physicochemically tuned. For example, in these studies, the linker group in these studies is a component that can have 1 of 3 different properties (short, Alkane or PEG) that can be, for example, combined with agonist density, which represents another component that can have a range of values (e.g., varying agonist density from 1-10 mol% 7/8a). It was hypothesized that certain physicochemical properties, such as high densities of TLR-7/8a attached to the polymer (agonist density = component 1) scaffold through flexible PEG linkers (linker group = component 2) may enhance biological activity by enhancing avidity of TLR-7 binding and / or promoting TLR-7 clustering that enhances downstream signalling. To evaluate how these different parameters influence biological activity, a combinatorial library was prepared by reacting three different densities of TLR-7/8a (component 1 = 2, 4 or 8 mol% 7/8a) using three different linker group compositions (component 2 = short, PEG or Alkane) to yield 9 unique Poly-7/8a conjugates (Figure 3.5). The number of unique compounds produced by combinatorial synthesis is equal to the product of the number of variables tested for each component (e.g., 3 agonist densities x 3 linker groups = 9 unique Poly-7/8a).

Combinatorial synthesis was used to generate over 300 unique Poly-7/8a that were screened in structure-activity relationship studies *in vitro*. However, only subsets of this expansive Poly-7/8a material library are discussed in this thesis because our initial *in vitro* studies were not predictive of *in vivo* biological activity. Thus, rather than including *in vitro* data that provides limited insights as to how physiochemical

properties of different Poly-7/8a influence biological activity *in vivo,* the remainder of this thesis focuses on small subsets of the total Poly-7/8a material library that were evaluated in more robust *in vivo* studies in mice. Moreover, as a means of reducing the number of animals required for these studies, the *in vivo* studies described herein focused on evaluating specific trends between structure and activity using limited, but focused, subsets of the Poly-7/8a combinatorial library.

The next sections describe the characterisation and *in vivo* evaluation of the 9 unique Poly-7/8a that were produced by the combinatorial process shown in Figure 3.4B.

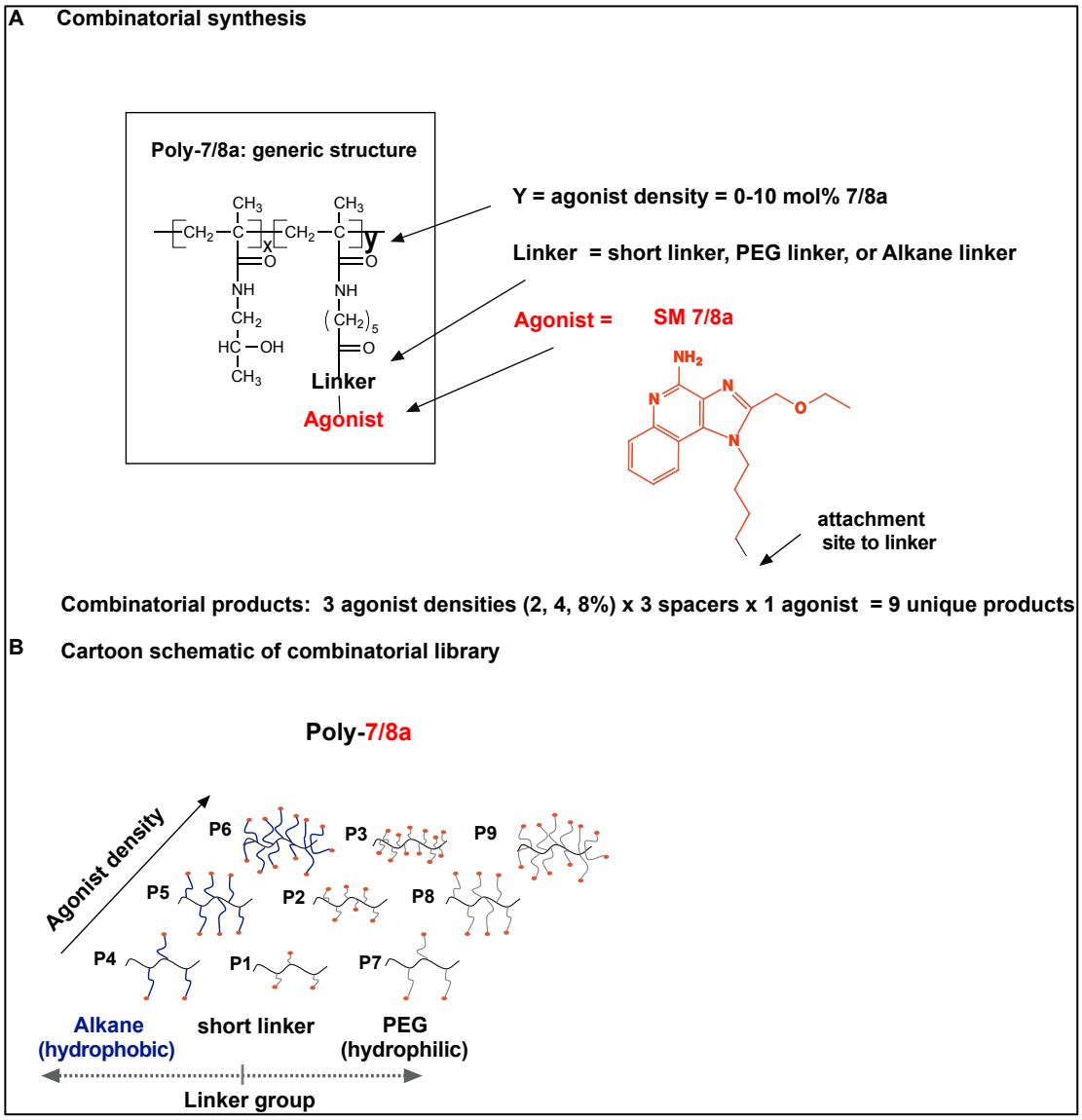

Figure 3.5: Combinatorial synthesis of Poly-7/8a. (A) A combinatorial library of Poly-7/8a was generated by attaching TLR-7/8a to HPMA-based copolymers at different densities (~ 2, 4, 8 mol %) using either a short, alkane or PEG linker. By reacting TLR-7/8a at 3 different densities, using 3 different linkers, there are 9 unique products that can be generated, as represented in the cartoon schematic (B). Note that the agonist and polymer composition represent additional variables that can be tuned but were not evaluated here.

Poly-7/8a generated by the combinatorial process were purified using dialysis and / or size-exclusion chromatography, both of which are used to separate the polymer from unreacted monomers and small molecule precursors based on differences in molecular weight (see materials and methods for details). All Poly-7/8a were then evaluated for physicochemical properties, including TLR-7/8a content (amount and density attached) and molecular weight. Additional characterisation modalities are discussed in later sections.

An example of the physicochemical properties determined for Poly-7/8a is shown in Table 3-1 for a combinatorial library of 9 different Poly-7/8a with varying agonist density (2-9 mol% 7/8a) and linker group (short, Alkane and PEG). The measured agonist density closely conforms to the theoretical agonist densities (2, 4 and 8 mol% 7/8a), which confirms the efficiency of the addition-elimination reaction used to incorporate the TLR-7/8a into the polymer backbone. Additionally, it should be noted that the incorporation of the TLR-7/8a into the polymers had little impact on the resulting molecular weights of the polymer conjugate, which ranged from about 40-60 kDa. This reflects that attaching < 10 mol% 7/8a represents a fractional change in the overall molecular weight of the polymer. The relatively high Polydispersity (Mw/Mn) is a result of the radical polymerization process that results in broad distribution in the resulting polymer molecular weight. Note that different doses of Poly-7/8a (μg) must be used to normalize for the dose of TLR-7/8a (nmoles) (see table 3-1).

Description		Physicochemical parameters					In vivo dose	
Polymer #	Agonist-linker	Agonist density (mol% 7/8a)	TLR-7/8a per polymer	M_w [g/mol]	M_n [g/mol]	M_w/M_n	TLR-7/8a (nmoles)	Polymer (ug)
P1	7/8a-short	3.1	10	51,880	32,650	1.59	12.5	62
P2	7/8a-short	5.7	19	42,640	26,440	1.61	12.5	36
P3	7/8a-short	8.5	28	49,760	33,930	1,47	12.5	26
P4	7/8a-Alkane	2.4	8	44,790	29,790	1.50	12.5	81
P5	7/8a-Alkane	4.7	16	53,960	35,220	1.53	12.5	45
P6	7/8a-Alkane	8.2	27	54,660	35,660	1.53	12.5	29
P7	7/8a-PEG	2.4	8	48,490	28,300	1.71	12.5	83
P8	7/8a-PEG	4.0	13	59,470	32,430	1.83	12.5	52
P9	7/8a-PEG	7.9	26	55,680	33,850	1.65	12.5	30

Table 3-1: Physicochemical properties of Poly-7/8a produced by combinatorial synthesis. Agonist density = (moles 7/8a / moles of monomers)*100; TLR-7/8a per polymer = (mol % 7/8a / 100)*degree of polymerization; Mw = weight average molecular weight determined by light scattering; Mn = number average molecular weight determined by refractometry; Mw/Mn = Polydispersity. Note that by normalizing for dose of TLR-7/8a (nmoles), different masses of Poly-7/8a (µg) were required. A 12.5 nmoles dose of TLR-7/8a is approximately equal to 4 µg of R848 (12.5 nmoles x 0.314 µg/nmoles R848 ~ 4 µg)

3.6 *In vivo* screening of a combinatorial library of polymer-TLR-7/8a conjugates

Structure-activity relationship (SAR) studies were used to evaluate how continua of different physicochemical properties of Poly-7/8a influences biological activity. Initial efforts to screen activity of the combinatorial libraries of Poly-7/8a relied on *in vitro* assays. Importantly, however, results from the *in vitro* (see section 3.10) screens did not predict *in vivo* activity. To evaluate activity more directly, combinatorial libraries of Poly-7/8a were subcutaneously administered to mice and proximal draining lymph nodes were screened for cytokine production 24 h after administration. Evaluation of lymph node cytokines takes into account how pharmacokinetics, uptake by immune cells and the dynamic processes of cellular migration and tissue remodelling influence activity at the site of T cell priming (e.g.,

draining lymph nodes). Note that the 24 h timepoint was selected based on preliminary screening showing that evaluation of earlier timepoints provided limited sensitivity and that cytokine responses peak between 1-4 days after administration.

A combinatorial library of 9 unique Poly-7/8a with varying agonist density (mol% 7/8a) and linker group compositions was evaluated for lymph node cytokine production (Figure 3.6). Though the same dose of TLR-7/8a was delivered (12.5 nmoles), a wide range of innate immune activity was observed. Increasing agonist density was associated with significantly increased production of IL-12 and IP-10, two cytokines that are critical for priming, differentiating and expanding both Th1-type CD4 and CD8 T cell responses. This trend was observed across all linker groups used: increasing agonist density from ~ 2 to 8% resulted in an ~ 5-fold increase in lymph node cytokine production. Poly-7/8a with the TLR-7/8a attached through the PEG linker resulted in the highest lymph node cytokine production and, based on this enhanced activity, the PEG linker was used for TLR-7/8a attachment to the polymer for all subsequent studies.

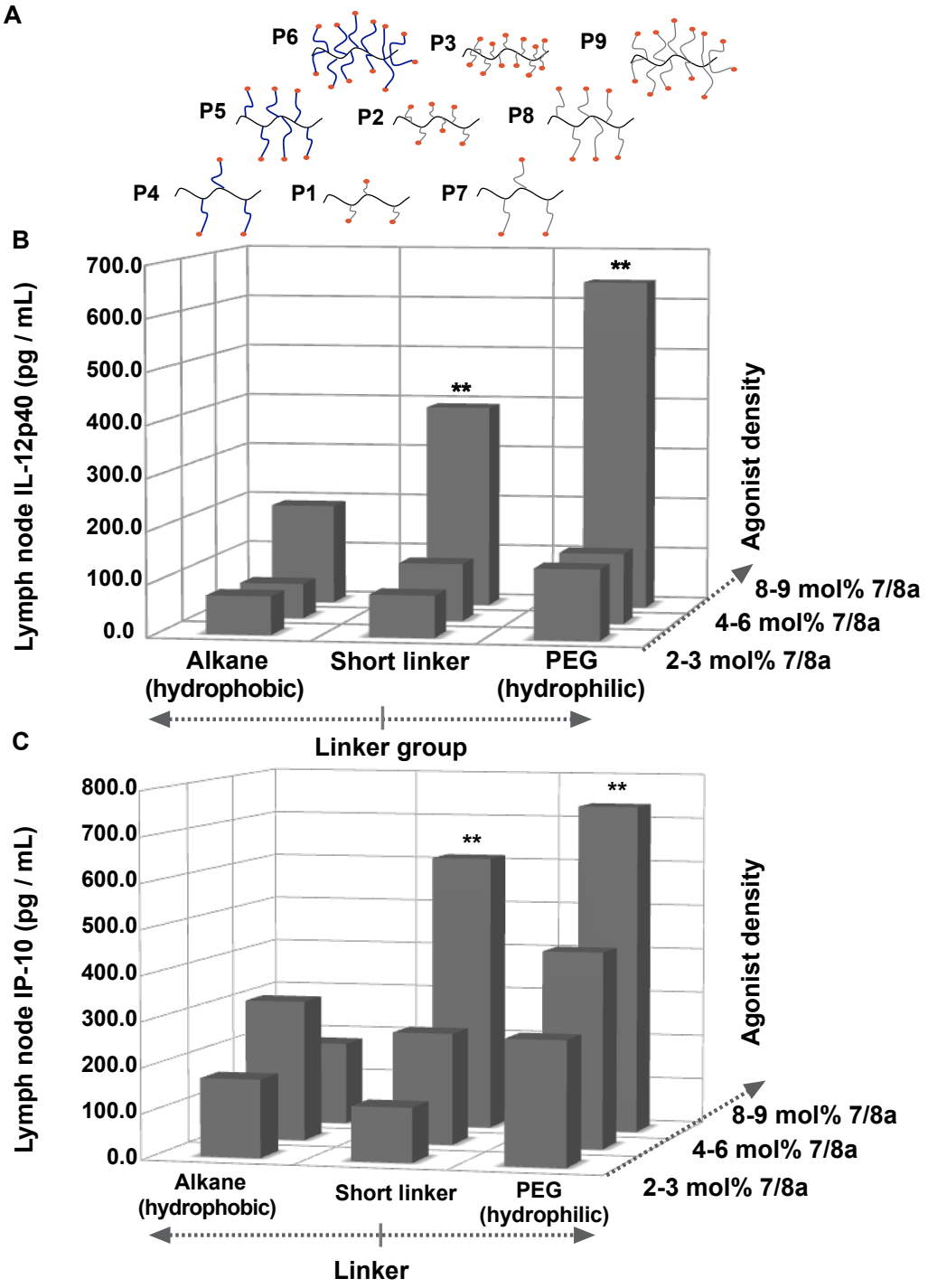

Figure 3.6: In vivo screening of a combinatorial library of Poly-7/8a. (A) Cartoon schematic of a combinatorial library of Poly-7/8a. (B-C) Poly-7/8a (normalized for TLR-7/8a dose, 12.5 nmoles) were subcutaneously administered into both hind footpads of C57BL/6 mice. Draining lymph nodes (n = 4) were harvested 24 h after administration and were processed to generate a cell suspension that was cultured overnight. ELISA was used to measure IL-12 and IP-10 in the supernatant. Data are represented as mean; significance is reported relative to naïve.

3.7 Increasing TLR-7/8a density on polymers induces particle formation

Increasing densities of TLR-7/8a attached to the polymer scaffolds was associated with an increased tendency of Poly-7/8a to assemble into particles in aqueous conditions (Figure 3.7). Particle size and distribution were determined by light scattering and Cryo-electron microscopy (Cryo-EM) and representative data are shown in Figure 3.7. Poly-7/8a with low agonist density (~ 1-2 mol% 7/8a) adopt random coil confirmations, referred to as polymer coils (PC, ~ 10 nm diameter); Poly-7/8a with intermediate agonist density (~ 4 mol% 7/8a) exist predominantly as PC but are in equilibrium with nanometre-sized supramolecular associates; Poly-7/8a with high agonist density (8-10 mol% 7/8a) assemble into submicron polymer particles (PP, ~ 700 nm diameter).

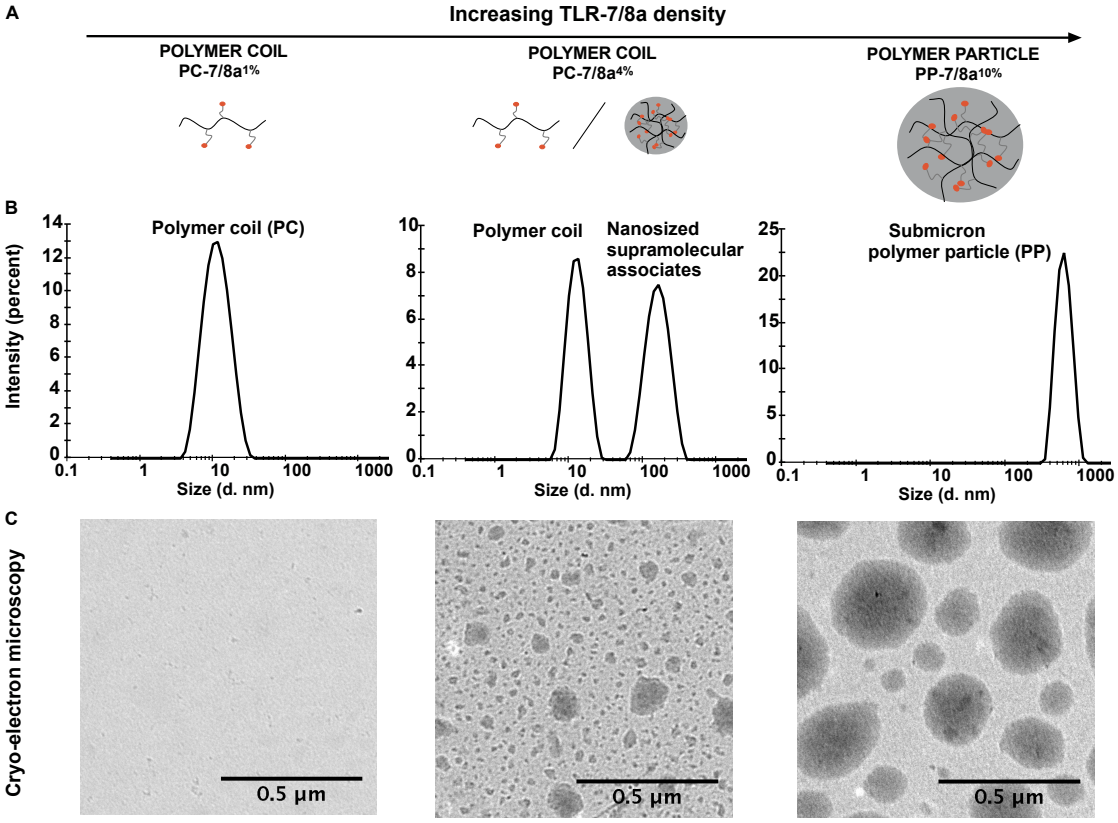

Figure 3.7: Increasing agonist density on polymers induces particle formation in aqueous conditions. (A) Poly-7/8a were prepared with 1, 4 or 10 mol% 7/8a. Aqueous solutions of Poly-7/8a were characterized by (B) dynamic light scattering and (C) Cryo-electron microscopy (EM). PC = polymer coil; PP = polymer particle.

3.8 Increasing TLR-7/8a density and particle formation are associated with increased lymph node cytokine production

The above results show that increasing agonist density (mol% 7/8a) is associated with increasing lymph node cytokine production and increased tendency of Poly-7/8a to assemble into particles. It is possible that cytokine production could be a result of the physicochemical properties (high agonist density and polymer particle morphology) of the Poly-7/8a that are independent of TLR-7/8a signalling. To account for this possibility, control polymers were prepared with high densities of 2-aminopyridine

(AP), a heterocyclic base that is structurally related to TLR-7/8a (Figure 3.8A). AP ligands were attached to the polymer backbone through either a hydrophilic PEG linker or an amphiphilic (AMPH) linker (Figure 3.8B). Whereas high densities of AP attached to HPMA-based polymers through a PEG linker results in polymer coil (PC) morphologies (PC control), AP attached through the AMPH linker results in polymer particle formation (PP control), which provides a control that is matched for the physicochemical properties of Poly-7/8a with high TLR-7/8a agonist density (8-10 mol% 7/8a) that assemble into polymer particles.

To further evaluate the association between agonist density, particle formation and lymph node cytokine production, Poly-7/8a with 1-10 mol% 7/8a, polymer controls and a small molecule TLR-7/8a were evaluated for the capacity to induce lymph node cytokine production. Only polymer particle (PP)-forming Poly-7/8a with agonist densities of 8 and 10 mol% 7/8a, referred to as PP-7/8$^{8\%}$ and PP-7/8$^{10\%}$, respectively, induced significant levels of IL-12, IP-10, IFN-α and IFN-γ in draining lymph nodes (Figure 3.8C-F). In contrast, Poly-7/8a with 1, 2 and 4 mol% 7/8a, as well as the small molecule TLR-7/8a (SM 7/8a) and both PC and PP controls, did not induce lymph node cytokine production. The observation that the polymer controls (PC and PP) do not induce cytokine production in lymph nodes suggests that the polymer scaffolds alone are immunologically inert and require TLR-7/8a for activity. Altogether, these results suggest that high agonist density, particle formation, or both, are critical to the capacity of Poly-7/8a to induce lymph node cytokine production.

A

	Physicochemical parameters			In vivo dose	
Adjuvant / Control	Agonist-linker or *Control-linker	Agonist density (mol% 7/8a)	Diameter nm.	TLR-7/8a (nmoles)	Polymer mass (ug)
PC	*AP-PEG	9.0	13 (±5)		220
PP	*AP-AMPH	8.3	603 (±48)		52
SM 7/8a	----	1.0	N.A.	12.5	N.A.
PC-7/8a$^{1\%}$	7/8a-PEG	0.8	13 (±6)	12.5	220
PC-7/8a$^{2\%}$	7/8a-PEG	2.4	22 (±17)	12.5	83
PC-7/8a$^{4\%}$	7/8a-PEG	4.0	142 (±67)	12.5	52
PP-7/8a$^{8\%}$	7/8a-PEG	7.9	547 (±66)	12.5	30
PP-7/8a$^{10\%}$	7/8a-PEG	10.5	688 (±55)	12.5	24

B

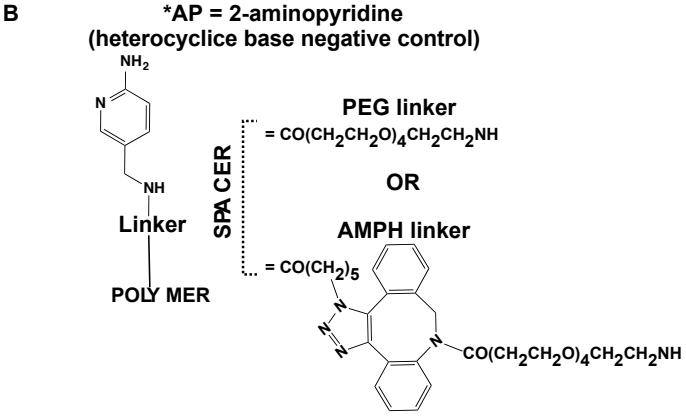

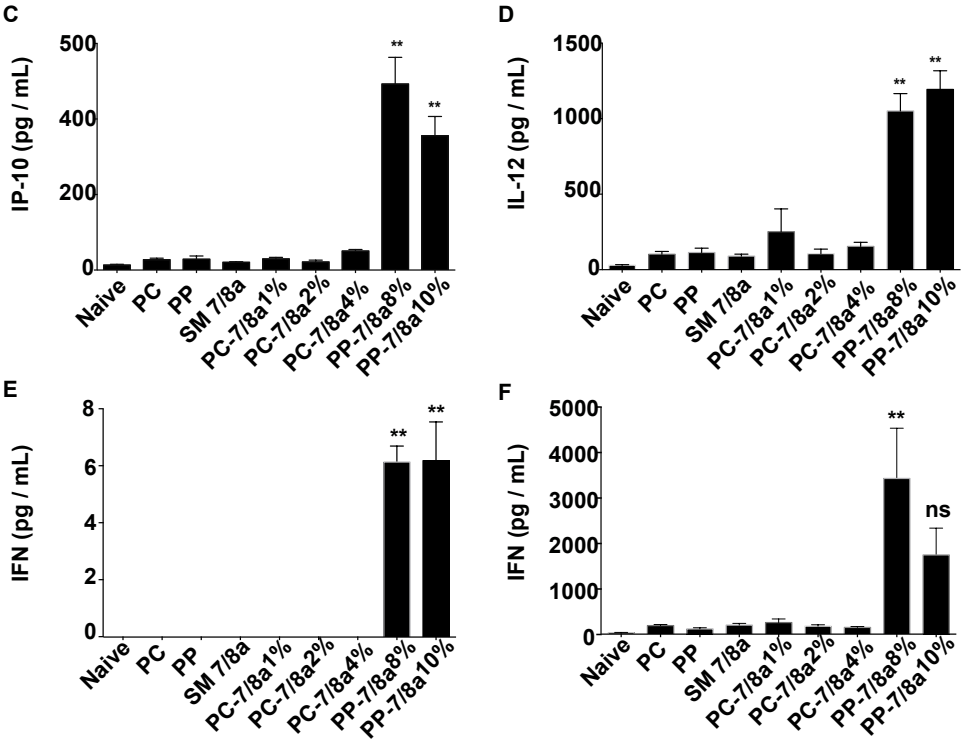

Figure 3.8: Increasing density of agonists on polymers results in particle formation and is associated with enhanced local innate immune activity. (A) Properties of Poly-7/8a, SM 7/8a and control polymers are summarized in the table. (B) Negative control polymers were prepared using 2-aminopyridine (AP) to account for the contribution of

the aromatic amine present on the imidazoquinoline-based TLR-7/8a used in this study. AP was attached to polymers either through a PEG or amphiphilic (AMPH) spacer to prepare polymer coil (PC) and polymer particle (PP) controls, respectively. (C-F) Poly-7/8a, SM 7/8a or polymer controls normalized for TLR-7/8a dose (12.5 nmoles) were subcutaneously administered into both hind footpads of C57BL/6 mice. Draining lymph nodes (n = 4) were harvested 24 h after administration and were processed to generate a cell suspension that was cultured overnight and assessed for (C) IP-10, (D) IL-12, (E) IFN-α or (F) IFN-γ by ELISA. All data are represented as mean ± SEM; statistical significance is relative to all other groups.

3.9 Lymph node cytokine production is dependent on TLR-7 but independent of the Inflammasome

The previous studies demonstrated a prominent trend between increasing agonist density and both particle formation and lymph node cytokine production, with particle forming Poly-7/8a with 8-10 mol% 7/8a (PP-7/8a$^{8\text{-}10\%}$) inducing significantly higher levels of cytokine production as compared with controls. To evaluate whether lymph node cytokine production is TLR-7 dependent, PP-7/8a$^{10\%}$ was administered to both wild type (WT) and TLR-7 knockout (KO) mice and lymph node cytokines were evaluated 24 h after administration. While PP-7/8a$^{10\%}$ induced high levels of IL-12 (~ 3,000 pg/mL) and IP-10 (~ 200 pg/mL) in the draining lymph nodes of WT mice, cytokines were undetectable in TLR-7 KO mice, suggesting that TLR-7 is critical to the capacity of particle forming Poly-7/8a with high agonist density to induce lymph node cytokine production. Moreover, CpG, a TLR-9 agonist, was able to induce the production of both IL-12 and IP-10 in TLR-7 KO mice, demonstrating that other TLR-9 signalling pathways and cytokine production are intact in these mice.

Prior studies have shown that particles alone can induce innate immune activation through the NALP3 Inflammasome[26]. It is possible that some of the innate cytokine

production induced by PP-7/8a$^{10\%}$ could be due to the polymer particles activating specific Inflammasome pathways. To evaluate this possibility, PP-7/8a$^{10\%}$ was administered to mice that are deficient in Caspase 1/11 and lymph node cytokines were evaluated 24 h after administration. Lymph node cytokine production was notably increased in Caspase 1/11 KO mice as compared with the WT mice, which suggests that cytokine production in WT mice is not dependent on this dominant Inflammasome pathway. Note that cytokine supernatants underwent 2 freeze-thaw cycles prior to analysis, which may account for the lower cytokine responses observed in panels C-D, as compared with WT mice observed in panels A-B. These data, together with the observation that the polymer alone induces no cytokine production (Figure 3.8, C-F), suggests that Poly-7/8a activity is mediated through TLR-7 and not due to intrinsic activity associated with physical or chemical properties of the polymer.

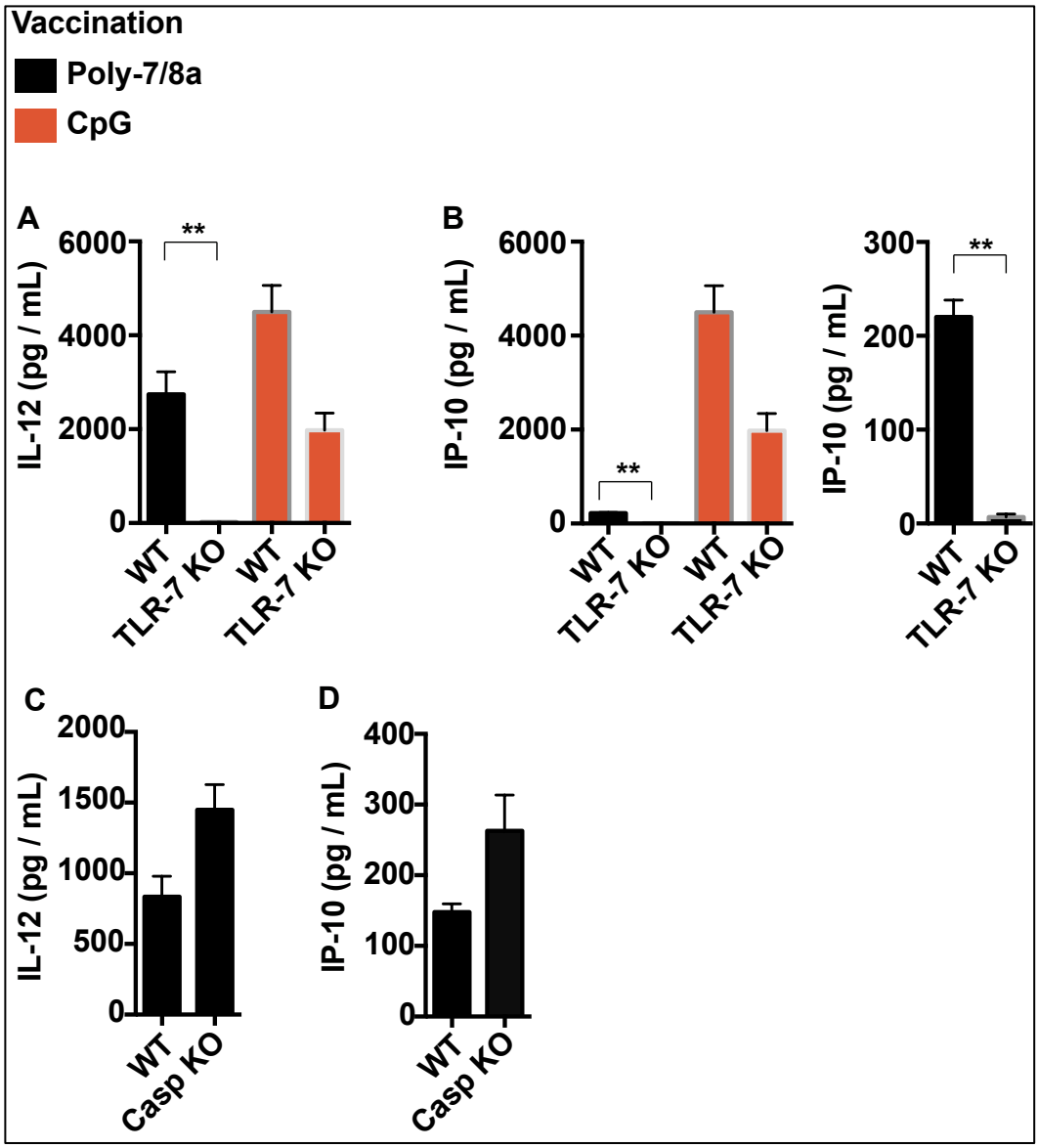

Figure 3.9: In vivo activity by particle forming Poly-7/8a is dependent on TLR-7 but independent of the inflammasome. Poly-7/8a$^{10\%}$ (12.5 nmoles) was subcutaneously administered into both hind footpads of either (A-B) wild type (WT) and TLR-7 knockout (TLR-7 KO) mice, or (C-D) WT and Caspase 1/11 (Inflammasome) KO mice. (A-D) Draining lymph nodes (n = 4) were harvested 24 h after administration and were processed to generate a cell suspension that was cultured overnight and assessed for IL-12 and IP-10 by ELISA. All data are represented as mean ± SEM.

3.10 Polymer-TLR-7/8a conjugates are inactive *in vitro*

Early evaluation of combinatorial libraries of Poly-7/8a used *in vitro* assays to evaluate activity. A subset of this data is shown in Figure 3.10. Notably, while particle-forming Poly-7/8a induces nearly 1000-fold higher lymph node cytokine production as compared with SM 7/8a *in vivo* (Figure 3.8), a reverse trend was observed *in vitro* (Figure 3.10). This discrepancy between *in vitro* and *in vivo* activity has been recently described and suggests that *in vitro* assays may be inadequate for the evaluation of certain adjuvant delivery platforms[124].

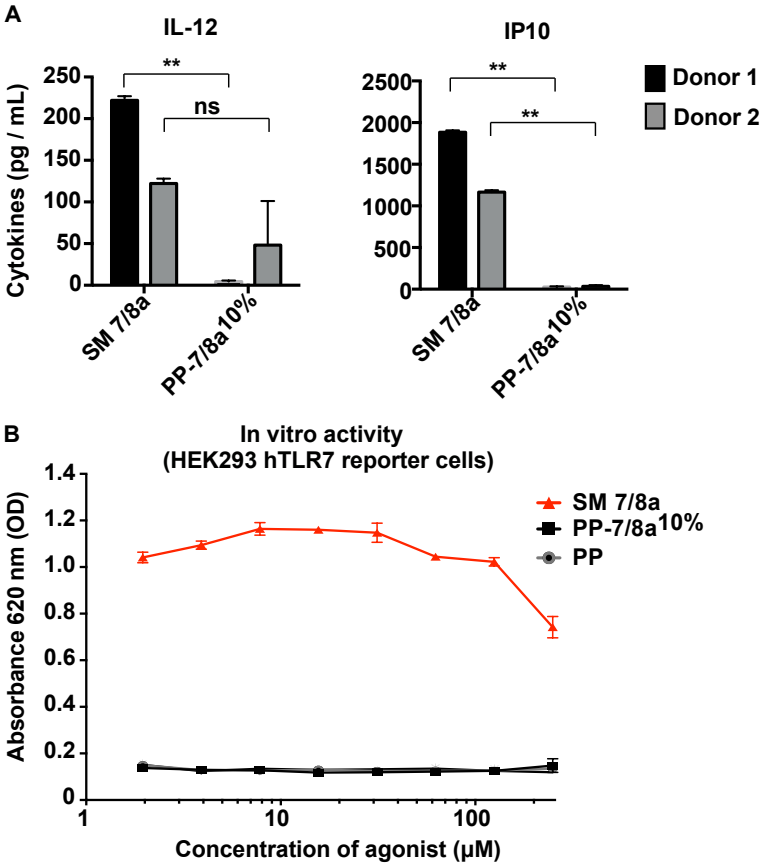

Figure 3.10: Poly7/8a (PP-7/8a$^{10\%}$) is inactive in vitro. (A) PP-7/8a$^{10\%}$ or SM 7/8a normalized for TLR-7/8a dose (5 nmoles) were incubated with freshly isolated human PBMCs overnight and evaluated for presence of IL-12 or IP-10 by ELISA. (B) PP-7/8a$^{10\%}$ and SM 7/8a were serially diluted and added to *in vitro* cultures of HEK293 hTLR7 reporter cells. Absorbance at 620 nm is proportional to signalling downstream of TLR7 binding. All data are represented as mean ± SEM.

3.11 Discussion

In vivo structure-activity relationship studies identified that linker group, and either TLR-7/8a density (mol% 7/8a), carrier morphology, or both, are important factors that influence Poly-7/8a activity *in vivo*. In contrast to many prior studies that have relied on either *in vitro* or downstream measures of innate activity *in vivo* (e.g., antibody and T cell responses), the results herein show that the direct evaluation of innate activity *in vivo* is critical for yielding insights as to how structure influences activity in draining lymph nodes, the site of T cell priming following vaccination.

As biomarkers for the pharmacodynamics of Poly-7/8a, as well as a proxy for the capacity of Poly-7/8a to induce innate immune responses sufficient for priming, differentiating and expanding T cells, this study focused on the evaluation of four cytokines: IL-12, IP-10, IFNγ, and IFNα. These four, among many other candidate biomarkers, were chosen because of their critical importance in eliciting adaptive Th1-type CD4 and CD8 T cell mediated immunity. Specifically, IL-12 and IFNγ have been shown to be important for inducing Th1-type CD4 cells while inhibiting differentiation of Th2-type CD4 cells[167-170]; IFNα is required for promoting cross-presentation of exogenously delivered antigen in mice[52, 171]; IP-10 promotes the recruitment of CD8 T cells and has been shown to enhance Th1 type immunity, possibly through a positive feedback loop[53, 172]; and, finally, IL-12 plays a direct role in the expansion of CD8 T cells by promoting their upregulation of the high affinity IL-2 receptor[54, 55]. While other cytokines certainly play important roles in the innate and adaptive immune responses, the cytokines evaluated herein were selected as biomarkers based on their high sensitivity, low cost and specificity as gene products downstream of TLR-7/8a activity.

These studies are the first to describe an agonist density-dependent increase in the propensity of the carrier to assemble into particles, which is associated with increased capacity to induce lymph node cytokine production. A critical question, however, is whether the activity of particle forming Poly-7/8a is dependent on the particulate morphology of the carrier or whether high agonist density is important for promoting TLR-7 clustering in APCs. Indeed, earlier strategies directly attaching TLR-7/8a to protein antigen found that aggregation of protein-TLR-7/8a conjugates, or their adsorption to particulate delivery systems, was required for elicitation of T cell responses[108, 116]. While these data suggest that particle formation is important for activity, both conjugates evaluated had a fixed density of agonist and provide limited information as to how agonist density influences activity. The influence of agonist density and morphology are evaluated in greater depth in Chapter 4.

Earlier studies have reported that particles with diverse physiochemical properties (PLGA, Polystyrene and Alum) activate the Inflammasome through NALP3[26, 173]. In this study, lymph node cytokine production by Poly-7/8a in caspase 1/11 deficient mice was found to be similar to that observed in WT mice, suggesting that the NALP3 inflammasome is not critical to the production of IL-12 and IP-10 by Poly-7/8a. However, while production of IL-12 and IP-10 was not decreased in Caspase 1/11 deficient mice in response to Poly-7/8a, certain pro-inflammatory cytokines that are more characteristic of the Inflammasome pathway, such as IL-1β may be affected and have a biologically meaningful role in the activity of Poly-7/8a. Thus, it is possible to conclude that the production of certain cytokines (IL-12 and IP-10) by Poly-7/8a does not depend on signalling through Caspase 1/11, but this data does not preclude the possibility that the Inflammasome has a role in the activity of Poly-7/8a

in vivo. While the exact role of the Inflammasome in Poly-7/8a activity may be unclear, knocking out TLR-7 completely abrogates cytokine production, confirming that production of IL-12 and IP-10 by Poly-7/8a is TLR-7 dependent.

Finally, the observation that the free TLR-7/8a but not particulate carriers of TLR-7/8a are active *in vitro* is consistent with recent reports in the literature and suggests that *in vitro* assays may not be adequate for the assessment of particulate adjuvant delivery systems[121, 124]. Part of this discrepancy between *in vitro* and *in vivo* assays could relate to the inability of *in vitro* systems to fully recapitulate the *in vivo* environment. In particular, *in vitro* assays do not contain many important serum proteins, such as complement and lectins, which bind to reactive surfaces and sugars, respectively. While complement, lectin and other humoral factors (e.g., antibodies) can bind to particles and facilitate their uptake into APCs through receptor-mediated endocytosis *in vivo*[148], these mechanisms are not present *in vitro* and may, therefore, explain the differences observed between *in vitro* and *in vivo* activity by Poly-7/8a in the studies herein.

Altogether, this chapter shows that combinatorial synthesis and *in vivo* screening are effective strategies for systematically identifying physicochemical properties that are critical for the capacity of adjuvant delivery systems to induce innate immune activation.

4 Influence of Poly-7/8a pharmacokinetics and DC uptake on the location, magnitude and duration of innate immune activation

4.1 Introduction

In the previous chapter, increasing TLR-7/8a density and particle formation were associated with increased lymph node cytokine production by Poly-7/8a. An important consideration is how these properties independently influence pharmacokinetics and uptake by DCs in lymph nodes.

Improved adaptive immune responses induced by small molecule TLR-7/8a formulated with particulate carriers suggests that spatially restricting agonist distribution and increasing local (i.e. lymph node) persistence (through retention of the carriers within the draining lymphatics) may be critical to the activity of TLR-7/8a[119-121, 123, 124]. However, it has not been characterized how different physicochemical properties of TLR-7/8a formulations—that affect biodistribution, kinetics and cellular localization—influence the location, magnitude and duration of innate immune activation. Without these insights, the relative contributions that different components of adjuvant delivery have on downstream immune responses remain unknown.

The principal objective of this chapter was to determine how physicochemical parameters of TLR-7/8a formulation directly influence the magnitude and spatiotemporal characteristics of innate immune activation *in vivo* and how these responses translate to protective cellular immunity in the context of vaccination. These studies identify that particle formation has a strong positive impact on the activity of Poly-7/8a. Biodistribution and kinetics studies together with analysis of DC populations in lymph nodes were used to mechanistically define how particle-forming Poly-7/8a enhance innate immune activation in lymph nodes by increasing local retention and promoting DC uptake. Whereas particulate morphology is a major determinant of TLR-7/8a activity, increasing agonist density (mol% 7/8a), potency and dose all led to increased persistence and magnitude of lymph node cytokine production. Importantly, the persistence, rather than the magnitude, of lymph node cytokine production was found to be critical to the elicitation of CD8 T cell responses to a co-administered protein antigen.

Experimental aims:

1. Evaluate how morphology of the carrier and density of the TLR-7/8a influence biodistribution and kinetics
2. Characterize how morphology and agonist density influence uptake by DCs in draining lymph nodes
3. Characterize the magnitude, location (lymph node vs. spleen) and duration (1-15 days) of innate immune activation induced by Poly-7/8a, SM 7/8a or controls
4. Evaluate the capacity of Poly-7/8a, SM 7/8a or controls to elicit CD8 T cell responses to a co-administered protein antigen

4.2 Dye-labelled constructs for whole animal imaging and flow cytometry

A major objective of this chapter was to evaluate how TLR-7/8a carrier morphology (small molecule, polymer coil and polymer particle) and density of attached TLR-7/8a (3% and 10%) influence biodistribution, kinetics and uptake by migratory and lymph node resident DCs. Biodistribution and kinetics were evaluated using whole animal imaging in intact mice, and flow cytometry was used to evaluate material uptake by DCs that were isolated from lymph nodes.

To facilitate tracking using whole animal imaging and flow cytometry, it was necessary to label Poly-7/8a, SM 7/8a and polymer controls with fluorescent dyes (see Table 4-1). Note that an infrared (IR) dye, which absorbs and emits light at wavelengths optimal for soft tissue penetration (Excitation ~ 773 nm, Emission ~ 790 nm), was used in the whole animal imaging studies and was found to be sufficient for detecting dye-labelled constructs in draining lymph nodes (Figure 4.1). As infrared dyes are not suitable for the flow cytometer configuration used in these studies, alternative constructs were prepared with a green dye that is compatible with the laser and detector configuration of the instruments used herein.

Importantly, Poly-7/8a and controls were produced to independently assess how morphology and agonist density influences *in vivo* activity. To evaluate the influence of agonist density independent of the morphology of the carrier, two particle-forming Poly-7/8a were prepared with either low (Lo ~ 3%) or high (Hi ~ 10%) agonist density, referred to as PP-7/8a^{Lo} and PP-7/8a^{Hi}, respectively (Table 4-1). Furthermore, comparing the low agonist density polymer coil and polymer particle (PC-7/8a^{Lo} and

PP-7/8a^{Lo}), which are matched for TLR-7/8a dose and density, allows for the evaluation of the influence of morphology independent of agonist density.

Adjuvant or control	Agonist-linker or Control-linker	Agonist density (mol% 7/8a)	Particle size diameter, nm (± std dev)	TLR 7/8a dose (nmoles)	Polymer mass (g)
SM-7/8a	7/8a	N.A.	N.A.	62.5	∅
PC	AP-PEG	10	13 (±5)	∅	300
PC-7/8a^{Lo}	7/8a-PEG	3	12 (±4)	62.5	300
PP	AP-AMPH	8	603 (±48)	∅	120
PP-7/8a^{Lo}	7/8a-PEG / A PAMPH	3 / 5	817 (± 200)	62.5	300
PP-7/8a^{Hi}	7/8a-PEG	10	688 (±55)	62.5	120

Morphology
Small molecule (SM)
Polymer coils (PC)
Polymer particles (PP)

Table 4-1: Infrared-dye (IR Dye 800cw) labelled Poly-7/8a, small molecule and polymer controls. Note: polymer-dye conjugates were prepared with either ~ 0.5 mol% Alexa fluorophore 488 (AF488) or 0.5 mol% IR-Dye800cw using the same polymer precursor. The small molecule TLR 7/8a is conjugated to a single dye molecule. Particle size was evaluated by dynamic light scattering and is reported as mean ± SD (n = 3). See materials and methods for additional details.

4.3 Biodistribution and kinetics of SM 7/8a and Poly-7/8a

Dual-modality imaging was used to evaluate how different physicochemical parameters influence localization of materials at various timepoints following subcutaneous administration. As shown in the example in Figure 4.1, anatomical localization of the fluorescence signal was determined in a three-step protocol: (1) epifluorescence was used to visualize and quantify the fluorescence signal; (2) an X-ray image was obtained to visualize tissues with contrasting densities, and (3) the two images were merged to identify the anatomical origin of the fluorescence signal. In the example, image overlay confirms that a dye-labelled polymer localizes to the site of injection and the proximal draining lymph node following subcutaneous administration.

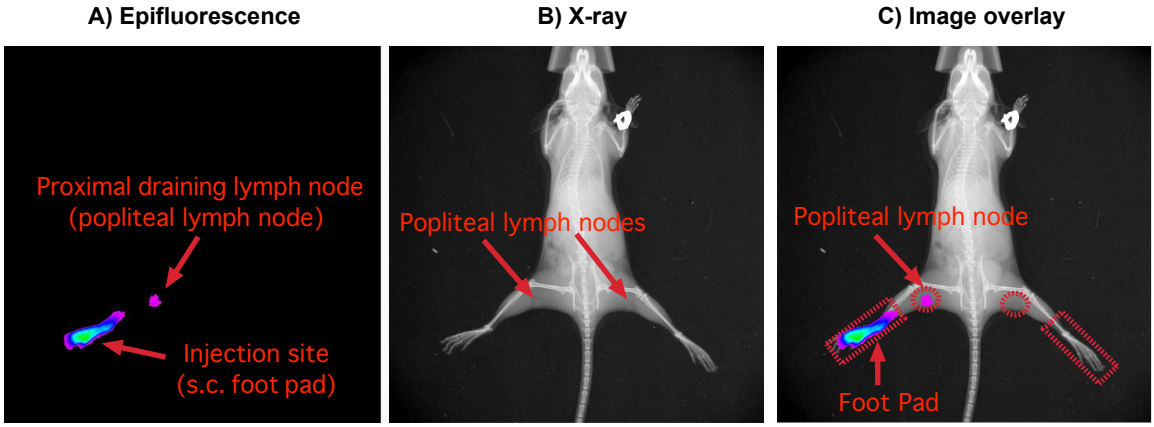

Figure 4.1: Example of dual-modality imaging protocol used to assess biodistribution and kinetics. Poly-7/8a (PP-7/8a^{Hi}) labelled with IR-Dye800cw was subcutaneously administered into the left rear footpad of a mouse. Images were acquired 24 hours after administration: (A) The site of injection and proximal draining lymph node (popliteal) are both readily evident in the epifluorescence image. (B) Popliteal lymph nodes are visible in the X-ray image with prominent lymphadenopathy observed in the draining lymph node but not the lymph node contralateral to the injection site. (C) Image overlay confirms that the dye-labelled polymer is predominantly localized to the injection site and the proximal draining lymph node.

Biodistribution

Following subcutaneous footpad administration of dye-labelled materials (Table 4-1), mice were imaged serially for up to 20 days. A subset of the images is shown in Figure 4.2 and provides a visual representation of the kinetics data shown in Figure 4.3. The small molecule (SM 7/8a) exhibited rapid systemic distribution and was present at high concentrations in the bladder at 6 hours after administration, suggesting high tissue extravasation and renal elimination. After 24 hours, the small molecule TLR-7/8a was undetectable. In contrast, all variants of Poly-7/8a and polymer controls were retained locally and were detectable in draining lymph nodes for over 20 days (see kinetics data for full time course: Figure 4.3).

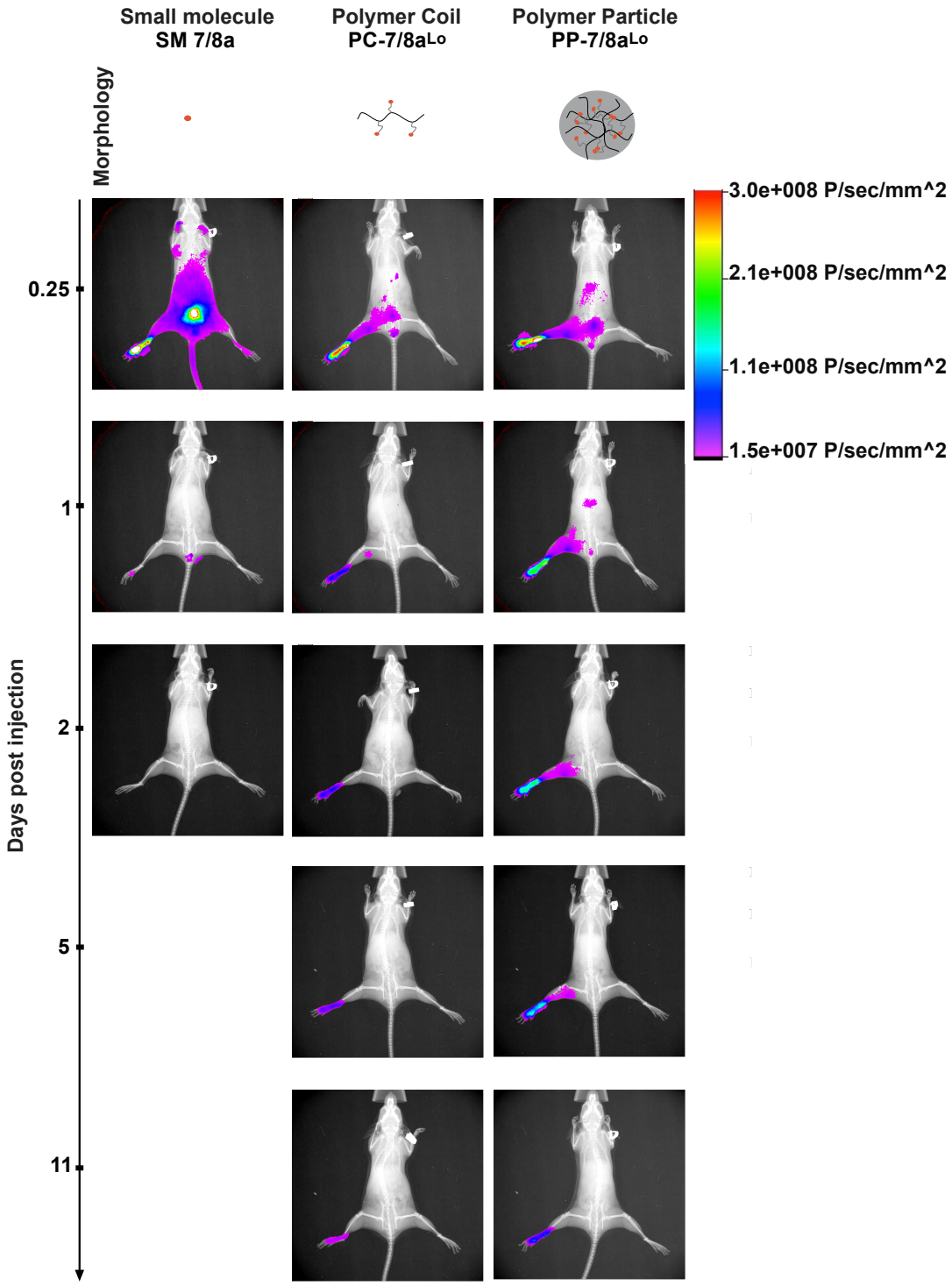

Figure 4.2: Biodistribution of IR dye-labelled small molecule TLR-7/8a (SM 7/8a), polymer coil (PC-7/8a^{Lo}) and polymer particle-forming Poly-7/8a (PP-7/8a^{Lo}). Mice (n = 3) received a single subcutaneous injection at t = 0 and were imaged serially at timepoints thereafter. The above images show the fluorescence and X-ray image overlay for a representative mouse from each group for up to 11 days after vaccination.

Kinetics

Standard curves that relate fluorescence emission (photons/sec) to TLR-7/8a concentration were used to determine the amount of TLR-7/8a (nmoles) in popliteal lymph nodes. As shown in Figure 4.3, TLR-7/8a morphology had the largest influence on lymph node kinetics. The maximum dose of the small molecule (SM 7/8a) that was detected in the draining lymph nodes was less than 1/10th that of all variants of Poly-7/8a. While the SM 7/8a was undetectable in draining lymph nodes after 2 days, all variants of Poly-7/8a and polymer controls were detected in the draining lymph nodes for up to 20 days. Importantly, the dose of polymer particles was nearly 2-fold higher at 4 days and nearly 5-fold higher at 20 days as compared with the polymer coils. These data suggest that size / morphology of the carrier has the largest influence on biodistribution and is largely independent of the pharmacological activity of the agonist.

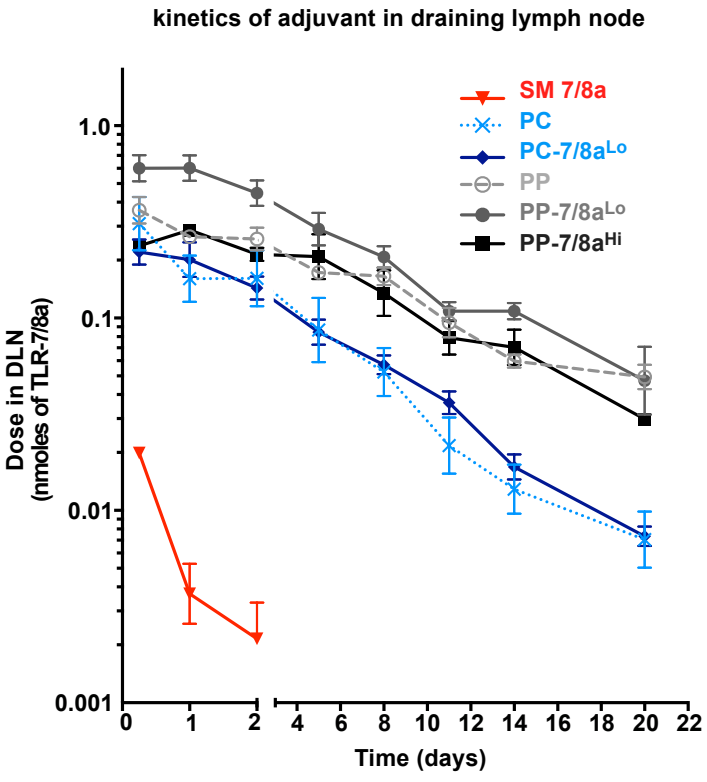

Figure 4.3: Kinetics of IR dye-labelled materials in popliteal lymph node. Materials were normalized for TLR-7/8a dose (62.5 nmoles) and administered subcutaneously into mice (n = 3) that were serially imaged at various timepoints thereafter. Data are reported as mean ± SEM. Data are representative of two independent experiments. Note that evaluation of TLR-7/8a dose for *ex vivo* lymph nodes yielded comparable results.

4.4 Adjuvant uptake by lymph node DC populations

The previous studies evaluated the influence of carrier morphology and TLRa density on anatomical distribution and kinetics. The next studies assessed how these properties influence uptake by the major dendritic cell (DC) populations in lymph nodes.

Following subcutaneous administration of different dye-labelled materials in mice, the major $CD11c^+$ DC populations in the proximal draining lymph node were evaluated for adjuvant uptake and activation by flow cytometry. As shown in the gating tree, Figure 4.4, applying gates that defined single (non-aggregated) leukocytes removed events related to blood cells, platelets and other debris. Non-viable cells, as well as $CD3^+$ (T cells), $NK1.1^+$ (natural killer) and $CD19^+$ (B cells) cells were gated out. The remaining cells were gated for $CD11c^+$ events, which represent total DCs. The total DC population can be divided into three subsets: (1) $CD8^-$ / $B220^-$ DC, which represent a heterogeneous population comprised of migratory DCs and lymph node resident $CD8^-$ conventional DC ($CD8^-$ cDC); (2) lymph node resident $CD8^+$ cDC, which are specialised for antigen cross-presentation; and, (3) $B220^+$, pDCs, which are known to produce high amounts of Type I IFN. Importantly, while the migratory DCs, resident $CD8^-$ DCs and pDCs express TLR-7 and have been shown to produce cytokines in response to TLR-7 stimulation *in vitro*[34], $CD8^+$ DCs show limited TLR-7 expression but do upregulate co-stimulatory molecules in response to

TLR-7/8a exposure *in vivo*[174], suggesting an indirect role for the activation of these DCs by TLR-7/8a. Total DCs, or individual DC subsets, were then evaluated for material uptake (AF488^{+}) and activation (CD80 and CD86 expression).

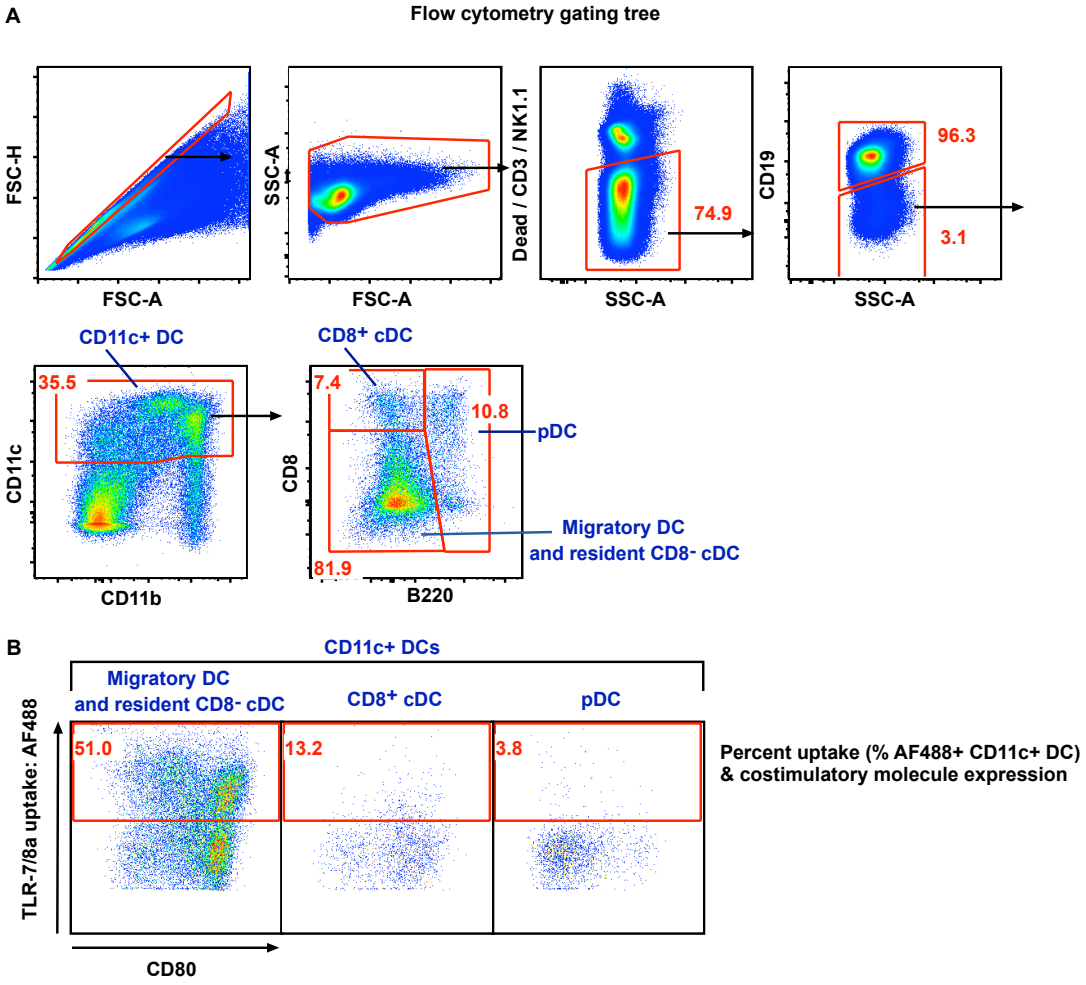

Figure 4.4: In vivo tracking of Alexa-fluorophore 488 (AF488) dye-labelled constructs. (A) Example gating tree that was used to quantify the number, costimulatory molecule expression (CD80 and CD86) and adjuvant uptake (AF488+) status of the major DC populations in draining lymph nodes and spleen. DC = dendritic cells; cDC = conventional DC; pDC = plasmacytoid DC.

The proportion of DCs positive for adjuvant uptake in draining lymph nodes was evaluated following subcutaneous administration of the different dye-labelled constructs (PP-7/8a^{Hi}, PP-7/8a^{Lo}, PC-7/8a^{Lo}, SM 7/8a and PP and PC controls Table 4-1). Independent of agonist density or morphology, all Poly-7/8a localized with 30-60% of the migratory and resident cDC populations over the first 8 days (Figure 4.5B-C), whereas the percentage of pDCs positive for uptake of any variant of Poly-7/8a was less than 10% over the first 4 days, and was less than 1% by day 8 (Figure 4.5D). These data show that all variants of Poly-7/8a, independent of agonist density or morphology of the carrier, primarily localize with migratory and resident cDC populations, rather than pDCs. In contrast, the SM 7/8a localized with all DC populations to a similar extent on day 1 but was undetectable after 4 days.

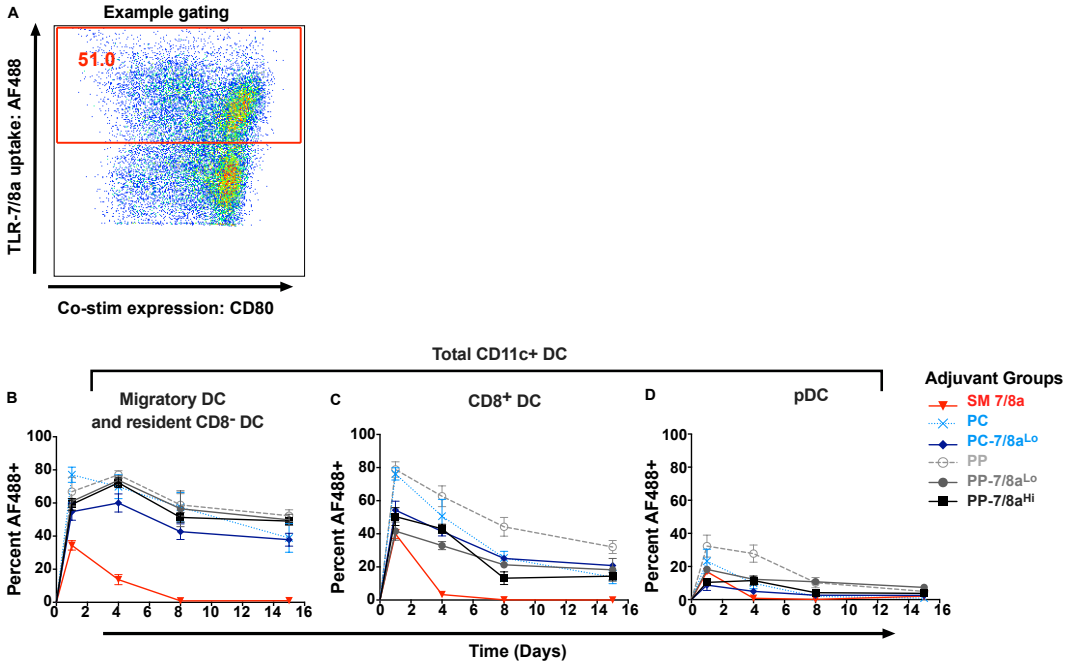

Figure 4.5: Cellular localization of Alexa-fluorophore 488 (AF488) dye-labelled constructs. Dye-labelled materials normalized for TLR-7/8a dose (62.5 nmoles) were delivered subcutaneously to the left footpad of mice and draining lymph nodes (n = 3) were harvested at serial timepoints and evaluated by flow cytometry. (A) Example gate of AF488 uptake and CD80 expression. (B-D) Different DC subsets were evaluated for adjuvant uptake (% AF488+). All data are represented as mean ± SEM.

While Figure 4.5 shows the proportion of each DC population that stain positive for dye-labelled constructs, it does not account for the relative amount of material uptake on a per cell basis. As a semi-quantitative means of material uptake, the median fluorescence intensity (MFI) of AF488 was evaluated for total adjuvant positive $CD11c^{+}$ DCs. Note that the low event rate for adjuvant uptake by pDCs does not permit calculation of population statistics (e.g., MFI) and therefore the aggregate $AF488^{+}$ $CD11c^{+}$ DC population was used for the calculation of the AF488 MFI shown in Figure 4.6.

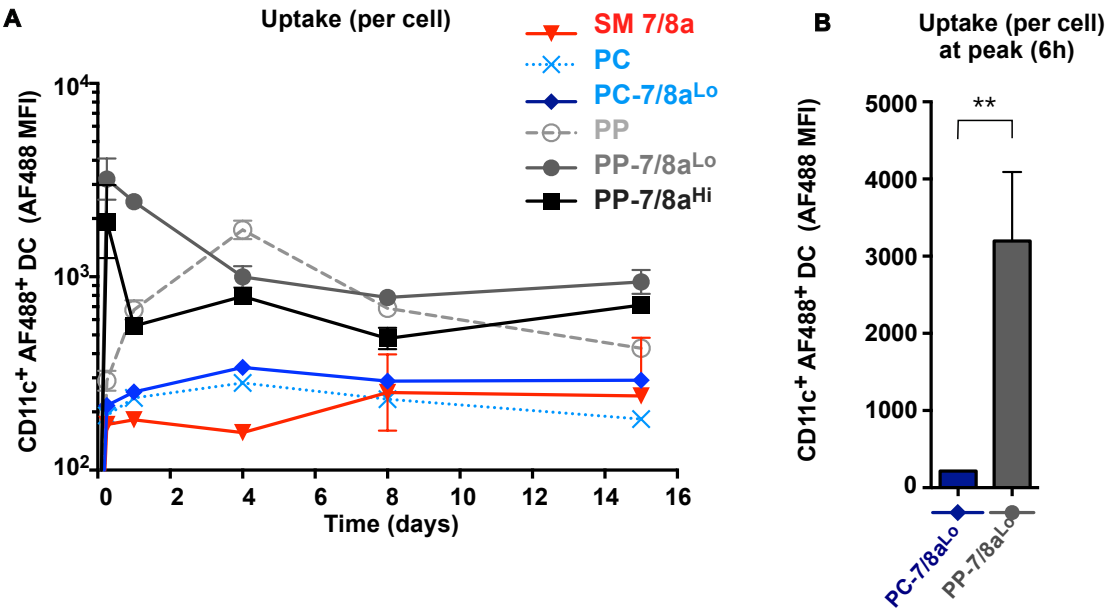

Figure 4.6: Particles promote enhanced uptake by DCs. Relative adjuvant uptake by total CD11c+ AF488+ DC was evaluated by measuring the median fluorescence intensity (MFI), which is proportional to material uptake on a per cell basis. (A) Uptake efficiency for all groups at serial time points. (B) Comparison of TLR-7/8a dose- and density-matched Poly-7/8a with polymer coil and polymer particle morphologies (PC-7/8^{Lo} vs. PP-7/$8a^{Lo}$) allows for evaluation of the influence of morphology on uptake. All data are represented as mean ± SEM (n = 3).

Morphology was the primary factor influencing Poly-7/8a uptake by DCs. Nearly 10-fold higher levels of AF488 (MFI) were observed for polymer particles (PP-7/8^{Hi}, PP-7/8^{Lo} and PP) as compared with the polymer coils (PC-7/8^{Lo} and PC) and SM-7/8a

(Figure 4.6). This trend is especially evident when comparing the low agonist density polymer particle (PP-7/8a^{Lo}) with the low agonist density polymer coil (PC-7/8^{Lo}), which are matched for both agonist density (3 mol% 7/8a) and TLR-7/8a dose (62.5 nmoles): the polymer particle is taken up nearly 20-fold higher than the polymer coil (Figure 4.6B). In contrast, all polymer particles (PP-7/8a^{Hi}, PP-7/8a^{Lo} and PP) exhibited similar uptake on a per cell basis, suggesting that the agonist has little influence on cellular uptake. Altogether, these data show that size / morphology, independent of the type or density of agonist attached, are critical factors that influence DC uptake.

4.5 Magnitude and spatiotemporal characteristics of innate immune activation

The prior sections established that particulate morphologies are important for local retention and uptake by APCs. To evaluate how these factors influence downstream DC recruitment and activation, lymph node DCs from immunized mice were quantified and characterized for the expression of co-stimulatory molecules (CD80 and CD86). The particle-forming Poly-7/8a (PP-7/8a^{Hi} and PP-7/8^{Lo}) led to significantly higher (~ 10-20 fold) levels of DC recruitment across all populations (Figure 4.7A). The largest increases were observed for the migratory DC and CD8^{-} DC population, where the lymph node DC population increased from 1,000 to about 20,000 cells over 15 days. Higher magnitudes of cellular recruitment was also associated with significant increases in the magnitude and duration of co-stimulatory molecule expression by migratory and resident cDC, but not pDCs (Figure 4.7B-C). In contrast, poorly retained SM 7/8a did not enhance DC recruitment but did induce transient (< 24 h) increases in the activation of all DC subsets. Notably, the polymer

coil Poly-7/8a (PC-7/8a^{Lo}) did not promote the recruitment or activation of DCs in draining lymph nodes. Moreover, polymer coil-based Poly-7/8a (PC-7/8a^{Lo}) across a range of precisely defined molecular weights (~ 5 to 300 kDa) were all found to be incapable of inducing cytokine production in lymph nodes (data not shown), suggesting that the Poly-7/8a that exist predominantly as polymer coils in aqueous conditions are inactive *in vivo*. Altogether, these data demonstrate that particulate morphology is a critical determinant of Poy-7/8a activity, which requires high lymph node retention and efficient DC uptake to induce high levels of DC recruitment and activation.

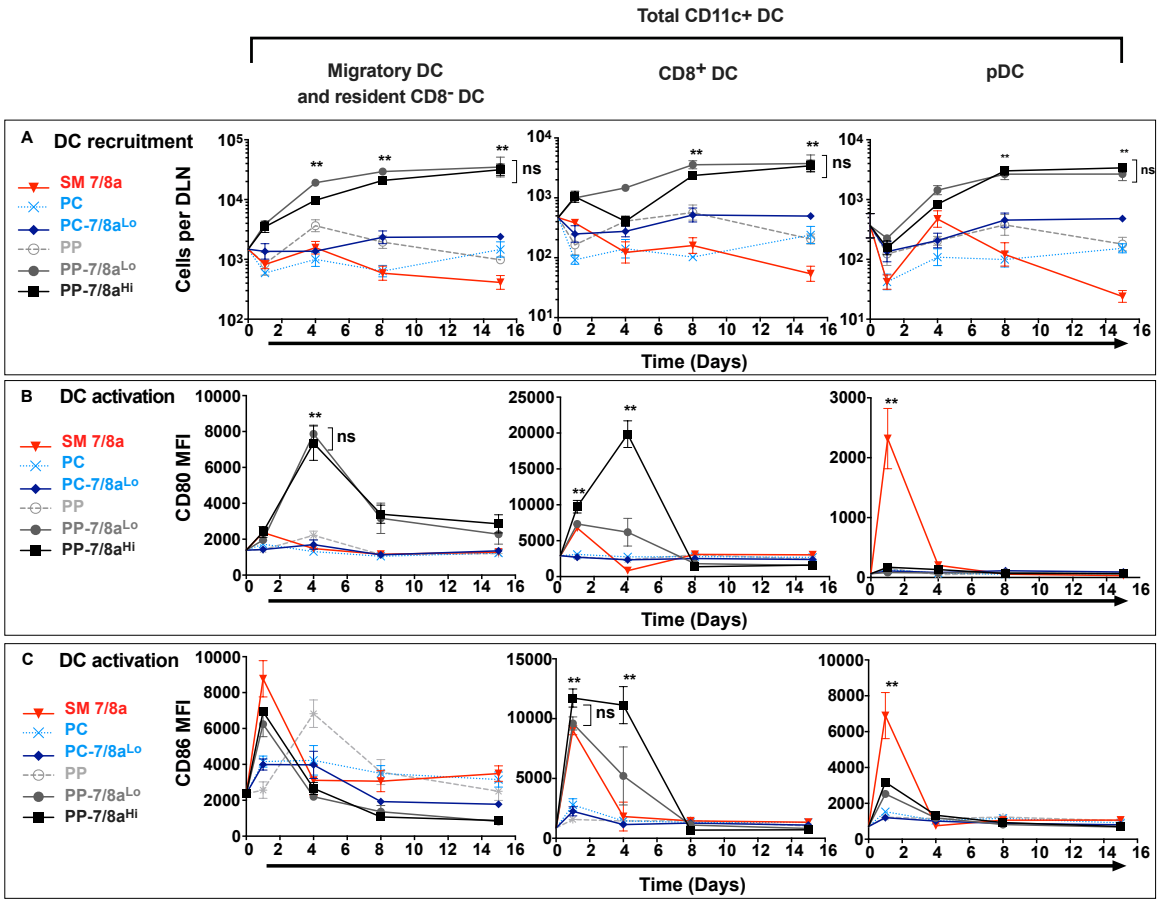

Figure 4.7: Recruitment and activation of CD11c^{+} DC in draining lymph nodes. Following subcutaneous administration of dye-labelled materials normalized for TLR-7/8a dose (62.5 nmoles), draining lymph nodes (n = 3) were harvested at serial timepoints and evaluated by flow cytometry. Subsets of total CD11c^{+} DC were (A) quantified and evaluated for expression of the co-stimulatory molecules (B) CD80 and (C) CD86. All data are represented as mean ± SEM.

The prior data demonstrate that local retention of particle-forming Poly-7/8a leads to persistent innate immune activation in draining lymph nodes. The next studies assessed whether SM 7/8a or Poly-7/8a induce the activation of splenic DCs following subcutaneous administration (Figure 4.8). While no variant of Poly-7/8a induced splenic DC activation above background levels (Figure 4.8), systemic distribution of the SM-7/8a was associated with ~ 4-fold increases in expression of CD80 and CD86 by all $CD11c^{+}$ DC populations in the spleen.

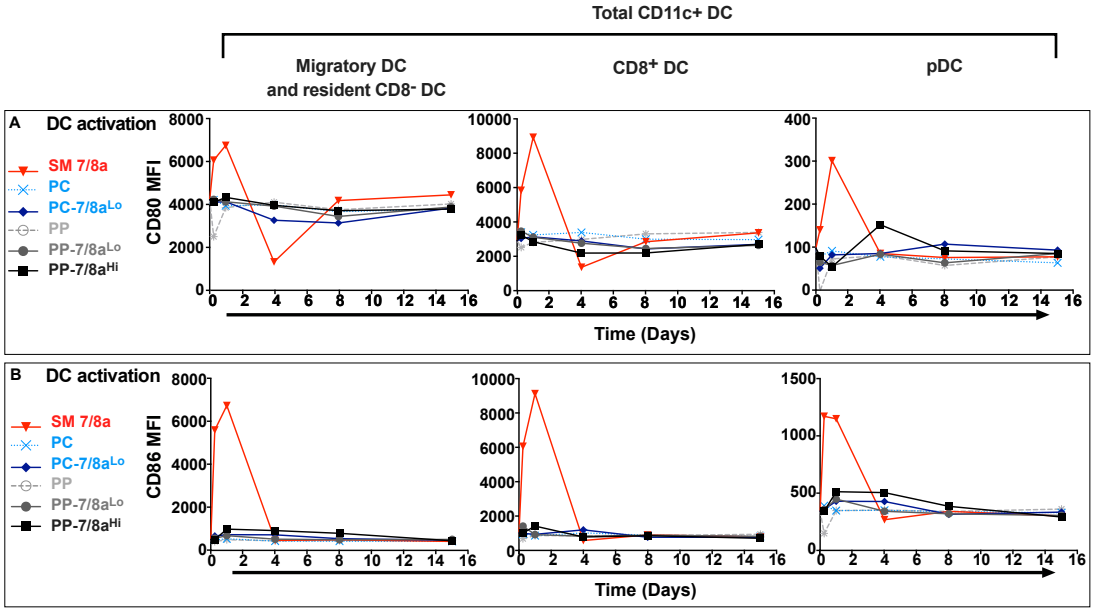

Figure 4.8: Activation of $CD11c^{+}$ DC in spleen following local adjuvant delivery. Following subcutaneous administration of dye-labelled materials normalized for TLR-7/8a dose (62.5 nmoles), spleens (n = 1) were harvested at serial timepoints and evaluated by flow cytometry. (A) Subsets of total $CD11c^{+}$ DC were evaluated for expression of the co-stimulatory molecules (B) CD80 and (C) CD86.

4.6 Magnitude and spatiotemporal characteristics of cytokine production

Whereas flow cytometry was used to characterize phenotypic markers of DC activation (CD80 and CD86 expression), IL-12 production from lymph nodes and serum were used as biomarkers downstream of DC activation. The timing and location of IL-12 production (Figure 4.9) was closely associated with the kinetics of DC activation observed in Figure 4.7 and Figure 4.8. The SM 7/8a that induced transient and high levels of splenic DC activation induced high levels of serum IL-12 but limited production of lymph node IL-12. In contrast, the locally retained particle forming Poly-7/8a (PP-7/8^{Hi} and PP-7/8^{Lo}) that induces significant DC recruitment and activation in lymph nodes leads to significantly higher lymph node IL-12 production as compared with all other groups. Whereas particulate morphology is a critical determinant of the magnitude of innate immune responses in draining lymph nodes, increasing agonist density (3 to 10 mol% 7/8a) on PP-7/8a was associated with increased persistence of lymph node IL-12 production.

Altogether, these data (Figure 4.7, Figure 4.8, Figure 4.9) demonstrate that the location and kinetics of APC activation closely follow that of cytokine production. Locally retained particle-forming Poly-7/8a that induce persistent lymph node DC activation lead to persistent lymph node IL-12 production, whereas the systemically distributed SM 7/8a that induces robust splenic DC activation leads to high levels of transient cytokine production.

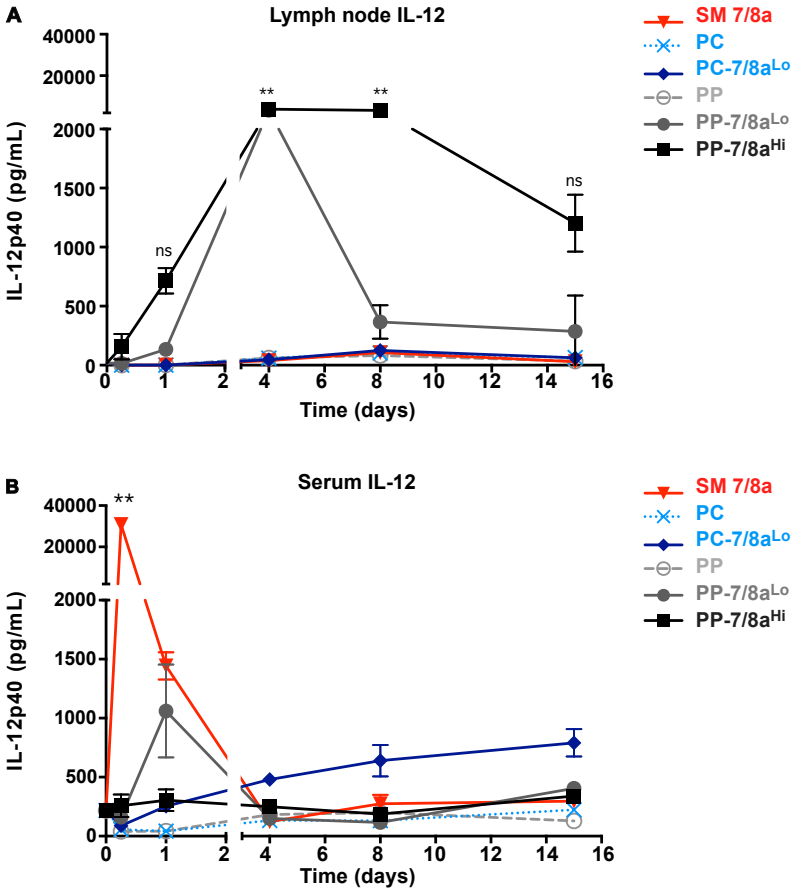

Figure 4.9: Particle-forming Poly-7/8a induce persistent lymph node but not systemic IL-12 production. Following subcutaneous administration of Poly-7/8a, SM 7/8a and polymer controls normalized for dose (see Table 4-1), either (A) lymph node cell suspensions (n = 4) or (B) serum (n = 5) were evaluated for IL-12 by ELISA. All data are represented as mean ± SEM.

4.7 CD8 T cell and antibody responses to a model immunogen

To assess how the location, magnitude and duration of innate immune activation influences adaptive immune responses, a model antigen, ovalbumin (OVA), was co-administered with SM 7/8a, Poly-7/8a or controls in a homologous prime-boost immunization scheme (Figure 4.12). Two weeks following two immunizations, whole blood was evaluated for the proportion of total CD8 T cells that bind a tetramer (MHC I molecule bound to the immunodominant CD8 peptide from OVA, SIINFEKL), which defines the majority of the antigen-specific CD8 T cell response

to OVA. As shown in Figure 4.12, the particle-forming Poly-7/8a with high agonist density (PP-7/8a^{Hi}) resulted in significantly higher CD8 T cell responses (~ 8%) as compared with the particle-forming poly-7/8 with low agonist density (PP-7/8a^{Lo}) that induces similar magnitude but less persistent lymph node innate immune responses. These data suggest that persistent local innate immune activation is critical for inducing CD8 T cell responses. Consistent with this observation, the SM 7/8a that induces only transient lymph node innate immune activation did not elicit CD8 T cells to OVA. Limited CD8 T cell responses (< 0.1%) were also observed for OVA co-administered with either the polymer controls (PP or PC) or OVA administered without adjuvant.

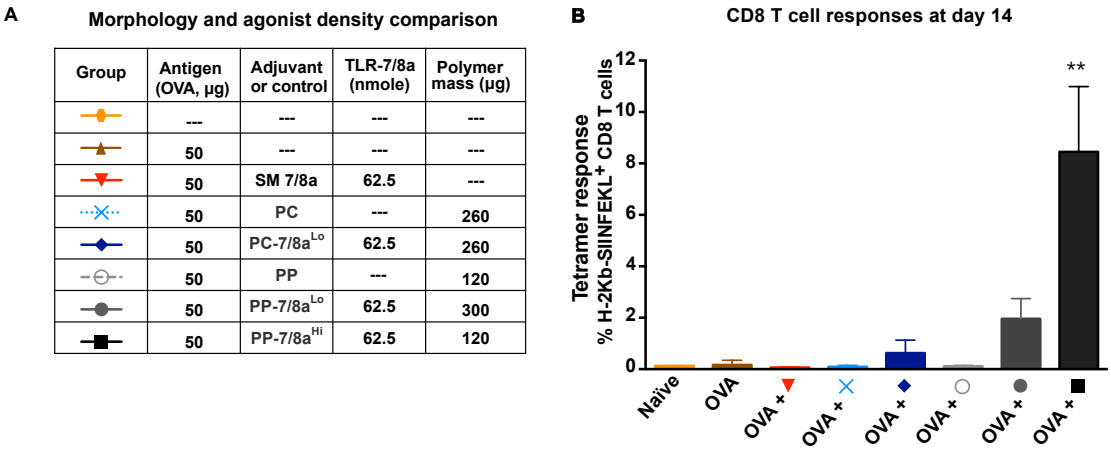

Group	Antigen (OVA, µg)	Adjuvant or control	TLR-7/8a (nmole)	Polymer mass (µg)
	---	---	---	---
	50	---	---	---
	50	SM 7/8a	62.5	---
	50	PC	---	260
	50	PC-7/8a^{Lo}	62.5	260
	50	PP	---	120
	50	PP-7/8a^{Lo}	62.5	300
	50	PP-7/8a^{Hi}	62.5	120

Figure 4.10: Particle-forming Poly-7/8a enhances the magnitude of CD8 T cell and antibody responses to a co-administered protein antigen. (A) Doses of OVA and adjuvant administered to C57BL/6 mice (n = 5) at days 0 and 14. (B) At day 28, tetramer^{+} CD8 T cell responses were evaluated from whole blood of vaccinated mice. All data are represented as mean ± SEM; statistical significance is relative to all other groups.

The durability of the CD8 T cell responses induced by the particle forming Poly-7/8a (PP-7/8a^{Hi}), relative to controls, was assessed following immunizations at day 0 and 14. The CD8 T cell responses measured at day 28 (~ 6%) were significantly higher than those observed with OVA either co-administered with the SM 7/8a or polymer controls, or OVA administered alone. Moreover, the responses induced by PP-7/8a^{Hi} were maintained above 1% up to 10 weeks after the last vaccination, indicating that the Poly-7/8a optimized for prolonged lymph node innate immune activation leads to high magnitude and durable CD8 T cell responses.

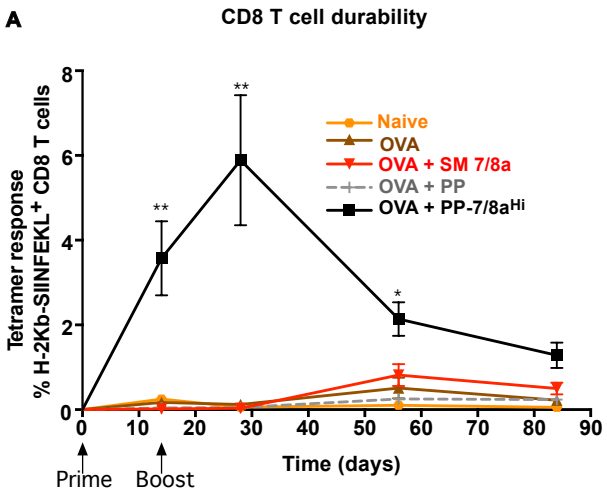

Figure 4.11: PP-7/8a^{Hi} induces durable tetramer^{+} CD8 T cell responses. PP-7/8a^{Hi}, SM 7/8a or a control were formulated with 50 µg of OVA in PBS and given subcutaneously to C57BL/6 mice (n = 5) at days 0 and 14. Mice (n = 5) were bled at days 14, 28, 56 and 84 and antigen-specific CD8 T cell responses were evaluated using a tetramer. All data are represented as mean ± SEM; statistical significance is relative to all other groups.

To assess the influence of the formulation of the TLR-7/8a on humoral immunity, mice were bled 10 days after the second immunization and serum antibodies were measured against OVA (Figure 4.12). The magnitude of antibody responses against OVA were comparable to that observed for the CD8 T cell responses. PP-7/8a^{Hi} elicited the highest anti-OVA IgG titre; however, unlike the CD8 T cell data, all Poly-

7/8a—independent of morphology or agonist density—induced similar anti-OVA total IgG endpoint titres (~ 10^6). As observed with the CD8 T cell responses, the antibody responses elicited by the SM 7/8a or polymer controls co-administered with OVA were indistinguishable from the responses induced by OVA protein administered without adjuvant. Serum from immunized mice was also evaluated for hapten antibodies against the ligands (either the TLR-7/8a or AP) arrayed on the Poly-7/8a and polymer controls. The data show that all Poly-7/8a formulations induce hapten antibodies, but that the particulate formulations of Poly-7/8a (PP-7/8a) lead to the highest hapten antibody titres.

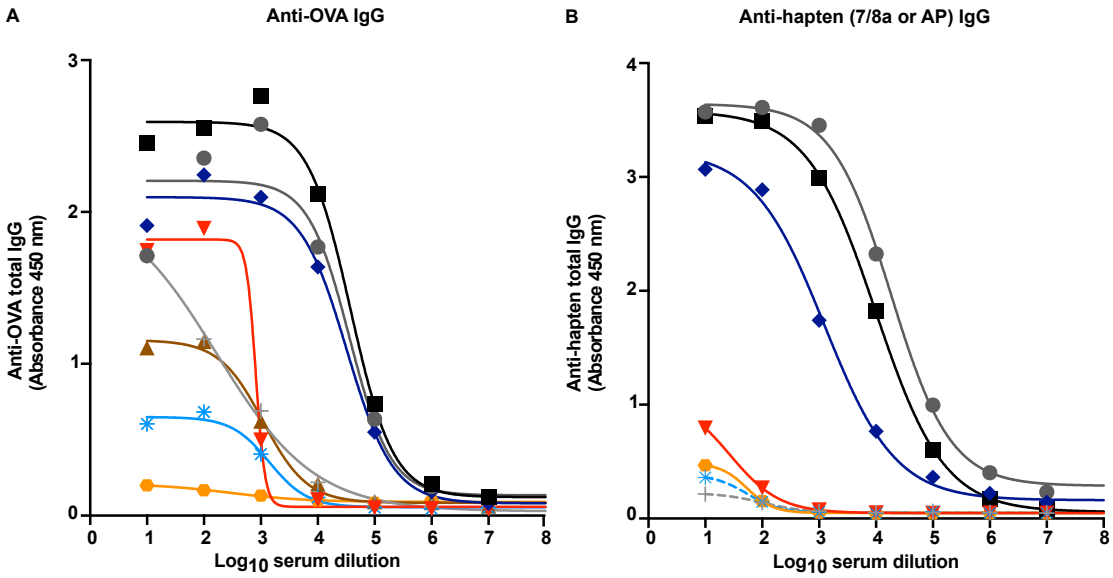

Figure 4.12: Particle-forming Poly-7/8a enhances the magnitude of antibody responses to a co-administered protein antigen. Serum from vaccinated mice was evaluated for (A) total IgG antibodies against OVA and (B) total IgG against the small molecule haptens (TLR-7/8a or AP). Notably, all Poly-7/8a induce antibodies against the TLR-7/8a, whereas vaccination with the small molecule, SM 7/8a, does not elicit hapten antibodies. All data are represented as mean ± SEM; statistical significance is relative to small molecule TLR-7/8a and polymer controls.

4.8 Poly-7/8a co-administered with protein antigen ensures efficient co-delivery to lymph node DCs

Prior studies suggest that co-delivery of protein antigen and TLR-7/8a to DCs is important for inducing T cell responses as well as preventing tolerance[136, 137, 139-141] Accordingly, co-delivery can be achieved by physically linking TLRa to protein antigen[106, 107, 116]. While ensuring efficient co-delivery of protein and TLRa, these strategies can lead to covalent modification of epitopes on proteins that are important for recognition by neutralizing antibodies. Alternatively, co-administering protein with adjuvants that are taken up efficiently by APCs can promote efficient co-delivery without the need for modifying the protein antigen.

The next studies assessed the efficiency of co-delivery of antigen and adjuvant (co-localization with DCs) following the co-administration of OVA with either the small molecule (SM 7/8a) or polymer particle with high agonist density (PP-7/8a^{Hi}). To facilitate tracking by flow cytometry, the SM 7/8a and PP-7/8a^{Hi} were labelled with AF488, and OVA was labelled with AF647. Following subcutaneous footpad administration, lymph nodes were isolated at 1, 3 and 7 days and total CD11c^{+} DC were evaluated for uptake of either adjuvant, protein, or both Figure 4.13. Representative flow plots are shown for the peak timepoint for protein uptake by draining lymph node DCs (day 3). The SM 7/8a is poorly retained and does not effectively recruit DCs to the lymph node, resulting in < 10% co-delivery to lymph node DCs. In contrast, the high lymph node retention of PP-7/8a^{Hi} leads to a significant increase in DC recruitment and results in ~ 80, 70% and 90% of the protein antigen co-delivered with TLR-7/8a at days 1, 3 and 7. These data show that

co-administration of a protein antigen with a locally retained polymer-based adjuvant (PP-7/8a^{Hi}) leads to efficient co-delivery.

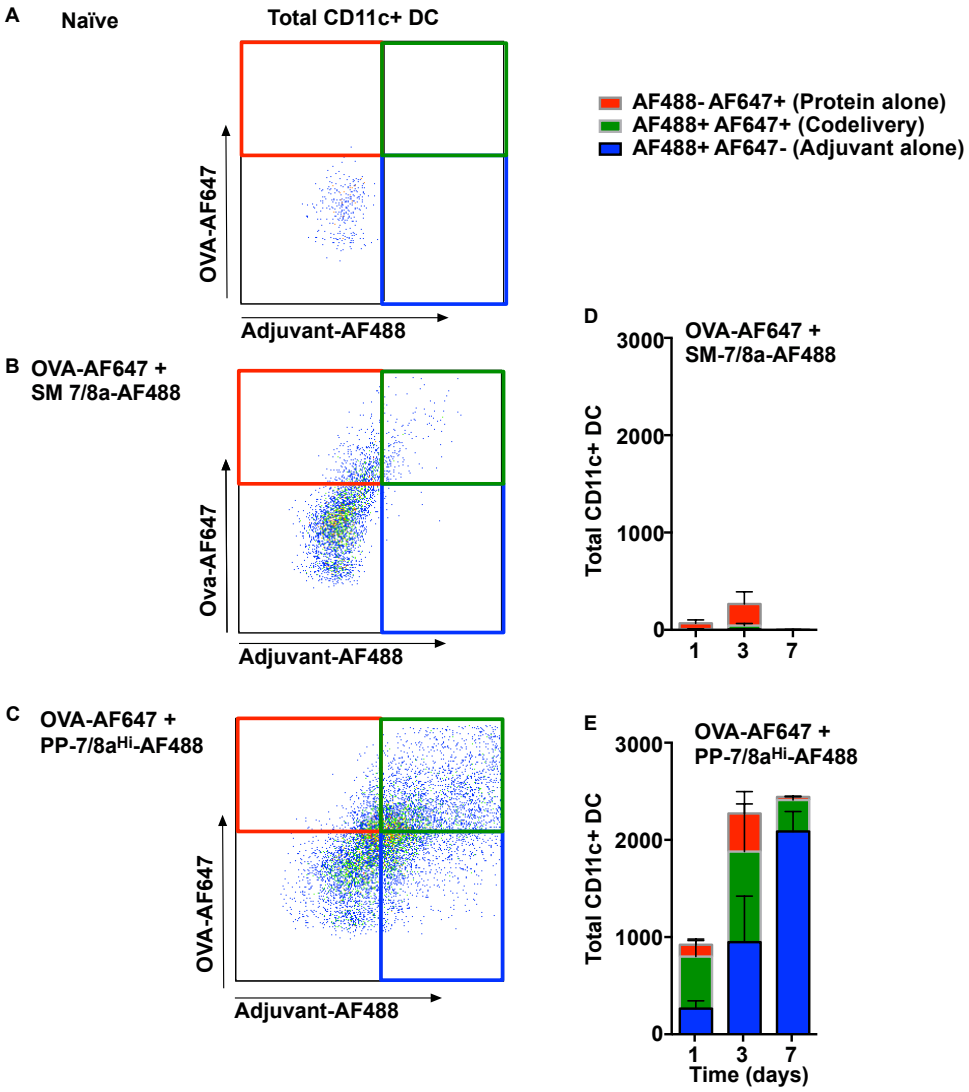

Figure 4.13: Co-administration of OVA with PP-7/8a^{Hi} leads to efficient co-delivery to CD11c^{+} DCs in draining lymph nodes. OVA-AF647 (50 µg) and either PP-7/8a^{Hi}-AF488 or SM 7/8a-AF488 (62.5 nmoles) were administered to C57BL/6 mice. At serial timepoints thereafter, popliteal lymph nodes (n = 3) were evaluated by flow cytometry. Total CD11c+ DCs (per draining lymph node) were evaluated for uptake of antigen (OVA-AF647+) and adjuvant (AF488+). Representative flow plots for (A) naïve, (B) OVA-AF647 + SM 7/8a-AF488 and (C) OVA-AF647 + PP-7/8a^{Hi}-AF488 vaccine groups for the day 3 time point are shown. (D, E) The magnitude of total CD11c^{+} DCs per lymph node that are either positive for protein alone (AF488- AF647+), adjuvant alone (AF488+ AF647-) or have taken up both protein and adjuvant (co-delivery, AF488+ AF647+) was quantified by flow cytometry. All data are represented as mean ± SEM.

4.9 Increasing agonist potency and dose are associated with persistent lymph node cytokine production and higher magnitude CD8 T cell responses

The next studies evaluated the influence of agonist potency and dose on the magnitude and persistence of innate immune activity as well as the elicitation of CD8 T cells in the context of vaccination.

A compound structurally related to SM 7/8a was prepared as recently described[69, 155] and evaluated for activity *in vitro* (Figure 4.14). Note that *in vitro* assays are valid for evaluating potency of small molecules, as cellular uptake and access to endosomally localized TLRa are not considered rate-limiting processes. Whereas the R848 analogue (SM 7/8a) has a half maximal effective concentration (EC50) of ~ 2 μM, modifying the side group and linker on SM 7/8a to increase hydrophobic character and planarity enhances the potency and reduces the EC50 to ~ 0.1 μM; for simplicity, this compound with a 20-fold greater potency (as compared with SM 7/8a) is referred to as SM 20x7/8a (Figure 4.14).

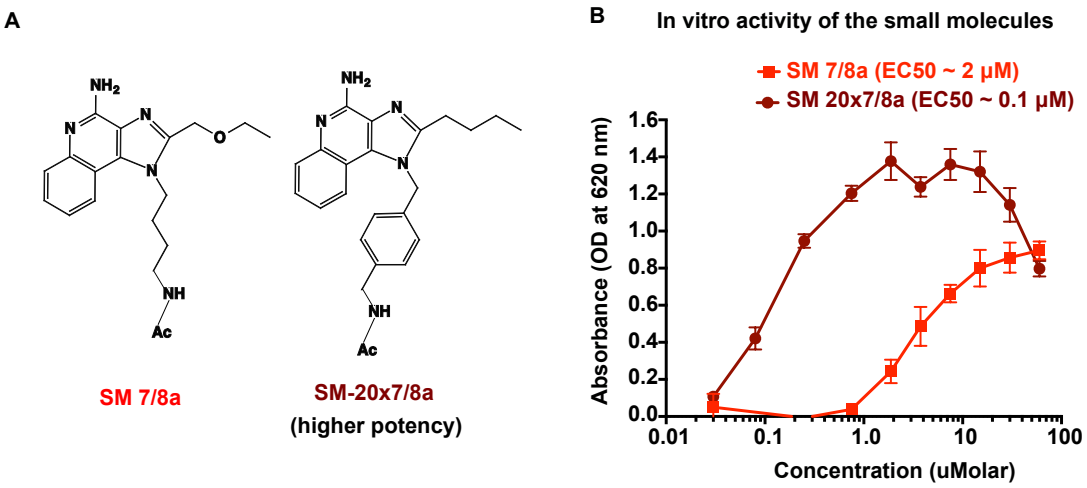

Figure 4.14: Structure and activity of SM 7/8a and SM 20x7/8a. (A) Structures of acetylated (CH3CO) agonist; note that acetylated agonists were used as this small molecule derivative most closely represents the physical and chemical properties of the TLR-7/8a when attached to the polymer backbone through an amide bond. (B) The potency of the TLR-7/8a was evaluated in vitro using HEK293 hTLR7 reporter cells; absorbance at 620 nm is proportional to TLR7 binding.

To evaluate how agonist potency and dose influences innate immune activation, Poly-7/8a were prepared with high densities (~ 10 mol%) of either SM 7/8a or SM 20x7/8a (Figure 4.15A), and these materials were evaluated for the capacity to induce lymph node production of IL-12 at different timepoints after subcutaneous footpad administration. Increasing doses of Poly-7/8a led to saturation of the magnitude of IL-12 production between 1 and 4 days after immunization, with the major differences arising only at later timepoints (Figure 4.15). When comparing PP-7/8a^{Hi} with the dose matched (12.5 nmoles) Poly-7/8a carrying the 20-fold more potent agonist (PP-20x7/8a^{Hi}), the more potent Poly-7/8a induced similar early magnitude but more persistent lymph node cytokine production. While earlier studies in this chapter used both flow cytometry and innate cytokine production as readouts for activity of different formulations of Poly-7/8a, the flow cytometry data was found to be redundant as the observed APC activation (by flow cytometry) closely paralleled the

magnitude and duration of lymph node IL-12 production (determined by ELISA). Therefore, based on the capacity of the IL-12 kinetic to provide a comparable but lower cost and more rapid assay than flow cytometry, lymph node IL-12 kinetics were used as a screening tool to assess the magnitude and duration of innate immune activation for different adjuvant formulations for the remainder of the experiments in this thesis.

To evaluate how the magnitude and persistence of lymph node cytokine production influences the elicitation of antigen-specific CD8 T cells, mice were immunized with OVA co-administered with either PP-7/8a^{Hi} at different doses, or with PP-20x7/8a^{Hi} administered at a fixed dose. The persistence of local cytokine production correlated with the magnitude of CD8 T cell responses induced by the different doses and potencies of Poly-7/8a. These data substantiate the idea that persistence of lymph node cytokine production is critical for promoting CD8 T cell responses to co-administered protein antigen.

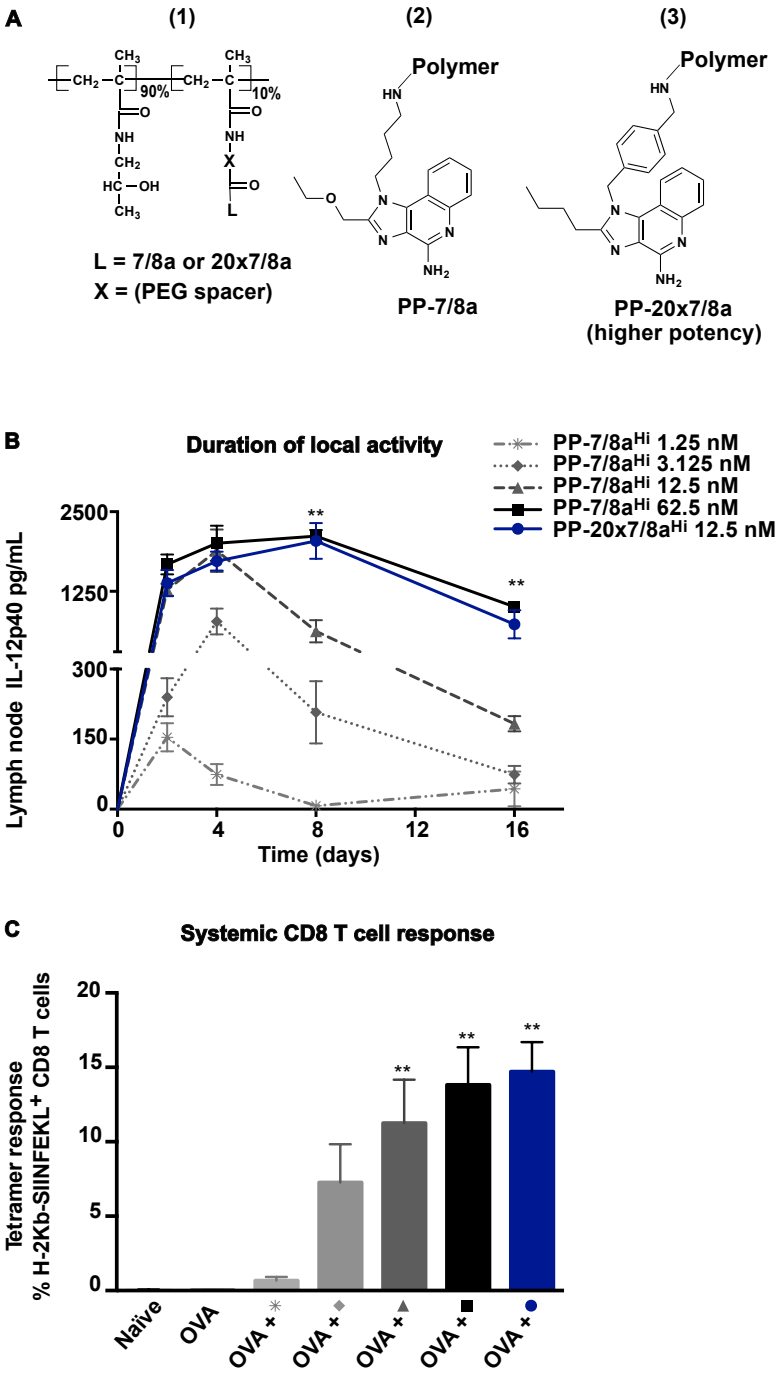

Figure 4.15: Increasing TLR-7/8a potency and dose are associated with prolonged innate immune activation and higher magnitude CD8 T cell responses. (A) Poly-7/8a (1) were prepared with high densities (~ 10 mol%) of either SM 7/8a (2) or SM 20x7/8a (3), yielding PP-7/8a^{Hi} and PP-20x7/8a^{Hi}, respectively. (B) PP-7/8a^{Hi} (1.25, 3.125, 12.5 and 62.5 nmoles) and PP-20x7/8a^{Hi} (12.5 nmoles) were subcutaneously administered into both hind footpads of C57BL/6 mice and proximal draining lymph nodes (popliteal, n = 4) were evaluated for the presence of IL-12p40. (C) Different doses of PP-7/8a^{Hi} (1.25-62.5 nmoles) or PP-20x7/8a^{Hi} (12.5 nmoles) formulated with 50 µg of OVA were delivered subcutaneously into the hind footpad of C57BL/6 mice (n = 5) at days 0 and 14. Tetramer^{+} CD8 T cells responses were evaluated at day 24 (10 days post boost).

4.10 Discussion

Accounting for biodistribution, kinetics and uptake by different DC subsets *in vivo* reveals how different physicochemical parameters of both the TLR-7/8a and polymer carrier influence the location, magnitude and duration of innate immune activation *in vivo*. These studies establish that particulate carriers of TLR-7/8a displaying high densities and potencies of the agonist are critical for inducing high magnitude and persistent (> 8 days) innate immune activation in lymph nodes that is necessary for eliciting durable CD8 T cell responses to co-administered protein antigen.

Biodistribution is the most important factor dictating the balance between local (lymph node) innate immune activity and systemic inflammation. Consistent with earlier findings, small molecule TLR-7/8a distributed systemically and resulted in high levels of transient (< 24h) systemic inflammation[83, 97, 103]. However, polymeric particle carriers of TLR-7/8a (e.g., PP-7/8a^{Hi}) were retained locally for 2-4 weeks and induced persistent local innate immune activation. Indeed, while earlier studies have shown improved activity of TLRa delivered on macromolecular or particulate carriers[107, 116, 124], or TLRa formulated within particles[121], this is the first study to demonstrate that the capacity of formulations to restrict agonist biodistribution and, therefore, increase local retention, is critical to the capacity of these delivery systems to enhance vaccine immunogenicity.

Local retention is critical but not sufficient for adjuvant activity. Despite improved retention by all polymer-based macromolecular carriers of TLR-7/8a, only Poly-7/8a that assemble into particles are taken up efficiently by APCs and induce robust and persistent innate immune responses in lymph nodes. These findings define the

mechanisms to explain earlier observations[108, 116] that protein-TLR-7/8a conjugates are markedly more immunogenic after aggregation or when adsorbed to particles, as this renders both the TLR-7/8 and protein antigen particulate.

Another consideration is how particle size influences trafficking to lymph nodes and cellular localization. Earlier work has shown that small particles (< 100 nm) passively traffic to lymph nodes and target subcapsular macrophages and lymph node resident DCs, whereas larger particles (100-1000 nm) require uptake and trafficking to lymph nodes primarily by migratory and monocyte-derived DCs[148-150]. The patterns of DC uptake observed for the particulate Poly-7/8a (~ 700 nm) are consistent with earlier findings that ~ 100-1000 nm particles are primarily trafficked to lymph nodes through uptake by migratory and monocyte-derived DCs. Indeed, our current efforts are focused on the development of Poly-7/8a that assemble into uniformly sized 100-150 nm particles that will be used to evaluate how different sizes of particles of Poly-7/8a influence *in vivo* activity. However, it is presently unclear whether passive trafficking to lymph nodes using small particles (~ 100 nm) or reverse targeting[22] using submicron or micron sized particles that stay at the site of injection will be preferable for eliciting protective immune responses using protein-based vaccines.

In addition to particle formation, increasing TLR-7/8a density, potency and dose were also associated with enhanced persistence of local innate immune activation. Potency and dose likely relate to receptor occupancy. However, improved activity by higher densities of TLR-7/8a along the polymer backbone may be accounted for by higher avidity[144] interactions and / or by the capacity of the densely arrayed TLR-7/8a to promote favourable receptor clustering[142, 143] critical for initiating intracellular

signalling cascades[36, 73]. Additional mechanisms may relate to how multimeric display of the TLR-7/8a influences TLR signalling and cytokine production[145-147], or may relate to the observation by Shukla et al that multimeric display leads to increased TLR-7 activity at the expense of TLR-8[175]. Indeed, additional mechanistic studies will be required to fully understand how agonist density influences activity.

Altogether, this work demonstrates that accounting for the pharmacokinetics and cellular localization of the adjuvant platform is critical to understanding how different properties of adjuvant delivery influence the magnitude and spatiotemporal characteristics of innate immune responses, as well as the development of downstream adaptive T cell immunity.

5 Polymer-TLR-7/8a conjugates elicit protective CD8 T cell and Th1-type CD4 T cell responses

5.1 Introduction

Prolonged innate immune activation and antigen presentation in draining lymph nodes is critical for promoting cellular immune responses to protein antigen[128-131]. However, it is presently unclear whether innate immune responses should be restricted locally at the draining lymph nodes or whether systemic (blood and spleen) innate immune responses also play a role in T cell priming to locally administered vaccines. While several studies have shown that spatially restricting adjuvant distribution to the sites of vaccine administration and draining lymph nodes using particulate carriers of TLRa enhances T cell responses while reducing systemic toxicity[121, 124, 176], the mechanism of action of many of the most effective pre-clinical adjuvants (ISCOMs[177], pICLC[56] and CpG[54] etc.) has been associated with their capacity to induce high levels of systemic innate immune activation. Thus, it is presently unclear whether purely local, systemic or a combination of local and systemic innate immune activation is critical for enhancing T cell response during vaccination. To clarify this discrepancy, there is presently a need for more thorough investigations of how location, magnitude and duration of innate immune activation influences cellular immune responses. These insights will be important for rationally engineering vaccine adjuvants with optimal characteristics for innate immune activation.

A primary aim of this chapter was to assess whether the capacity of the Poly-7/8a to focus and prolong adjuvant activity locally in draining lymph nodes is necessary and sufficient for eliciting protective cellular immunity. The activity of Poly-7/8a was benchmarked against the imidazoquinoline-based TLR-7/8, R848, and a TLR-9 agonist, CpG ODN 1826. Prior studies have shown that both R848 and CpG induce systemic immune responses[56] but that CpG also induces robust local innate immune activation (unpublished results). CpG has also been used as a gold-standard adjuvant for eliciting protective CD4 and CD8 T cell responses in several mouse models[178]. By comparing Poly-7/8a, which only induces local innate immune activation, with R848 and CpG, it is possible to evaluate how the location of innate immune activation (local vs. systemic vs. both) influences the elicitation of adaptive immune responses to a locally administered protein antigen. Innate responses induced by the different adjuvants was correlated with their capacity to elicit adaptive Th1-type CD4 and CD8 T cells in parallel with their ability to mediate protection in two challenge models.

Experimental aims:

1. Characterize the innate responses induced by Poly-7/8a and other adjuvants
2. Evaluate CD8 T cell responses and protection using an experimental system based on challenge with genetically modified *Listeria monocytogenes*
3. Evaluate the capacity of particle forming Poly-7/8a to induce protective Th1-type CD4 T cell responses using an experimental system based on challenge with *Leishmania major*

5.2 Magnitude and spatiotemporal characteristics of innate immune activation

To benchmark innate activity, the lead Poly-7/8a (PP-7/8a^{Hi}) was compared with two commercially available TLRa, the small molecule TLR-7/8a, R848 (Resiquimod), and a TLR-9 agonist, CpG, which is especially potent in mice due to broad expression of TLR-9 across multiple murine APC subsets[28, 34]. Following subcutaneous administration of each of these adjuvants, serum and lymph node cytokines were evaluated at serial timepoints (Figure 5.1). Consistent with earlier reports[56], both R848 and CpG induced significantly elevated (>10,000 pg/mL) serum IL-12, with peak responses observed 6 h after administration. Despite inducing high levels of systemic IL-12, R848 provided no measurable lymph node IL-12 production, whereas both CpG and PP-7/8a^{Hi} induced significantly elevated lymph node IL-12 between 1 and 8 days after vaccine administration.

Of note, while IL-12 was selected as a biomarker for adjuvant pharmacodynamics, it is likely that evaluation of different cytokines would have yielded distinct kinetics. Earlier studies have shown that IFNs peak early in both lymph nodes and serum, whereas inflammatory cytokines (e.g., IL-6, IL-12) tend to peak later[56]. Furthermore, IP-10 was found to be biphasic, with peak timepoints at days 1 and 8, which was also recently reported in the literature[179].

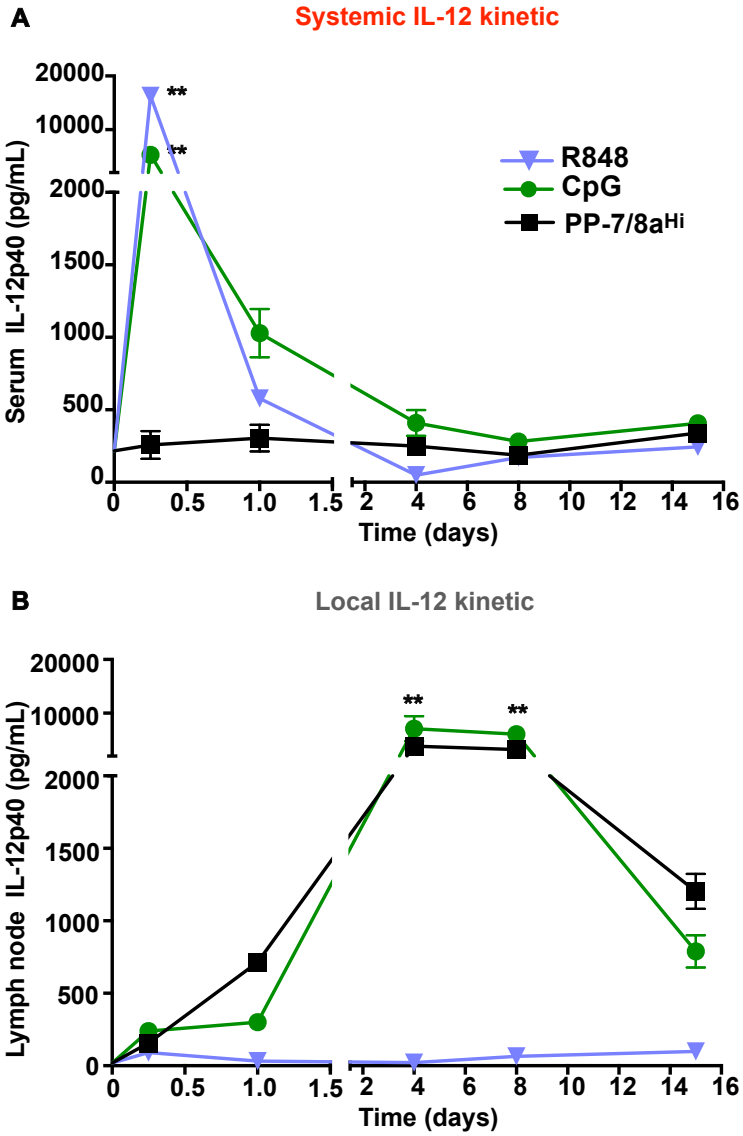

Figure 5.1: PP-7/8a^{Hi}, R848 and CpG induce unique profiles of local and systemic cytokine production. Following subcutaneous administration of PP-7/8a^{Hi}, CpG or R848, either (A) serum (n = 5) or (B) lymph nodes (n = 4) were assessed for IL-12 production by ELISA. All data are represented as mean ± SEM. Significance is relative to naïve.

APC recruitment to draining lymph nodes

Differences in the timing at which peak systemic (6 hours) and peak local (4 days) cytokines are observed likely relate to immune cell availability in lymph nodes (Figure 5.2): for CpG and PP-7/8a^{Hi}, the magnitude (fold change relative to naïve) of each major APC population in draining lymph nodes increased 5-fold by day 4, with increases up to 20-fold by day 15. Consistent with the IL-12 kinetic observed in Figure 5.1, the magnitude and kinetics of APC recruitment to the draining lymph node was comparable for both CpG and PP-7/8a^{Hi}, with no increases in lymph node APC populations observed for R848. Notably, while peak levels of IL-12 occurred at day 4, the magnitude of APCs in lymph nodes did not peak until day 15. These data suggest that the kinetic of lymph node cytokine production (Figure 5.1) is likely a product of the TLR-7/8a concentration (which peaks early and decays logarithmically) and magnitude of APC populations present in the draining lymph node.

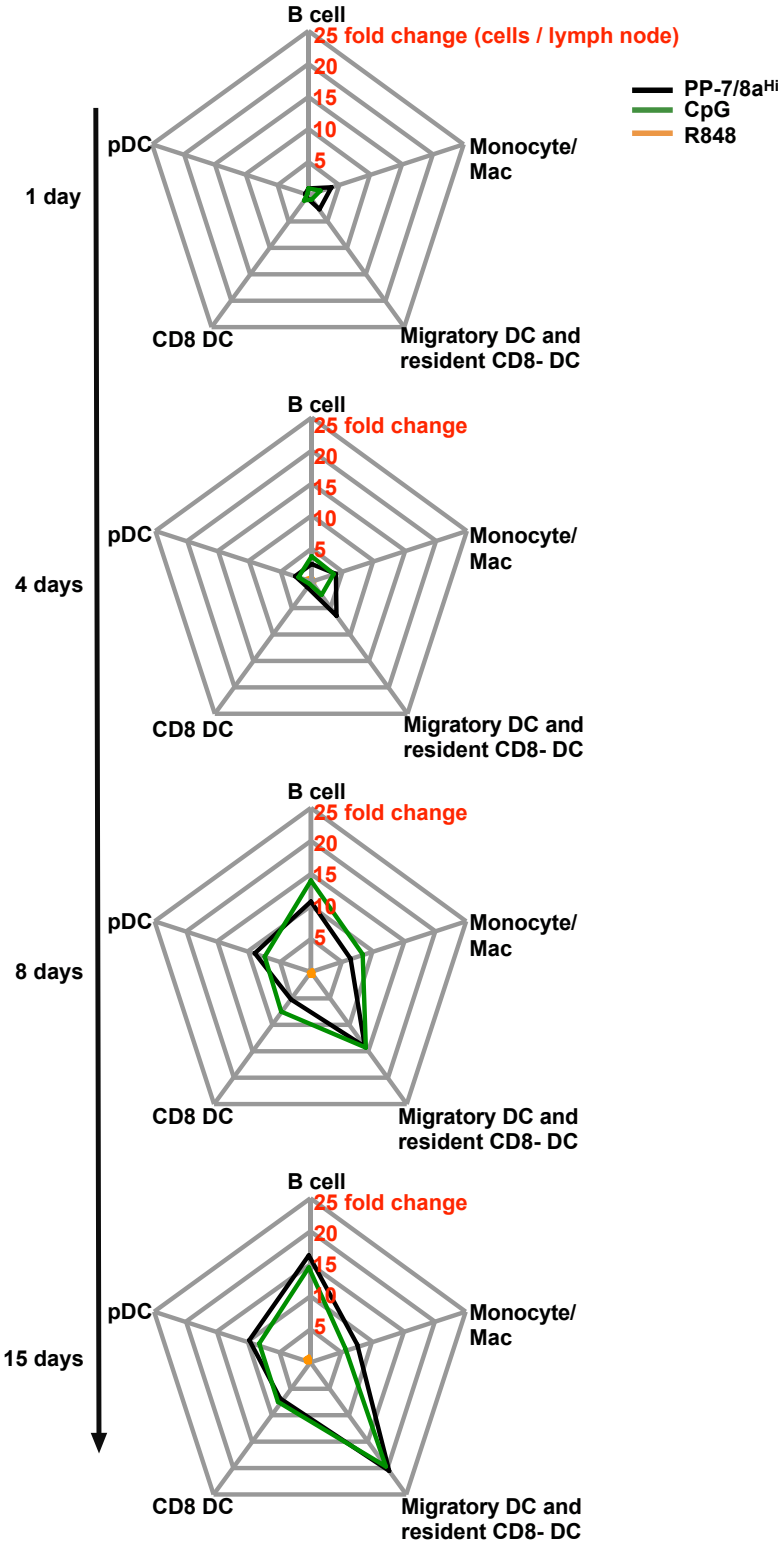

Figure 5.2: Magnitude (fold-change relative to naïve) of major APC populations in draining lymph nodes. Following subcutaneous administration of PP-7/8a^{Hi}, R848 or CpG, draining lymph nodes (n = 3) were harvested at serial timepoints and evaluated by flow cytometry. The major APC populations were quantified and are represented as fold change relative to the number of each population found in the lymph node of a naïve mouse. All data are represented as mean fold-change.

While IL-12 production serves as a valuable biomarker for TLR binding and the downstream capacity of the adjuvant to induce cellular immune responses, additional cytokines and chemokines are known to play important roles in shaping the magnitude and phenotypic characteristics of adaptive immune response. Using cytokine bead array, PP-7/8a^{Hi}, R848 and CpG were assessed for their capacity to induce various cytokines and chemokines associated with inflammation (IL-6, TNFα); cross-presentation (IFNα and IP-10); and, skewing of CD4 helper T cell responses towards Th1 (IFNα, IFNγ and IL-12), Th2 (IL-4), Th17 (IL-17) or Treg (IL-10) phenotypes.

Serum and lymph node cytokines were evaluated at 6 and 24 h after vaccination, respectively. These timepoints represent intermediate timepoints for the detection of many cytokines in both lymph nodes and serum (see kinetic: Figure 5.1B). Consistent with earlier reports that TLR-7/8 and TLR-9 agonists predominantly induce pro-inflammatory and Th1-polarizing cytokines[21, 56], each of the adjuvants induced significant increases in IFNγ, IL-12 and IL-6, but low to undetectable levels of IL-4, IL-10 and IL-17 (Figure 5.3). However, there was a marked difference in the location of cytokine production between the adjuvants. Whereas R848 only induced systemic (sera) cytokines (Figure 5.3A), locally retained PP-7/8^{Hi} predominantly induced lymph node cytokines (Figure 5.3B), characterized by significantly enhanced production of Th1-polarizing cytokines IFNγ and IL-12. In contrast to both R848 and PP-7/8^{Hi}, CpG induced high levels of both local and systemic cytokine production.

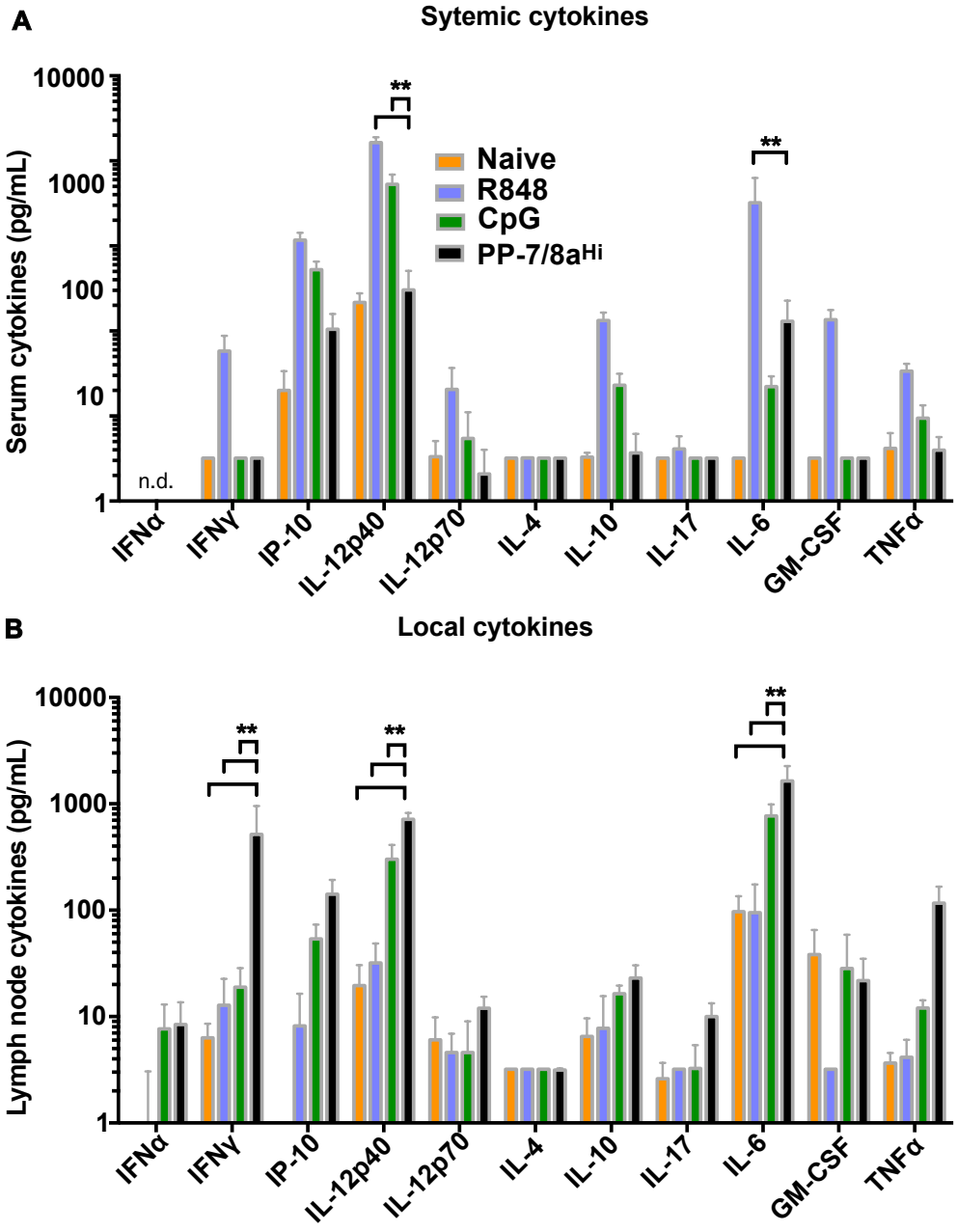

Figure 5.3: PP-7/8^{Hi}, R848 and CpG induce Th1-polarizing and pro-inflammatory cytokines but exhibit differences in localization of cytokine production. Following subcutaneous administration of PP-7/8^{Hi}, R848 or CpG, (A) serum (n = 5) and (B) lymph nodes (n = 4) were assessed for cytokine and chemokine production by cytokine bead array. All data are represented as mean ± SEM. Significance is relative to naïve. n.d. = not determined

Prior studies have shown that systemic cytokine production in humans leads to a "flu-like" syndrome characterized by pyrexia, nausea, and, in some cases, even hypotension[39, 83, 91, 97]. Here, weight loss was used as a proxy for morbidity following subcutaneous administration of PP-7/8a^{Hi}, R848 and CpG in mice. Systemic inflammation induced by R848 and CpG was associated with transient decreases in mouse body weight (Figure 5.4A), with the kinetics of weight loss closely following that of serum cytokine production (Figure 5.1). For mice that received R848 and CpG, weight loss decreased by 6% and 8%, respectively, whereas fluctuations in body weight for mice that received PP-7/8a^{Hi} was indistinguishable from weight fluctuations observed for untreated mice. These data show that systemic, but not local, innate immune activation is associated with weight loss in mice.

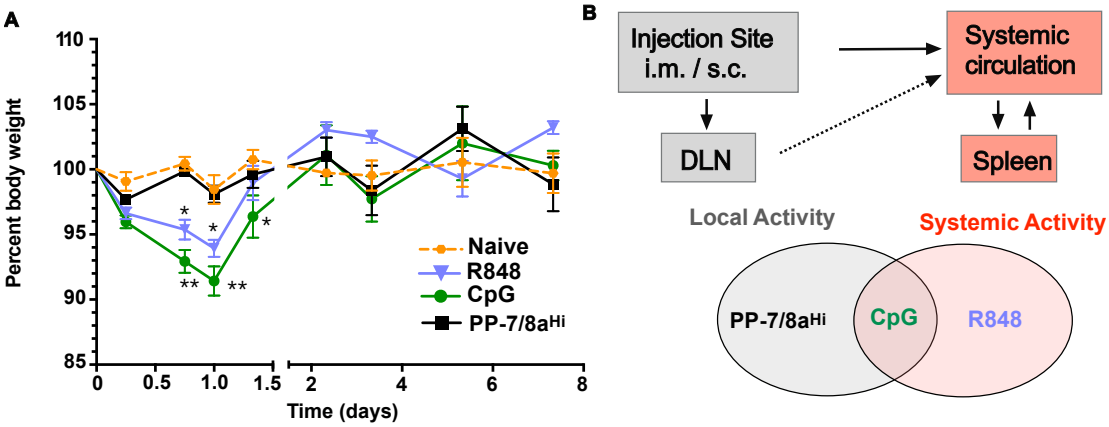

Figure 5.4: Systemic cytokine production by CpG and R848 is associated with transient decreases in mouse body weight. (A) Mouse (n = 3) body mass was evaluated immediately prior to, and at serial timepoints following, subcutaneous administration of PP-7/8a^{Hi}, R848 and CpG. Body weight is expressed as the percentage of body mass measured at t = 0. (B) Venn diagram for the localization of the different adjuvants assessed in this study. All data are represented as mean ± SEM. Significance is relative to naïve.

5.3 Magnitude and protective efficacy of CD8 T cell responses elicited by immunization with ovalbumin

The next studies assessed whether local innate immune activation, systemic activation, or both, are important for the capacity of adjuvants to elicit protective CD8 T cell responses to co-administered protein antigen. OVA protein was used as a model immunogen that was co-administered with PP-7/8a^{Hi}, R848 or CpG. CD8 T cell responses from whole blood were evaluated 10 days after two immunizations. As shown in Figure 5.5A, OVA admixed with PP-7/8a^{Hi} elicited significantly higher CD8 T cell responses (~ 11%) as compared with OVA alone or OVA admixed with R848 but provided comparable responses to those observed with OVA co-administered with CpG (~ 8%).

To evaluate the capacity of the CD8 T cell responses to mediate protection, mice were challenged intravenously with *Listeria monocytogenes* expressing OVA (*LM*-OVA). Prior studies have shown that *LM*-OVA can infect splenocytes and that bacterial burden in the spleen (e.g., CFU/spleen) is inversely related to the magnitude of the antigen (OVA)-specific CD8 T cell response[160, 161]. Two days after intravenous challenge, spleens from infected mice were isolated and evaluated for bacterial burden (Figure 5.5B). Protection (inverse of bacterial burden) closely followed the magnitude of CD8 T cell responses, with OVA + PP-7/8a^{Hi} reducing bacterial burden in the spleen of infected mice by nearly 5 orders of magnitude. CpG also induced significant levels of protection that were comparable to that observed with PP-7/8a$^{Hi.}$

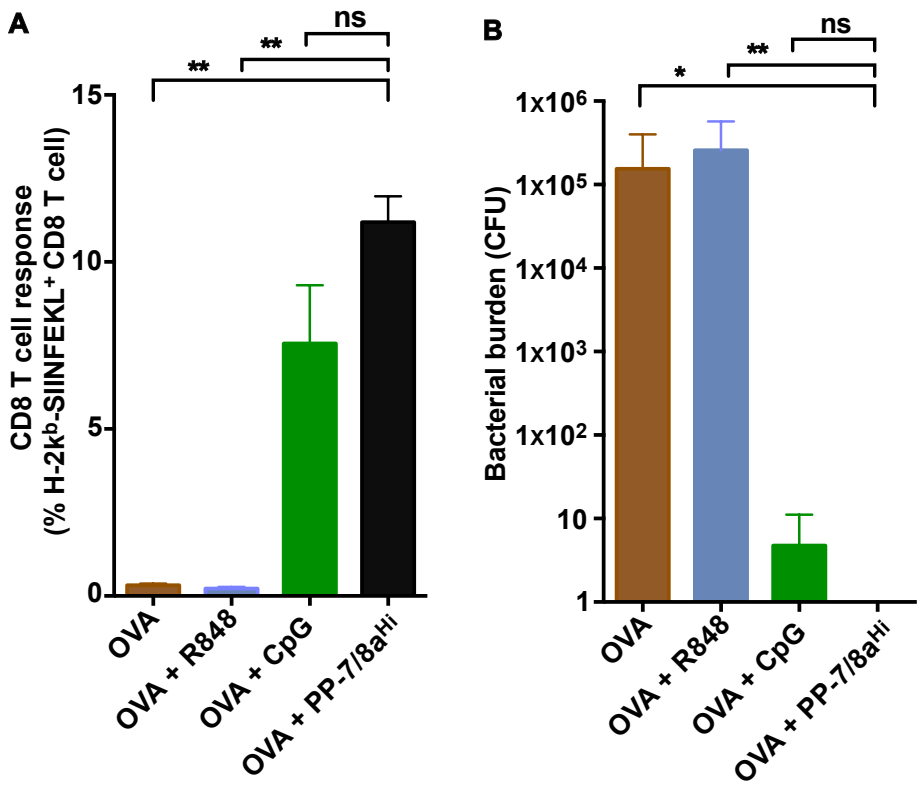

Figure 5.5: Persistent local innate immune activation is necessary and sufficient for inducing protective CD8 T cell responses. C57BL/6 mice (n = 6) received a single subcutaneous footpad injection of 50 µg of OVA admixed with adjuvant at days 0 and 14. (A) At day 24, tetramer$^+$ CD8 T cell responses from whole blood were evaluated by flow cytometry. (B) Mice (n = 6) were challenged intravenously at day 28 with LM-OVA and bacterial burden in spleens was evaluated on day 31. All data are represented as mean ± SEM.

In the same experiment as shown in Figure 5.5, additional control and experimental groups were evaluated and are shown in Figure 5.6. Note that OVA admixed with either the polymer particle control (PP) or with any of the small molecule TLR-7/8a (R848, SM 7/8a, or SM 20x7/8a) provided no improvement in CD8 T cell responses or protection as compared with OVA administered alone. Furthermore, the magnitude of CD8 T cells and protection elicited by the different doses and potencies of Poly-7/8a correlated with the persistence, but not magnitude, of lymph node cytokine production. Both PP-7/8a^{Hi} at 62.5 nmoles and PP-20x7/8a^{Hi} at 12.5 nmoles induce comparable magnitude of early lymph node cytokine production, as compared with PP-7/8a^{Hi} at 12.5 nmoles, but only the former, which induces high levels of persistent (> 8 days) lymph node cytokine production, was able to elicit significant protection against *LM*-OVA challenge. Altogether, these data support the hypothesis that persistent lymph node innate immune activation is critical for eliciting protective T cell responses.

A

	Controls			Small molecules			PP-7/8a			
Antigen (OVA, µg)	---	50	50	50	50	50	50	50	50	50
Adjuvant	---	---	PP	R848	SM 7/8a	SM 20x7/8a	PP-7/8a^{Hi}	PP-20x7/8a^{Hi}	PP-7/8a^{Hi}	CpG
Adjuvant dose (nM)	---	---	---	62.5	62.5	12.5	12.5	12.5	62.5	3.1

B

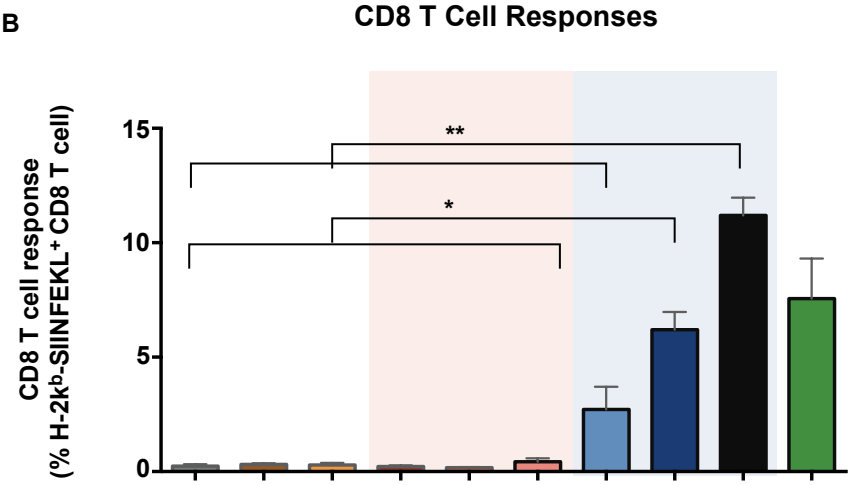

C

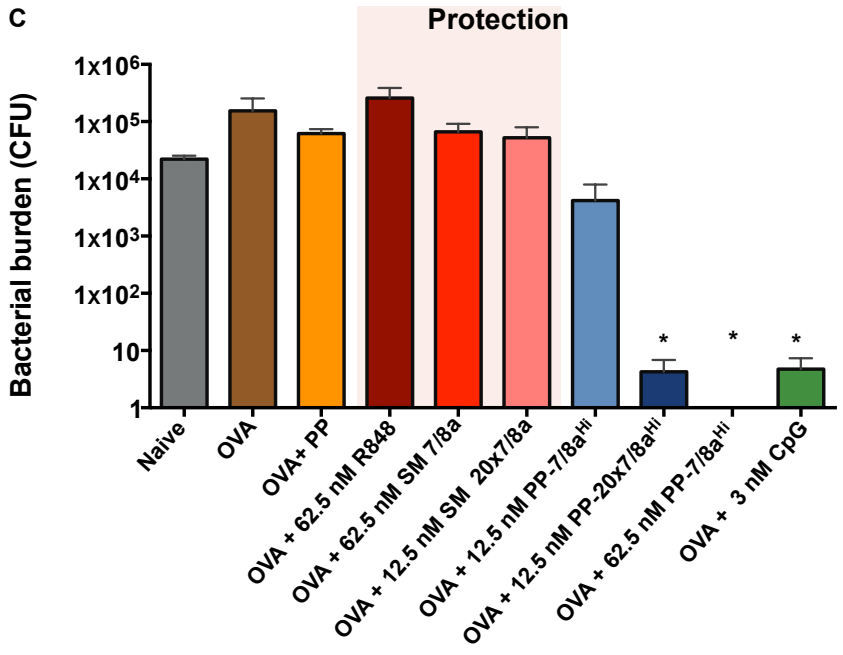

Figure 5.6: Persistent local innate immune activation is necessary and sufficient for inducing protective CD8 T cell responses. C57BL/6 mice (n = 6) received a single subcutaneous footpad injection of 50 µg of OVA formulated with adjuvant at days 0 and 14. (A) At day 24, tetramer$^+$ CD8 T cell responses from whole blood were evaluated by flow cytometry. (B) Mice (n = 6) were challenged intravenously at day 28 with LM-OVA and bacterial burden in the spleens was evaluated on day 31. All data are represented as mean ± SEM. Significance is relative to naïve.

5.4 Magnitude and isotype (Th1 vs. Th2) of antibodies elicited

An additional consideration is how innate immune activation influences the titre and isotype of antibodies elicited against the protein antigen. Serum from vaccinated mice was evaluated at 10 days after 2 immunizations and was evaluated for the mid-point titre of anti-OVA IgG1 and IgG2c antibodies (Figure 5.7). The highest magnitude responses were observed for OVA + PP-7/8a^{Hi}, which resulted in 40 and 400-fold increases in IgG1 and IgG2c anti-OVA antibodies (relative to OVA without adjuvant), respectively. Notably, whereas the high dose Poly-7/8a carrying the low potency agonist (PP-7/8a^{Hi} at 62.5 nmoles) induced high levels of both Th1- and Th2-skewed antibodies, the Poly-7/8a carrying the 20-fold more potent agonist (PP-20x7/8a^{Hi}) and CpG resulted in lower ratios of IgG1/IG2c, which relates to Th1-skewing. These data suggest that persistent local innate immune activation is critical for enhancing the magnitude of antibody responses, but that increasing the potency of the agonist (which allows for a relative decrease in the amount of polymer carrier that is administered) may be critical for skewing responses towards Th1-type antibody isotype responses (i.e., IgG2c).

Anti-OVA IgG titer by isotype

Vaccine	Anti-OVA IgG1 (Th2 Ab)	Anti-OVA IgG2c (Th1 Ab)	Ratio (IgG1/IgG2c)
OVA	1.6E+03	1.9E+02	8.35
OVA + PP	4.2E+03	1.1E+03	3.62
OVA + 62.5 nM R848	1.7E+04	2.4E+03	7.18
OVA + 62.5 nM SM 7/8a	5.0E+03	5.7E+02	8.71
OVA + 12.5 nM SM 20x7/8a	3.2E+04	4.2E+03	7.78
OVA + 12.5 nM PP-7/8a^{Hi}	2.8E+03	5.4E+03	0.52
OVA + 12.5 nM PP-20x7/8a^{Hi}	5.5E+03	4.2E+04	0.13
OVA + 62.5 nM PP-7/8a^{Hi}	8.0E+04	8.0E+04	1.00
OVA + CpG	2.1E+04	4.5E+04	0.46

Note: IgG1/IgG2c > 1 = Th2 skewed response
IgG1/IgG2c < 1 = Th1 skewed response

Figure 5.7: Poly-7/8a and CpG enhance the magnitude of anti-OVA IgG responses. C57BL/6 mice (n = 6) received a single subcutaneous footpad injection of 50 μg of OVA formulated with adjuvant at days 0 and 14. Serum was evaluated for the mid-point titre of anti-OVA IgG1 and IgG2c responses at day 24. The ratio of IgG1 (Th2-specific) and IgG2c (Th1-specific) titres provides a qualitative measure of Th1 versus Th2 skewing.

5.5 SIV Gag immunization: magnitude of CD8 T cell responses and protective efficacy

The prior studies in this thesis evaluated the capacity of Poly-7/8a to generate adaptive immune responses to a non-physiologically relevant antigen, OVA. Precursor frequencies of naïve OVA-specific CD8 T cells are exceptionally high as compared with other antigens[180] and this in part explains the relatively high magnitude of CD8 T cell responses to OVA that have been observed herein.

The next study assessed the capacity of the different adjuvants (PP-7/8a^{Hi}, R848 or CpG) to elicit protective CD8 T cell responses using a more physiologically relevant antigen, Gagp55 (Gag) derived from Simian Immunodeficiency Virus-1 (SIV-1, strain mac 239). The responses induced by Gag + PP-7/8a^{Hi} or CpG were modest (< 1%)

compared with the CD8 T cell responses induced by OVA + PP-7/8a^{Hi} or CpG (8-15% tetramer^{+} CD8 T cells) and were associated with only limited protection following intravenous challenge with *LM*-expressing full-length SIV Gag. The trends in protection were consistent with the magnitude of CD8 T cell responses, with highet levels of protection observed in mice immunized with Gag + PP-7/8a^{Hi}, followed by Gag + CpG, Gag + R848 and then Gag alone. While the magnitude of CD8 T cell responses were lower than those observed with OVA, these data are consistent with the previous findings that persistent local innate immune activation by PP-7/8a^{Hi} is superior to systemic activation alone (R848) for promoting generation of protective T cell immunity to co-administered protein antigen.

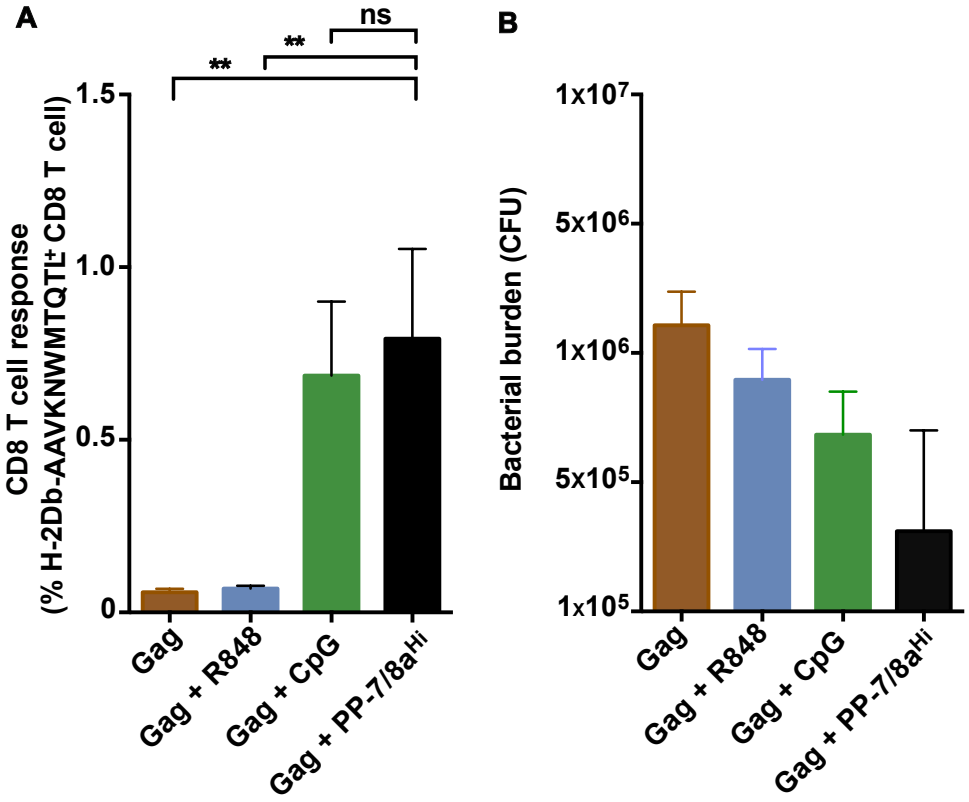

Figure 5.8: CD8 T cell responses and protection following immunization with SIV Gag protein. C57BL/6 mice (n = 6) received a single subcutaneous footpad injection of 20 µg of Gag formulated with adjuvant at days 0 and 14. (A) At day 24, tetramer^{+} CD8 T cell responses from whole blood were evaluated by flow cytometry. (B) Mice (n = 6) were challenged intravenously at day 28 with LM-Gag and bacterial burden in spleens was evaluated on day 31. All data are represented as mean ± SEM.

5.6 Magnitude and quality of Th1-type CD4 T cell responses elicited by immunization with the MML protein derived from *Leishmania major*

Vaccines that are capable of eliciting durable Th1-type CD4 cells are needed for certain parasitic infections and tuberculosis[45, 181]. Thus, the capacity of Poly-7/8a to induce protective Th1-type CD4 T cell responses was assessed in a mouse vaccination and challenge model of *Leishmania major*. *L. major* is a protozoan parasite that infects phagocytic cells. Th1 cells play a critical role in clearing these, and other, intracellular parasites by producing cytokines, such as IFNγ, that directly activate infected cells to kill the parasite[44]. While Th1 cells promote clearance of the parasite, Th2 and Th17 cells have been implicated in parasite growth, dissemination, or even increased disease pathology[44, 178, 182]. Thus, the *L. major* immunization and challenge model provides an effective system for determining whether a vaccine can elicit protective Th1-type CD4 T cells.

Mice were immunized with MML, a recombinant polyprotein derived from *L. major*, either alone or admixed with adjuvant. At 1 week and 4 weeks post 3 immunizations, splenocytes from vaccinated mice were stimulated *in vitro* with antigen (MML) and evaluated for production of Th1-characteristic cytokines (IFNγ, IL-2 or TNFα). Cells that produced combinations of these cytokines define the antigen-specific Th1-type CD4 T cell population in vaccinated mice. As observed in Figure 5.9, MML co-administered with either Poly-7/8a or CpG led to significant increases in the magnitude of CD4 T cell responses. Consistent with earlier findings in this thesis, MML co-administered with the polymer particle control (PP) or with the small molecule TLR-7/8a (SM 7/8a or SM 20x7/8a) provided no improvement in CD4 T cell responses as compared with MML administered without adjuvant. Comparing responses induced by the different doses and potencies of Poly-7/8a, a prominent dose effect was observed for PP-7/8a^{Hi}: increasing the dose from 12.5 nmoles to 62.5 nmoles led to a significant increase in the magnitude of CD4 T cell responses elicited (~ 0.2 and 1.5%, respectively, at 4 weeks post 3 immunizations). Increasing potency for dose matched Poly-7/8a (PP-7/8a versus PP-20x7/8a) was associated with only modestly higher CD4 T cell responses as compared with dose-matched PP-7/8a^{Hi}.

A

	Controls			Small molecules		PP-7/8a			
Antigen (MML, µg)	---	40	40	40	40	40	40	40	40
Adjuvant	---	---	PP	SM 7/8a	SM 20x7/8a	PP-7/8a^{Hi}	PP-20x7/8a^{Hi}	PP-7/8a^{Hi}	CpG
Adjuvant dose (nM)	---	---	---	62.5	12.5	12.5	12.5	62.5	3.1

B

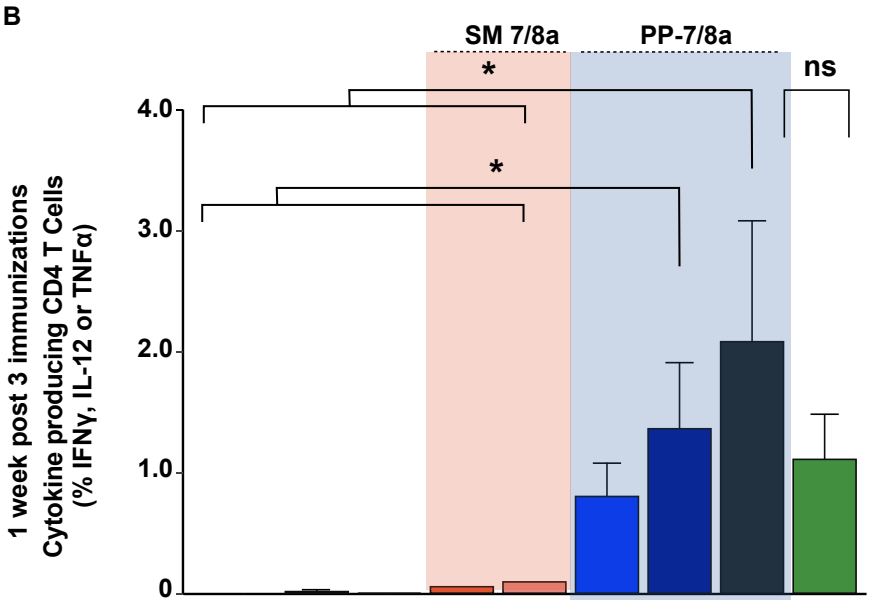

C

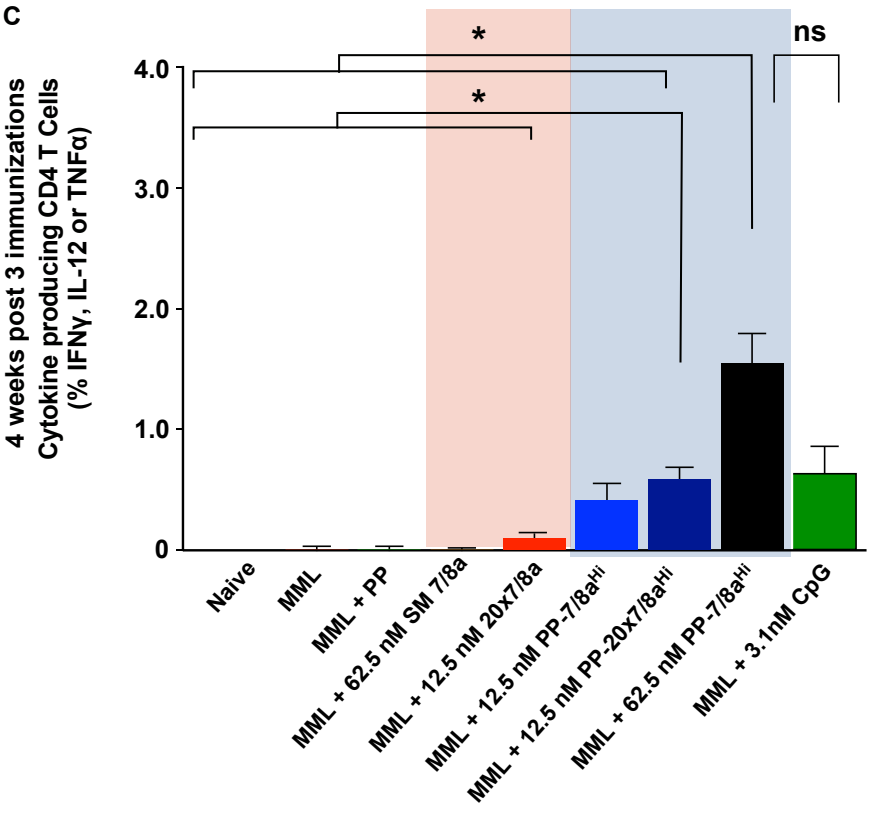

Figure 5.9: Poly-7/8a enhances the magnitude of Th1-type CD4 T cells. C57BL/6 mice (n = 5) received subcutaneous immunizations of 20 μg of MML protein either alone or formulated with an adjuvant on days 0, 21 and 42. (A) Table of vaccines groups. (B) Splenocytes were isolated on day 70 and stimulated *in vitro* with an MML peptide pool. Antigen-specific cytokine producing CD4 T cells in the mixed splenocyte cultures were quantified by flow cytometry (n = 5) for their capacity to produce Th1 characteristic cytokines (IFNγ, IL-2 and TNFα). All data are represented as mean ± SEM.

Prior studies have established that the "quality" of antigen-specific CD4 T cell responses is related to the functional properties of those cells.[44, 45]. In this model, CD4 T cells that produce multiple effector cytokines (e.g., IFNγ, IL-2 or TNFα) are considered qualitatively superior to double and single cytokine producing CD4 T cells. The functional superiority of triple cytokine producing cells has been suggested in the control of HIV infection as well as the mouse model of *L major*, whereby disease burden inversely correlates with the frequency of multifunctional CD4 T cells[44, 45].

The magnitude of triple, double and single-cytokine producing CD4 T cells is shown in Figure 5.10 at 1 and 4 weeks following 3 immunizations with MML admixed with adjuvant or given alone. MML + Poly-7/8a (at all doses and potencies) leads to a high frequency (0.5-1%) of triple cytokine-producing CD4 T cells at 1 week, which represents > 50% of the total antigen-specific CD4 T cell responses observed in Figure 5.9. At 4 weeks post immunization, the "high quality" multi-functional CD4 T cells (producing 2 or more effector cytokines) are maintained at more than 1% of the total CD4 T cell population in mice that received MML+ PP-7/8^{Hi} at 62.5 nmoles. Qualitatively similar, but lower magnitude, responses were observed for the other doses and potencies of Poly-7/8a (PP-7/8a^{Hi} and PP-20x7/8a^{Hi} at 12.5 nmoles) as well

as CpG. Altogether, these results show that Poly-7/8a optimized for persistent local innate immune activation can induce high magnitude and quality Th1-type CD4 T cell responses against co-administered protein antigen.

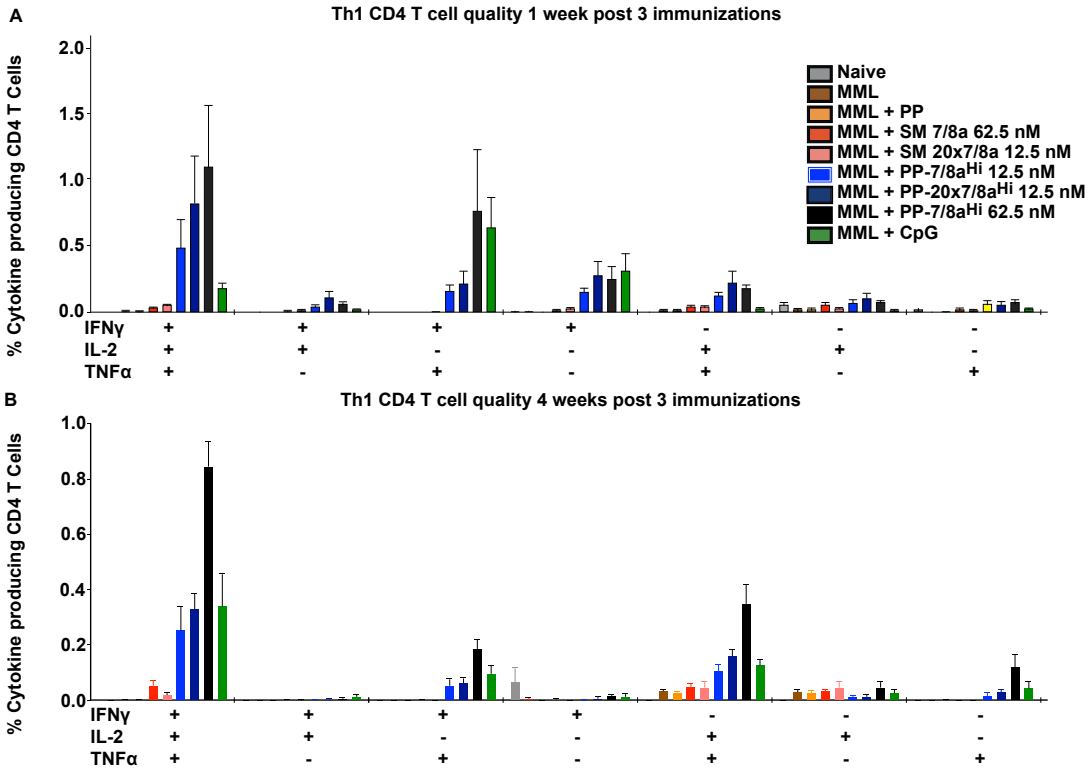

Figure 5.10: Poly-7/8a enhance the quality of Th1 CD4 T cells. C57BL/6 mice (n = 5) received subcutaneous immunizations of 20 µg of MML protein either alone or formulated with an adjuvant on days 0, 21 and 42. Splenocytes were isolated on day 70 and stimulated *in vitro* with an MML peptide pool. Antigen-specific cytokine producing CD4 T cells in the mixed splenocyte cultures were quantified by flow cytometry and Boolean gating was used to determine the frequency of triple, double or single cytokine producing cells.

5.7 Th1-type CD4 T cells induced by Poly-7/8a mediate protection following infectious challenge with *Leishmania major*

The capacity of the Th1-type CD4 T cell responses to be mediate protection was assessed by challenging mice intradermally in the ear with *L major* parasites (promastigote stage). *L major* is known to infect intradermal phagocytic cells and induce inflammation that results in a cutaneous ear lesion. The size of this lesion has been shown to correlate with the parasite burden, both in terms of number of parasites as well as parasite RNA levels[44, 178]. The lesion sizes for the different vaccine groups were assessed weekly and are shown in Figure 5.11.

Both the highest dose of the particle-forming Poly-7/8a (PP-7/8a^{Hi} at 62.5 nmoles) and the lower dose Poly-7/8a with higher potency agonist (PP-20x-7/8a^{Hi} at 12.5 nmoles) induced significant reductions in ear lesion size compared with controls, and these responses were comparable to those observed with MML + CpG, which is considered a gold-standard adjuvant for inducing protective Th1-type CD4 T cell responses in the mouse model of *L major*. Notably, the lower dose of PP-7/8a^{Hi} (12.5 nmoles) did not provide protection, despite eliciting a comparable magnitude and quality of Th1-type CD4 T cell responses as compared with PP-20x7/8a^{Hi} and CpG. Altogether, these results show that Poly-7/8a optimized for agonist dose, density and potency are effective for eliciting Th1-type CD4 T cell responses that can mediate protection against infectious challenge.

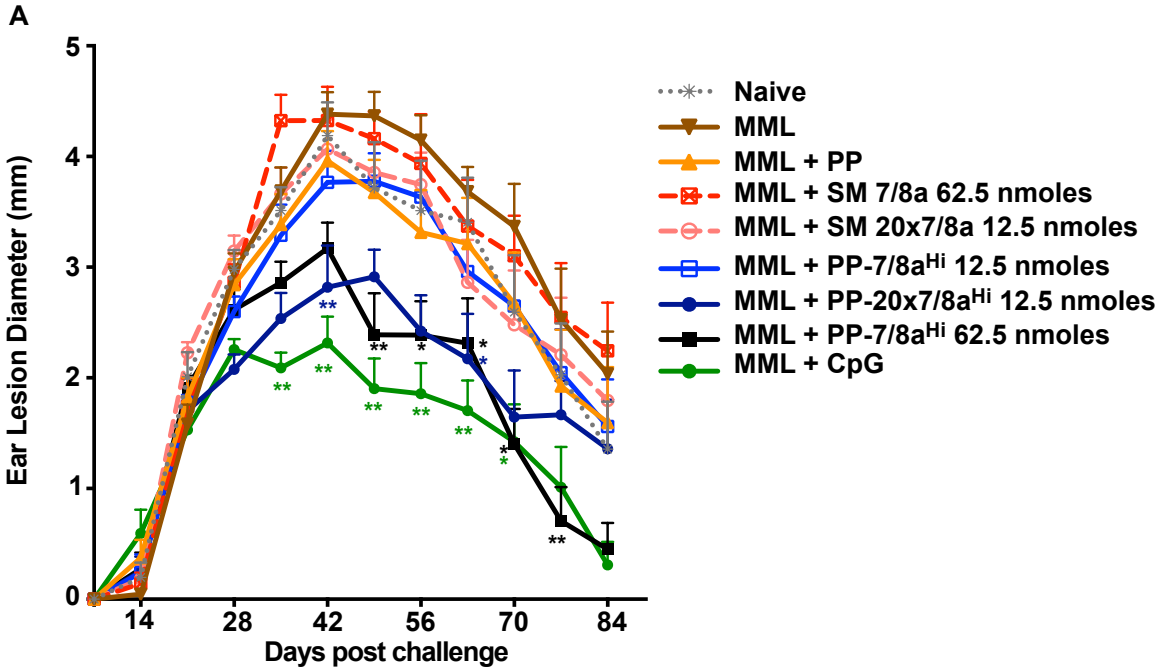

Figure 5.11: Poly-7/8a and CpG induce protective Th1-type CD4 T cells that mediate protection against L major. C57BL/6 mice (n = 6) received subcutaneous immunizations of 20 µg of MML protein either alone or admixed with adjuvant on days 0, 21 and 42. Mice (n = 6) were challenged intradermally in both ears with L major at day 70. Personnel blinded to group assignment measured ear lesion diameters weekly after infection. All data are represented as mean ± SEM; statistical significance is relative to naïve, MML alone and MML + SM 7/8a.

5.8 Discussion

The results presented in this chapter show that the prolonged innate immune activation that is spatially restricted to draining lymph nodes that is induced Poly-7/8a (optimized for agonist density, potency and dose) is necessary and sufficient for eliciting robust Th1-type CD4 and CD8 T cell responses that mediate protection following infectious challenge.

The magnitude and spatiotemporal characteristics of innate immune activation induced by Poly-7/8a was benchmarked against commercially available adjuvants, R848 (TLR-7/8a) and CpG (TLR-9a). Whereas the locally retained Poly-7/8a induced persistent local cytokine production, the small molecule TLR-7/8a, R848, induced high magnitude but only transient systemic cytokine responses. In contrast, CpG induced both transient systemic and persistent local cytokine production. While previous studies have reported that both R848 and CpG induce transient systemic cytokines[56], this is the first study to characterize the magnitude and kinetics of cytokine production in the serum (systemic) and lymph nodes (local).

A critical question is how the location of innate immune activation contributes to toxicity and morbidity. This question has been partly answered by clinical trials evaluating the safety and efficacy of small molecule TLR-7/8a[77, 83, 96, 97]. In these studies, serum concentrations of TLR-7/8a have been shown to correlate with the magnitude of pharmacodynamic biomarkers (e.g., IFNs and pro-inflammatory cytokines) in serum, and both of these measures are closely associated with the onset and duration of adverse events, including fever, vomiting and lymphopenia. These data, together with our observation that the kinetics of serum cytokine production

induced by both R848 and CpG closely follows the onset and duration of body weight decreases in mice, suggests that systemic innate immune activation, rather than robust local innate immune activation, accounts for the adjuvant morbidity.

Prior studies have reported that systemic cytokine production is critical to the capacity of many adjuvants, including CpG and poly(IC), to induce T cell responses to co-administered protein antigens[54, 56]. However, these studies did not evaluate cytokine production in draining lymph nodes (the site of T cell priming) and instead relied solely on evaluation of serum cytokines. Thus, the role of local cytokines was unaccounted for in these earlier studies. Moreover, we observe that a Poly-7/8a that induces limited systemic cytokine production but focuses adjuvant activity locally in the draining lymph nodes is able to elicit significantly higher magnitude T cell responses as compared with the purely systemic adjuvant, R848. In contrast, locally acting Poly-7/8a induces comparable magnitude of responses as compared with CpG, which induces both local and systemic activity. These results suggest that lymph node cytokines, but not systemic cytokine production, are important for eliciting CD8 T cell responses and that systemic cytokines are dispensable to CD8 T cell priming and expansion. Indeed, these findings are supported by prior studies demonstrating that particulate carriers of adjuvants that restrict adjuvant activity to the sites of immunization and draining lymph nodes are able to elicit robust antibody and T cell responses to co-administered protein antigen[121, 124, 127, 176, 183].

A critical aspect for priming T cell immunity is to provide sufficient quality (type of cytokines) and duration of innate immune activation[128, 129, 184]. Here, we show that particulate formulations of Poly-7/8a (PP-7/8a) induce persistent (> 8 days) innate

immune activation in lymph nodes, which correlates with their capacity to elicit protective CD4 and CD8 T cell responses. In contrast to earlier reports[54, 56], however, systemic cytokine production, which is limited for particulate formulations of TLR-7/8a, appears to be dispensable for CD8 T cell priming and expansion. The findings that lymph node cytokines, but not systemic cytokine production, are important for inducing CD8 T cell responses may explain what previous reports have referred to as the "temporal conundrum" relating to the discordance between when systemic cytokines and CD8 T cell responses peak, 2-6 hours and ~ 7-10 days after vaccination, respectively[54].

While particle formation was found to be critical to Poly-7/8a activity, a potential concern is that these platforms may induce unwanted polarization of cellular immunity towards Th2-type CD4 T cell responses through NALP3 Inflammasome activation[26]. Indeed, several prior studies report that particulate carriers of TLR agonists induce mixed Th1/Th2 responses, with TLR agonist dose-dependent Th1 skewing[121, 185]. Consistent with these findings, we observed that Poly-7/8a induced a Th1 dominant cellular immune response that provided protection against infectious challenge with *L major,* suggesting that robust production of Th1-skewing cytokines by Poly-7/8a is sufficient for overcoming Th2 skewing by the carrier alone. Though both CpG and Poy-7/8a elicited Th1-type CD4 T cell responses that mediated protection against *L major,* it is important to note that the genetic background of the mice also plays an important role in determining CD4 T cell differentiation towards certain stimuli. Accordingly, it is well documented that, whereas naïve C57BL/6 mice (used herein) exposed to *L major* naturally develop Th1-type CD4 T cell responses that mediate protection against the parasite, BALB/c mice exposed to *L major*

develop Th2 responses and are unable to clear the infection, which eventually results in the development of fatal disseminated infection[186]. The differential capacity of these mouse strains to develop protective Th1 responses has been associated with the inability of BALB/c mice to downmodulate Th2 responses in response to many inflammatory stimuli, including natural infection by *L major*[187]. Therefore, these data suggest that, while the Poly-7/8a was able to elicit protective Th1-type CD4 T cell mediated protection using C57BL/6 mice, the outcomes may have been different depending on the genetic background of the mouse strain, which highlights not only the importance of the adjuvant but also the role of the genetic background of the recipient in determining immunological outcomes to vaccination and natural infection.

Altogether, these results define the spatiotemporal characteristics of innate immune activation that are required for inducing protective cellular immunity.

6 Second-generation polymer-TLR-7/8a conjugates

6.1 Introduction

The prior chapters identified that particle formation is critical to the capacity of Poly-7/8a to induce high magnitude innate immune activation that is localized to draining lymph nodes. Moreover, the persistence of this activity was associated with increasing dose, density and potency of agonists attached to the polymers. Building on these findings, the next studies used novel synthetic chemical schemes to prepare 2nd-generation Poly-7/8a that address the limitations of the 1st generation technologies.

Delayed onset of innate immune activation

There is currently a need for adjuvants that can be programmed to delay the onset of innate immune activation. This observation is based on findings that the magnitude of adaptive immune responses elicited by DNA and adenoviruses is proportional to the levels of *in vivo* gene expression[188], which inversely correlates with innate immune activation (e.g., number of CpG motifs or level of type-I IFNs)[189]. While gene expression can be reduced by innate immune responses, optimal T cell and antibody responses still require cytokines associated with innate immune activation[190]. Altogether, these findings suggest that optimal adaptive immune responses to gene delivery-based vaccines may require sufficient time for gene expression before the onset of innate immune activation. Towards addressing the need for delayed onset of innate immune activation, pro-drug based Poly-7/8a were developed that delay the onset of innate immune activation in draining lymph nodes by up to 8 days after

vaccine administration. The synthesis and preliminary evaluation of these pro-drug constructs is described herein.

Controlled particle formation of Poly-7/8a

A major limitation of the 1st-generation Poly-7/8a adjuvants is that particle formation was an unanticipated result of attaching high densities of the amphiphilic ligand (TLR-7/8a) to the hydrophilic HPMA-based polymer scaffold. This process resulted in a heterogeneous population of particles that ranged in size from about 0.2-2 μm. While these particles were highly immunogenic, smaller particles (< 100 nm) are likely needed for direct targeting of lymph node resident DC populations, particularly pDCs[149, 150]. It is, therefore, advantageous to develop strategies that permit greater control over the sizes of particles to not only permit direct targeting of lymph node resident DCs but also to provide a more chemically defined and reproducible product in terms of particle size and distribution.

This chapter introduces two novel technologies to address the need for greater control over Poly-7/8a particle formation. The first approach uses multi-block copolymers to form micelles of defined sizes in aqueous conditions. In this strategy, an inner hydrophobic core based on poly(propylene glycol), PPG, is used to induce particle formation. The synthesis and preliminary biological evaluation of a micelle-forming Poly-7/8a is described herein.

The second approach offers an alternative to pre-formed particles by using thermoresponsive particle-forming Poly-7/8a (TRPP-7/8a) that exist as single water-soluble macromolecules during manufacturing and storage but undergo temperature-

driven particle formation *in vivo*. TRPP-7/8a were found to induce high levels of lymph node innate immune activation and elicited protective CD8 T cell responses. Altogether, TRPP-7/8a combine the benefits of soluble adjuvants—high chemical definition, versatility, stability and permissibility to cost-effective sterile filtration—with the superior biological activity of particulate adjuvants for eliciting T cell immunity.

Experimental aims:

1. Delay onset of innate immune activation using pro-drug Poly-7/8a
2. Develop micelle-forming Poly-7/8a
3. Synthesize and evaluate thermoresponsive polymer adjuvants as a proof-of-concept for in situ particle formation

6.2 Controlling the timing of onset of innate immune activation

To mitigate decreases in transgene expression, pro-drug adjuvants that delay onset of innate immune activation may be important for improving adaptive immune responses to gene delivery-based vaccines. One method for blocking or delaying the activity of imidazoquinoline-based TLR-7/8a is to modify the C4 aryl amine, as shown in Figure 6.1. This has been demonstrated in both structural biology studies[73] and structure-activity relationship studies[66], which both independently identify that the C4-aryl amine is critical for TLR-7/8 binding. Subsequent *in vitro* studies have elaborated on these findings and shown that "pro-drug" TLR-7/8a can be produced by attaching labile groups to the C4 position[191]; while the labile group is attached, the compound is not active, but UV light-catalysed release of the labile group yields the active TLR-7/8a, thereby permitting control over the timing of activation.

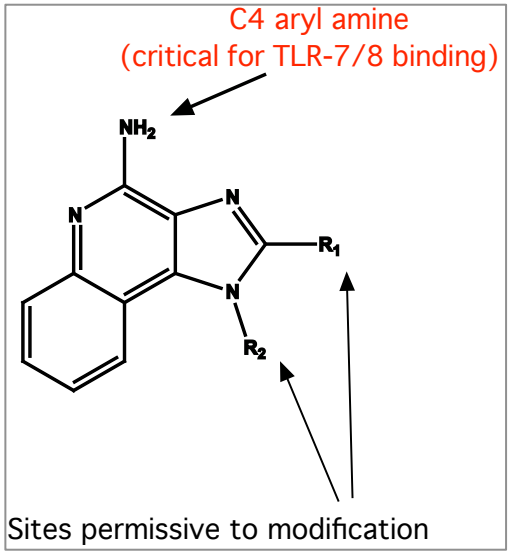

Figure 6.1: Generic structure of an imidazoquinoline-based TLR-7/8a. Note that the C4 aryl amine is critical for TLR7 binding. Modification of the C4 aryl amine abrogates activity. In contrast, positions denoted by R1 and R2 are permissive to chemical modification. The R2 site is used to link the TLR-7/8a to polymer backbones throughout the studies described herein and is referred to at the "native confirmation" of the molecule.

To delay the timing of onset of innate immune activation using polymer carriers of TLR-7/8a, high densities (10 mol%) of the high potency TLR-7/8a, 20x7/8a, were attached to the polymer backbone through a C4 hydrazine to yield a pro-drug variant of PP-20x7/8a^{Hi}, referred to as PP-pro20x7/8a^{Hi} (Figure 6.2A). Based on earlier findings, hydrazide and amide bonds linking TLR-7/8a to polymers appear to be hydrolysed slowly *in vivo*, possibly by cathepsins or other proteases. It was, therefore, hypothesized that attachment of 20x7/8a through the C4 position would either completely abrogate or delay the onset of innate immune activation and that activity would be restored through hydrolysis of the hydrazide bond (at the C4 amine position) *in vivo*. The capacity of PP-pro20x7/8a^{Hi} (pro-drug) and PP-20x7/8a^{Hi} (native form) to induce lymph node cytokine production was assessed at serial timepoints following their subcutaneous administration. Whereas PP-20x7/8a^{Hi} induced high levels of IL-12 and IP-10 at all time points evaluated (days 1-15), PP-pro20x7/8a^{Hi} did not induce measurable lymph node cytokine production until 8 days after administration (Figure 6.2B-C). To confirm this trend, PP-pro20x7/8a^{Hi} was subcutaneously administered at 2 different doses and was evaluated for the capacity to induce lymph node cytokine production up to 16 days after administration (Figure 6.2D-E). Consistent with Figure 6.2B-C, no lymph node cytokine production was induced by PP-pro20x7/8a^{Hi} until 8 days after administration and these responses were maintained up until day 16. Importantly, no lymph node cytokine production was observed for the small molecule pro-drug, pro20x7/8a, or the polymer particle, PP, which confirms the need for both the particle and TLR-7/8a to induce IL-12 and IP-10 production in lymph nodes.

Altogether, these studies suggest that polymer carriers may be an effective strategy for delaying the onset of innate immune activation by attaching the TLR-7/8a to the polymer backbone through the C4 position using chemically labile linkers. Additional studies evaluating the utility of this approach for use with gene delivery based vaccines are ongoing.

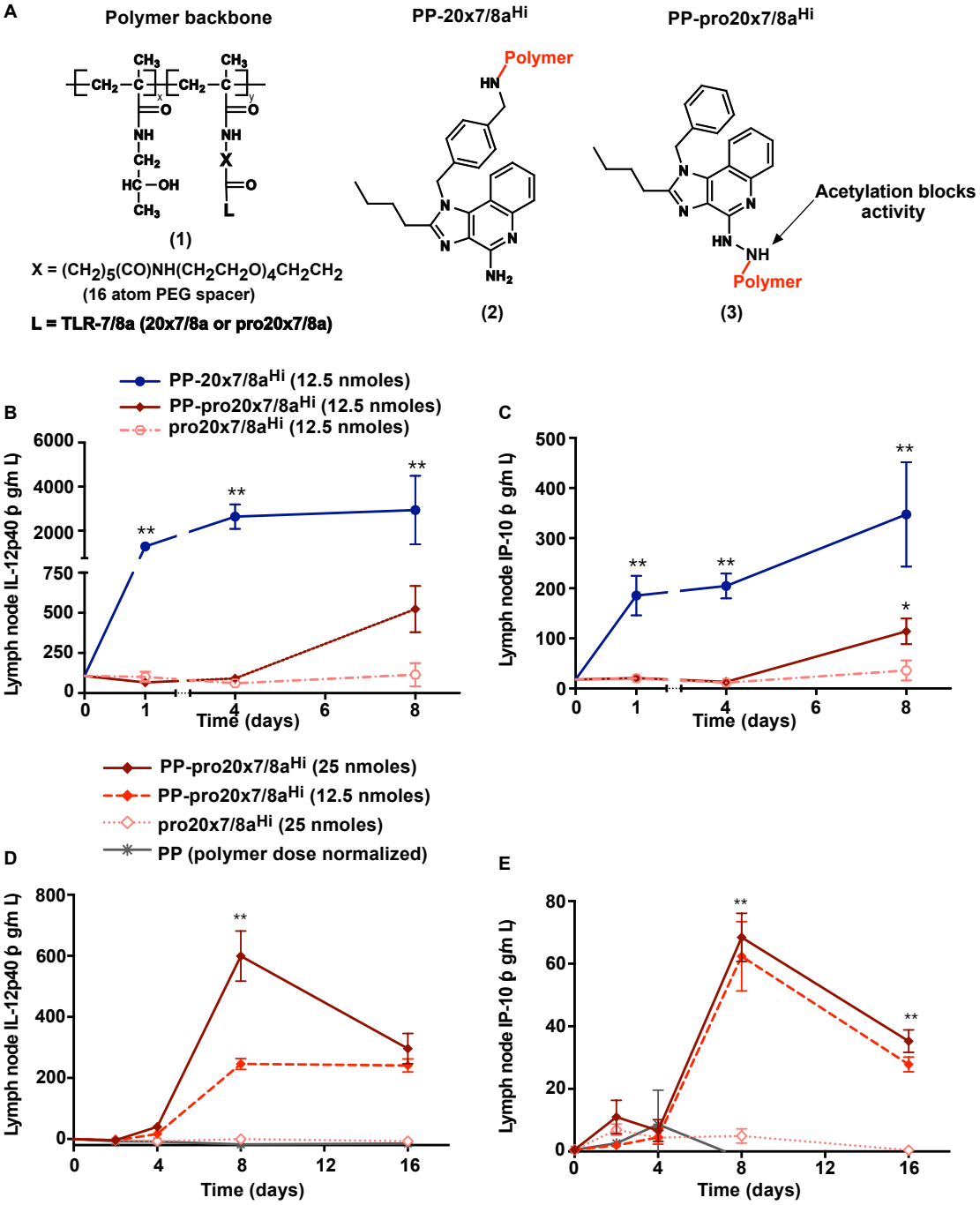

Figure 6.2: Delayed onset of innate immune activation using a pro-drug Poly-7/8a. (A) Poly-7/8a (1) were prepared with high densities (~ 10%) of either 20x7/8a (PP-20x7/8a^{Hi}, 2), or a pro-drug version of the molecule (pro20x7/8a) that was attached to the polymer backbone through a C4 aryl hydrazide (PP-pro20x7/8a^{Hi}, 3). (B-E) PP-20x7/8a^{Hi}, PP-pro20x7/8a^{Hi} and the small molecule (pro20x7/8a) and polymer control (PP) were subcutaneously administered into both hind footpads of C57BL/6 mice and proximal draining lymph nodes (popliteal, n = 4) were evaluated for the presence of either (B, D) IL-12p40 or (C, E) IP-10 by ELISA at serial timepoints thereafter. All data are represented as mean ± SEM. Significance is relative to naïve.

6.3 Micelle-forming Poly-7/8a

First-generation Poly-7/8a adjuvants described in chapters 3-5 were comprised of linear HPMA-based copolymers with TLR-7/8a statistically distributed along the length of the polymer backbone (Figure 6.3A). The capacity of the 1st-generation Poly-7/8a to form particles was dependent on high densities of TLR-7/8a introducing amphiphilic properties into the Poly-7/8a. To provide greater control over particle formation that is independent of TLR-7/8a density, micelle-forming Poly-7/8a were developed using HPMA and poly(propylene glycol) (PPG)-based multiblock copolymers (Figure 6.3B). Note that PPG allows for particle formation at low TLR-7/8a density (<3-5 mol% 7/8a) and that changing the length of the PPG-based hydrophobic core provides a means of tuning the sizes of micelles formed.

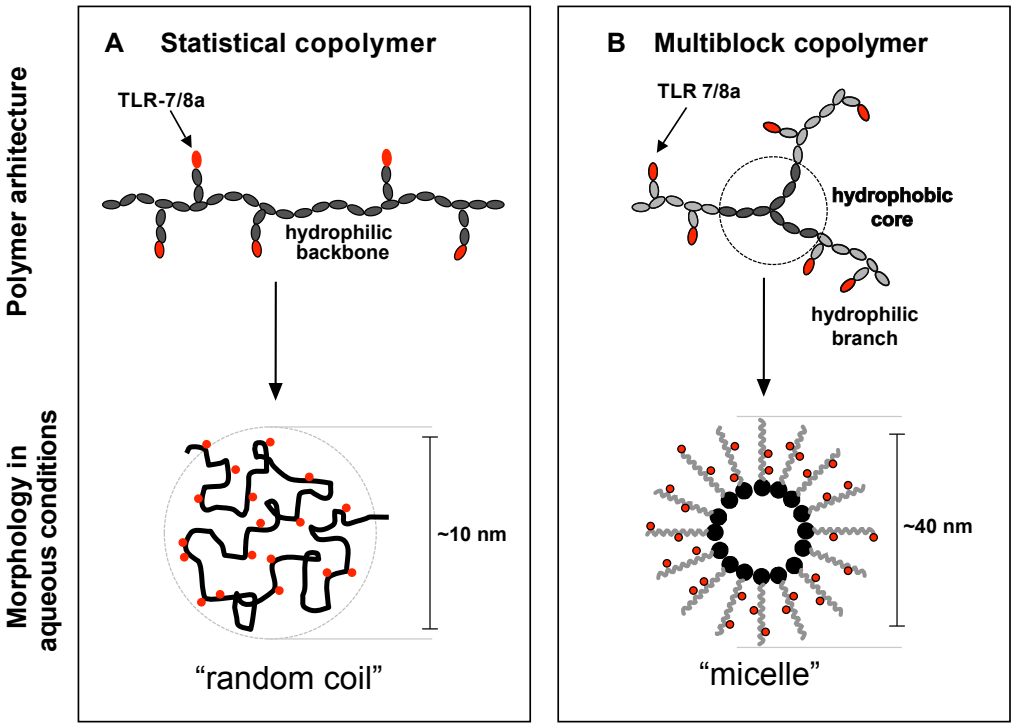

Figure 6.3: Statistical copolymer (1st-generation) and multi-block copolymer (2nd-generation)-based Poly-7/8a architecture and morphology in aqueous conditions. (A) First-generation Poly-7/8a were HPMA-based statistical copolymers. Statistical copolymers with low densities of TLR-7/8a adopt random coil confirmations (shown), whereas statistical copolymers with high densities of TLR-7/8a were found to assemble into polymer particles (not shown). (B) Structure of a 2nd-generation micelle-forming Poly-7/8a comprised of an HPMA and poly(propylene glycol) PPG-based multi-block copolymer. Note that 3 copolymer chains of HPMA containing TLR-7/8a radiate from the hydrophobic PPG-based core and that the hydrophobic core drives micelle formation.

Synthesis of second generation micelle-forming Poly-7/8 (Figure 6.4) was carried out in collaboration with Richard Laga at the Institute of Macromolecular Chemistry at Prague. In short, multiple azide group-containing small molecule TLR-7/8a (20x7/8a-azide) were conjugated to a multi-block copolymer using a Cu(I) Azide-Alkyne Cycloaddition (CuAAC) "click chemistry" reaction[192, 193]. As shown in Figure 6.4, the TLR-7/8a (20x7/8a) is linked to the polymer backbone through 1,2,3-triazole rings that are highlighted in red font. This synthetic procedure was used to prepare a

micelle-forming Poly-7/8a with ~ 3 mol % 7/8a (Table 6.1). Note that micelle-forming Poly-7/8a were prepared with low agonist densities (< 3 mol% 7/8a) so that the PPG core predominantly drives particle formation independent of the attached ligand.

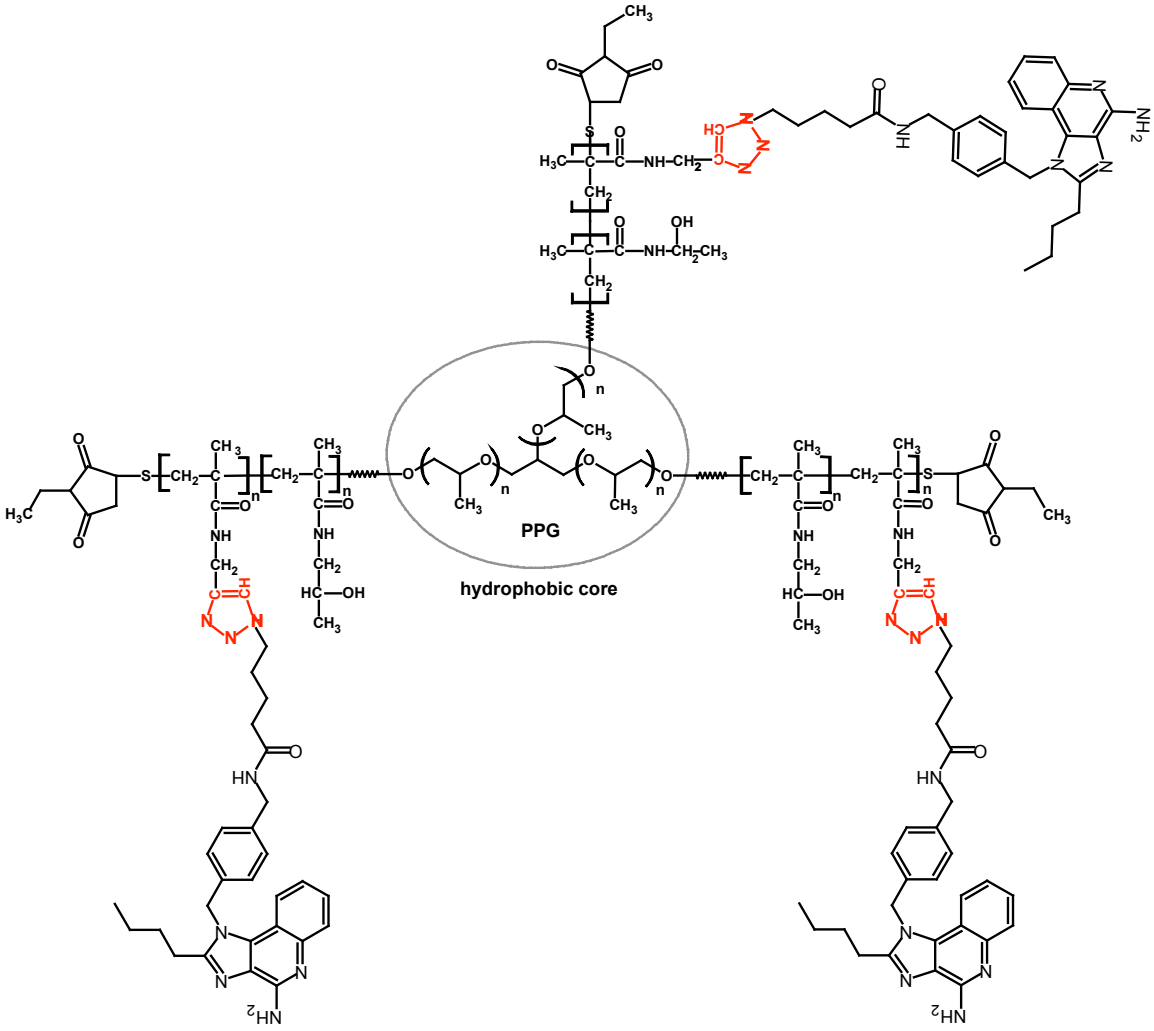

Figure 6.4: Structure of second-generation micelle forming Poly-7/8a. The A block of the multi-block copolymer is a hydrophobic core comprised of water insoluble poly(propylene glycol). The B block of the multi-block copolymer is comprised of a copolymer of HPMA and PGMA-TLR-7/8a. Note that the TLR-7/8a is attached to the monomer, PGMA, through a 1,2,3-triazole.

Adjuvant	Agonist-linker	Agonist density (mol% 7/8a)	Molecular weight (g/mol)	Particle size (d. nm)
PP-20x7/8$^{10\%}$	20x7/8a-PEG	~ 10	50,820	528 ± 43
PM-20x7/8a$^{3\%}$	20x7/8a-azide	~ 3	54,500	428 ± 233
PM	----	0	48,700	342 ± 125

Table 6.1: Physicochemical properties of 1st and 2nd-generation Poly-7/8a. PP-20x7/8a$^{10\%}$ is an HPMA-based statistical copolymer with ~ 10 mol% 7/8a. PM-20x7/8a is a multi-block copolymer with ~ 3 mol% 7/8a attached to the polymer backbone. PM is the multi-block copolymer control without TLR-7/8a attached. UV-Vis spectrophotometry, GPC and light scattering determined agonist density, molecular weight, and particle size, respectively (see materials and methods). Particle size is reported as mean ± SD (n = 3)

Particle size distribution and biological activity of the second-generation micelle-forming Poly-7/8a, PM-20x7/8a$^{3\%}$, was compared with the lead first-generation Poly-7/8a, PP-20x7/8a$^{10\%}$ and is shown in Figure 6.5. Whereas PP-20x7/8a$^{10\%}$ exists predominantly as submicron-sized polymer particles (530 ± 40 nm) in aqueous conditions, PM-20x7/8a$^{3\%}$ was found to be in equilibrium between single molecule "unimers" (~ 20 ± 15 nm) and multimeric "micelle" particles (430 ± 230 nm).

To evaluate biological activity, lymph node cytokine production was assessed following subcutaneous footpad administration of PP-20x7/8a$^{10\%}$, PM-20x7/8a$^{3\%}$ and both the small molecule (20x7/8a) and micelle-forming polymer (PM) controls. Consistent with previous findings, PP-20x7/8a$^{10\%}$ induced persistent IL-12 and IP-10 production and the small molecule, 20x7/8a, induced only transient IP-10 (< 24 h) and low to undetectable levels of IL-12 (Figure 6.5C-D). Notably, PM-20x7/8a$^{3\%}$ induced a similar kinetic but a significantly (~ 4-fold) lower magnitude of IL-12

production as compared with PP-20x7/8a$^{10\%}$. In contrast, PM-20x7/8a$^{3\%}$ induced a similar early magnitude of IP-10 production but these levels were significantly lower than those observed for PP-20x7/8a$^{10\%}$ at the day 8 timepoint. Altogether, these data show that the multi-block copolymer is an effective strategy for inducing particle formation of Poly-7/8a at low TLR-7/8a density but that the activity of these preliminary prototypes is lower than optimized 1st-generation Poly-7/8a (e.g., PP-20x7/8a$^{10\%}$) that assemble into submicron polymer particles.

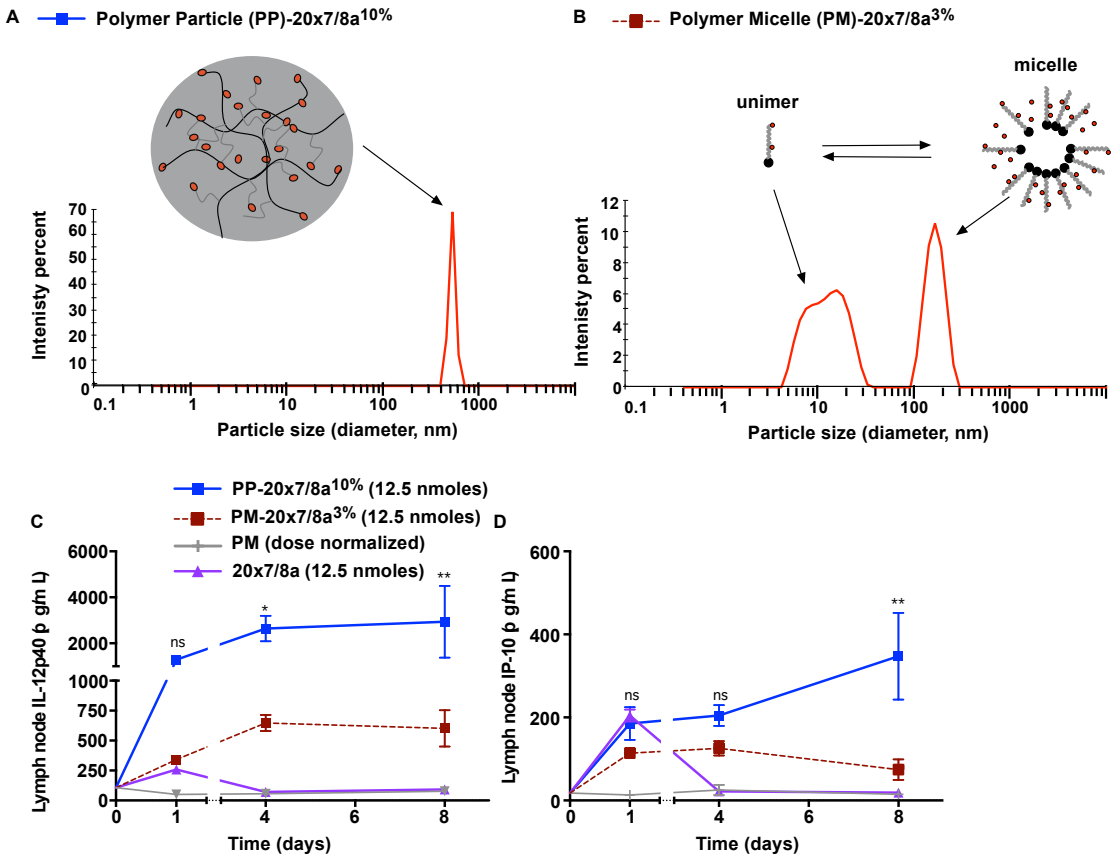

Figure 6.5: Particle size distribution and biological activity of 1st and 2nd-generation Poly-7/8a prototypes. (A-B) Cartoon representation and particle size distribution (diameter, nm) of (A) PP-20x7/8a$^{10\%}$ and (B) PM-20x7/8a$^{3\%}$; particle size distribution analysis was carried out using dynamic light scattering. (C-D) PP-20x7/8a$^{10\%}$, PM-20x7/8a$^{3\%}$, PM and 20x7/8a were subcutaneously administered into both hind footpads of C57BL/6 mice and proximal draining lymph nodes (popliteal, n = 4) were evaluated for the presence of either (C) IL-12p40 or (D) IP-10 by ELISA at serial timepoints thereafter. All data are represented as mean ± SEM. Significance is relative to the micelle-forming Poly-7/8a, PM-20x7/8a$^{3\%}$.

6.4 *In vivo* particle formation using thermoresponsive polymers

Many prior studies have established that particulate antigens and adjuvants are markedly more immunogenic than single, monomeric macromolecules[22, 24, 26, 108, 119, 135, 194]. Indeed, the studies presented herein (Chapters 3-5) corroborate these findings and show that particle formation is critical for local retention and DC uptake, which leads to higher magnitude and more persistent innate immune activation in tissue draining lymph nodes. However, two practical considerations limit the potential utility of many particle-based adjuvant systems: (1) many particulate adjuvants are too large to permit the use of cost-effective sterile filtration, which is only amenable to vaccine products that are smaller than filter pore sizes (~ 200 nm)[195]; and, (2) particulate adjuvants and vaccines often require specialized storage conditions to prevent particle aggregation[22].

To overcome the limitations associated with preformed particles, thermo-responsive polymer particle TLR-7/8a conjugates (TRPP-7/8a) were developed that exist as single water-soluble macromolecules during manufacturing and storage but undergo temperature-driven particle formation above an empirically defined transition temperature (Figure 6.6). The transition temperature is dependent on the composition of the polymer backbone and the attached ligands, properties that can be chemically tuned to permit control over the temperature range over which particle formation occurs.

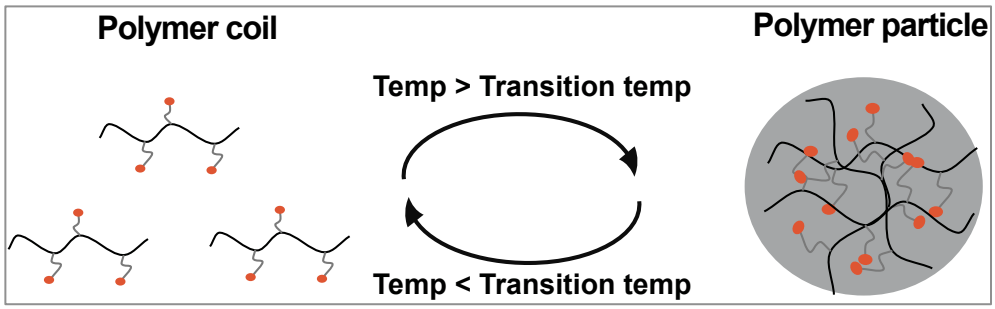

Figure 6.6 : Thermo-responsive polymer particle-7/8a conjugates (TRPP-7/8a). Cartoon schematic of TRPP-7/8a shown reversibly assembling into particles.

While there are several different classes of polymers that exhibit thermo-responsive properties[196-199], the studies herein focused on the use of N-isopropylacrylamide (NIPAM)-based copolymers that have similar physical and chemical properties to HPMA-based copolymers (see Figure 6.7). The mechanism for the thermo-responsive property of polymers is due to intramolecular hydrogen bonding. At temperatures below the transition temperature of a thermo-responsive polymer, the polymer chain is extended in aqueous solutions and individual monomers hydrogen bond predominantly with water molecules in the solvent. At temperatures above an empirically defined transition temperature, which is dependent on the exact composition of the material, the propensity of neighbouring monomer units along the polymer chain to undergo hydrogen-bonding increases[197]. This increase in intramolecular hydrogen bonding leads to compression of the polymer chain, which expels water molecules and results in even greater propensity of the polymer chain to undergo intramolecular hydrogen bonding through an autocatalytic process. The collapsing polymer chain excludes water molecules and leads to formation of a hydrophobic globular molecule that associates with other globules to assemble into sub-micron sized particles.

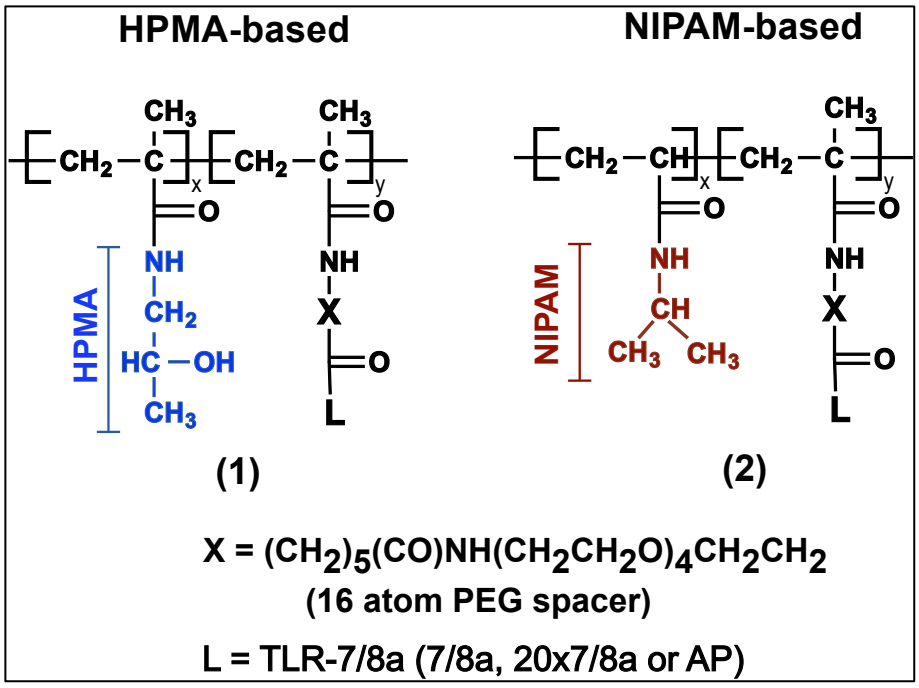

Figure 6.7: Generic structures of HPMA and NIPAM-based statistical copolymer carriers of TLR-7/8a. Note that NIPAM-based copolymers lack the hydroxyl group present on HPMA, which reduces water solubility and contributes to the capacity of NIPAM-based polymers to undergo temperature-dependent particle formation.

NIPAM-based TRPP-7/8a were synthesized according to the same protocol that was used to synthesize 1st-generation HPMA-based Poly-7/8a (see materials and methods). In short, amine-reactive NIPAM-based copolymer precursors were reacted with different amounts of 7/8a, 20x7/8a or a control ligand (4-aminopyridine, AP) to generate 8 unique TRPP conjugates described in Figure 6.8A. Note that increasing the density of either the TLR-7/8a (7/8a, or 20x7/8a) or control ligand (AP) attached to the NIPAM-based copolymers is associated with decreasing transition temperature (the temperature at which particle formation occurs). An example of the influence of ligand density on transition temperature is shown in Figure 6.8B, where increasing agonist density from 2.4 to 4.7 mol% 7/8a is associated with a transition temperature decrease from 43°C (above body temperature) to 34°C (below body temperature); the TRPP control with the 6 mol% AP ligand is shown and has a transition temperature of 32°C.

A

Adjuvant	Agonist-spacer	Agonist density	TT	Morphology at BT	M_W	M_n	M_W/M_N
TRPP-7/8a^{43C}	7/8a-PEG	2.4	43	Polymer coil	30,640	22,820	1.34
TRPP-7/8a^{34C}	7/8a-PEG	4.7	34	Polymer particle	34,840	26,000	1.34
TRPP-7/8a^{15C}	7/8a-PEG	5.4	<15	Polymer particle	37,240	27,290	1.36
TRPP-20x7/8a^{37C}	20x7/8a-PEG	1.2	37	Polymer coil	31,510	23,700	1.33
TRPP-20x7/8a^{34C}	20x7/8a-PEG	1.8	34	Polymer particle	31,790	23,790	1.34
TRPP-20x7/8a^{17C}	20x7/8a-PEG	2.8	17	Polymer particle	32,480	24,270	1.34
TRPP^{32C}	AP-AMPH	6.0	32	Polymer particle	49,120	41,070	1.20
TRPP^{29C}	AP-AMPH	9.0	29	Polymer particle	66,350	55,990	1.19

B

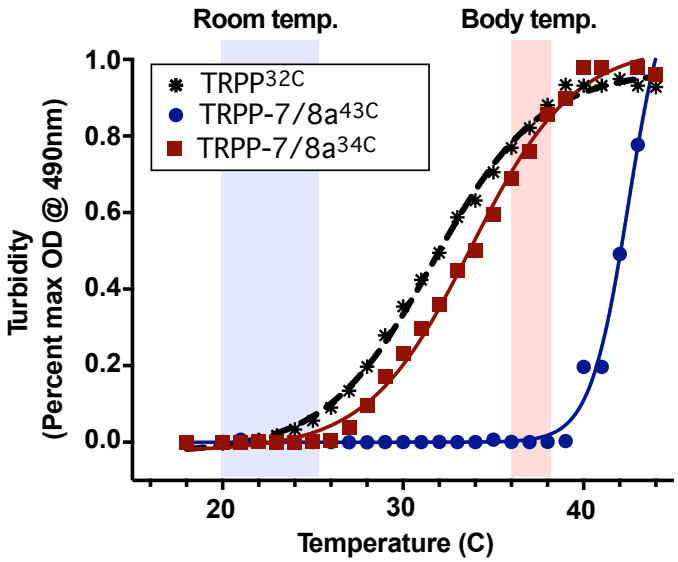

Figure 6.8: Thermo-responsive polymer particle-7/8a conjugates (TRPP-7/8a). (A) Table summarizing the thermo-responsive properties of a series of NIPAM-based TRPP-7/8a and TRPP controls that were produced with increasing densities of either SM 7/8a, SM 20x7/8a or the control ligand, 4-aminopyridine (AP). Note that increasing densities of the hydrophobic molecules leads to decreasing transition temperature (TT). (B) TT was empirically determined by measuring the turbidity (OD at 490 nm) of solutions of different TRPP and TRPP-7/8a in PBS over a range of temperatures; TT is defined as the temperature at 50% the max value of absorbance (horizontal asymptote).

To evaluate the dependence of transition temperature on *in vivo* activity, TRPP-7/8a with transition temperatures of 43 and 34°C (TRPP-7/8a^{43C} and TRPP-7/8a^{34C}, respectively) and a control TRPP with a transition temperature of 32°C (TRPP^{32C}) were evaluated for the capacity to induce lymph node cytokine production following subcutaneous administration. Whereas TRPP-7/8a^{34C}, which exists as a polymer particle at body temperature (T > 36°C), induced high levels of lymph node IL-12 and IP-10, the TRPP control (particle at body temperature) and TRPP-7/8a^{43C} (polymer coil at body temperature) induced low to undetectable levels of lymph node cytokine production (Figure 6.9B-C).

To evaluate whether local innate immune activation and lymph node cytokine production induced by TRPP-7/8a is sufficient for eliciting protective CD8 T cell mediated immunity, mice were immunized with either OVA alone, or OVA co-administered with TRPP-7/8a^{34C}, TRPP-7/8a^{43C} or the TRPP control (Figure 6.9B). Consistent with earlier findings, only TRPP-7/8a^{34C}, which forms particles at body temperature, induced significant T cell responses and protection against infectious challenge with *L mono* expressing OVA (*LM-OVA*); TRPP-7/8a^{43C} and TRPP did not improve CD8 T cell mediated protection as compared with OVA administered alone. These results substantiate the importance of particulate adjuvants for inducing immune responses and suggest that *in situ* particle formation using thermo-responsive carriers may be a suitable alternative to preformed particles for eliciting protective T-cell mediated immunity to a co-administered protein antigen.

A

Adjuvant	Agonist density	TT (°C)	Morphology at 20-25 °C	Morphology at T > 36 °C
✳ TRPP^{32C}	0	32	Polymer coil	Polymer Particle
● TRPP-7/8a^{43C}	2.4	43	Polymer coil	Polymer coil
■ TRPP-7/8a^{34C}	4.7	34	Polymer coil	Polymer Particle

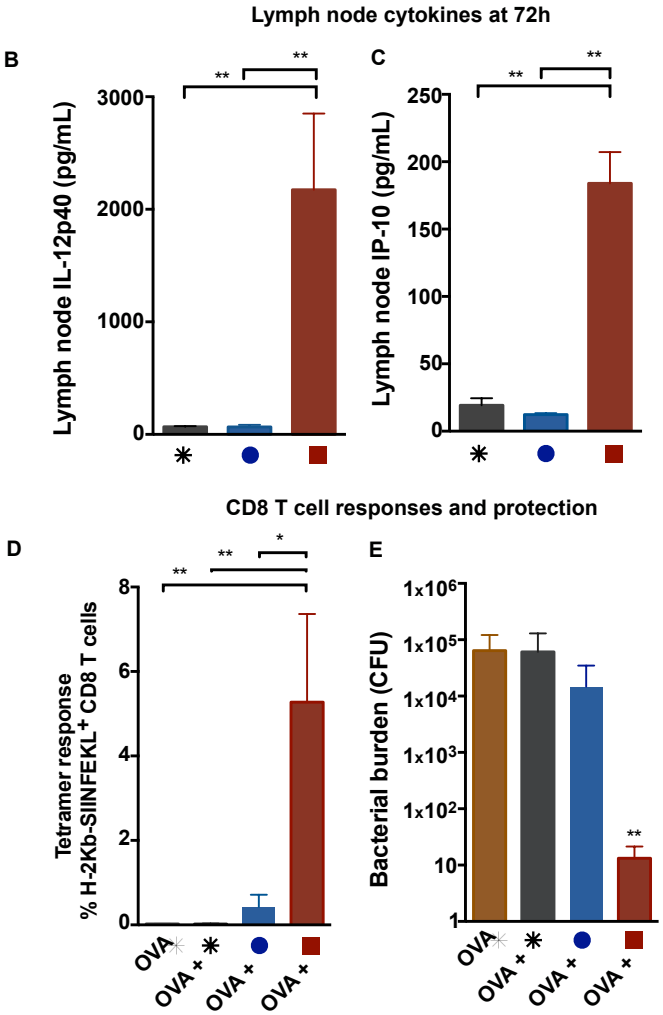

Figure 6.9: Thermo-responsive polymer particles (TRPP) permit in vivo particle assembly that leads to persistent innate immune activation sufficient for eliciting protective CD8 T cell responses. (A) Table summarizing the TRPP-7/8a and TRPP constructs evaluated in vivo. (B-C) TRPP-7/8a and TRPP controls were delivered subcutaneously into both hind footpads of C57BL/6 mice. Popliteal lymph nodes (n = 4) were harvested at 72 h and cultured *ex vivo* overnight. Supernatants were evaluated for the presence of (B) IL-12p40 or (C) IP-10. (D-E) C57BL/6 mice (n = 5) received subcutaneous administration of 50 μg of OVA formulated with adjuvant or control at days 0 and 14. (C) Tetramer^{+} CD8 T cell responses were evaluated at day 28. (D) Mice were challenged intravenously at day 28 with LM-OVA and bacterial burden in spleens was evaluated on day 31; significance is relative to OVA. All data are represented as mean ± SEM.

6.5 Discussion

Several novel synthetic chemical schemes were devised to allow for greater control over physicochemical properties of 2nd-generation Poly-7/8a. These strategies included the modification of the TLR-7/8a attachment site to develop a pro-drug Poly-7/8a that delays onset of immune activation in lymph nodes, as well as changes to the polymer backbone that influence how and when particle formation occurs. Altogether, these studies demonstrate how the chemical versatility and tunability of polymers can be used to overcome the contemporary limitations of vaccine adjuvants.

Delayed onset of innate immune activation

To control the onset of innate immune activation, an imidazoquinoline-based TLR-7/8a was linked to an HPMA-based scaffold through the C4 aryl amine position of the agonist to generate a pro-drug version of Poly-7/8a. Previous reports have shown that the C4 position is critical to TLR-7/8 dependent activity[66, 73, 191]. Consistent with earlier reports, pro-drug Poly7/8a (PP-pro20x7/8a^{Hi}) did not induce lymph node cytokine production at days 1-4, but significant levels of lymph node cytokine production were observed over days 8-16. These data suggest that the amide bond at the C4 position, which was used to link the TLR-7/8a to the polymer backbone, is able to undergo hydrolysis to release the active form of the compound *in vivo*. Indeed, these findings are consistent with recent reports that photolabile groups attached through the C4 position of TLR-7/8a can be used as switches to turn on activity through UV light-catalysed release of the photolabile group[191].

While these studies suggest that bond stability at the C4 position may be an effective means of controlling the exact timing of onset of innate immune activation, a critical question is whether these strategies will have any potential clinical utility. Towards addressing this question, ongoing studies are evaluating how delayed onset of innate immune activation influences gene expression and downstream T cell responses elicited by CpG-free plasmids expressing model transgene antigens.

Controlled particle formation using micelle-forming Poly-7/8a

To provide greater control over Poly-7/8a particle formation, multi-block copolymer carriers of TLR-7/8a (PM-20x7/8a$^{3\%}$) were developed that use hydrophobic PPG-based cores to drive particle formation. Micelle-forming carriers are attractive from a product development standpoint because of the reversibility of particle formation and the proven safety record of other micelle-forming particulate systems (e.g., pluronics) for human use[200-202]. However, as evidenced by the modest immune activation induced by the 2nd-generation micelle-forming Poly-7/8a as compared with the lead 1st-generation Poly-7/8a, additional development will be required to optimize micelle-forming Poyl-7/8a activity.

In situ particle formation using thermo-responsive polymer scaffolds

Thermo-responsive polymers were developed as a means of overcoming limitations associated with the manufacturing and storage of pre-formed particles while at the same time providing the superior biological activity associated with particulate adjuvants. While two prior studies have used thermo-responsive polymers to either entrap antigen[203] or use the polymers as an adjuvant alone[196], this is the first report to use thermoresponsive polymers as scaffolds for the delivery of adjuvants. These

proof-of-concept studies demonstrate that polymeric adjuvants with thermo-responsive properties can be used to induce high levels of innate immune activation in lymph nodes that is sufficient for eliciting protective CD8 T cell responses to a co-administered protein antigen. Combining high *in vivo* potency of a particulate adjuvant system with the high stability and chemical definition of soluble single molecule solutions provides a novel and potentially more cost-effective adjuvant delivery system than contemporary pre-formed particle-based adjuvants.

Altogether, the novel synthetic chemical approaches described herein demonstrate the tremendous versatility of polymer carriers as platforms for the delivery of TLR-7/8a and suggest that further research and development efforts are warranted to realise the full potential of this technology for clinical utility.

7 Conclusions and future directions

This section will summarize key findings and will propose next steps that should be undertaken to advance this work. A more in-depth discussion of the major findings of this thesis can be found within the discussion section of each results chapter.

7.1 Conclusions

Historically, particulate delivery systems based on aluminum salts (Alum)[204] and oil-in-water emulsions[205] have been used as stand alone adjuvants to enhance antibody responses to protein-based vaccines. More recently, small molecule immune potentiators, such as certain TLRa (e.g., Monophosphoryl Lipid A) have been formulated with these earlier generation particulate adjuvants to improve antibody responses for licensed vaccines against HPV and Influenza[206, 207]. However, currently licensed vaccine adjuvants are limited for inducing Th1 and CD8 T cell mediated immunity because they lack the appropriate innate immune stimulus needed to promote T cell priming and / or are inadequately formulated to provide sufficient magnitude and persistence of innate immune activation. Therefore, based on the ability of TLR-7/8a to induce broad-based APC activation and production of a cytokine milieu that promotes Th1 priming and antigen cross-presentation, this study focused on using a novel adjuvant delivery approach to define the physicochemical parameters of both the TLR-7/8a and delivery platform that directly influence the location, magnitude and duration of innate immune activation that are critical for promoting adaptive T cell immunity to protein antigens.

While several recent reports in the literature describe non-covalent formulations of TLR-7/8a with particulate delivery systems[121, 123, 124, 126], we introduce a purpose-built strategy whereby TLR-7/8a are covalently linked to linear biocompatible polymer carriers (Poly-7/8a). This strategy provides the advantage that many of the physicochemical properties of both the polymer (length, composition, etc.) and covalently attached TLRa (linker group composition, density and orientation of agonist, etc.) can be precisely chemically tuned to modulate biological activity. Screening combinatorial libraries of Poly-7/8a *in vivo* led us to identify many important structure-activity relationships. The most notable finding was that only Poly-7/8a that assembled into particles induced robust and persistent (> 8 days) lymph node innate immune activation and protective T cell responses. This finding guided our rational design of later generation Poly-7/8a that undergo temperature dependent particle formation, and, more broadly, these findings substantiate the importance of particulate delivery of TLRa for enhancing innate and adaptive immunity.

Consistent with recent reports, we observed that spatially restricting TLRa distribution *in vivo* is critical for enhancing local (lymph node) activity and limiting systemic inflammation[126, 176]. Indeed, while the importance of spatially restricting TLRa distribution was emphasized in a recent study, the data presented herein suggests that improved retention is necessary but not sufficient for enhancing T cell immunity. Despite improved retention at the injection site and draining lymph nodes by all polymer carriers of TLR-7/8a, we observed that only the particles (PP-7/8a) are taken up efficiently by APCs and enhance T cell immunity. In addition to focusing adjuvant activity locally, we also show that particulate formulations of Poly-7/8a (PP-7/8a) are necessary for prolonging (> 8 days) innate immune activation in lymph

nodes, which correlates with their capacity to elicit protective CD4 and CD8 T cell responses. These findings are corroborated by earlier work showing that prolonged innate immune activation is critical for optimizing T cell immunity[128, 129, 131, 184]. The capacity of particles to focus and prolong adjuvant activity in lymph nodes provides an *in vivo* mechanism to account for the observations by others and us that TLR-7/8a attached to protein antigens are markedly more immunogenic upon aggregation or when adsorbed to alum microparticles[108, 116], as this renders both the antigen and TLR-7/8a particulate.

Another important consideration is how particle size influences innate and adaptive immune responses. Consistent with earlier findings[148-150], the particle forming Poly-7/8a used in this thesis, which were ~ 500 nm in diameter, were taken up by a high proportion of migratory and monocyte-derived DCs, but not by pDCs. Despite limited uptake by pDCs and $CD8^+$ DCs, the particle forming Poly-7/8a were found to induce high levels of Type I IFNs and were able to elicit high magnitude CD8 and Th1-type CD4 T cell responses that mediated protection following infectious challenge. While some reports suggest that direct targeting of lymph node resident DCs using particles < 100 nm may be preferential for eliciting T cell responses[135, 148-150], the findings herein are consistent with recent reports that TLR-7/8a delivered on particles > 200 nm are effective for eliciting T cell responses despite limited uptake by $CD8^+$ DCs and pDCs[119, 121]. However, additional studies will be required to identify how precise sizes of particles carrying TLR-7/8a influence priming of protective T cell mediated immunity.

In addition to the importance of particle formation for activity, increasing TLR-7/8a density and potency led to more persistent innate immune activation in lymph nodes. Whereas potency likely relates to receptor occupancy, improved activity by higher densities of TLR-7/8a along the polymer backbone may be accounted for by higher avidity interactions or the capacity of the densely arrayed TLR-7/8a to promote favourable receptor clustering[142, 144]. Moreover, varying the orientation of the TLR-7/8a to block sites of the agonist (i.e., C4 amine) that are critical for receptor binding[73] delayed the onset of innate immune activation in draining lymph nodes. This finding, together with a recent *in vitro* study showing that chemically labile bonds can be used to block the C4 amine of the TLR-7/8a to temporally control innate immune activity[191], suggests that the orientation and sites of the agonist can be chemically tuned to temporally program the onset of innate immune activation *in vivo*, which may be useful for gene delivery strategies that require delayed onset of innate immune activity to optimize gene expression[188, 189].

While linear biocompatible polymers were used as scaffolds for the delivery of TLR-7/8a, the results herein suggest that other particle-based delivery platforms will also be useful and should focus on high agonist density and potency to achieve persistent innate immune activation required for generating protective cellular immunity and Th1-polarization. Indeed, PLGA-[120, 124], liposomal-[121] and Alum-based particulate delivery platforms that are currently being developed by Selecta, 3M and Novartis pharmaceutical companies, respectively, are suitable strategies that fulfil the physicochemical requirements identified and validated in this thesis. However, as highlighted in a recent review[22], particulate delivery systems used in vaccines can be unstable during long-term storage and often require specialized manufacturing and

storage conditions that can contribute significantly to cost. These considerations led us to develop thermo-responsive Poly-7/8 (TRPP-7/8a) that only assemble into particles at defined temperatures either under controlled conditions *in vitro* or at body temperature *in vivo*. This new approach could potentially overcome the manufacturing and storage limitations of preformed particles and may allow for the use of single-vial water-soluble preparations of antigen and adjuvant, which is ideal from a product development standpoint.

A final consideration is how the technology described herein compares with alternative subunit vaccine approaches for eliciting T cell immunity, such as the use of recombinant viral vectors, virus like particles (VLPs) bacteriophages, or even whole organism vaccines[1, 7, 10, 11, 15]. Whereas synthetic chemical approaches were used herein to produce non-naturally occurring materials for use in vaccines, recombinant viruses and VLPs offer the advantage that these are particulate platforms that combine antigens and adjuvants that are comprised of naturally occurring biomolecules. Moreover, the capacity of viruses to produce antigen endogenously allows for the generation of more robust T cell immunity as compared with exogenously delivered protein antigen[15]. Indeed, recombinant viral vectors have been shown to mediate protection against Ebola in primates[208] and have been shown to elicit high magnitude and durable CD8 T cell responses against HIV and malaria proteins as well[160, 209]. While subunit approaches may be preferred for generating immune responses against very well defined epitopes of antigens, whole organism based vaccines may be important when high breadth of immune responses may be needed to control infection, which may be useful for diseases such as Malaria[210]. Finally, while this thesis focused on the use of traditional vaccine approaches, genetic

technologies are emerging that could revolutionize medicine. Accordingly, a CMV vector that establishes stable infection was recently shown to mediate complete HIV clearance in infected primates[5], whereas an alternative genetic engineering approach whereby patient's T cells were engineered using a chimeric-antigen receptor (CAR) was shown to mediate complete clearance of a B cell lymphoma in patient's who were refractive to treatment with traditional chemotherapy regimens[211]. Overall, in addition to the adjuvant formulations described in this thesis, it's important to recognize that many alternative platform technologies exist for generating T cell responses that can mediate protection against infection and cancer.

In conclusion, polymer carriers of TLRa represent a diverse and versatile class of adjuvant delivery platform that can be systematically chemically tuned to achieve the optimal magnitude and spatiotemporal characteristics of innate immune activation required for eliciting protective T cell immunity. While TLR-7/8a were chosen as model adjuvants for these studies, both the systematic approach and modular platform described herein should be amenable for optimizing delivery of other immune potentiators and / or protein antigens for use in vaccines.

7.2 Future directions

To advance the technology described in this thesis, ongoing efforts are focused on improving the chemical definition and generalizability of the polymer adjuvants. These efforts are elaborated briefly here:

Greater programmability and biodegradability of thermo-responsive Poly-7/8a

The thermoresponsive Poly-7/8a platforms described in chapter 6 undergo particle formation at temperatures that depend on the density of attached agonists. This dependency on agonist density reduces the potential generalizability and modularity of this approach as it requires modulation of agonist density to achieve the desired transition temperature, which may not be preferable when the optimal agonist for biological activity and transition temperature are disparate. Thus, to allow for control over the transition temperature independent of the attached TLR-7/8a, we have recently begun to use a di-block copolymer that segregates the thermo-responsive block of the copolymer from the block where the TLR-7/8a is attached. This allows for thermo-responsiveness of the polymers to be tuned independent of the attached agonist. Moreover, in this di-block copolymer design, we have introduced a biodegradable ester bond that should allow for more efficient excretion of these materials following their *in vivo* use.

Site-specific incorporation of protein antigen

Prior studies have shown that optimizing T cell priming to protein antigens requires synchronous delivery of antigen with innate immune stimulation (i.e., TLRa) to APCs[138, 140]. Based on this requirement for optimizing T cell immunity, it will be necessary to ensure that protein antigen is co-delivered efficiently with the thermo-responsive Poly-7/8a adjuvants developed herein. Prior studies linking protein antigen to TLR-7/8a have used non-specific chemical conjugations methods that mask important epitopes of protein antigens that are needed for recognition by neutralizing antibodies[117]. Thus, to ensure efficient co-delivery of the TLR-7/8a with thermo-responsive Poly-7/8a, without masking potentially important epitopes of the antigen, we are currently evaluating site-specific linker strategies that provide a generalizable approach for attaching antigen to the polymer platforms that should preserve important antigenic sites[112].

Control over particle formation

As emphasized earlier, particle size is an important factor influencing whether materials passively traffic, or require active transport, to lymph nodes. A major focus of ongoing work is to use thermo-responsive polymer scaffolds that assemble into particles of defined sizes (~ 50-100 nm) for optimizing delivery of molecularly defined adjuvants and protein antigens. To control the sizes of the particles formed by thermoresponsive polymers, a multiblock copolymer strategy is being employed whereby a linear copolymer is comprised of a hydrophobic thermoresponsive block that drives particle formation and a hydrophilic block that stabilizes the particles and prevents flocculation.

8 Literature cited

1. Rappuoli, R., Mandl, C.W., Black, S. & De Gregorio, E. Vaccines for the twenty-first century society. *Nat Rev Immunol* **11**, 865-872 (2011).
2. Whitney, C.G. et al. Benefits from immunization during the vaccines for children program era - United States, 1994-2013. *MMWR. Morbidity and mortality weekly report* **63**, 352-355 (2014).
3. Vitoria, M. et al. The global fight against HIV/AIDS, tuberculosis, and malaria: current status and future perspectives. *American journal of clinical pathology* **131**, 844-848 (2009).
4. Van Braeckel-Budimir, N. & Harty, J.T. CD8 T-cell-mediated protection against liver-stage malaria: lessons from a mouse model. *Frontiers in microbiology* **5**, 272 (2014).
5. Hansen, S.G. et al. Immune clearance of highly pathogenic SIV infection. *Nature* **502**, 100-104 (2013).
6. Seder, R.A. et al. Protection against malaria by intravenous immunization with a nonreplicating sporozoite vaccine. *Science* **341**, 1359-1365 (2013).
7. Nabel, G.J. Designing tomorrow's vaccines. *N Engl J Med* **368**, 551-560 (2013).
8. Picker, L.J. & Deeks, S.G. HIV: Antibodies advance the search for a cure. *Nature* **503**, 207-208 (2013).
9. Li, Y. et al. Mechanism of neutralization by the broadly neutralizing HIV-1 monoclonal antibody VRC01. *J Virol* **85**, 8954-8967 (2011).
10. Ulmer, J.B., Valley, U. & Rappuoli, R. Vaccine manufacturing: challenges and solutions. *Nat Biotechnol* **24**, 1377-1383 (2006).
11. Plotkin, S.A. Vaccines: the fourth century. *Clinical and vaccine immunology : CVI* **16**, 1709-1719 (2009).
12. Laursen, N.S. & Wilson, I.A. Broadly neutralizing antibodies against influenza viruses. *Antiviral research* **98**, 476-483 (2013).
13. Kwong, P.D., Mascola, J.R. & Nabel, G.J. Rational design of vaccines to elicit broadly neutralizing antibodies to HIV-1. *Cold Spring Harbor perspectives in medicine* **1**, a007278 (2011).
14. Perrie, Y., Mohammed, A.R., Kirby, D.J., McNeil, S.E. & Bramwell, V.W. Vaccine adjuvant systems: enhancing the efficacy of sub-unit protein antigens. *Int J Pharm* **364**, 272-280 (2008).
15. Draper, S.J. & Heeney, J.L. Viruses as vaccine vectors for infectious diseases and cancer. *Nature reviews. Microbiology* **8**, 62-73 (2010).
16. Lindsay, R.W. et al. CD8+ T cell responses following replication-defective adenovirus serotype 5 immunization are dependent on CD11c+ dendritic cells but show redundancy in their requirement of TLR and nucleotide-binding oligomerization domain-like receptor signaling. *J Immunol* **185**, 1513-1521 (2010).
17. Casimiro, D.R. et al. Comparative immunogenicity in rhesus monkeys of DNA plasmid, recombinant vaccinia virus, and replication-defective adenovirus vectors expressing a human immunodeficiency virus type 1 gag gene. *J Virol* **77**, 6305-6313 (2003).
18. Roberts, D.M. et al. Hexon-chimaeric adenovirus serotype 5 vectors circumvent pre-existing anti-vector immunity. *Nature* **441**, 239-243 (2006).

19. Barouch, D.H. et al. International seroepidemiology of adenovirus serotypes 5, 26, 35, and 48 in pediatric and adult populations. *Vaccine* **29**, 5203-5209 (2011).
20. Catanzaro, A.T. et al. Phase 1 safety and immunogenicity evaluation of a multiclade HIV-1 candidate vaccine delivered by a replication-defective recombinant adenovirus vector. *The Journal of infectious diseases* **194**, 1638-1649 (2006).
21. Coffman, R.L., Sher, A. & Seder, R.A. Vaccine adjuvants: putting innate immunity to work. *Immunity* **33**, 492-503 (2010).
22. Brito, L.A. & O'Hagan, D.T. Designing and building the next generation of improved vaccine adjuvants. *Journal of controlled release : official journal of the Controlled Release Society* **190C**, 563-579 (2014).
23. Guy, B. The perfect mix: recent progress in adjuvant research. *Nature reviews. Microbiology* **5**, 505-517 (2007).
24. Nordly, P., Madsen, H.B., Nielsen, H.M. & Foged, C. Status and future prospects of lipid-based particulate delivery systems as vaccine adjuvants and their combination with immunostimulators. *Expert opinion on drug delivery* **6**, 657-672 (2009).
25. Lambrecht, B.N., Kool, M., Willart, M.A. & Hammad, H. Mechanism of action of clinically approved adjuvants. *Curr Opin Immunol* **21**, 23-29 (2009).
26. Sharp, F.A. et al. Uptake of particulate vaccine adjuvants by dendritic cells activates the NALP3 inflammasome. *Proc Natl Acad Sci U S A* **106**, 870-875 (2009).
27. Warshakoon, H.J. et al. Potential adjuvantic properties of innate immune stimuli. *Hum Vaccin* **5**, 381-394 (2009).
28. Iwasaki, A. & Medzhitov, R. Toll-like receptor control of the adaptive immune responses. *Nat Immunol* **5**, 987-995 (2004).
29. Poltorak, A. et al. Defective LPS signaling in C3H/HeJ and C57BL/10ScCr mice: mutations in Tlr4 gene. *Science* **282**, 2085-2088 (1998).
30. Medzhitov, R., Preston-Hurlburt, P. & Janeway, C.A., Jr. A human homologue of the Drosophila Toll protein signals activation of adaptive immunity. *Nature* **388**, 394-397 (1997).
31. Lee, J. et al. Activation of anti-hepatitis C virus responses via Toll-like receptor 7. *Proc Natl Acad Sci U S A* **103**, 1828-1833 (2006).
32. Gunzer, M. et al. Systemic administration of a TLR7 ligand leads to transient immune incompetence due to peripheral-blood leukocyte depletion. *Blood* **106**, 2424-2432 (2005).
33. Hornung, V. et al. Quantitative expression of toll-like receptor 1-10 mRNA in cellular subsets of human peripheral blood mononuclear cells and sensitivity to CpG oligodeoxynucleotides. *J Immunol* **168**, 4531-4537 (2002).
34. Edwards, A.D. et al. Toll-like receptor expression in murine DC subsets: lack of TLR7 expression by CD8 alpha+ DC correlates with unresponsiveness to imidazoquinolines. *Eur J Immunol* **33**, 827-833 (2003).
35. Sandor, F. & Buc, M. Toll-like receptors. II. Distribution and pathways involved in TLR signalling. *Folia Biol (Praha)* **51**, 188-197 (2005).
36. Napetschnig, J. & Wu, H. Molecular basis of NF-kappaB signaling. *Annual review of biophysics* **42**, 443-468 (2013).
37. Hoshino, K. et al. Critical role of IkappaB Kinase alpha in TLR7/9-induced type I IFN production by conventional dendritic cells. *J Immunol* **184**, 3341-3345 (2010).

38. Connolly, D.J. & O'Neill, L.A. New developments in Toll-like receptor targeted therapeutics. *Current opinion in pharmacology* **12**, 510-518 (2012).
39. Cristofaro, P. & Opal, S.M. The Toll-like receptors and their role in septic shock. *Expert opinion on therapeutic targets* **7**, 603-612 (2003).
40. Hood, J.D. et al. Immunoprofiling toll-like receptor ligands: Comparison of immunostimulatory and proinflammatory profiles in ex vivo human blood models. *Hum Vaccin* **6**, 322-335 (2010).
41. Steinman, R.M. Dendritic cells in vivo: a key target for a new vaccine science. *Immunity* **29**, 319-324 (2008).
42. Zhu, J. & Paul, W.E. CD4 T cells: fates, functions, and faults. *Blood* **112**, 1557-1569 (2008).
43. Mosmann, T.R., Cherwinski, H., Bond, M.W., Giedlin, M.A. & Coffman, R.L. Two types of murine helper T cell clone. I. Definition according to profiles of lymphokine activities and secreted proteins. *J Immunol* **136**, 2348-2357 (1986).
44. Darrah, P.A. et al. Multifunctional TH1 cells define a correlate of vaccine-mediated protection against Leishmania major. *Nature medicine* **13**, 843-850 (2007).
45. Seder, R.A., Darrah, P.A. & Roederer, M. T-cell quality in memory and protection: implications for vaccine design. *Nat Rev Immunol* **8**, 247-258 (2008).
46. Raphael, I., Nalawade, S., Eagar, T.N. & Forsthuber, T.G. T cell subsets and their signature cytokines in autoimmune and inflammatory diseases. *Cytokine* (2014).
47. Jovanovic, K., Siebeck, M. & Gropp, R. The route to pathologies in chronic inflammatory diseases characterized by T helper type 2 immune cells. *Clinical and experimental immunology* **178**, 201-211 (2014).
48. Erle, D.J. & Sheppard, D. The cell biology of asthma. *J Cell Biol* **205**, 621-631 (2014).
49. Nakayamada, S., Takahashi, H., Kanno, Y. & O'Shea, J.J. Helper T cell diversity and plasticity. *Curr Opin Immunol* **24**, 297-302 (2012).
50. Schmitt, E., Klein, M. & Bopp, T. Th9 cells, new players in adaptive immunity. *Trends Immunol* **35**, 61-68 (2014).
51. Fazilleau, N., Mark, L., McHeyzer-Williams, L.J. & McHeyzer-Williams, M.G. Follicular helper T cells: lineage and location. *Immunity* **30**, 324-335 (2009).
52. Le Bon, A. & Tough, D.F. Type I interferon as a stimulus for cross-priming. *Cytokine Growth Factor Rev* **19**, 33-40 (2008).
53. Padovan, E., Spagnoli, G.C., Ferrantini, M. & Heberer, M. IFN-alpha2a induces IP-10/CXCL10 and MIG/CXCL9 production in monocyte-derived dendritic cells and enhances their capacity to attract and stimulate CD8+ effector T cells. *Journal of leukocyte biology* **71**, 669-676 (2002).
54. Starbeck-Miller, G.R., Xue, H.H. & Harty, J.T. IL-12 and type I interferon prolong the division of activated CD8 T cells by maintaining high-affinity IL-2 signaling in vivo. *J Exp Med* **211**, 105-120 (2014).
55. Kim, M.T. & Harty, J.T. Impact of Inflammatory Cytokines on Effector and Memory CD8+ T Cells. *Frontiers in immunology* **5**, 295 (2014).
56. Longhi, M.P. et al. Dendritic cells require a systemic type I interferon response to mature and induce CD4+ Th1 immunity with poly IC as adjuvant. *J Exp Med* **206**, 1589-1602 (2009).

57. Rajagopal, D. et al. Plasmacytoid dendritic cell-derived type I interferon is crucial for the adjuvant activity of Toll-like receptor 7 agonists. *Blood* **115**, 1949-1957 (2010).
58. Ito, T. et al. Interferon-alpha and interleukin-12 are induced differentially by Toll-like receptor 7 ligands in human blood dendritic cell subsets. *J Exp Med* **195**, 1507-1512 (2002).
59. Villadangos, J.A. & Shortman, K. Found in translation: the human equivalent of mouse CD8+ dendritic cells. *J Exp Med* **207**, 1131-1134 (2010).
60. Liu, Y.J. IPC: professional type 1 interferon-producing cells and plasmacytoid dendritic cell precursors. *Annual review of immunology* **23**, 275-306 (2005).
61. Shortman, K. & Liu, Y.J. Mouse and human dendritic cell subtypes. *Nat Rev Immunol* **2**, 151-161 (2002).
62. Poulin, L.F. et al. Characterization of human DNGR-1+ BDCA3+ leukocytes as putative equivalents of mouse CD8alpha+ dendritic cells. *J Exp Med* **207**, 1261-1271 (2010).
63. Gorden, K.B. et al. Synthetic TLR Agonists reveal functional differences between human TLR7 and TLR8. *Journal of Immunology* **174**, 1259-1268 (2005).
64. Demaria, O. et al. TLR8 deficiency leads to autoimmunity in mice. *J Clin Invest* **120**, 3651-3662 (2010).
65. Martinez, J., Huang, X. & Yang, Y. Toll-like receptor 8-mediated activation of murine plasmacytoid dendritic cells by vaccinia viral DNA. *Proc Natl Acad Sci U S A* **107**, 6442-6447 (2010).
66. Gerster, J.F. et al. Synthesis and structure-activity-relationships of 1H-imidazo[4,5-c]quinolines that induce interferon production. *J Med Chem* **48**, 3481-3491 (2005).
67. Hemmi, H. et al. Small anti-viral compounds activate immune cells via the TLR7 MyD88-dependent signaling pathway. *Nat Immunol* **3**, 196-200 (2002).
68. Lan, T. et al. Stabilized immune modulatory RNA compounds as agonists of Toll-like receptors 7 and 8. *Proc Natl Acad Sci U S A* **104**, 13750-13755 (2007).
69. Shukla, N.M., Malladi, S.S., Mutz, C.A., Balakrishna, R. & David, S.A. Structure-activity relationships in human toll-like receptor 7-active imidazoquinoline analogues. *J Med Chem* **53**, 4450-4465 (2010).
70. Weterings, J.J. et al. 2-Azidoalkoxy-7-hydro-8-oxoadenine derivatives as TLR7 agonists inducing dendritic cell maturation. *Bioorg Med Chem Lett* **19**, 2249-2251 (2009).
71. Czarniecki, M. Small molecule modulators of toll-like receptors. *J Med Chem* **51**, 6621-6626 (2008).
72. Kurimoto, A. et al. Synthesis and evaluation of 2-substituted 8-hydroxyadenines as potent interferon inducers with improved oral bioavailabilities. *Bioorg Med Chem* **12**, 1091-1099 (2004).
73. Tanji, H., Ohto, U., Shibata, T., Miyake, K. & Shimizu, T. Structural reorganization of the Toll-like receptor 8 dimer induced by agonistic ligands. *Science* **339**, 1426-1429 (2013).
74. Diebold, S.S., Kaisho, T., Hemmi, H., Akira, S. & Reis e Sousa, C. Innate antiviral responses by means of TLR7-mediated recognition of single-stranded RNA. *Science* **303**, 1529-1531 (2004).
75. Heil, F. et al. Species-specific recognition of single-stranded RNA via toll-like receptor 7 and 8. *Science* **303**, 1526-1529 (2004).

76. Dudek, A.Z. et al. First in human phase I trial of 852A, a novel systemic toll-like receptor 7 agonist, to activate innate immune responses in patients with advanced cancer. *Clin Cancer Res* **13**, 7119-7125 (2007).
77. Pockros, P.J. et al. Oral resiquimod in chronic HCV infection: safety and efficacy in 2 placebo-controlled, double-blind phase IIa studies. *Journal of hepatology* **47**, 174-182 (2007).
78. Sullivan, T.P., Dearaujo, T., Vincek, V. & Berman, B. Evaluation of superficial basal cell carcinomas after treatment with imiquimod 5% cream or vehicle for apoptosis and lymphocyte phenotyping. *Dermatologic surgery : official publication for American Society for Dermatologic Surgery [et al.]* **29**, 1181-1186 (2003).
79. Lebwohl, M. et al. Imiquimod 5% cream for the treatment of actinic keratosis: results from two phase III, randomized, double-blind, parallel group, vehicle-controlled trials. *Journal of the American Academy of Dermatology* **50**, 714-721 (2004).
80. Geisse, J.K. et al. Imiquimod 5% cream for the treatment of superficial basal cell carcinoma: a double-blind, randomized, vehicle-controlled study. *Journal of the American Academy of Dermatology* **47**, 390-398 (2002).
81. Schon, M. & Schon, M.P. The antitumoral mode of action of imiquimod and other imidazoquinolines. *Curr Med Chem* **14**, 681-687 (2007).
82. A, A.G., Tyring, S.K. & Rosen, T. Beyond a decade of 5% imiquimod topical therapy. *Journal of drugs in dermatology : JDD* **8**, 467-474 (2009).
83. Savage, P. et al. A phase I clinical trial of imiquimod, an oral interferon inducer, administered daily. *British journal of cancer* **74**, 1482-1486 (1996).
84. Witt, P.L. et al. Phase I trial of an oral immunomodulator and interferon inducer in cancer patients. *Cancer Res* **53**, 5176-5180 (1993).
85. Mark, K.E. et al. Topical resiquimod 0.01% gel decreases herpes simplex virus type 2 genital shedding: a randomized, controlled trial. *The Journal of infectious diseases* **195**, 1324-1331 (2007).
86. St Pierre, S.A. et al. In situ photoimmunotherapy: a surgery- and limb-sparing approach to the treatment of cutaneous metastases in advanced melanoma. *Archives of dermatology* **146**, 831-834 (2010).
87. Schon, M.P. & Schon, M. Imiquimod: mode of action. *Br J Dermatol* **157 Suppl 2**, 8-13 (2007).
88. Schiessl, C., Wolber, C., Tauber, M., Offner, F. & Strohal, R. Treatment of all basal cell carcinoma variants including large and high-risk lesions with 5% imiquimod cream: histological and clinical changes, outcome, and follow-up. *Journal of drugs in dermatology : JDD* **6**, 507-513 (2007).
89. Cooksley, W.G. The role of interferon therapy in hepatitis B. *MedGenMed : Medscape general medicine* **6**, 16 (2004).
90. Lampkin, B.C., Levine, A.S., Levy, H., Krivit, W. & Hammond, D. Phase II trial of a complex polyriboinosinic-polyribocytidylic acid with poly-L-lysine and carboxymethyl cellulose in the treatment of children with acute leukemia and neuroblastoma: a report from the Children's Cancer Study Group. *Cancer Res* **45**, 5904-5909 (1985).
91. Lampkin, B.C., Levine, A.S., Levy, H., Krivit, W. & Hammond, D. Phase II trial of poly(I,C)-LC, an interferon inducer, in the treatment of children with acute leukemia and neuroblastoma: a report from the Children's Cancer Study Group. *Journal of biological response modifiers* **4**, 531-537 (1985).

92. Matsuda, F. et al. Anti-interferon-alpha neutralizing antibody is associated with nonresponse to pegylated interferon-alpha plus ribavirin in chronic hepatitis C. *Journal of viral hepatitis* **19**, 694-703 (2012).
93. da Silva, L.C. et al. [Recombinant alfa interferon in the treatment of chronic B and non-A, non-B hepatitis: preliminary results]. *Revista do Hospital das Clinicas* **44**, 201-206 (1989).
94. Boonstra, A. et al. Potent immune activation in chronic hepatitis C patients upon administration of an oral inducer of endogenous interferons that acts via Toll-like receptor 7. *Antiviral therapy* **17**, 657-667 (2012).
95. Bergmann, J.F. et al. Randomised clinical trial: anti-viral activity of ANA773, an oral inducer of endogenous interferons acting via TLR7, in chronic HCV. *Alimentary pharmacology & therapeutics* **34**, 443-453 (2011).
96. Dummer, R. et al. An exploratory study of systemic administration of the toll-like receptor-7 agonist 852A in patients with refractory metastatic melanoma. *Clin Cancer Res* **14**, 856-864 (2008).
97. Harrison, L.I., Astry, C., Kumar, S. & Yunis, C. Pharmacokinetics of 852A, an imidazoquinoline Toll-like receptor 7-specific agonist, following intravenous, subcutaneous, and oral administrations in humans. *Journal of clinical pharmacology* **47**, 962-969 (2007).
98. Chang, B.A., Cross, J.L., Najar, H.M. & Dutz, J.P. Topical resiquimod promotes priming of CTL to parenteral antigens. *Vaccine* **27**, 5791-5799 (2009).
99. Holcmann, M., Drobits, B. & Sibilia, M. How imiquimod licenses plasmacytoid dendritic cells to kill tumors. *Oncoimmunology* **1**, 1661-1663 (2012).
100. Drobits, B. et al. Imiquimod clears tumors in mice independent of adaptive immunity by converting pDCs into tumor-killing effector cells. *J Clin Invest* **122**, 575-585 (2012).
101. Stary, G. et al. Tumoricidal activity of TLR7/8-activated inflammatory dendritic cells. *J Exp Med* **204**, 1441-1451 (2007).
102. Chaperot, L. et al. Virus or TLR agonists induce TRAIL-mediated cytotoxic activity of plasmacytoid dendritic cells. *J Immunol* **176**, 248-255 (2006).
103. Soria, I. et al. Effect of food on the pharmacokinetics and bioavailability of oral imiquimod relative to a subcutaneous dose. *International journal of clinical pharmacology and therapeutics* **38**, 476-481 (2000).
104. Baenziger, S. et al. Triggering TLR7 in mice induces immune activation and lymphoid system disruption, resembling HIV-mediated pathology. *Blood* **113**, 377-388 (2009).
105. Wille-Reece, U. et al. HIV Gag protein conjugated to a Toll-like receptor 7/8 agonist improves the magnitude and quality of Th1 and CD8+ T cell responses in nonhuman primates. *Proc Natl Acad Sci U S A* **102**, 15190-15194 (2005).
106. Wille-Reece, U., Wu, C.Y., Flynn, B.J., Kedl, R.M. & Seder, R.A. Immunization with HIV-1 Gag protein conjugated to a TLR7/8 agonist results in the generation of HIV-1 Gag-specific Th1 and CD8+ T cell responses. *J Immunol* **174**, 7676-7683 (2005).
107. Wille-Reece, U. et al. Toll-like receptor agonists influence the magnitude and quality of memory T cell responses after prime-boost immunization in nonhuman primates. *J Exp Med* **203**, 1249-1258 (2006).

108. Kastenmuller, K. et al. Protective T cell immunity in mice following protein-TLR7/8 agonist-conjugate immunization requires aggregation, type I IFN, and multiple DC subsets. *J Clin Invest* **121**, 1782-1796 (2011).
109. Shukla, N.M. et al. Toward self-adjuvanting subunit vaccines: model peptide and protein antigens incorporating covalently bound toll-like receptor-7 agonistic imidazoquinolines. *Bioorg Med Chem Lett* **21**, 3232-3236 (2011).
110. Shah, N.H., Dann, G.P., Vila-Perello, M., Liu, Z. & Muir, T.W. Ultrafast protein splicing is common among cyanobacterial split inteins: implications for protein engineering. *Journal of the American Chemical Society* **134**, 11338-11341 (2012).
111. Jung, B. & Theato, P. in Bio-synthetic Polymer Conjugates, Vol. 253. (ed. H. Schlaad) 37-70 (Springer Berlin Heidelberg, 2013).
112. Pechar, M. & Pola, R. The coiled coil motif in polymer drug delivery systems. *Biotechnology advances* **31**, 90-96 (2013).
113. Fierer, J.O., Veggiani, G. & Howarth, M. SpyLigase peptide-peptide ligation polymerizes affibodies to enhance magnetic cancer cell capture. *Proc Natl Acad Sci U S A* **111**, E1176-1181 (2014).
114. Prescher, J.A. & Bertozzi, C.R. Chemistry in living systems. *Nature chemical biology* **1**, 13-21 (2005).
115. Witus, L.S. et al. Site-specific protein transamination using N-methylpyridinium-4-carboxaldehyde. *Journal of the American Chemical Society* **135**, 17223-17229 (2013).
116. Vecchi, S. et al. Conjugation of a TLR7 agonist and antigen enhances protection in the S. pneumoniae murine infection model. *European journal of pharmaceutics and biopharmaceutics : official journal of Arbeitsgemeinschaft fur Pharmazeutische Verfahrenstechnik e.V* **87**, 310-317 (2014).
117. Feng, Y. et al. Chemical cross-linking of HIV-1 Env for direct TLR7/8 ligand conjugation compromises recognition of conserved antigenic determinants. *Virology* **446**, 56-65 (2013).
118. Fujita, Y. & Taguchi, H. Overview and outlook of Toll-like receptor ligand-antigen conjugate vaccines. *Therapeutic delivery* **3**, 749-760 (2012).
119. Kasturi, S.P. et al. Programming the magnitude and persistence of antibody responses with innate immunity. *Nature* **470**, 543-547 (2011).
120. Tacken, P.J. et al. Targeted delivery of TLR ligands to human and mouse dendritic cells strongly enhances adjuvanticity. *Blood* **118**, 6836-6844 (2011).
121. Smirnov, D., Schmidt, J.J., Capecchi, J.T. & Wightman, P.D. Vaccine adjuvant activity of 3M-052: an imidazoquinoline designed for local activity without systemic cytokine induction. *Vaccine* **29**, 5434-5442 (2011).
122. Scott, E.A. et al. Dendritic cell activation and T cell priming with adjuvant- and antigen-loaded oxidation-sensitive polymersomes. *Biomaterials* **33**, 6211-6219 (2012).
123. Vicente, S. et al. Co-delivery of viral proteins and a TLR7 agonist from polysaccharide nanocapsules: a needle-free vaccination strategy. *Journal of controlled release : official journal of the Controlled Release Society* **172**, 773-781 (2013).
124. Ilyinskii, P.O. et al. Adjuvant-carrying synthetic vaccine particles augment the immune response to encapsulated antigen and exhibit strong local immune activation without inducing systemic cytokine release. *Vaccine* **32**, 2882-2895 (2014).

125. Heuking, S. & Borchard, G. Toll-like receptor-7 agonist decoration enhances the adjuvanticity of chitosan-DNA nanoparticles. *J Pharm Sci* (2011).
126. Wu, T.Y. et al. Rational design of small molecules as vaccine adjuvants. *Sci Transl Med* **6**, 263ra160 (2014).
127. Wu, C.C. et al. Immunotherapeutic activity of a conjugate of a Toll-like receptor 7 ligand. *Proc Natl Acad Sci U S A* **104**, 3990-3995 (2007).
128. Storni, T., Ruedl, C., Renner, W.A. & Bachmann, M.F. Innate immunity together with duration of antigen persistence regulate effector T cell induction. *J Immunol* **171**, 795-801 (2003).
129. Obst, R., van Santen, H.M., Mathis, D. & Benoist, C. Antigen persistence is required throughout the expansion phase of a CD4(+) T cell response. *J Exp Med* **201**, 1555-1565 (2005).
130. Bachmann, M.F. et al. Long-lived memory CD8+ T cells are programmed by prolonged antigen exposure and low levels of cellular activation. *Eur J Immunol* **36**, 842-854 (2006).
131. Shaulov, A. & Murali-Krishna, K. CD8 T cell expansion and memory differentiation are facilitated by simultaneous and sustained exposure to antigenic and inflammatory milieu. *J Immunol* **180**, 1131-1138 (2008).
132. Tabata, Y. & Ikada, Y. Effect of the size and surface charge of polymer microspheres on their phagocytosis by macrophage. *Biomaterials* **9**, 356-362 (1988).
133. Storni, T., Kundig, T.M., Senti, G. & Johansen, P. Immunity in response to particulate antigen-delivery systems. *Advanced drug delivery reviews* **57**, 333-355 (2005).
134. Ahsan, F., Rivas, I.P., Khan, M.A. & Torres Suarez, A.I. Targeting to macrophages: role of physicochemical properties of particulate carriers--liposomes and microspheres--on the phagocytosis by macrophages. *Journal of controlled release : official journal of the Controlled Release Society* **79**, 29-40 (2002).
135. Bachmann, M.F. & Jennings, G.T. Vaccine delivery: a matter of size, geometry, kinetics and molecular patterns. *Nat Rev Immunol* **10**, 787-796 (2010).
136. Hawiger, D. et al. Dendritic cells induce peripheral T cell unresponsiveness under steady state conditions in vivo. *J Exp Med* **194**, 769-779 (2001).
137. Steinman, R.M., Hawiger, D. & Nussenzweig, M.C. Tolerogenic dendritic cells. *Annual review of immunology* **21**, 685-711 (2003).
138. Nair-Gupta, P. et al. TLR signals induce phagosomal MHC-I delivery from the endosomal recycling compartment to allow cross-presentation. *Cell* **158**, 506-521 (2014).
139. Blander, J.M. & Medzhitov, R. Regulation of phagosome maturation by signals from toll-like receptors. *Science* **304**, 1014-1018 (2004).
140. Blander, J.M. & Medzhitov, R. Toll-dependent selection of microbial antigens for presentation by dendritic cells. *Nature* **440**, 808-812 (2006).
141. Blander, J.M. & Medzhitov, R. On regulation of phagosome maturation and antigen presentation. *Nat Immunol* **7**, 1029-1035 (2006).
142. Cairo, C.W., Gestwicki, J.E., Kanai, M. & Kiessling, L.L. Control of multivalent interactions by binding epitope density. *Journal of the American Chemical Society* **124**, 1615-1619 (2002).
143. Gestwicki, J.E., Cairo, C.W., Strong, L.E., Oetjen, K.A. & Kiessling, L.L. Influencing receptor-ligand binding mechanisms with multivalent ligand

architecture. *Journal of the American Chemical Society* **124**, 14922-14933 (2002).
144. Kitov, P.I. & Bundle, D.R. On the nature of the multivalency effect: a thermodynamic model. *Journal of the American Chemical Society* **125**, 16271-16284 (2003).
145. Honda, K. et al. Spatiotemporal regulation of MyD88-IRF-7 signalling for robust type-I interferon induction. *Nature* **434**, 1035-1040 (2005).
146. Haas, T., Schmitz, F., Heit, A. & Wagner, H. Sequence independent interferon-alpha induction by multimerized phosphodiester DNA depends on spatial regulation of Toll-like receptor-9 activation in plasmacytoid dendritic cells. *Immunology* **126**, 290-298 (2009).
147. Wu, C.C., Lee, J., Raz, E., Corr, M. & Carson, D.A. Necessity of oligonucleotide aggregation for toll-like receptor 9 activation. *J Biol Chem* **279**, 33071-33078 (2004).
148. Reddy, S.T. et al. Exploiting lymphatic transport and complement activation in nanoparticle vaccines. *Nat Biotechnol* **25**, 1159-1164 (2007).
149. Reddy, S.T., Rehor, A., Schmoekel, H.G., Hubbell, J.A. & Swartz, M.A. In vivo targeting of dendritic cells in lymph nodes with poly(propylene sulfide) nanoparticles. *Journal of controlled release : official journal of the Controlled Release Society* **112**, 26-34 (2006).
150. Manolova, V. et al. Nanoparticles target distinct dendritic cell populations according to their size. *Eur J Immunol* **38**, 1404-1413 (2008).
151. Cinelli, M.A., Cordero, B., Dexheimer, T.S., Pommier, Y. & Cushman, M. Synthesis and biological evaluation of 14-(aminoalkyl-aminomethyl)aromathecins as topoisomerase I inhibitors: Investigating the hypothesis of shared structure-activity relationships. *Bioorgan Med Chem* **17**, 7145-7155 (2009).
152. Kaminski, Z.J. 2-Chloro-4,6-Dimethoxy-1,3,5-Triazine - a New Coupling Reagent for Peptide-Synthesis. *Synthesis-Stuttgart*, 917-920 (1987).
153. Nanba, R.J., Iizuka, Takao (JP), Ishii, Takeo (JP) (TERUMO CORP (JP), 1999).
154. Russo, C. et al. Small molecule Toll-like receptor 7 agonists localize to the MHC class II loading compartment of human plasmacytoid dendritic cells. *Blood* **117**, 5683-5691 (2011).
155. Shukla, N.M. et al. Syntheses of fluorescent imidazoquinoline conjugates as probes of Toll-like receptor 7. *Bioorg Med Chem Lett* **20**, 6384-6386 (2010).
156. Subr, V. & Ulbrich, K. Synthesis and properties of new N-(2-hydroxypropyl)-methacrylamide copolymers containing thiazolidine-2-thione reactive groups. *React Funct Polym* **66**, 1525-1538 (2006).
157. Hruby, M. et al. New bioerodable thermoresponsive polymers for possible radiotherapeutic applications. *Journal of controlled release : official journal of the Controlled Release Society* **119**, 25-33 (2007).
158. Neron, S. et al. Characterization of mononuclear cells remaining in the leukoreduction system chambers of apheresis instruments after routine platelet collection: a new source of viable human blood cells. *Transfusion* **47**, 1042-1049 (2007).
159. Neron, S., Dussault, N. & Racine, C. Whole-blood leukoreduction filters are a source for cryopreserved cells for phenotypic and functional investigations on peripheral blood lymphocytes. *Transfusion* **46**, 537-544 (2006).

160. Quinn, K.M. et al. Comparative analysis of the magnitude, quality, phenotype, and protective capacity of simian immunodeficiency virus gag-specific CD8+ T cells following human-, simian-, and chimpanzee-derived recombinant adenoviral vector immunization. *J Immunol* **190**, 2720-2735 (2013).
161. Foulds, K.E., Rotte, M.J. & Seder, R.A. IL-10 is required for optimal CD8 T cell memory following Listeria monocytogenes infection. *J Immunol* **177**, 2565-2574 (2006).
162. Weterings, J.J. et al. Synthesis of 2-alkoxy-8-hydroxyadenylpeptides: towards synthetic epitope-based vaccines. *Bioorg Med Chem Lett* **16**, 3258-3261 (2006).
163. Duncan, R. & Vicent, M.J. Do HPMA copolymer conjugates have a future as clinically useful nanomedicines? A critical overview of current status and future opportunities. *Advanced drug delivery reviews* **62**, 272-282 (2010).
164. Seymour, L.W., Duncan, R., Strohalm, J. & Kopecek, J. Effect of Molecular-Weight (Mbarw) of N-(2-Hydroxypropyl)Methacrylamide Copolymers on Body Distribution and Rate of Excretion after Subcutaneous, Intraperitoneal, and Intravenous Administration to Rats. *J Biomed Mater Res* **21**, 1341-1358 (1987).
165. Seymour, L.W. et al. Hepatic drug targeting: phase I evaluation of polymer-bound doxorubicin. *J Clin Oncol* **20**, 1668-1676 (2002).
166. Liu, X.M., Miller, S.C. & Wang, D. Beyond oncology--application of HPMA copolymers in non-cancerous diseases. *Advanced drug delivery reviews* **62**, 258-271 (2010).
167. Manetti, R. et al. Natural killer cell stimulatory factor (interleukin 12 [IL-12]) induces T helper type 1 (Th1)-specific immune responses and inhibits the development of IL-4-producing Th cells. *J Exp Med* **177**, 1199-1204 (1993).
168. Trinchieri, G. Interleukin-12 and its role in the generation of TH1 cells. *Immunology today* **14**, 335-338 (1993).
169. Trinchieri, G. et al. Producer cells of interleukin-12. *Immunology today* **14**, 237-238 (1993).
170. Trinchieri, G. Interleukin-12 and the regulation of innate resistance and adaptive immunity. *Nat Rev Immunol* **3**, 133-146 (2003).
171. Le Bon, A. et al. Direct stimulation of T cells by type I IFN enhances the CD8+ T cell response during cross-priming. *J Immunol* **176**, 4682-4689 (2006).
172. Gangur, V., Simons, F.E. & Hayglass, K.T. Human IP-10 selectively promotes dominance of polyclonally activated and environmental antigen-driven IFN-gamma over IL-4 responses. *FASEB journal : official publication of the Federation of American Societies for Experimental Biology* **12**, 705-713 (1998).
173. Dostert, C. et al. Innate immune activation through Nalp3 inflammasome sensing of asbestos and silica. *Science* **320**, 674-677 (2008).
174. Doxsee, C.L. et al. The immune response modifier and Toll-like receptor 7 agonist S-27609 selectively induces IL-12 and TNF-alpha production in CD11c+CD11b+CD8- dendritic cells. *J Immunol* **171**, 1156-1163 (2003).
175. Shukla, N.M. et al. Potent adjuvanticity of a pure TLR7-agonistic imidazoquinoline dendrimer. *PLoS One* **7**, e43612 (2012).
176. Liu, H. et al. Structure-based programming of lymph-node targeting in molecular vaccines. *Nature* **507**, 519-522 (2014).

177. Fries, L.F., Smith, G.E. & Glenn, G.M. A recombinant viruslike particle influenza A (H7N9) vaccine. *N Engl J Med* **369**, 2564-2566 (2013).
178. Shah, J.A. et al. Dendritic cells are responsible for the capacity of CpG oligodeoxynucleotides to act as an adjuvant for protective vaccine immunity against Leishmania major in mice. *J Exp Med* **198**, 281-291 (2003).
179. Raghavan, S., Nystrom, J., Fredriksson, M., Holmgren, J. & Harandi, A.M. Orally administered CpG oligodeoxynucleotide induces production of CXC and CC chemokines in the gastric mucosa and suppresses bacterial colonization in a mouse model of Helicobacter pylori infection. *Infection and immunity* **71**, 7014-7022 (2003).
180. Jenkins, M.K. & Moon, J.J. The role of naive T cell precursor frequency and recruitment in dictating immune response magnitude. *J Immunol* **188**, 4135-4140 (2012).
181. Andersen, P. & Woodworth, J.S. Tuberculosis vaccines--rethinking the current paradigm. *Trends Immunol* **35**, 387-395 (2014).
182. Lopez Kostka, S. et al. IL-17 promotes progression of cutaneous leishmaniasis in susceptible mice. *J Immunol* **182**, 3039-3046 (2009).
183. Chan, M. et al. Synthesis and immunological characterization of toll-like receptor 7 agonistic conjugates. *Bioconjug Chem* **20**, 1194-1200 (2009).
184. Itano, A.A. et al. Distinct dendritic cell populations sequentially present antigen to CD4 T cells and stimulate different aspects of cell-mediated immunity. *Immunity* **19**, 47-57 (2003).
185. Jewell, C.M., Lopez, S.C. & Irvine, D.J. In situ engineering of the lymph node microenvironment via intranodal injection of adjuvant-releasing polymer particles. *Proc Natl Acad Sci U S A* **108**, 15745-15750 (2011).
186. Reiner, S.L. & Locksley, R.M. Lessons from Leishmania: a model for investigations of CD4+ subset differentiation. *Infectious agents and disease* **1**, 33-42 (1992).
187. Reiner, S.L. & Locksley, R.M. The regulation of immunity to Leishmania major. *Annual review of immunology* **13**, 151-177 (1995).
188. Hensley, S.E. et al. Type I interferon inhibits antibody responses induced by a chimpanzee adenovirus vector. *Mol Ther* **15**, 393-403 (2007).
189. Hyde, S.C. et al. CpG-free plasmids confer reduced inflammation and sustained pulmonary gene expression. *Nat Biotechnol* **26**, 549-551 (2008).
190. Hemmi, M. et al. The early activation of CD8+ T cells is dependent on type I IFN signaling following intramuscular vaccination of adenovirus vector. *BioMed research international* **2014**, 158128 (2014).
191. Ryu, K.A., Stutts, L., Tom, J.K., Mancini, R.J. & Esser-Kahn, A.P. Stimulation of Innate Immune Cells by Light-Activated TLR7/8 Agonists. *Journal of the American Chemical Society* **136**, 10823-10825 (2014).
192. Pola, R., Braunova, A., Laga, R., Pechar, M. & Ulbrich, K. Click chemistry as a powerful and chemoselective tool for the attachment of targeting ligands to polymer drug carriers. *Polymer Chemistry* **5**, 1340-1350 (2014).
193. Kolb, H.C. & Sharpless, K.B. The growing impact of click chemistry on drug discovery. *Drug Discovery Today* **8**, 1128-1137 (2003).
194. Moon, J.J. et al. Enhancing humoral responses to a malaria antigen with nanoparticle vaccines that expand Tfh cells and promote germinal center induction. *Proc Natl Acad Sci U S A* **109**, 1080-1085 (2012).
195. Wendorf, J. et al. A practical approach to the use of nanoparticles for vaccine delivery. *Journal of Pharmaceutical Sciences* **95**, 2738-2750 (2006).

196. Shakya, A.K., Holmdahl, R., Nandakumar, K.S. & Kumar, A. Characterization of chemically defined poly-N-isopropylacrylamide based copolymeric adjuvants. *Vaccine* **31**, 3519-3527 (2013).
197. Keerl, M., Smirnovas, V., Winter, R. & Richtering, W. Copolymer microgels from mono- and disubstituted acrylamides: Phase behavior and hydrogen bonds. *Macromolecules* **41**, 6830-6836 (2008).
198. Iwai, R., Kusakabe, S., Nemoto, Y. & Nakayama, Y. Deposition Gene Transfection Using Bioconjugates of DNA and Thermoresponsive Cationic Homopolymer. *Bioconjugate Chem* **23**, 751-757 (2012).
199. Diab, C., Akiyama, Y., Kataoka, K. & Winnik, F.M. Microcalorimetric study of the temperature-induced phase separation in aqueous solutions of poly(2-isopropyl-2-oxazolines). *Macromolecules* **37**, 2556-2562 (2004).
200. Ballas, S.K. et al. Safety of purified poloxamer 188 in sickle cell disease: phase I study of a non-ionic surfactant in the management of acute chest syndrome. *Hemoglobin* **28**, 85-102 (2004).
201. Daniels, S., Reader, S., Berry, P. & Goulder, M. Onset of analgesia with sodium ibuprofen, ibuprofen acid incorporating poloxamer and acetaminophen--a single-dose, double-blind, placebo-controlled study in patients with post-operative dental pain. *European journal of clinical pharmacology* **65**, 343-353 (2009).
202. Tran, P.H. et al. Physical properties and in vivo bioavailability in human volunteers of isradipine using controlled release matrix tablet containing self-emulsifying solid dispersion. *Int J Pharm* **450**, 79-86 (2013).
203. Chou, H.Y. et al. Hydrogel-delivered GM-CSF overcomes nonresponsiveness to hepatitis B vaccine through the recruitment and activation of dendritic cells. *J Immunol* **185**, 5468-5475 (2010).
204. De Gregorio, E., Tritto, E. & Rappuoli, R. Alum adjuvanticity: unraveling a century old mystery. *Eur J Immunol* **38**, 2068-2071 (2008).
205. O'Hagan, D.T., Ott, G.S., Nest, G.V., Rappuoli, R. & Giudice, G.D. The history of MF59((R)) adjuvant: a phoenix that arose from the ashes. *Expert review of vaccines* **12**, 13-30 (2013).
206. Garcon, N. et al. Development of an AS04-adjuvanted HPV vaccine with the adjuvant system approach. *BioDrugs : clinical immunotherapeutics, biopharmaceuticals and gene therapy* **25**, 217-226 (2011).
207. Garcon, N., Segal, L., Tavares, F. & Van Mechelen, M. The safety evaluation of adjuvants during vaccine development: the AS04 experience. *Vaccine* **29**, 4453-4459 (2011).
208. Sullivan, N.J. et al. CD8+ cellular immunity mediates rAd5 vaccine protection against Ebola virus infection of nonhuman primates. *Nature medicine* **17**, 1128-1131 (2011).
209. Hill, A.V. et al. Prime-boost vectored malaria vaccines: progress and prospects. *Hum Vaccin* **6**, 78-83 (2010).
210. Epstein, J.E. et al. Live attenuated malaria vaccine designed to protect through hepatic CD8(+) T cell immunity. *Science* **334**, 475-480 (2011).
211. Porter, D.L., Levine, B.L., Kalos, M., Bagg, A. & June, C.H. Chimeric antigen receptor-modified T cells in chronic lymphoid leukemia. *N Engl J Med* **365**, 725-733 (2011).